



FACULTY OF MEDICINE
AND HEALTH SCIENCES

**CONNEXIN CHANNELS PROVIDE A TARGET TO
MANIPULATE CALCIUM DYNAMICS AND BLOOD BRAIN
BARRIER PERMEABILITY**

MARIJKE DE BOCK

Promoter: Prof. Dr. Luc Leybaert

Thesis submitted in fulfillment of the requirements for the degree of
'Doctor of Biomedical Sciences'

Faculty of Medicine and Health Sciences
Department of Basic Medical Sciences
Physiology Group

Thesis submitted in fulfillment of the requirements for the degree of ‘Doctor of Biomedical Sciences’
July 02, 2012

Promotor: Prof. Dr. Luc Leybaert
Ghent University, Belgium

Members of the Examination Committee:

Prof. Dr. Vincent Berezowski
Université d’Artois, France

Prof. Dr. Laurent Combettes
Université paris Sud, France

Prof. Dr. Jan Gettemans
Ghent University, Belgium

Prof. Dr. Michael Sanderson
University of Massachusetts, USA

Prof. Dr. Hubert Thierens
Ghent University, Belgium

Prof. Dr. Bert Vanheel
Ghent University, Belgium

Chairman: Prof. Dr. Claude Cuvelier
Ghent University, Belgium

Cover illustration: ‘Blood vessels’ from the website of the alzheimer’s association (www.alz.org).
With permission

Research funded by a PhD grant of the Institute for the promotion of
Innovation through Science and Technology in Flanders (IWT
Vlaanderen, grant number 63352)



agentschap voor Innovatie
door Wetenschap en Technologie

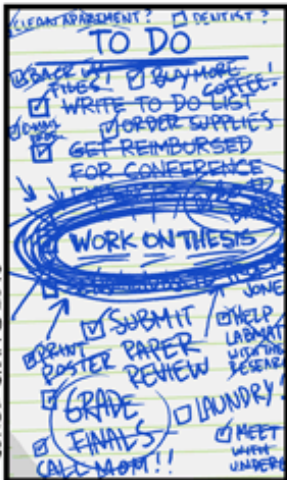
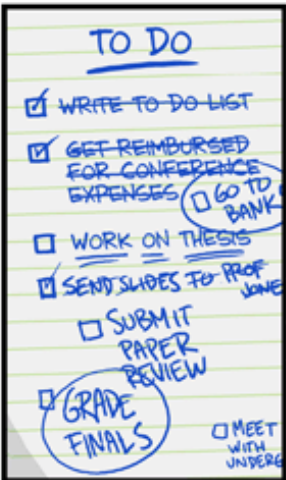
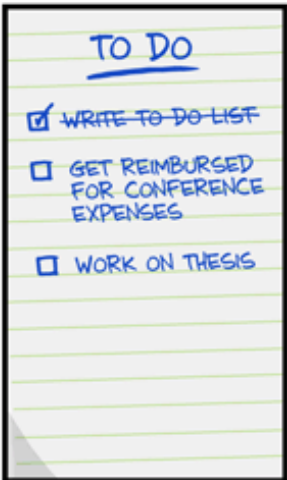


TABLE OF CONTENTS

List of frequently used abbreviations	9
Summary	13
Samenvatting	17
Chapter 1: Introduction.....	21
1.1 Preface.....	23
1.2 Cell-cell communication: Gap junctions and Hemichannels	24
1.2.1 The connexin protein family	26
1.2.1.1 Molecular characterization of connexin-based channels	27
1.2.1.2 The connexin life cycle.....	28
1.2.2 Permeability and pore selectivity of connexin channels	31
1.2.3 Gating of connexin channels.....	34
1.2.3.1 Voltage gating.....	35
1.2.3.2 Chemical gating	37
1.2.3.2.1 pH gating.....	37
1.2.3.2.2 Channel gating by post-translational modifications.....	38
1.2.3.2.3 Modulation of connexin channels by Ca ²⁺	40
Gap junctions.....	40
Connexin hemichannels.....	42
1.2.4 The innexin/pannexin protein family	47
1.2.5 Pharmacological properties of connexins and pannexins	50
1.2.5.1 Connexin mimetic peptides	52
1.3 Ca ²⁺ homeostasis and Ca ²⁺ signaling.....	55
1.3.1 Ca ²⁺ homeostasis.....	55
1.3.2 Intracellular and intercellular Ca ²⁺ signaling	57
1.3.2.1 [Ca ²⁺] _i elevation and restoration mechanisms.....	57
1.3.2.2 Spatiotemporal organization of Ca ²⁺ signals	61
1.3.2.2.1 Ca ²⁺ oscillations	62
Ca ²⁺ oscillations based on intrinsic InsP ₃ receptor properties	65
Ca ²⁺ oscillations driven by InsP ₃ dynamics	68
Role of Ca ²⁺ entry in the Ca ²⁺ oscillation mechanism	70
Other players of the Ca ²⁺ oscillation machinery	73
1.3.2.2.2 Propagation of Ca ²⁺ signals.....	74
1.4 Endothelial Ca ²⁺ dynamics and blood-brain barrier function.....	81
1.4.1 The blood-brain barrier	81
1.4.1.1 The blood-brain barrier from a historical point of view	81
1.4.1.2 Blood-brain barrier anatomy.....	82
1.4.1.2.1 Tight junctions	82
1.4.1.2.2 Adherens junctions.....	84
1.4.1.3 The neurovascular unit	86
1.4.2 Ca ²⁺ as a major determinant of BBB function	88
1.4.2.1 Bradykinin	90
1.4.2.2 LPA and histamine	91
1.4.2.3 Thrombin	92
1.4.2.4 Glutamate.....	92
1.4.2.5 Vascular endothelial growth factor.....	93

1.4.2.6 BBB permeation by pathogens and leukocytes	94
1.4.2.7 Ca ²⁺ dependent pathways converge on tight junction proteins and the actin cytoskeleton	96
1.4.3 Spatiotemporal organization of Ca ²⁺ signals and BBB function.....	102
1.4.3.1 Brain microvessel endothelial cells display Ca ²⁺ oscillation and intercellular Ca ²⁺ wave activity	102
Chapter 2: Aim of the study	109
Chapter 3: Results.....	113
3.1 Connexin channels provide a target to manipulate brain endothelial calcium dynamics and blood brain barrier permeability.....	115
3.1.1 Introduction.....	116
3.1.2 Materials and Methods.....	118
3.1.2.1 Cell culture	118
3.1.2.2 Chemicals and reagents	118
3.1.2.3 Ca ²⁺ imaging.....	119
3.1.2.4 Caged-InsP ₃ loading and photoliberation	120
3.1.2.5 Gap junction dye coupling studies.....	120
3.1.2.6 Hemichannel assays.....	121
3.1.2.7 Cell death studies.....	121
3.1.2.8 <i>In vitro</i> endothelial permeability	122
3.1.2.9 <i>In vivo</i> BBB permeability	122
3.1.2.10 siRNA treatment	123
3.1.2.11 Electrophoresis and western blotting.....	124
3.1.2.12 Polymerase chain reaction	124
3.1.2.13 Immunofluorescence.....	125
3.1.2.14 Statistical analysis.....	125
3.1.3 Results.....	125
3.1.3.1 BK triggers Ca ²⁺ oscillations that involve connexin hemichannel opening and purinergic signaling.....	125
3.1.3.2 ATP triggers Ca ²⁺ oscillations that are not associated with hemichannel opening.....	131
3.1.3.3 BK, but not ATP, increases BCEC permeability in a [Ca ²⁺] _i -dependent and Gap27-inhibitable manner	132
3.1.3.4 Effects of BK and Gap27 treatment on tight junction and cytoskeletal proteins.....	134
3.1.4 Discussion.....	136
3.2 low extracellular Ca ²⁺ conditions induce an increase in brain endothelial permeability that is largely mediated by triggering intercellular Ca ²⁺ waves	141
3.2.1 Introduction	142
3.2.2 Materials and Methods.....	144
3.2.2.1 Cell culture	144
3.2.2.2 Chemicals and reagents	144
3.2.2.3 Ca ²⁺ imaging.....	145
3.2.2.4 Endothelial transport studies.....	146
3.2.2.5 Hemichannel assays.....	146
3.2.2.6 Electrophoresis and western blotting.....	146
3.2.2.7 Statistical analysis.....	147
3.2.3 Results.....	148
3.2.3.1 Low extracellular Ca ²⁺ induces intercellular Ca ²⁺ waves in brain endothelial cells.....	148
3.2.3.2 BAPTA-AM and Gap27 inhibit endothelial permeability-increases induced by low extracellular [Ca ²⁺]	150
3.2.3.3 PKC, CaMKII and cytoskeletal involvement in endothelial permeability-increases induced by low extracellular [Ca ²⁺].....	151

3.2.3.4 Ca ²⁺ oscillations triggered by bradykinin provoke a limited endothelial permeability increase that is not mediated by PKC, CaMKII or actomyosin contraction.....	152
3.2.4 Discussion.....	154
3.3 Connexin-43 hemichannels contribute to cytoplasmic Ca ²⁺ oscillations by providing a bimodal Ca ²⁺ -dependent Ca ²⁺ entry pathway	159
3.3.1 Introduction.....	160
3.3.2 Materials and methods	162
3.3.2.1 Cell culture	162
3.3.2.2 Chemicals and reagents	163
3.3.2.3 Ca ²⁺ imaging.....	163
3.3.2.4 Electroporation loading	165
3.3.2.5 Caged compound loading and photoliberation	165
3.3.2.6 Hemichannel assays.....	166
3.3.2.7 Gap junction dye coupling studies.....	166
3.3.2.8 Ectonucleotidase activity	167
3.3.2.9 Apoptosis assay	167
3.3.2.10 siRNA treatment	167
3.3.2.11 Electrophoresis and Western blot analysis	168
3.3.2.12 Statistical analysis.....	168
3.3.3 Results.....	169
3.3.3.1 Concentration and InsP ₃ -dependency of BK- and ATP-induced Ca ²⁺ oscillations	169
3.3.3.2 Connexin-channel blockers inhibit BK-induced Ca ²⁺ oscillations but not those triggered by ATP.....	171
3.3.3.3 Lowering extracellular Ca ²⁺ differentially affects BK- and ATP-induced oscillations ..	176
3.3.3.4 ATP-induced Ca ²⁺ oscillations are inhibited by CytC while BK-induced oscillations are inhibited by both CytC and Cx43-targeting CT9 peptide.....	178
3.3.3.5 BK triggers TEER changes that can be inhibited by BAPTA-AM and carbenoxolone..	185
3.3.4 Discussion.....	186
Chapter 4: General discussion	191
4.1 Connexin hemichannels contribute to BK-triggered Ca ²⁺ oscillations.....	193
4.2 Ca ²⁺ dynamics modulate BBB permeability in concert with other signaling cascades	197
4.3 The nexus: where connexins meet Ca ²⁺ and junctional proteins	202
4.4 Future perspectives	210
References.....	213
Dankwoord.....	247
Curriculum Vitae.....	251

LIST OF FREQUENTLY USED ABBREVIATIONS

2-APB	2-aminoethoxydiphenyl borate
2-MeS-ATP	2-methylthio-ATP
Å	Ångstrom
AC	adenylyl cyclase
ADP	adenosine 5'-diphosphate
AMP	adenosine 5'-monophosphate
Ang-1	angiopoietin-1
ARC	arachidonate-activated channel
ATP	adenosine 5'-triphosphate
AUC	area under the curve
BAPTA-AM	1,2-bis-(2-aminophenoxy)-ethane- <i>N,N,N',N'</i> -tetraacetic-acid acetoxy methyl ester
BBB	blood brain barrier
BCEC	bovine brain capillary endothelial cells
bFGF	basic fibroblast growth factor
BK	bradykinin
$[Ca^{2+}]_{i/e}$	intra/extracellular Ca^{2+} concentration
cADPR	cyclic adenosine 5'-diphosphoribose
CaM	calmodulin
CaMKII	Ca^{2+} /CaM-dependent kinase II
cAMP	cyclic AMP
Cbx	carbenoxolone
CCE	capacitative Ca^{2+} entry
CFDA-AM	carboxyfluorescein diacetate acetoxy methyl ester
cGMP	cyclic guanosinemonophosphate
CICR	Ca^{2+} -induced Ca^{2+} release
CKAR	C kinase activity reporter
CL	cytoplasmic loop
CNS	central nervous system
CO ₂	carbon dioxide
CRAC	Ca^{2+} release activated channel
CT	carboxy-terminal
CytC	Cytochrome C
Da	Dalton
DAG	diacylglycerol
DF	dextran fluorescein
DMEM	Dulbecco's modified eagle medium
DTR	Dextran Texas Red
EGTA	ethylene glycol-bis-(β-aminoethyl ether)- <i>N,N,N',N'</i> -tetraacetic acid
EL	extracellular loop
ER	endoplasmic reticulum
ERK	extracellular signal-regulated kinase

FCS	fetal calf serum
FFA	flufenamic acid
FM	frequency modulation
FRAP	fluorescence recovery after photobleaching
GA	glycyrrhetic acid
GDNF	glial cell-derived neurotrophic factor
GFP	green fluorescent protein
G _j	junctional conductance
GPCR	G-protein coupled receptor
HBSS	Hank's balanced salt solution
HRP	horseradish peroxidase
ICAM	intercellular adhesion molecule
I _{CRAC}	CRAC-mediated currents
IL	interleukine
InsP ₃	inositol 1,4,5 trisphosphate
InsP ₄	inositol 1,3,4,5 tetrakisphosphate
InsP ₃ R	InsP ₃ receptor
Inx	innexin
IP	intraperitoneal
IV	intravenous
JAM	junction adhesion molecule
LPA	lysophosphatidic acid
LY	Lucifer yellow
MAPK	mitogen-activated protein kinase
MCP	monocyte chemoattractant protein
MDCK	madine darby canine kidney cells
MDR	multidrug resistance protein
MEM	minimal essential medium
mGluR	metabotropic glutamate receptor
MLC	myosin light chain
MLCK	MLC kinase
MLCP	MLC phosphatase
MMP	matrix-metalloproteinase
MW	molecular weight
NAADP	nicotinic acid adenine dinucleotide phosphate
NAD ⁺	nicotinamide adenine dinucleotide
NFA	niflumic acid
NFAT	nuclear factor of activated T-cells
NFκB	nuclear factor κB
NO	nitric oxide
NOS	nitric oxide synthase
NT	amino-terminal

Panx	pannexin
PAR	protease-activated receptor
PBS	phosphate-buffered saline
PDGF-B	platelet-derived growth factor B
Pe	Permeability coefficient
P-gp	P-glycoprotein
pH _{i/e}	intra/extracellular pH
PI	propidium iodide
PIP ₂	phosphatidylinositol bisphosphate
PKA	protein kinase A
PKC	protein kinase C
PKG	protein kinase G
PLA ₂	phospholipase A ₂
PLC	phospholipase C
PMCA	plasma membrane Ca ²⁺ ATPase
P _o	open probability
PPADS	pyridoxal phosphate-6-azo(benzene-2,4-disulfonic acid) tetrasodium salt
pS	picosiemens
PS	permeability-surface product
RBE	rat brain endothelial cells
ROCK	Rho kinase
ROS	reactive oxygen species
(R)PTK	(receptor) protein tyrosine kinase
RT	Room temperature
RyR	ryanodine receptor
s/pGC	soluble/particulate guanylyl cyclase
S1P	sphingosine-1-phosphate
SCaMPER	sphingolipid Ca ²⁺ -release mediating protein of the ER
SERCA	sarco-endoplasmic reticulum Ca ²⁺ ATPase
SOC	store-operated Ca ²⁺ channel
STIM	stromal interaction molecule
TEER	transendothelial electrical resistance
TGFβ	transforming growth factor β
TRP	transient receptor potential channel
VASP	vasodilator-stimulated phosphoprotein
VE-cadherin	vascular endothelial cadherin
V _j	transjunctional voltage
V _m	transmembrane potential
ZO	zonula occludens
γ _i	single channel conductance

SUMMARY

A typical feature of multicellular organisms is their capacity to communicate with surrounding cells, coordinating organ function. In vertebrate tissues, the integration of cellular functions is mediated by gap junctions, *i.e.* cell-cell channels that connect the cytoplasm of two neighboring cells. These channels are composed of two half gap junction channels or 'hemi'channels that, on their turn, enclose 6 connexin proteins. Over the years it has become evident that hemichannels are not mere building blocks of gap junction channels, but function by themselves as a tightly regulated conduit between the cell's interior and the extracellular space. Connexin channels, both gap junctions and hemichannels, are implicated in many tissue functions and their contribution to, for instance, Ca^{2+} signaling (changes in the intracellular Ca^{2+} concentration $[\text{Ca}^{2+}]_i$) has been very well characterized. Ca^{2+} signals are highly organized in time and space, presenting as intracellular Ca^{2+} oscillations and intercellular Ca^{2+} waves respectively. Two mechanisms have been identified supporting the latter. The first mechanism relies on the diffusion of Ca^{2+} or Ca^{2+} mobilizing messengers through gap junction channels. Alternatively, paracrine signaling involves the release of a Ca^{2+} mobilizing messenger into the extracellular space where it binds on its corresponding receptor and activates downstream signaling pathways in neighboring cells. Connexin hemichannels are likely candidates for the release of these messengers.

In addition to their proposed role in Ca^{2+} wave propagation, evidence is accruing that hemichannels may be involved in Ca^{2+} oscillations. The aim of this work was to define the mechanism by which hemichannels are involved in Ca^{2+} oscillations. Oscillations are based on positive and negative $[\text{Ca}^{2+}]_i$ feedback on InsP_3 receptor (InsP_3R) opening and Ca^{2+} release from the endoplasmic reticulum. Connexin hemichannels too are Ca^{2+} -permeable plasma membrane channels that are controlled by $[\text{Ca}^{2+}]_i$; therefore they may have an active contribution to the Ca^{2+} oscillation machinery as well. We applied different agonists that trigger Ca^{2+} oscillations and determined the involvement of connexin hemichannels in immortalized and long term cultured, primary brain endothelial cells that express Cx37 and Cx43. Bradykinin-triggered Ca^{2+} oscillations were inhibited by interfering with connexin channels making use of the pan-connexin channel inhibitor carbenoxolone, Cx37/Cx43 knockdown or Gap27, a peptide blocker of Cx37/Cx43 channels. Gap27 inhibition of the oscillations was rapid (within minutes), indicating the involvement of hemichannels (not gap

junctions). Work with connexin hemichannel-permeable dyes provided evidence for bradykinin-triggered hemichannel opening and we furthermore found that a bradykinin-activated purinergic signaling loop contributes to the oscillations. In contrast, Ca^{2+} oscillations provoked by exposure to ATP were not affected by carbenoxolone or Gap27. In Madine Darby Canine Kidney (MDCK) cells expressing Cx32 and Cx43, bradykinin-induced oscillations were rapidly and reversibly inhibited by the connexin mimetic peptides $^{32}\text{Gap27}/^{43}\text{Gap26}$ and by Cx43 gene silencing, while ATP-induced oscillations were again unaffected. These peptides also inhibited the bradykinin-triggered release of hemichannel-permeable dyes. Furthermore, bradykinin-induced oscillations, but not those induced by ATP, were sensitive to lowering extracellular Ca^{2+} to 0.5 mM. Alleviating the negative feedback of $[\text{Ca}^{2+}]_i$ on InsP_3Rs using CytC inhibited both bradykinin- and ATP-induced oscillations. Similar to the InsP_3R , Cx32 and Cx43 hemichannels are activated by $[\text{Ca}^{2+}]_i < 500$ nM but are inhibited by higher concentrations. CT9 peptide (last 9 amino acids of the Cx43 C-terminal tail) removed the inhibition by $[\text{Ca}^{2+}]_i > 500$ nM. Unlike interfering with the bell-shaped dependence of InsP_3Rs to $[\text{Ca}^{2+}]_i$ with CytC, CT9 peptide only prevented bradykinin-induced oscillations. Furthermore, hemichannel opening was not sufficient to set off oscillations by itself but a contribution of hemichannels was crucial as their inhibition stopped the oscillations.

Repetitive changes in $[\text{Ca}^{2+}]_i$ are documented to initiate a myriad of cellular processes, but little is known on the effect of $[\text{Ca}^{2+}]_i$ dynamics on blood-brain barrier (BBB) function. This barrier is present between the systemic circulation and the brain, and protects the nervous tissue from potentially toxic, circulating substances while securing a specialized environment for proper neuronal signaling. The BBB is formed by capillary endothelial cells that are characterized by an extremely low pinocytotic activity thus limiting non-specific transcellular access to the brain tissue. BBB endothelial cells are furthermore equipped with a tight and complex junctional network which, aided by the actin cytoskeleton, results in a restriction of the paracellular permeability. The latter route has been the subject of extensive research as an increase in paracellular permeability is often associated with a wide range of central nervous system pathologies and underlies brain edema and inflammation.

In second instance we aimed to define a functional link for connexin-based Ca^{2+} dynamics (oscillations and waves) on BBB function. In particular, we explored the effects of hemichannel-supported Ca^{2+} oscillations on BBB endothelial permeability. Bradykinin

triggered Ca^{2+} oscillations and increased endothelial permeability in immortalized and long term cultured, primary BBB endothelial cells. This was prevented by buffering intracellular Ca^{2+} changes with BAPTA indicating that Ca^{2+} oscillations are crucial in the permeability changes. Moreover, Gap27 inhibited the bradykinin-triggered endothelial permeability increase in *in vitro* and *in vivo* experiments. ATP, which induced oscillations that did not require hemichannels, did not disturb endothelial permeability. At the protein level we found bradykinin-induced alterations in the intermediate filament vimentin, but not in the tight junction proteins occludin and ZO-1. Again, these changes could be counteracted by Gap27 and were not found in cells treated with ATP. Exposing brain endothelial cells to low extracellular Ca^{2+} conditions triggered intercellular Ca^{2+} waves in the endothelial cultures. These waves elicited an increase in endothelial permeability that was inhibited by buffering $[\text{Ca}^{2+}]_i$ changes, indicating a crucial role for $[\text{Ca}^{2+}]_i$ changes, and by the connexin channel blocker Gap27. Although, the cell mass participating in either Ca^{2+} oscillations or Ca^{2+} waves was comparable, the permeability-increase triggered by low extracellular Ca^{2+} conditions largely exceeded that brought about by bradykinin, suggesting that intercellular Ca^{2+} waves are more efficient in modulating barrier function. Inhibiting protein kinase C, Ca^{2+} /calmodulin-dependent kinase II and actomyosin contraction interfered with the permeability-increase brought about by Ca^{2+} -free solution but did not influence the permeability increase triggered by bradykinin.

Collectively, our data indicate that connexin hemichannels contribute to bradykinin-induced oscillations by allowing Ca^{2+} -entry and/or release of ATP that acts in an autocrine manner, and that such hemichannel-supported oscillations increase BBB permeability. Additionally, intercellular Ca^{2+} waves that propagate by means of the different connexin channels result in more pronounced changes in BBB permeability. Currently, there are no tools available to limit BBB opening and our work shows that endothelial connexin channels may serve as a novel target to counteract a BBB permeability increase.

SAMENVATTING

Cel-cel communicatie is uiterst belangrijk voor de coördinatie van verschillende cellen en is daarom karakteristiek voor multicellulaire organismen. In vertebrate weefsels wordt zulke cel-cel communicatie gemedieerd door gap juncties. Gap juncties verbinden het cytoplasma van twee naburige cellen en zijn opgebouwd uit twee halve gap junctie kanalen of ‘hemi’kanalen die op hun beurt zijn opgebouwd uit 6 connexine eiwitten. Hemikanalen zijn niet enkel bouwstenen voor gap juncties, maar vormen zelf ook een streng gecontroleerde diffusieweg tussen het cytoplasma en de extracellulaire ruimte. Connexine kanalen, zowel gap juncties als hemikanalen, zijn betrokken bij verschillende weefselfuncties. Zo is hun rol in Ca^{2+} signaal communicatie uitgebreid gekend. Ca^{2+} signalen (wijzigingen in de intracellulaire Ca^{2+} concentratie $[\text{Ca}^{2+}]_i$) zijn georganiseerd in tijd en ruimte en komen voor als Ca^{2+} oscillaties en Ca^{2+} golven. Twee mechanismen kunnen de propagatie van zulke Ca^{2+} golven ondersteunen. Het eerste mechanisme omvat de diffusie van een Ca^{2+} mobiliserende boodschapper doorheen gap juncties. Het tweede behelst de loslating van een Ca^{2+} mobiliserende boodschapper in de extracellulaire ruimte waar hij diffundeert naar naburige cellen, daar bindt op zijn respectievelijke receptor en stroomafwaarts gelegen signaaltransductiecascade activeert. Connexine hemikanalen vormen een mogelijke loslatingsweg voor deze Ca^{2+} mobiliserende boodschappers.

Naast hun goed gekende rol in de propagatie van Ca^{2+} golven, is er ook meer en meer evidentie voor een mogelijke contributie van hemikanalen tot Ca^{2+} oscillaties. In deze thesis trachten we zulke bijdrage verder op te helderen. Ca^{2+} oscillaties worden aangedreven door positieve en negatieve feedback acties op InsP_3 receptor opening en Ca^{2+} vrijstelling uit het endoplasmatisch reticulum. Connexine hemikanalen zijn eveneens Ca^{2+} -permeabele kanalen wiens activiteit gecontroleerd wordt door $[\text{Ca}^{2+}]_i$. Net om deze reden kunnen ook hemikanalen actief bijdragen tot het oscillatie mechanisme. Met behulp van verschillende stimuli werden oscillaties opgewekt in geïmmortaliseerde en langdurig gecultiveerde, primaire cerebrale endotheelcellen die Cx37 en Cx43 tot expressie brengen. Ca^{2+} oscillaties die gestimuleerd werden door bradykinine werden onderdrukt door de connexine kanaal blokker carbenoxolone, door Cx37/Cx43 knockdown en door Gap27, een peptide dat specifiek Cx37/Cx43 kanalen blokkeert. Het effect van Gap27 was daarenboven snel (enkele minuten) wat pleit voor een bijdrage van hemikanalen en niet van gap juncties. Bradykinine-

gestimuleerde opening van hemikanalen werd onthuld met behulp van connexine-permeabele kleurstoffen. Verder konden we ook een bradykinine-getriggerde purinerge signaallus aantonen die bijdraagt tot de Ca^{2+} oscillaties. In tegenstelling tot bradykinine-geïnduceerde oscillaties konden oscillaties getriggerd door ATP niet geïnhibeerd worden door carbenoxolone of Gap27. In Madine Darby Canine Kidney (MDCK) cellen, die Cx32 en Cx43 tot expressie brengen, werden bradykinine-gestimuleerde oscillaties belemmerd door de connexine mimetische peptiden $^{32}\text{Gap27}/^{43}\text{Gap26}$ en Cx43 gensuppressie terwijl dit opnieuw geen effect had op oscillaties aangedreven door ATP. $^{32}\text{Gap27}/^{43}\text{Gap26}$ blokkeerden eveneens bradykinine-gestimuleerde vrijstelling van hemikanaal-permeabele kleurstoffen. Bovendien bleken bradykinine-gestimuleerde oscillaties afhankelijk van extracellulair Ca^{2+} terwijl deze aangewakkerd door ATP ongevoelig waren aan een vermindering van de extracellulaire Ca^{2+} concentratie (tot 0.5 mM). Het afzwakken van negatieve $[\text{Ca}^{2+}]_i$ feedback op de InsP_3 receptor (InsP_3R) door middel van cytochrome C (CytC) inhibeerde zowel bradykinine- als ATP-gestimuleerde oscillaties. Net zoals de InsP_3R worden Cx32 en Cx43 hemikanalen gestimuleerd door $[\text{Ca}^{2+}]_i < 500$ nM maar geïnactiveerd door hogere Ca^{2+} concentraties. Het CT9 peptide (laatste 9 aminozuren van het Cx43 C-terminale domein) voorkomt deze inactivatie door $[\text{Ca}^{2+}]_i > 500$ nM. In tegenstelling tot interferentie met de bimodale $[\text{Ca}^{2+}]_i$ -regulatie van InsP_3R , kon het CT9 peptide enkel bradykinine-geïnduceerde oscillaties verhinderen. Hemikanaal activatie/inactivatie op zich was onvoldoende om oscillaties te stimuleren, maar hun contributie tot het oscillatie mechanisme staat buiten kijf aangezien het inhiberen van deze kanalen Ca^{2+} oscillaties voorkomt.

Repetitieve wijzigingen in $[\text{Ca}^{2+}]_i$ zijn algemeen bekend als de drijvende kracht achter verschillende cellulaire processen. Er is echter weinig gekend betreffende het effect van $[\text{Ca}^{2+}]_i$ oscillaties/golven op de functie van de bloed-hersenbarrière (BHB). Deze barrière is aanwezig tussen de systemische circulatie en de hersenen en beschermt het hersenweefsel tegen potentieel toxische, circulerende substanties terwijl ze ook een gespecialiseerde omgeving creëert waarin neuronale signalisatie optimaal kan verlopen. De BHB wordt opgebouwd uit capillaire endotheelcellen die gekenmerkt worden door een extreem lage pinocytotische activiteit wat resulteert in een sterk gelimiteerde transcyclulaire toegang tot het hersenweefsel. BHB endotheelcellen vertonen bovendien een zeer hecht en complex netwerk van intercyclulaire juncties dat, geholpen door het actine cytoskelet, verantwoordelijk is voor een restrictie van de paracyclulaire permeabiliteit. Deze laatste is het onderwerp van menig onderzoek aangezien een verhoogde paracyclulaire permeabiliteit frequent geassocieerd wordt

met diverse pathologieën van het centraal zenuwstelsel en aanleiding geeft tot hersenoedeem en inflammatie.

In tweede instantie trachtten we een functionele link aan te tonen tussen connexine-dependente Ca^{2+} signalisatie (oscillaties en golven) enerzijds en de werking van de BHB anderzijds. Hierbij besteedden we bijzondere aandacht aan de effecten van hemikanaal-aangedreven Ca^{2+} oscillaties op (BHB) endotheliale permeabiliteit. Bradykinine induceerde Ca^{2+} oscillaties in geïmmortaliseerde en langdurig gecultiveerde, primaire BHB endotheelcellen en daarbij observeerden we ook een verhoogde endotheliale permeabiliteit. Deze permeabiliteitsverhoging kon tegengegaan worden door intracellulaire Ca^{2+} wijzigingen te verhinderen met behulp van BAPTA. Dit impliceert een cruciale rol van Ca^{2+} oscillaties in de permeabiliteitswijzigingen. Daarenboven konden zowel *in vitro* als *in vivo* permeabiliteitswijzigingen geïnhibeerd worden door Gap27. ATP, dat hemikanaal-ongerelateerde oscillaties induceert, had geen effect op de endotheliale permeabiliteit. Alteraties op het niveau van de tight junctie-eiwitten occludine en ZO-1 konden niet worden aangetoond, maar modificaties in de structuur van het intermediaire filament vimentine bleken geassocieerd met de permeabiliteitsverhoging. Deze modificaties konden opnieuw worden tegengegaan met Gap27 en waren niet aanwezig in cellen blootgesteld aan ATP. Intercellulaire Ca^{2+} golven konden opgewekt worden in BHB endotheelcellen door een vermindering van de extracellulaire Ca^{2+} concentratie. Deze golven bleken eveneens geassocieerd met een toegenomen permeabiliteit en beiden werden opnieuw verhinderd door BAPTA, wat een cruciale rol voor $[\text{Ca}^{2+}]_i$ wijzigingen impliceert, en door de connexine kanaal inhibitor Gap27. Hoewel het aantal oscillerende cellen bij blootstelling aan bradykinine niet verschillend was van het aantal cellen dat participeert in laag extracellulair Ca^{2+} -geïnduceerde Ca^{2+} golven, was de toename in permeabiliteit veroorzaakt door bradykinine beduidend lager dan de toename die volgt op een verlaging van de extracellulaire Ca^{2+} concentratie. Dit suggereert dat intercellulaire Ca^{2+} golven efficiënter zijn in regulatie van de barrièrefunctie. Proteïne kinase C, Ca^{2+} /calmoduline-dependente kinase en actomyosine contracties dragen bij tot de laag Ca^{2+} -geïnduceerde permeabiliteitswijzigingen, maar niet tot de door bradykinine opgewekte wijzigingen.

Uit onze data blijkt dat hemikanalen bijdragen tot het bradykinine-geïnduceerde oscillatie mechanisme. Deze bijdrage bestaat uit Ca^{2+} influx en/of vrijstelling van ATP dat een autocriene, purinerge signaallus activeert. Hemikanaal-dependente Ca^{2+} oscillaties hebben

daarenboven een fysiologische impact op de werking van de BHB. Daarnaast propageren intercellulaire Ca^{2+} golven met behulp van connexine hemikanalen en/of gap juncties naar naburige endotheelcellen. Deze Ca^{2+} golven resulteren in meer uitgesproken alteraties in BHB permeabiliteit. Op dit moment bestaan er geen tools om BHB opening te verhinderen en ons werk toont aan dat endotheliale connexine kanalen een potentieel doelwit vormen om een verhoogde permeabiliteit van de BHB tegen te gaan.

Chapter 1

Introduction

1.1 PREFACE

Over 50 % of the worldwide population is at risk for developing a central nervous system (CNS) disorder [Cardoso et al., 2010]. These diseases can be largely classified in pathologies with a primary vascular or primary neuronal origin. In the former, endothelial cells can directly affect neuronal and synaptic functions through changes in blood flow and function of the blood-brain barrier (BBB), an endothelial interface that strictly controls all passage to and from the brain. In the other case, vascular abnormalities are secondary to neuronal malfunctioning, yet they can further contribute to the progression of the disease. Stroke is an example with an indisputable vascular origin whereas for Alzheimer's disease and Parkinson's disease a neuronal origin is more or less accepted. However, for other CNS disorders, like epilepsy and multiple sclerosis, the cause is less clear. In Alzheimer's and Parkinson's disease, changes in BBB morphology and function, including fragmentation of vessels, redistribution of interendothelial junctions and reduced activity of transporters, have been revealed whereas multiple sclerosis is associated with increased transport of activated T-cells across the BBB [Oby and Janigro, 2006; Stamatovic et al., 2008; Zlokovic, 2008]. Further elucidation of the nature of pathological events at the BBB is part of understanding how these diseases progress and therapeutically useful targets may be found. However, there's another side to the story: due to the BBB's unique properties, most (~98%) drugs are incapable of entering the brain, therefore, there is only a limited number of therapeutics available for treatment of brain disorders [Cardoso et al., 2010]. A better knowledge of BBB physiology can thus not only learn us more on the pathological events occurring at this level, it can also identify novel routes for drug delivery to the CNS. In this thesis we focus on the role of Ca^{2+} signaling and connexin channels in regulation of BBB permeability. Connexin channels are well known for their role in intercellular Ca^{2+} signaling. Furthermore, several lines of evidence indicate altered Ca^{2+} homeostasis and/or signaling in ageing and in different neurodegenerative diseases including Alzheimer's and Parkinson's disease [Bezprozvanny, 2009]. Thus, Ca^{2+} regulation of barrier function and the contribution of connexins therein may improve our insights in the role of BBB disturbances associated with these diseases. Recently, connexin channels have been identified as part of the interendothelial junctional complex, [Nagasawa et al., 2006], placing them at the correct position for influencing barrier permeability. To keep a clear overview, the introduction will embark on the common

knowledge on cell-cell communication and connexin channels before proceeding to basic Ca^{2+} signaling mechanisms and the role of Ca^{2+} signaling in BBB regulation.

1.2 CELL-CELL COMMUNICATION: GAP JUNCTIONS AND HEMICHANNELS

The appearance of multicellular organisms in evolution has led to the necessity of a system that harmonizes increasingly large cell populations, establishing a biochemical and electrical syncytium that is of utmost importance in tissue homeostasis. Therefore, a typical feature of these organisms is their capacity to endure direct communication between neighboring cells, coordinating and synchronizing cellular responses to external stimuli. Cell-cell coupling in the different *regna* emerged independently and are mediated by structurally distinct plasmodesmata (*plantae*), septal pores (*fungi*) or gap junctions (*metazoa*) [Barbe et al., 2006]. The latter are aqueous channels that are unique in that they span the intercellular cleft, allowing the direct exchange of ions, metabolites and second messengers between the cytoplasm of two coupled cells. Gap junction channels are assembled by the docking of two half gap junction channels, known as connexons or hemichannels, that are composed of 6 connexin proteins [Bruzzone et al., 1996]. Connexin hemichannel docking occurs in specialized plasma membrane regions termed ‘gap junction plaques’ which can be found in nearly all mammalian cell types and which coordinate different functions like development, differentiation, synchronization of electrical signals in the heart, smooth muscle contraction, metabolism, neuronal signal transmission, pattern formation during development, oncogenic transformation and growth control [Bruzzone et al., 1996; Kumar and Gilula, 1996].

During the last two decades it became increasingly clear that unapposed connexin hemichannels are more than mere gap junction precursors. They can, by themselves, form a strictly regulated conduit between the cytoplasm and the extracellular environment. Due to their rather large permeability, it was originally believed that these channels remain in a closed state until they dock with apposed hemichannels. Keeping hemichannels closed would prevent cell death caused by the loss of essential metabolites, energy sources and diffusible second messengers, and the collapse of ionic gradients. The latter will result in a loss of membrane potential and abolish normal transport functions. Indeed, a first report highlighting the existence of active hemichannels indicated that transfection of oocytes with Cx46, a connexin isotype that forms hemichannels which are open at physiological membrane

potentials, resulted in massive cell death [Paul et al., 1991]. In contrast, brief and controlled opening of connexin hemichannels does not lead to cell loss, suggesting that cells can at least cope with some degree of connexin hemichannel opening [Stout et al., 2002]. Connexin hemichannel activity can be regulated by Ca^{2+} , voltage, pH, redox potential and post-translational modifications (see 1.2.3: ‘Gating of connexin channels’). Although it was originally believed that hemichannel opening was merely an artefact, observed in exogenous expression systems where the protein is forced into an environment that normally not supports the presence of connexin channels, this is contested now by evidence of endogenous connexin hemichannels that are sensitive to the intracellular ($[\text{Ca}^{2+}]_i$) and extracellular ($[\text{Ca}^{2+}]_e$) Ca^{2+} concentration, free radicals, intracellular redox potential [Ramachandran et al., 2007; Retamal et al., 2006; Retamal et al., 2007a; Retamal et al., 2007b], metabolic inhibition [Contreras et al., 2002] or ischemia [Bargiotas et al., 2009], and mechanical stimulation or fluid flow shear stress [Siller-Jackson et al., 2008]. Connexin hemichannel function has been implicated in primary cells (glia [Hofer and Dermietzel, 1998; Retamal et al., 2007a], leukocytes [Eltzschig et al., 2006], retinal horizontal cells [DeVries and Schwartz, 1992], ventricular cardiomyocytes [Shintani-Ishida et al., 2007], taste cells [Romanov et al., 2007], monocytes [Wong et al., 2006] and neutrophils [Eltzschig et al., 2006]), organotypic slices from cochlea [Anselmi et al., 2008], medulla oblongata [Huckstepp et al., 2010], spinal cord [O’Carroll et al., 2008] and hippocampus [Stridh et al., 2008], in the isolated heart [Hawat et al., 2010] and recently also the brain *in vivo* [Davalos et al., 2005]. Although the role of connexin hemichannel function remains to be resolved they have been implicated in Ca^{2+} signaling (see 1.3 ‘ Ca^{2+} homeostasis and Ca^{2+} signaling’), ephaptic signaling [Kamermans et al., 2001], central chemoreception [Huckstepp et al., 2010], development of atherosclerotic plaques [Wong et al., 2006], astrogliosis [O’Carroll et al., 2008] and propagation of cell death [Decrock et al., 2009]. Thus far, *in vivo* hemichannel activity has mainly been identified in the nervous tissue. Microgliosis, *i.e.*, the accumulation of activated microglia in brain tissue is a hallmark of many neurodegenerative diseases [Takeuchi et al., 2011]. The microglial cells appear to be guided to the site of brain injury by an extracellular ATP gradient that originates from laserlight-ablated cortical astrocytes. Because this gradient was abolished by application of the connexin channel inhibitors carbenoxolone and flufenamic acid (see 1.2.5 ‘Pharmacological properties of connexins and pannexins’), it was suggested that it results from hemichannel-mediated ATP release [Davalos et al., 2005; Kim and Dustin, 2006]. In addition, blockade of exuberant hemichannel-mediated glutamate release from activated microglia has been shown to suppress disease progression in mouse models of amyotrophic

lateral sclerosis and Alzheimer's disease [Takeuchi et al., 2011]. Inhibition of hemichannels also improves recovery of brain activity and reduces seizure size following ischemia [Davidson et al., 2012]. Finally, preliminary data reveal enhanced hemichannel dye uptake in astrocytes from two murine models of Alzheimer's disease [Mei, 2010]. The following paragraphs will sketch important findings on connexin channel structure and gating.

1.2.1 THE CONNEXIN PROTEIN FAMILY

The structural protein subunits of hemi- and gap junction channels were named connexins (Cx) as they form channels that physically connect adjacent cells [Beyer et al., 1987]. To date, 21 connexin isoforms have been identified in the human genome (**figure 1**) and for most of them orthologs are present in other mammals.

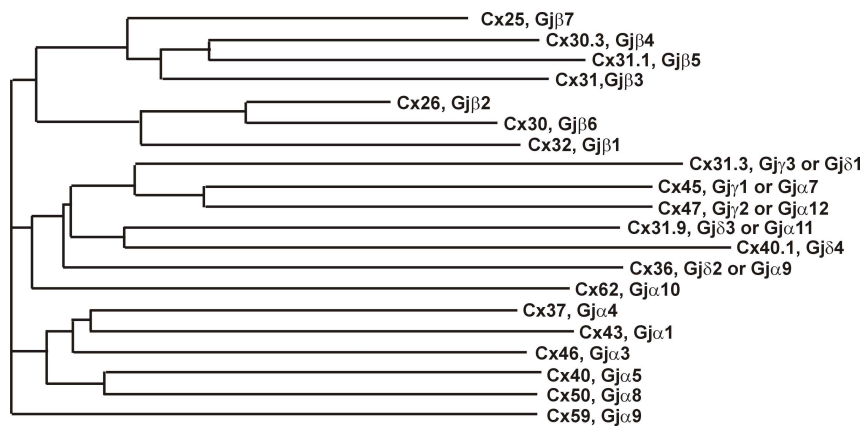


Figure 1. Evolutionary relationship between the different human connexins. The phylogram shows alignments of human connexin protein sequences that reveal varied degrees of similarity among the connexin isoforms. The different connexins are denoted by the two current nomenclatures. Figure adapted from [Alexander and Goldberg, 2003].

Two adequate nomenclatures are currently in use to designate the different connexin isoforms. A rather accepted manner of naming connexins depends on the species from which they were derived and on their molecular mass. A connexin is thus named aCx_B with the prefix a describing the species and the suffix B giving the predicted molecular weight in kDa; hCx43 for example, is a human connexin of approximately 43 kDa [Beyer et al., 1987]. An alternative manner of classifying connexins is to categorize connexins into subfamilies with respect to their degree of sequence homology and length of the cytoplasmic domains. Connexins are then denoted Gj x y with Gj standing for gap junction protein, x representing the

subfamily (α , β , γ , δ) and γ giving a serial number describing their order of discovery [Sohl and Willecke, 2003; Sohl and Willecke, 2004]. This nomenclature is mostly used for the corresponding gene names. To give an example, Cx43 is also known as Gj α 1 (or GJA1 according to its gene name is *Gjal*) as it was the first one to be discovered in the α -group. Because for some connexins there is no consensus yet on their classification, these connexins are designated by two names, until further notice.

1.2.1.1 Molecular characterization of connexin-based channels

Hydropathy plots reveal that all connexin proteins share a common topology, displaying four hydrophobic, α -helical transmembrane domains (M1-4) that are connected by two extracellular loops (EL1 and EL2) and one cytoplasmic loop (CL). The carboxyterminal (CT) and aminoterminal (NT) regions are facing the cytoplasm (**figure 2**). The best conserved protein regions are the extracellular loops and the transmembrane domains, whereas the CT- and CL-regions show marked divergence [Peracchia and Wang, 1997; Saez et al., 2003; Willecke et al., 2002; Yeager and Nicholson, 1996]. Six connexin proteins oligomerize into a connexin hemichannel. General features of the pore of each hemichannel include a funnel-like shape with a wide vestibule located on the cytoplasmic end, pronounced narrowing of the pore at the membrane borders and again a discrete widening in the region of the intercellular gap [Yeager and Harris, 2007]. There is no consensus yet on what residues line the channel pore. M1 is the only amphipatic transmembrane domain and was therefore believed to line the inner pore. However, others put M3 forward as the pore lining element. This is also supported by the recently discovered crystal structure of Cx26 [Bruzzone et al., 1996; Maeda et al., 2009; Peracchia and Wang, 1997; Yeager and Nicholson, 1996]. Then again, mutagenic and structural studies emphasize the possibility of two α -helices lining the inner pore wall [Unger et al., 1999; Zhou et al., 1997]. Analysis of Cx32 defined M3 as the major pore-lining unit, with M1 and M2 contributing to the wider segment of the pore that faces the cytoplasm [Skerrett et al., 2002]. M4 is located at the perimeter of the pore [Yeager and Harris, 2007]. The N- and C-terminal domains are important for channel gating [Kyle et al., 2009; Maeda et al., 2009] (see 1.2.3: ‘Gating of connexin channels’). Three-dimensional maps of Cx26 hemichannels show a ‘plug’ in the centre of the pore that physically blocks the channel, but it remains undetermined whether this plug is constituted by C-terminal, N-terminal or CL domains [Oshima et al., 2007].

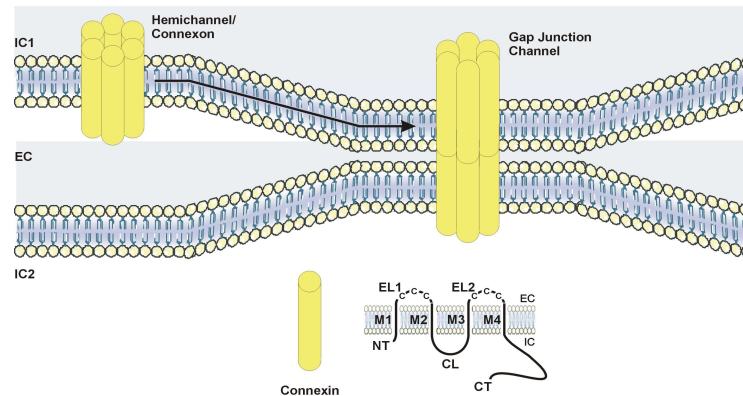


Figure 2: Molecular architecture of connexin channels and connexin topology. All connexins share a common topology: 4 α -helical domains (M1-4) span the plasma membrane and are connected by two extracellular loops (EL1 and EL2) and one cytoplasmic loop (CL). Both the C- and N-terminal domains are facing the cytoplasm (IC). Six of these connexins oligomerize into a connexon or connexin hemichannel and two of such ‘half’ channels diffuse to gap junction plaques where they dock head-to-head with an apposed hemichannel from a neighboring cell to form a gap junction channel. This figure was produced using Servier Medical Art.

1.2.1.2 The connexin life cycle

Connexin subunits are co-translationally integrated into the rough endoplasmic reticulum (ER) membrane where they adapt their native transmembrane configuration [Falk, 2000]. The subsequent oligomerization of the connexin subunits into a hemichannel starts in the ER and progresses in the Golgi apparatus [Das Sarma et al., 2002; He et al., 2005; Laird, 2006; Musil and Goodenough, 1993; Thomas et al., 2005; Vanslyke et al., 2009]. From there, vesicles with pre-formed hemichannels are transported along microtubules to the cell surface and inserted into the plasma membrane (**figure 3**). Biotinylation assays have estimated that connexin hemichannels in the plasma membrane constitute approximately 4-15% of the total cellular connexin protein amount [Musil and Goodenough, 1991; Retamal et al., 2006; Sanchez et al., 2009]. The connexin hemichannels can be traced back in the plasma membrane as small aggregates at sites of unapposed plasma membranes [Dermietzel et al., 2003; Lal et al., 1995; Segretain and Falk, 2004]. Eventually they will diffuse in the plane of the membrane towards the outer margins of gap junction plaques where they dock head-to-head with apposing hemichannels [Bruzzone et al., 1996; Falk, 2000; Gaietta et al., 2002]. Gap junction plaques in the plasma membrane are characterized in freeze-fracture microscopy by clusters of condense membrane particles on the plasma membrane with central depressions

corresponding to the channel pores. The plaques contain from less than a dozen to up to 200,000 units and may extend from several nanometers to a few micrometers in diameter [Bruzzone et al., 1996; Evans and Leybaert, 2007; Falk, 2000].

Docking of two connexin hemichannels to form a gap junction channel depends on non-covalent interactions that are sufficiently strong to keep the channel sealed and prevent leakage into the extracellular environment [Dahl et al., 1991; Foote et al., 1998; Maeda et al., 2009; Oshima et al., 2007; Rackauskas et al., 2010; Sosinsky and Nicholson, 2005]. The conserved amino acid motifs QPG and SHVR in EL1 and SRPTEK in EL2 are involved in hemichannel docking [Bruzzone et al., 1996; Warner et al., 1995], yet a true interaction between apposed motifs has not been shown thus far. Although the extracellular loops are highly homologous, not all connexin hemichannels will pair with one another. As much as the primary sequence seems to play a role in connexin hemichannel docking, the spatial relationships of individual residues, which are equally important for gap junction channel formation, are dictated by the tertiary structure of the extracellular loops [Foote et al., 1998]. The extracellular loops are characterized by conserved patterns that contain three cysteine residues at identical positions in all known connexin proteins (CX₆CX₃C in EL1 and CX_{4/5}CX₅C in EL2). Intramolecular disulfide bridges in and between the loops stabilize their tertiary structure [Bruzzone et al., 1996; Dahl et al., 1991; Foote et al., 1998; Sohl and Willecke, 2004]. Different mutagenic studies have emphasized a role for the cysteine residues in determining the tertiary structure of the loops and either substitution of individual cysteine residues by serine [Dahl et al., 1992] or interloop switching of the cysteines caused a distortion in normal loop folding and compromised channel function [Foote et al., 1998]. Based on these observations, a model was proposed in which the extracellular loops of each connexin interdigitate with the extracellular loops of an apposed hemichannel [Foote et al., 1998].

Once formed, gap junction channels move laterally towards the centre of the plaque where the oldest channels are internalized [Gaietta et al., 2002]. By budding off whole pieces of the plaque, the plasma membranes of both cells are internalized. These double-membraned gap junction-containing vesicles are known as annular gap junctions or connexosomes [Laird, 2006] and are degraded via the lysosomal [Qin et al., 2003] or proteasomal network [He et al., 2005; Musil et al., 2000; Saez et al., 2003] (**figure 3**). It is currently unknown if all hemichannels become incorporated into gap junctions before degradation or whether channels

with a hemichannel ‘fate’ and gap junction ‘fate’ follow distinct recycling pathways. Connexins have a relatively short half-life (1-6 hours) [Herve et al., 2007; Segretain and Falk, 2004] and hemichannels are thus continuously synthesized, trafficked to the plasma membrane, assembled into gap junctions, internalized and degraded again. This constant aggregation and degradation of gap junctions likely provides a means to rapidly tune cell-cell communication in response to environmental changes [Rackauskas et al., 2010].

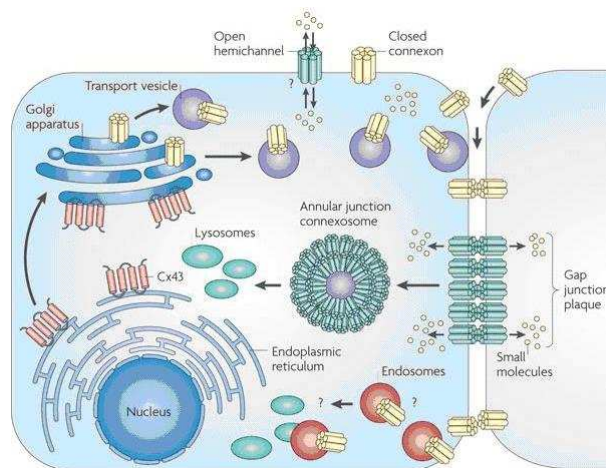


Figure 3. The connexin life cycle. The figure displays the life cycle of Cx43, the most common connexin in the human body. Connexins acquire their tertiary structure in the ER and oligomerize into hemichannels while trafficking through the Golgi apparatus. After transport to the cell surface, connexin hemichannels can function as strictly regulated channels that allow the exchange of small molecules between the cytoplasm and the extracellular environment. Subsequently, hemichannels dock with their adjacent counterparts from a neighboring cell to form gap junction channels that aggregate into gap junction plaques. Gap junctions internalize into annular junctions or connexosomes before degradation via the lysosomal and/or proteasomal pathway. Figure adapted from [Naus and Laird, 2010].

Connexins are expressed in an overlapping spatio-temporal and cell-type specific pattern. As tissues express different connexins, hemichannels can be either homomeric (6 identical connexins) or heteromeric (different connexins isoforms) (**figure 4**). The assembly of connexins into heteromeric connexin hemichannels is not *ad random* but occurs only when connexin isotypes are compatible with each other. Exactly how this compatibility is achieved is still a question mark, but 3 hypotheses have been put forward: *i*) non-compatible connexins are synthesized in different ER-regions and never come into physical contact with one another, *ii*) specific chaperones bind to compatible connexins, regulating their interaction and *iii*) specific compatibility signals are encoded into the connexin polypeptide sequence. These include an ‘assembly signal’ embedded in M3 that allows connexins to recognize each other

and an N-terminal ‘selectivity signal’ that determines compatibility [Falk et al., 1997; Segretain and Falk, 2004]. Furthermore, all heteromeric hemichannels thus far identified, are composed of two members of the same subgroup (α or β). In analogy to connexin hemichannels, gap junction channels can be either homo- or heterotypic, the former consisting of 2 identical hemichannels and the latter containing two different ones. Theoretically there are 196 possible types of gap junction channels, formed out of the 21 human connexins identified [Bukauskas and Verselis, 2004]. However, like the compatibility requirement in heteromeric hemichannels, the formation of heterotypic channels strictly depends on the expression of congruent connexins [Elfgang et al., 1995]. Construction of chimeric connexins with swapped EL domains indicated that such compatibility is determined by EL2 [White et al., 1994] though the detailed mechanisms of hemichannel docking are highly complex and remain uncharacterized.

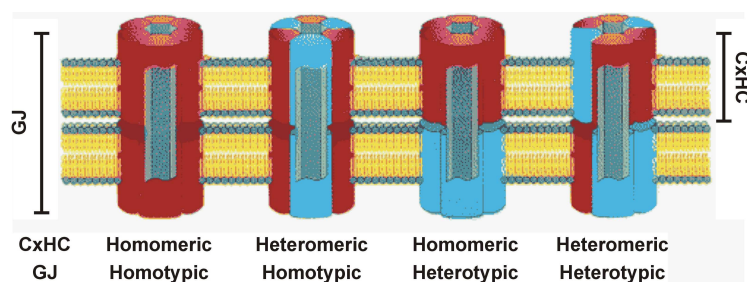


Figure 4. Different types of hemi- and gap junction channels. Connexin hemichannels (CxHC) can contain six identical or different connexin proteins, forming homo- or heteromeric channels respectively. Gap junction channels from their part can be composed of two identical or two different hemichannels, constituting homo- and heterotypic channels. Figure adapted from [Kumar and Gilula, 1996].

1.2.2 PERMEABILITY AND PORE SELECTIVITY OF CONNEXIN CHANNELS

More than anything, connexin permeability and selectivity are at the core of connexin channel function. Although historically, gap junctions have been portrayed as non-specific intercellular pores, recent developments in the field have demonstrated that connexin channels are unique in terms of their conductance, gating and permeability to specific molecules. It is becoming increasingly clear that connexin composition strongly influences the diffusion of molecules through the pore, and that passage is subject to size, charge and shape of the permeant, as well as to the effective pore size of the channel and the affinities between the pore wall and the permeants. A conceptually simple approach to study channel permeability is

to introduce a tracer molecule into a cell and observe whether it moves towards adjacent cells. These tracers must be hydrophilic enough to prevent direct transfer through the plasma membrane and they must be small enough to fit the aqueous pore of gap junction channels [Alexander and Goldberg, 2003]. Indeed, size is clearly one factor in the discrimination of molecules by different connexin channels. The general consensus is that gap junctions and connexin hemichannels are permeable to molecules with molecular weights (MWs) < 1.5 kDa or 1.5 nm in diameter [Loewenstein, 1981]. Based on work with dyes of different MW, it was estimated that Cx32 and Cx43 form the largest channels, that Cx26, Cx40 and Cx45 channels have smaller pores and that Cx37 and Cx46 are the most restrictive [Gong and Nicholson, 2001; Harris, 2007; Sosinsky and Nicholson, 2005; Weber et al., 2004]. Size-exclusion of dyes can become even more complex considering heteromeric and heterotypic channels. The latter appear to have selectivities that are intermediate between their homotypic counterparts and are dominated by the more restrictive hemichannel [Goldberg et al., 2004; Heyman et al., 2009; Weber et al., 2004]. Still, permselectivity is not based on size alone; charge is another important determinant for connexin channel permeability. The degree of selectivity is not inversely correlated with unitary conductance, that is, selectivity is not necessarily greater in channels with smaller conductances [Harris, 2001]. While they vary widely in unitary conductances (see 1.2.3.1 'voltage gating'), most connexins display the same sequence of cation selectivity [Goldberg et al., 2004; Wang and Veenstra, 1997]. Still, connexins can be subdivided according to their selectivity to cations or anions. For instance, Cx26, Cx40, Cx45, Cx46 and Cx50 are permeable to cations whereas their anion permeability is low [Beblo and Veenstra, 1997; Eskandari et al., 2002; Sanchez et al., 2010; Trexler et al., 1996]. Cx32 is preferentially permeable to anions [Bennett et al., 2003; Bukauskas and Verselis, 2004; Contreras et al., 2002] whereas Cx43 is poorly charge selective, exhibiting equal permeability to both negatively and positively charged molecules [Bennett et al., 2003; Contreras et al., 2002].

The molecular basis of charge selectivity is unknown but possibly implicates the presence of an electrostatic field associated with the channel pore [Beblo and Veenstra, 1997; Harris, 2001; Wang and Veenstra, 1997]. Fixed negative charges in EL1 of Cx46 hemichannels result in a predominance of cations to reside in the pore [Trexler et al., 2000]. Substitution of each of these residues by a positively charged one severely reduces charge transfer across the channel [Kronengold et al., 2003]. Despite all, connexin channel selectivity is still not easily explained in terms of charge and size alone. It also relates to the permeating molecule's chemistry (shape, H-bonds, flexibility, hydration, etc.). Indeed, the channels allow differential

exchange of molecules that would not necessarily be expected from predictions of pore and charge selectivity but are likely based on cooperative interactions between the channel pore and the permeant molecules [Cao et al., 1998; Orellana et al., 2011a]. Such discrepancies are mostly observed when comparing connexin channel permeability with small, charged tracer dyes like Ethidium bromide (EtBr, 395 Da, +1), Propidium iodide (PI, 668 Da, +2), Lucifer Yellow (LY, 457 Da, -2) or DAPI (277 Da, +2).

While the differential permeabilities to these synthetic probes are instructive, the ultimate interest is to understand the selectivity towards natural permeants [Sosinsky and Nicholson, 2005]. Gap junctions and hemichannels allow the passage of inositol 1,4,5 trisphosphate (InsP₃) [Beltramello et al., 2005; Boitano et al., 1992; Gossman and Zhao, 2008], reactive oxygen species (H₂O₂) [Ramachandran et al., 2007], prostaglandins (PGE₂) [Siller-Jackson et al., 2008], glutamate [Parpura et al., 2004; Takeuchi et al., 2006; Ye et al., 2003], glutathione [Stridh et al., 2010], cAMP [Harris, 2008], ATP and its metabolites ADP, AMP and adenosine [Goldberg et al., 2002; Kang et al., 2008], and glucose [Harris, 2007; Retamal et al., 2007a] (**table 1**). Again, permeability to these molecules is hard to predict when only considering their size and charge. For instance, cGMP and cAMP, which are largely of the same size (~330-350 Da) and charge (-1), pass equally well through Cx32 channels, whereas Cx26:32 heteromeric channels are more permissive to cGMP than to cAMP [Bevans et al., 1998]. ATP passes more efficiently through Cx43 channels than through channels composed of Cx32, but calcein (623 Da, -4), which has about the same size and charge as ATP (507 Da, -4), diffuses better through Cx32 channels. These two examples could be explained by a different chemistry of the permeants that influences its interactions with the channel pore [Goldberg et al., 1999; Goldberg et al., 2002]. Such interaction has been shown for InsP₃ and Cx26. Beltramello et al. (2005) indicated that a point mutation in the M2 region of Cx26 (V84L) produced no change in ion or LY transfer but severely compromised the flux of InsP₃ (420 Da, charge -6) through the channel [Beltramello et al., 2005]. These data indicate a structural modification of the pore that somehow hinders the passage of InsP₃, but not of other molecules or ions. Finally, despite their larger size, siRNA and polypeptides pass through connexin channels as well. Cx43 gap junctions were shown to be permeable to synthetic and endogenous peptides in the range of 1-1.9 kDa. The transfer rate decreased with increasing size and only peptides exhibiting a linear conformation were permeable whereas circular peptides could not be transferred through the cell-cell junctions. This indicates that the tertiary structure of peptides determines their permeability through gap junctions [Neijssen et al.,

2005]. Cx43, but not Cx32 or Cx26 gap junctions were permeable to synthetic oligonucleotides that mimic endogenous siRNA and that have MW's approaching 4 kDa [Spray et al., 2006; Valiunas et al., 2005].

<u>Molecule</u>	<u>MW (Da)</u>	<u>Charge</u>
glutamate	147	-1
aspartate	171	-1
glucose	180	0
adenosine	267	0
cAMP	329	-1
sucrose	342	0
cGMP	345	-1
AMP	347	-2
InsP ₃	414	-6
ADP	427	-3
ATP	507	-4
glutathione	612	-1
NAD ⁺	741	+1
Peptide	1000-1900	n.a.
RNA	4000	n.a.

Table 1. Connexin channel permeability to biologically relevant molecules. Overview of second messengers and other biologically relevant molecules that are permeable to connexin channels. The net-charge indicated is at neutral pH. The table is based on findings reported in [Harris, 2007]. 'n.a.': no data available.

1.2.3 GATING OF CONNEXIN CHANNELS

Changes in transjunctional voltage, intracellular acidification and an increase in $[Ca^{2+}]_i$ generally cause uncoupling of gap junctions, isolating damaged cells and protecting their healthy neighbors. Uncoupling occurs without any detectable change in the integrity of the gap junction plaque. Gap junctions thus close while they are still present in the plasma membrane, before being internalized. This closure can be ascribed to either conformational changes, intrinsic to the connexins, or to associated adaptor molecules that induce channel gating. Gating implies a fast and reversible molecular transition that leads to the complete opening or closure of a channel, or at least results in a relative change in the channel's conductive properties. The extent of electrical coupling (G_j) is dependent on the product of 3 gating parameters: $G_j = \gamma_j \times P_o \times N$. The unitary conductance γ_j denotes the channel's individual permeability to ions. The open probability P_o (ranging from 0 to 1) describes the

fraction of the total time a channel spends in the open configuration. Experimental determination of the mean open time (MOT) and mean closed time (MCT) will allow calculation of P_o through the formula $P_o = \text{MOT}/(\text{MOT}+\text{MCT})$. For a yet unknown reason, gap junction channels have a very low P_o (~0.1) [Bukauskas et al., 2000]. Finally, N stands for the number of channels; however, this is not a true gating parameter as assembly/disassembly does not imply a fast process nor does it suggest a molecular change in the channel structure. Similar to electrical coupling, dye coupling can be expressed as $\text{Perm} \times P_o \times N$ with ‘Perm’ reflecting the permeability of the channel to a dye of interest [Cottrell et al., 2003; Herve et al., 2007; Moreno and Lau, 2007].

1.2.3.1 Voltage gating

The ease by which ions pass a single gap junction channel is known as the junctional conductance G_j (expressed in picosiemens, pS) and is sensitive to the voltage difference between two paired cells, a.k.a. the transjunctional voltage (V_j). For homotypic junctions, G_j reaches its maximum when V_j is ~0 mV (i.e. when the transmembrane potentials V_m of the apposed cells are equal) and decreases to a residual substate (10-30% of the maximal G_j) symmetrically with both positive and negative V_j values [Bukauskas et al., 2001; Hoang et al., 2010]. Monitoring of single channel activity in intact cells has indicated that G_j values vary depending on the connexin subtype and that the unitary conductance of connexin hemichannels (γ_j) approximates the double value of that of homotypic gap junction channels, as predicted from a simple series arrangement of the hemichannels. Values for connexin hemichannel conductances vary from 20 pS for Cx31.9 [Bukauskas et al., 2006] to ~600 pS for Cx37 [Wang et al., unpublished observations] (**table 2**).

Voltage gating of the different connexins varies widely in terms of polarity, voltage sensitivity and kinetics. Many different V_j gating phenotypes exist, and this complexity progresses even further with the existence of heterotypic and heteromeric channels [Gonzalez et al., 2007]. Generally stated, gap junctions are operative at inside negative potentials and close when depolarization in one of the apposed cells generates a change in V_j , but they are largely insensitive to changes in V_m . In contrast, connexin hemichannels are highly sensitive to V_m : they remain preferentially ‘silent’ at inside negative potentials but are activated upon depolarization to positive ones by a slow (~10 ms) gating mechanism that resembles gating

transitions associated with the docking of extracellular loop domains; therefore slow gating is also referred to as loop gating [Bukauskas and Verselis, 2004; Gonzalez et al., 2006; Trexler et al., 1996; Verselis et al., 2009]. Loop gating is inherent to all connexin hemichannels and represents transitions between the fully open and closed states; in contrast, fast (1 ms) hemichannel gating involves transitions to residual substates. Fast gating can be activated by either positive or negative potentials; consequently, the voltage behaviour of connexin hemichannels can be either uni- or bipolar. For bipolar hemichannels, currents will increase with depolarization (slow gate), but will then decrease to substates (fast gating) when inside potentials become positive. For unipolar connexin hemichannels, currents will continue to increase with depolarization, even when V_m is in the positive range [Gonzalez et al., 2007; Valiunas, 2002].

Cx	GJ	CxHC	References
Cx31.9	9 pS	20 pS	[Bukauskas et al., 2006]
Cx36	15 pS	n.a.	[Srinivas et al., 1999]
Cx45	25 pS	57 pS	[Valiunas, 2002; Veenstra et al., 1994]
Cx57	30 pS	n.a.	[Manthey et al., 1999]
Cx32	50 pS	90 pS	[Gomez-Hernandez et al., 2003; Valiunas et al., 1999]
Cx47	55 pS	n.a.	[Teubner et al., 2001]
Cx43	50-110 pS	220 pS	[Contreras et al., 2003; Giaume et al., 1991]
Cx30	120-150 pS	283 pS	[Valiunas and Weingart, 2000; Yum et al., 2007]
Cx26	80-135 pS	300 pS	[Gonzalez et al., 2006; Suchyna et al., 1999; Yum et al., 2007]
Cx46	140 pS	300 pS	[Srinivas et al., 2005]
Cx40	198 pS	n.a.	[Bukauskas et al., 1995]
Cx50	220 pS	470 pS	[Srinivas et al., 2005]
Cx37	220 pS	600 pS	[Veenstra et al., 1994; Wang et al., unpublished observations]

Table 2. Unitary conductance of hemi- and gap junction channels, composed by different connexins.

Connexin hemichannels (CxHC) have single channel conductances varying between 20 pS and 600 pS. Gap junction channels (GJ) exhibit unitary conductances that are about half of those observed in their hemichannel counterparts. ‘n.a.’: no data available.

Connexin hemichannel opening/closure by the slow gating mechanism involves a movement of the M1-EL1 regions, resulting in a tilt of all six M1 domains and an increase/decrease of the pore diameter [Tang et al., 2009; Verselis et al., 2009]. Additionally, substitution of pore-lining residues in M1 abolished slow gating but left fast gating intact [Pfahnl and Dahl, 1999]. The N-terminal domain has also been implicated in slow gating as addition of green-

fluorescent protein (GFP) to the N-terminal domain prevented Cx43 hemichannel currents at positive V_m [Contreras et al., 2003]. Finally, slow gating transitions most likely represent concerted conformational changes in all 6 of the connexin hemichannel subunits whereas fast transitions reflect structural changes in single connexin subunits leading to rapid but incomplete closure [Bukauskas and Verselis, 2004; Oh et al., 2000]. The location of the fast gating voltage sensor still has to be determined. Residues in M2 [Ri et al., 1999; Suchyna et al., 1993], the N-terminal domain [Trexler et al., 1996; Verselis et al., 1994] and the C-terminus [Anumonwo et al., 2001; Bukauskas et al., 2001; Contreras et al., 2003; Maass et al., 2007; Moreno et al., 2002; Revilla et al., 1999] have been implicated in the fast V_j gating mechanism.

1.2.3.2 Chemical gating

1.2.3.2.1 pH gating

Lowering of the intracellular pH (pH_i) inhibits gap junctional communication in a dose dependent manner in nearly all cell types studied. Mild cytosolic acidification is a side effect of metabolic reactions (glycolysis and oxidative phosphorylation) and is intensified upon bursts of activity. Severe acidification occurs with ischemia, when oxygen is lacking and anaerobic energy production generates lactate, pyruvate and protons (H^+). A pH_i of 6.2 was measured in ischemic cardiac cells [Casey et al., 2010; Liu et al., 1993; Yao and Haddad, 2004]. Intracellular pH values that block gap junctions generally vary around 6 and are slightly different for the diverse connexin subtypes [Dakin and Li, 2006; Firek and Weingart, 1995; Liu et al., 1993; Wang and Peracchia, 1996]. Uncoupling by decreasing pH_i is rapid, practically coinciding with the onset of perfusion with acid-containing or CO_2 -saturated solutions [Spray et al., 1982; Trexler et al., 1999]. In addition, connexin hemichannels appear sensitive to the extracellular pH (pH_e) [Beahm and Hall, 2002; Ripps et al., 2004]. Most likely, H^+ ions enter the cell through activated hemichannels and closed them from the intracellular site in a similar way as gap junctions are closed by cytoplasmic H^+ [Beahm and Hall, 2002]. Therefore, the molecular mechanisms underlying the decrease in junctional communication and connexin hemichannel inhibition by low pH_i are probably of the same kind [Trexler et al., 1999]. Modulation of coupling could be due to direct connexin protonation [Spray et al., 1982; Trexler et al., 1999] or due to changes in $[Ca^{2+}]_i$ [Peracchia,

1990] and/or activation of calmodulin (CaM) [Peracchia et al., 2000]. Cytosolic Ca^{2+} levels increase upon acidification by the following mechanism: Na^+/H^+ exchangers are hyperactivated and Na^+ accumulates in the cell, reversing $\text{Na}^+/\text{Ca}^{2+}$ exchange and increasing $[\text{Ca}^{2+}]_i$ [Casey et al., 2010]. Ca^{2+} gating of connexin channels is described further down this chapter; yet, the role of Ca^{2+} in pH_i -induced connexin channel closure is heavily debated as a $[\text{Ca}^{2+}]_i$ increase seems to occur only when acidification is rather large ($\text{pH}_i \sim 4$). When acidification is less severe ($\text{pH}_i \sim 6$) no $[\text{Ca}^{2+}]_i$ changes were observed although gap junctions were uncoupled [Abudara et al., 2001]. In favour for a direct effect of H^+ ions on connexin channels is the observation that gap junction uncoupling and hemichannel inactivation are very fast. Furthermore, even in inside-out membrane patches where the bathing solution mimics the intracellular environment but no cytosolic proteins are present, Cx46 hemichannels close upon lowering of the pH [Trexler et al., 1999]. Direct protonation of the Cx43 and Cx50 has been described as well [Beahm and Hall, 2002; Ek et al., 1994]. Furthermore, acidification induces a conformational change in the extracellular domains of Cx26 that reduces the channel entrance diameter and closed the pore [Yu et al., 2007]. Additionally, pH_i gating of connexins was explained by a ‘ball-and-chain’ or ‘particle-receptor’ model whereby the CT-domain acts as a pore blocking particle. Accumulation of positive charges in the CL domain leads to a conformational change guiding the negatively charged C-terminal end to the channel vestibule where it occludes the hydrophilic pore [Ek et al., 1994; Ek-Vitorin et al., 1996; Liu et al., 1993; Peracchia and Wang, 1997; Seki et al., 2004]. This ball-and-chain model is thus far only applicable to Cx37, Cx40, Cx43 and Cx50 [Ek-Vitorin et al., 1996; Stergiopoulos et al., 1999] but not to Cx32 [Liu et al., 1993], Cx45 [Stergiopoulos et al., 1999] or Cx46 [Eckert, 2002; Trexler et al., 1999]. As C-terminal truncated Cx43 exhibits some residual sensitivity to pH_i , there must be an additional, yet unknown, pH sensor, upstream of this domain [Liu et al., 1993].

1.2.3.2.2 Channel gating by post-translational modifications

Post-translational modifications of connexins affect preferentially amino acid residues located in the C-terminal domain and include palmitoylation (addition of $\text{CH}_3(\text{CH}_2)_{14}\text{COOH}$), myristoylation (addition of $\text{CH}_3(\text{CH}_2)_{12}\text{COOH}$), S-nitrosylation, protease cleavage and phosphorylation. So far, no connexins are known to be glycosylated and there are no consensus sequences for glycosylation in the connexin extracellular domains [Bennett et al., 2003]. For most of these modifications, no clear role has been identified yet [Saez et al.,

2010]. S-nitrosylation has been observed in Cx43 hemichannels that are activated upon addition of NO or by metabolic inhibition [Retamal et al., 2006]. This common protein modification occurs in situations of oxidative stress and is characterized by the covalent attachment of a nitric oxide (NO) group to the thiol side chain of cysteine and nitration of tyrosine by peroxynitrite (ONOO⁻), the product of NO reaction with superoxide. S-nitrosylation of Cx43 takes part on 3 C-terminally located cysteine residues, creating an S-nitrosothiol (R-SNO) group. Cysteines in EL1/2 were not affected. As connexin hemichannel activation was fast and no increase in the surface level of connexin hemichannels was observed, most likely, S-nitrosylation increases the open probability or the unitary conductance of these channels.

Of all protein modifications, connexin phosphorylation is best characterized. Most of the connexin proteins are phosphoproteins containing different kinase consensus phosphorylation sites. Connexin phosphorylation is visualized by the direct incorporation of radioactive ³²P or by a shift in the electrophoretic mobility when analyzed by denaturing gel electrophoresis. Various connexins demonstrate multiple electrophoretic isoforms including a faster migrating, non-phosphorylated (NP) form, and at least two slower migrating forms, commonly termed P1 and P2 [Lampe and Lau, 2004; van Veen et al., 2000]. After treatment with alkaline phosphatase, P1 and P2 bands collapse to the faster migrating NP band, suggesting that phosphorylation is the primary post-translational modification detected by gel electrophoresis [Solan and Lampe, 2007; Solan and Lampe, 2009]. The C-terminal region appears to be the primary target region for different classes of kinases though some of the connexins (Cx36 and Cx56) can be phosphorylated in the cytoplasmic loop as well. Up to today, the N-terminal domain has never been identified as a target for kinases in any of the connexins studied [Lampe and Lau, 2004; Solan and Lampe, 2009]. The majority of phosphorylation events occur on serine residues but tyrosine phosphorylation is abundant as well. Kinases that are implicated in connexin phosphorylation include cAMP-dependent protein kinase (PKA), cGMP-dependent kinase (PKG), protein kinase C (PKC), Ca²⁺/CaM-dependent kinase II (CaMKII), the Rous sarcoma virus v-Src, cellular c-Src, casein kinases, mitogen-activated protein kinase (MAPK) and cyclinB/p34^{cdc2} [Kwak et al., 1995; Lampe and Lau, 2004] (**figure 5**). Various phosphatases, including PP1, PP2A, PP2B (calcineurin) and alkaline phosphatase are implicated in the gating of connexin channels [Herve and Sarrouilhe, 2002].

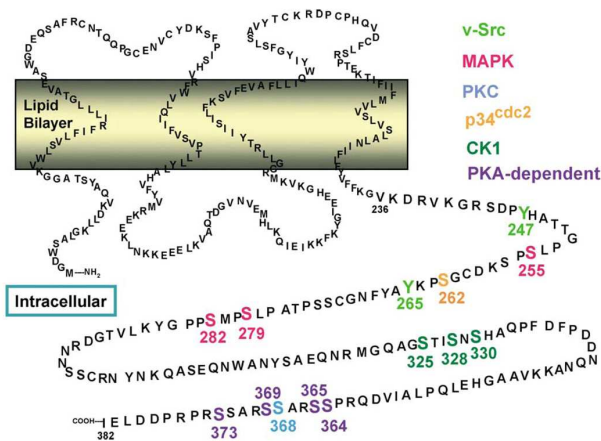


Figure 5. Consensus sites for different kinases in Cx43. Phosphorylation sites and corresponding kinases are represented in different colours. Most kinase target-sites are located in the C-terminal region [Lampe and Lau, 2004].

Both under basal and stimulated conditions, connexin channel activity appears to be regulated by ongoing phosphorylation-dephosphorylation events. Phosphorylation is implicated in trafficking from the cytosol to the plasma membrane and is essential for incorporation of connexin hemichannels into gap junction plaques [Solan and Lampe, 2007]; hence in both connexin hemichannels and gap junction channels, connexin subunits display at least some basal degree of phosphorylation. Presumably, the main reason for maintaining a basal phosphorylation state is to keep connexin hemichannels in a closed conformation [Lampe and Lau, 2004], both when they travel from ER and *trans*-Golgi towards the cell surface and when they are located inside the plasma membrane [Moreno, 2005]. Upon treatment with phorbol esters, phosphatases, growth factors or other stimuli, connexin channels are differentially modulated by their phosphorylation status, depending on the connexin isoform, the kinase/phosphatase, the stimulus and the cell type involved [De Vuyst et al., 2007; Kwak et al., 1995].

1.2.3.2.3 Modulation of connexin channels by Ca²⁺

Gap junctions

Ca²⁺ was the first cytoplasmic factor identified to regulate gap junction function, even long before the building blocks of gap junctions were discovered: microinjection of Ca²⁺ (~50 μM) in the vicinity of gap junction channels largely uncoupled these channels. Other gap junction

channels that were laying further away from the microinjection site were unaffected, unless a global $[Ca^{2+}]_i$ increase was manifested after addition of a Ca^{2+} ionophore [Loewenstein and Rose, 1978; Rose and Loewenstein, 1976]. Superfusion of one cytoplasmic face of the junctional membrane of a coupled cell pair with 100 μM free Ca^{2+} solutions did not reduce cell-cell coupling, in contrast to solutions containing 300-1000 μM free Ca^{2+} [Spray et al., 1982]. In neonatal rat cardiomyocytes the threshold for gap junction uncoupling was in the same range (400 μM) [Firek and Weingart, 1995]. Such concentrations are far outside the physiological range of $[Ca^{2+}]_i$ but can occur during cell death, when the plasma membrane is disrupted; therefore, gap junction uncoupling at elevated $[Ca^{2+}]_i$ is believed to isolate damaged cells and to protect their healthy neighbors [Spray et al., 1982]. Despite all observations there is still no clarity on whether gap junctions are only affected by these massive increases or also by more physiological elevations in $[Ca^{2+}]_i$. Ample evidence at least supports the latter. A reduction of astrocyte coupling was observed when $[Ca^{2+}]_i$ reached values of $\sim 2 \mu M$ [Cotrina et al., 1998a]. In Novikoff hepatoma cells expressing Cx43, gap junction uncoupling occurred when $[Ca^{2+}]_i$ was in the nanomolar range with both the magnitude and the time constant of inhibition being a function of $[Ca^{2+}]_i$. $[Ca^{2+}]_i$ approaching 126 nM was without effect but a $[Ca^{2+}]_i$ of 500 nM reduced coupling [Lazrak and Peracchia, 1993; Lazrak et al., 1994]. Similar observations were made in bovine lens cells but not in chicken lens cells that also express Cx43 [Crow et al., 1994]. The number of dye-coupled HeLaCx43 cells drastically diminished with $[Ca^{2+}]_i > 360$ nM [Lurtz and Louis, 2007]. Notably, many of these data are gathered by dialyzing or perfusing ruptured cells with solutions of known Ca^{2+} concentration. Damaging of the cell membrane can however profoundly alter Ca^{2+} homeostasis. Using the non-invasive LAMP technique (local activation of a molecular fluorescent probe) it was shown recently that a single Ca^{2+} spike or sustained Ca^{2+} oscillations did not abolish dye coupling whereas activation of capacitative Ca^{2+} entry (see 1.3: ' Ca^{2+} homeostasis and Ca^{2+} signaling'), despite its low magnitude (0.3 μM), drastically reduced coupling after ~ 8 minutes [Dakin et al., 2005]. These data confirm earlier observations where Ca^{2+} entry is required for block of cell-cell coupling [Lazrak et al., 1994, Chanson, 1999 #851]. Ca^{2+} entry channels possibly reside in close proximity to gap junctions and one can presume that local $[Ca^{2+}]_i$ at the cytoplasmic mouth of the channel pore reaches hundreds of micromolars which is sufficient to close them [Dakin and Li, 2006].

Loewenstein et al. (1978) indicated for the first time that a gradual increase in $[Ca^{2+}]_i$ results in the progressive diminution of the effective channel pore size: between 0.1 and 10 μM

$[Ca^{2+}]_i$, permeability changes manifested in a graded manner, depending on the size of the tracer molecule. Modest increases in $[Ca^{2+}]_i$ only blocked the diffusion of fluorescein but the flow of ions was unaffected [Loewenstein and Rose, 1978]. A narrowing of the pore has been explained by various molecular mechanisms, but thus far no consensus has been reached. At either $[Ca^{2+}]_i$ (physiological or higher) the decrease in cell-cell coupling is not a direct effect of Ca^{2+} but involves CaM [Lurtz and Louis, 2003; Lurtz and Louis, 2007]. This is supported by a lasting uncoupled state long after $[Ca^{2+}]_i$ has been restored [Cotrina et al., 1998a]. The rapid Ca^{2+} -block suggests a direct interaction of CaM with the connexin protein, rather than a secondary effect of CaM-dependent enzymes like CaMKII, calcineurin or NO synthase [Peracchia, 2004]. Consistently, CaM inhibition abolished the Ca^{2+} -block of dye coupling whereas inhibition of CaMKII did not have such an effect [Lurtz and Louis, 2007]. The CaM interaction site remains elusive though. On the one hand, CaM was found to bind a C-terminal peptide of Cx36 in a Ca^{2+} -dependent manner. The interaction site was believed to be a hydrophobic 10 amino acid sequence in the C-terminal domain but this sequence is barely conserved amongst the connexin family members [Burr et al., 2005]. A naturally occurring C-terminal truncated isoform of Cx50 was shown to lack CaM binding [Zhang and Qi, 2005], but in contrast, deletion of a large portion of the C-terminal domain in Cx43 did not abolish inhibition of dye coupling by Ca^{2+} /CaM [Lurtz and Louis, 2007]. Accordingly, it was recently demonstrated that CaM binds part of the Cx43 cytoplasmic loop [Myllykoski et al., 2009]. Upon an increase in $[Ca^{2+}]_i$ CaM will physically obstruct the channel pore. Indeed, each of the CaM lobes is $\pm 25 \text{ \AA}$ in diameter and fits the cytoplasmic mouth of the pore. This type of gating was presented as the cork-type gating model and has thus far only been proposed for Cx32 [Peracchia, 2004]. A direct effect of intracellular Ca^{2+} ions on connexins is not expected to occur. Such an effect would require clusters of negatively charged residues facing the cytosol. Connexin hemichannels do contain 6 glutamate residues (1 of each connexin) at the cytoplasmic face; however, these are insufficient to bind Ca^{2+} with high affinity, which is necessary for gating at physiological $[Ca^{2+}]_i$, nor are they located near the channel pore. EF-hands would be adequate structures for high affinity Ca^{2+} binding, but these have not been identified in any of the connexins [Peracchia, 2004].

Connexin hemichannels

Whereas gap junction channels are only sensitive to $[Ca^{2+}]_i$, connexin hemichannel activity is modulated both by changes in $[Ca^{2+}]_i$ and $[Ca^{2+}]_e$. $[Ca^{2+}]_e$ (normally 1-1.3 mM in mammals

[Parfitt, 1993; Xiong and MacDonald, 1999]) is subject to regional fluctuations under physiological conditions. Variations in $[Ca^{2+}]_e$ of 0.5 - 1 mM have for instance been observed in the rat neocortex upon application of excitatory neurotransmitters and fluctuations of 200 μ M were seen during a single heartbeat as well as during neuronal depolarization [Hofer, 2005; Massimini and Amzica, 2001; Torres et al., 2012]. Furthermore, $[Ca^{2+}]_e$ is decreased in pathologic conditions such as hypoglycemia, ischemia and epilepsy [Kristian et al., 1993; Somjen et al., 1986; Vezzani et al., 1988]. During hypoglycemia, $[Ca^{2+}]_e$ values drop to 0.02 mM whereas in ischemia they fall to 0.1 mM [Kristian et al., 1993]. However, due to cell swelling, ischemia is also associated with a decrease in the extracellular fluid space (about 50%). Combined with a decline in $[Ca^{2+}]_e$ one might expect that almost all extracellular Ca^{2+} will be translocated into the cells. In such conditions $[Ca^{2+}]_i$ can rise to \sim 30-60 μ M [Kristian and Siesjo, 1998]. Finally, some fluids in the body have an unusually low physiological Ca^{2+} content; the cochlear sensory epithelium for instance bathes in endolymph that contains only 20 μ M of free Ca^{2+} [Anselmi et al., 2008].

Lowering of $[Ca^{2+}]_e$ has been shown to trigger connexin hemichannel opening in various experimental approaches. One of the earliest publications identified Cx43 hemichannels in Novikoff hepatoma cells. The channels were activated upon lowering of the extracellular Ca^{2+} concentration and were responsible for the uptake of low MW dyes (LY, 6-carboxyfluorescein) in the cells [Li et al., 1996]. Omission of Ca^{2+} from the bathing medium has also been shown to trigger Cx43 hemichannel-mediated release of the antioxidant GSH (reduced form of glutathione) and glutamate from primary glial cells and organotypic hippocampal slices [Stridh et al., 2010; Stridh et al., 2008; Ye et al., 2003]. Depletion of extracellular Ca^{2+} furthermore increased activity of Cx43 [Contreras et al., 2003], Cx45 [Valiunas, 2002] and Cx26 hemichannels [Ripps et al., 2004] while the presence of Ca^{2+} in the cell medium elevated the threshold for Cx46 hemichannel activation [Ebihara et al., 2003; Ebihara and Steiner, 1993; Pfahnl and Dahl, 1999]. Extracellular Co^{2+} and Ni^{2+} also reduced connexin hemichannel activity but Mg^{2+} had no effect [Ebihara and Steiner, 1993]. Similar results were obtained for Cx37 hemichannels where depletion of Ca^{2+} and Mg^{2+} was sufficient to trigger Cx37 hemichannel activity at negative V_m [Puljung et al., 2004; Wang et al., unpublished observations]. Lowering $[Ca^{2+}]_e$ to 0.5 mM increased the Cx32 hemichannel unitary conductance from 18 pS to 90 pS. Substitution of Ca^{2+} in the external medium with other divalent cations inhibited Cx32 hemichannel activation as well ($Cd^{2+} > Co^{2+}$, $Ca^{2+} > Mg^{2+} > Ba^{2+}$). The half-maximal inhibitory concentration (IC_{50}) was 107 μ M for Ca^{2+} and Hill

coefficients were > 1 indicating that multiple ions act in a cooperative manner to block the channel [Gomez-Hernandez et al., 2003].

The molecular basis of extracellular Ca^{2+} regulation of Cx32 hemichannels was traced back to a ring of twelve aspartate residues to which six Ca^{2+} ions can bind. Each Cx32 subunit contains 2 aspartates, D169 and D178, that reside in EL2 and it is the interaction of D169 of one subunit with D178 of an adjacent subunit that creates a Ca^{2+} binding site. The six Ca^{2+} binding sites are located at the narrowest site of the pore in the external vestibule, which is expected to be 5-7 Å in diameter. Knowing that one Ca^{2+} ion is about 1-2 Å in diameter, it is expected that the binding of just a few Ca^{2+} ions would be sufficient to occlude the channel lumen. Based on sequence alignment, several other connexins (Cx30, Cx34.7, Cx35, Cx38, Cx43, Cx44 and Cx46) are possibly regulated in a similar way [Gomez-Hernandez et al., 2003]. Although a ring of 12 negatively charged residues is also present in Cx37 hemichannels, it was suggested that divalent cations block the channel from the cytoplasmic site [Puljung et al., 2004]. At negative potentials and physiological $[\text{Ca}^{2+}]_e$, the electric field acts on Ca^{2+} driving it to the intracellular binding site. At positive potentials the electric field repels Ca^{2+} ions from the connexin so that hemichannel activation is possible, even when $[\text{Ca}^{2+}]_e$ is high. Putative intracellular binding sites are the N- and C-terminal domains that are rich in acidic residues [Puljung et al., 2004]. Ca^{2+} blockage of Cx46 hemichannels possibly occurs via a similar mechanism [Pfahnl and Dahl, 1999] but it has also been reported that in Cx46 hemichannels, Ca^{2+} ions are channel modulators rather than gating particles [Verselis and Srinivas, 2008]. Many connexins are indeed believed to be regulated in another, yet unidentified, manner. In this respect, it was already hypothesized long time that connexin hemichannel closure is not achieved by Ca^{2+} ions blocking the channel pore [DeVries and Schwartz, 1992]. Electron microscopy studies revealed conformational changes dependent on the ambient $[\text{Ca}^{2+}]_e$. When Ca^{2+} is absent, connexin subunits are aligned parallel to the channel axis. When Ca^{2+} is added to the culture medium, subunits rotate so that they are now diagonally positioned around the central pore, closing the channel [Unwin and Ennis, 1983]. Similarly, atomic force microscopy showed a reversible decrease in the connexin hemichannel pore diameter upon addition of Ca^{2+} in the bathing solution [Allen et al., 2011; Muller et al., 2002; Thimm et al., 2005] (**figure 6**). The decrease in pore diameter results from conformational changes at the extracellular and cytoplasmic mouth of the pore [Allen et al., 2011; Thimm et al., 2005]. Extracellularly, EL1 and EL2 refold so that hydrophobic domains that were exposed to the extracellular environment move together, closing the channel pore

[Thimm et al., 2005]. A neutral alanine residue at position 40, located at the M1/EL1 boundary, is unlikely to create a Ca^{2+} binding site, but appears essential for regulation of Cx26 hemichannels by extracellular Ca^{2+} [Sanchez et al., 2010]. Alternatively, the ball-and-chain model can also apply for $[\text{Ca}^{2+}]_e$ -regulation of connexin hemichannels: Liu et al. (2006) indicate that upon addition of Ca^{2+} to the bathing solution a conformational change in Cx43 hemichannels masks the C-terminal domain from antibody-binding, as in this condition it is most likely associated with the ‘receptor’-domain [Liu et al., 2006].

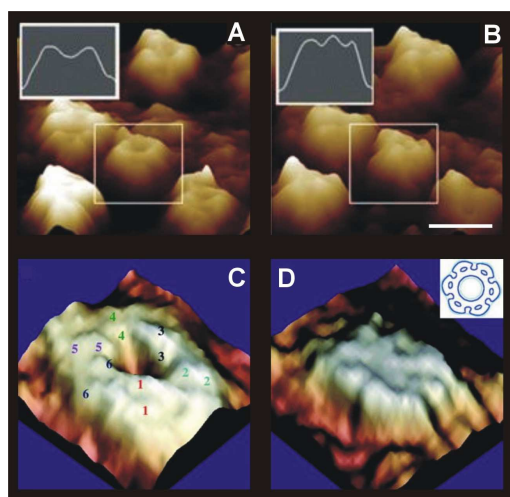


Figure 6. $[\text{Ca}^{2+}]_e$ dependent opening and closure of connexin hemichannels. (A-B) High resolution atomic force microscopy images of the extracellular face of reconstituted Cx40 hemichannels in the absence (A) and presence (B) of extracellular Ca^{2+} (3.6 mM). Scale bar is 10 nm [Allen et al., 2011]. (C-D) 3D height images of the extracellular face of Cx43 hemichannels imaged in Ca^{2+} -free buffer (C) or in the presence of 1.8 mM Ca^{2+} (D). Putative EL1 and EL2 for each of the 6 subunits are denoted by the numbers 1-6 [Thimm et al., 2005].

Generally, as described in many publications that handle on Ca^{2+} signaling, extracellular Ca^{2+} depletion inhibits intracellular Ca^{2+} responses, it usually not evokes them. However, lowering of $[\text{Ca}^{2+}]_e$ has also been shown to trigger an increase in $[\text{Ca}^{2+}]_i$. The exact process behind this phenomenon remains obscure and varying hypotheses have been postulated [Zanotti and Charles, 1997]. Candidate mechanisms include *i*) the electrochemical gradient that drives Ca^{2+} out of the cell, causing a drop in $[\text{Ca}^{2+}]_i$ and subsequent Ca^{2+} release from the ER, *ii*) activation of the $\text{Na}^+/\text{Ca}^{2+}$ exchanger, *iii*) activation of the Ca^{2+} -sensing receptor that uses Ca^{2+} as a first messenger and senses small changes of ~ 0.1 mM or less [Dhein et al., 2008] and *iv*) activation of voltage-dependent Ca^{2+} channels that are triggered by depolarization, which on its turn is brought about by lowering $[\text{Ca}^{2+}]_e$ [Zanotti and Charles, 1997]. Most recent evidence points to low $[\text{Ca}^{2+}]_e$ -activated connexin hemichannels that mediate ATP release as a point source originating from ‘trigger cells’ [Anselmi et al., 2008], and subsequent autocrine actions in surrounding cells via the activation of purinoceptors.

The modulation of connexin hemichannel activity in response to changes in $[Ca^{2+}]_i$ has only been outlined quite recently and connexin hemichannels seem to be differentially affected by $[Ca^{2+}]_i$ when compared to gap junctions. The first indication that connexin hemichannels are sensitive to an increase in $[Ca^{2+}]_i$ was provided by Cotrina et al. (1998) who showed connexin hemichannel-mediated ATP release triggered by activation of $InsP_3$ -linked purinoceptors [Cotrina et al., 1998b]. Subsequently, a role for intracellular Ca^{2+} was confirmed as Cx32 and Cx43 hemichannel-mediated ATP release was related to photoliberation of caged $InsP_3$ and caged Ca^{2+} , or exposure to Ca^{2+} ionophores [Braet et al., 2003b; De Vuyst et al., 2006; Schalper et al., 2008]. ATP release was furthermore suppressed when cytosolic Ca^{2+} ions were chelated or when Ca^{2+} release from $InsP_3$ - and ryanodine-sensitive stores was inhibited [Braet et al., 2003b; De Vuyst et al., 2006]. These data are in agreement with another report showing Ca^{2+} -dependent connexin hemichannel ATP release from retinal pigment epithelium [Pearson et al., 2005] but oppose observations made in taste cells where chelating intracellular Ca^{2+} had no effect on connexin hemichannel ATP release [Romanov et al., 2007]. Expressing connexin hemichannel responses as a function of $[Ca^{2+}]_i$ demonstrated that the magnitude of $[Ca^{2+}]_i$ is a critical factor with $[Ca^{2+}]_i$ between 200-1000 nM successfully triggering connexin hemichannel activation. The maximal response was observed at a $[Ca^{2+}]_i$ of 500 nM. Either very small or large $[Ca^{2+}]_i$ increases were inadequate triggers for connexin hemichannel activation [De Vuyst et al., 2006; De Vuyst et al., 2009]. Absence of Cx43 hemichannel activation at high $[Ca^{2+}]_i$ was confirmed in cardiomyocytes where $[Ca^{2+}]_i$ above a threshold of ~500 nM closed the channels [Shintani-Ishida et al., 2007].

The activation of connexin hemichannels by Ca^{2+} runs via a signaling cascade that involves CaM and arachidonic acid. However, unlike increasing $[Ca^{2+}]_i$, increasing CaM activity never resulted in hemichannel silencing thus, other mediators must be involved [De Vuyst et al., 2009]. Recently we suggested that Cx43 hemichannel closure at high $[Ca^{2+}]_i$ is related to a disruption of a CT-CL interaction. Addition of a peptide containing the last 10 C-terminal residues prevented connexin hemichannel closure by high $[Ca^{2+}]_i$ and restored hemichannel activity of C-terminally truncated channels [Ponsaerts et al., 2010]. Inhibition of Cx43 hemichannels by $[Ca^{2+}]_i > 500$ nM likely proceeds via actomyosin contraction that pulls the CT-tail away from the intracellular loop, leading to closure of the channel [Ponsaerts et al., 2010] (**figure 7**). These data point to an opposite regulation of connexin hemichannels and gap junction channels, gap junctions require a CT-CL interaction for closure while hemichannels need CT-CL interactions for opening. Cytoskeletal rearrangements might also

explain the previously observed inhibition of connexin hemichannel responses by thrombin, a potent activator of actomyosin contraction [D'Hondt et al., 2007b; Ponsaerts et al., 2008]. However, in marked contrast stands the observation that thrombin, via $[Ca^{2+}]_i$, Rho kinase (ROCK) and actomyosin promotes ATP release through connexin hemichannels [Seminario-Vidal et al., 2009]. Possible reasons for this discrepancy might involve a different cellular background (cornea endothelium *versus* lung carcinoma), a different protease-activated receptor (PAR) (PAR1 *versus* PAR3) or the fact that thrombin was used as an initial trigger in the latter but was applied to mechanically stimulated cells in the former.

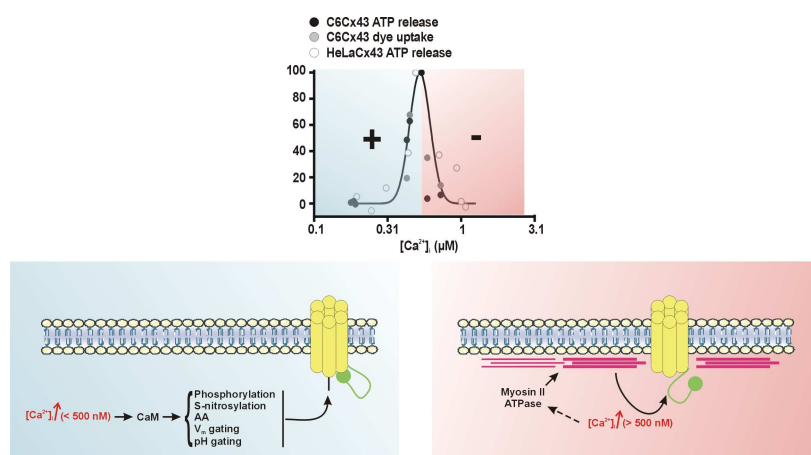


Figure 7. Connexin hemichannel opening and closing is influenced by $[Ca^{2+}]_i$. Connexin hemichannel-mediated ATP release and dye uptake are regulated by $[Ca^{2+}]_i$ in a bimodal manner with $[Ca^{2+}]_i < 500$ nM opening hemichannels and $[Ca^{2+}]_i > 500$ nM closing them again [De Vuyst et al., 2009]. Connexin hemichannel opening is regulated by arachidonic acid (AA), post-translational modifications (phosphorylation, S-nitrosylation), voltage gating and pH gating, which all can be linked to $[Ca^{2+}]_i$ changes. Ca^{2+} -dependent hemichannel opening is dependent on CaM activation [De Vuyst et al., 2009]. Hemichannel opening necessitates an interaction between the cytoplasmic loop and the C-terminal tail of Cx43 (green particle). Hemichannel closure by high $[Ca^{2+}]_i$ may be achieved by pulling away the C-terminal tail from the loop domain. Ca^{2+} -triggered actomyosin stress fiber formation has been proposed to be responsible for the latter (red subplasmalemmal fibers) [Ponsaerts et al., 2010]. This figure was produced using Servier Medical Art.

1.2.4 THE INNEXIN/PANNEXIN PROTEIN FAMILY

Gap junctions are common to all multicellular life forms, but despite this functional conservation a partition exists at the molecular level. Invertebrates indeed also display direct cell-cell coupling through gap junction channels but no connexins have been found in these systems [Cruciani and Mikalsen, 2006]. In contrast, functional gap junction molecules with

no sequence homology to connexins were identified in invertebrates (insects and nematodes) and they were named innexins (invertebrate analog of connexins) [Phelan et al., 1998]. The name ‘innexin’ was not valid though for the innexin-like genes that were identified in vertebrates. These vertebrate homologs were hence called pannexins, from the Latin *pan* which means ‘throughout’ or ‘all’ [Baranova et al., 2004; Panchin et al., 2000] but do not share any homology with their all-vertebrate counterparts, connexins [Yen and Saier, 2007]. In the mouse and human genomes, 3 pannexin genes, *PANX1*, *PANX2* and *PANX3* were described and these genes were highly conserved in invertebrate creatures like worms and insects [Baranova et al., 2004]. Despite the lack of sequence similarity, innexins and pannexins proteins have the same topology as connexins: they are tetra-span proteins that have their C- and N-terminus located intracellularly [Baranova et al., 2004; Bruzzone et al., 2003]. Pannexin hemichannel trafficking to the plasma membrane follows the same route as that described for connexins. Pannexin mRNA translates in the ER before pannexins are further processed and assembled in the ER/Golgi and delivered to the cell surface [Bhalla-Gehi et al., 2010]. Furthermore, unlike innexins and connexins, pannexins are glycosylated which negatively affects hemichannel docking [Boassa et al., 2007; Penuela et al., 2007; Penuela et al., 2009]. Pannexin western blots reveal three bands corresponding to G₀, a non-glycosylated state; G₁ that marks a high mannose-type glycoprotein and G₂, the fully processed glycoprotein that is present in the plasma membrane [Boassa et al., 2007]. The degree of glycosylation determines their retention in the ER and their assembly into heteromeric channels [Penuela et al., 2009]. This degree of glycosylation however differs between tissues: in endothelium only G₀ Panx1 is identified [Boassa et al., 2007], and this non-glycosylated protein was also found on the cell surface of human embryonic kidney cells [Penuela et al., 2009].

The first indication that pannexins form functional channels was given by Bruzzone *et al.* [Bruzzone et al., 2003]. Expression of Panx1 and Panx2 in *Xenopus* oocytes resulted in the formation of homomeric Panx1 hemichannels or heteromeric Panx1:Panx2 channels that were activated upon depolarization. These channels furthermore assembled into intercellular channels [Bruzzone et al., 2003]. Pannexin-mediated cell-cell coupling was observed when Panx1 and Panx3 were overexpressed in C6 glioma cells [Lai et al., 2007] and C2C12 myoblast cells [Ishikawa et al., 2011] respectively; however, little is left of the original idea that pannexins form gap junctions *in vivo*. Indeed, pannexin gap junction formation was only observed in ectopic expression systems and the presence of bulky carbohydrate moieties on

EL2 would interfere with pannexin docking (note though that G_0 pannexins are also found in the plasma membrane [Penuela et al., 2009]). Despite the controversy on pannexin gap junctions, ample evidence continues to support a role for pannexin hemichannels. The discovery of Panx1 mediated ATP release in erythrocytes, a cell type that does not express connexins, emphasized that pannexin hemichannels may have a functional role [Locovei et al., 2006a]. Different triggers are now known to activate pannexin hemichannels, including mechanical and hypotonic stress [Locovei et al., 2006a], depolarization [Bruzzone et al., 2003], ischemia [Thompson et al., 2006], and an increase in $[Ca^{2+}]_i$ [Locovei et al., 2006b], but opposed to connexin hemichannels, pannexin hemichannels are refractory to changes in $[Ca^{2+}]_e$ [Bruzzone et al., 2005] but in oocyte expression systems they do display $[Ca^{2+}]_i$ -sensitivity. Ca^{2+} activation of pannexin hemichannels was observed over a wide range of $[Ca^{2+}]_i$, up to unusually high concentrations (10 μM $[Ca^{2+}]_i$ or addition of 200 μM ionophore) which did not result in pannexin hemichannel closure [Locovei et al., 2006b]. Panx1 hemichannels were suggested as the large pore (900 Da) pathway activated by the purinergic and ionotropic P2X₇ receptor (P2X₇R) [Locovei et al., 2007; Pelegrin and Surprenant, 2006]. It co-immunoprecipitates with P2X₇R and inhibition of Panx1 prevents P2X₇R-mediated dye uptake. Rather high concentrations (> 100 μM) of extracellular ATP are required for P2X₇R activation. Such high concentrations are only present at sites of inflammation, suggesting that Panx1 channels play a role in activation of the inflammasome [Pelegrin and Surprenant, 2006].

Xenopus oocyte injection of innexin mRNA derived from *C. elegans*, lobster (*Homarus gammarus*) and leech (*Hirudo medicinalis*) indicated that different innexins are capable of forming gap junctions and couple two neighboring cells both electrically and metabolically [Chuang et al., 2007; Ducret et al., 2006; Dykes et al., 2004; Landesman et al., 1999; Li et al., 2003; Phelan et al., 1998]. Like connexins, gap junctions made of innexins are sensitive to changes in $[Ca^{2+}]_i$ [Baux et al., 1978], but unlike vertebrate channels, innexin gap junctions were sensitive to transmembrane voltage (V_m) in addition to V_j gating. Equal and simultaneous hyperpolarization (V_j remains 0) of an insect cell pair caused G_j to increase to a maximum whereas depolarization decreased G_j to ~ 0 [Bukauskas and Verselis, 2004]. Ectopic expression of leech Inx1, Inx2, Inx3 and Inx6 in *Xenopus* oocytes furthermore revealed that innexins, in addition to pannexins and connexins, can form functional hemichannels [Bao et al., 2007]. Depolarization to -20 mV induced innexin hemichannel ATP release and electrical currents with unitary conductances highly similar to those measured for Panx1 hemichannels

(~550 pS) [Thompson et al., 2006]. Furthermore, Inx2 and Inx3 mediated the loss of 6-carboxyfluorescein *in situ* [Bao et al., 2007]. Lowering $[Ca^{2+}]_i$ triggered the activation of hemichannels composed of the *C. elegans* innexin NSY-5, indicating they are regulated by $[Ca^{2+}]_i$ as well [Chuang et al., 2007]. Three butterfly cell lines furthermore showed hemichannel-mediated dye uptake under control conditions. Remarkably, here, the addition of divalent cations in the bath solution potentiated dye uptake, suggesting that they are positive regulators of innexin hemichannel activity [Luo and Turnbull, 2011]. Very recently, Inx2 hemichannel mediated ATP release from leech glial cells was triggered by an increase in $[Ca^{2+}]_i$ and was shown to mediate microglial movement towards the site of injury after mechanical stimulation [Samuels et al., 2010]. These data are the first to highlight a role for innexin hemichannels *in vivo*.

1.2.5 PHARMACOLOGICAL PROPERTIES OF CONNEXINS AND PANNEXINS

Inhibition of gap junction intercellular communication may be achieved by various approaches including inhibition of connexin gene expression (knockout or siRNA technology), inhibition of post-translational modifications (e.g. phosphorylation), alteration of the connexin lipid environment, etc. However, research in the field of connexin channels by the use of pharmacological tools has two major handicaps. The first obstacle is the absence of selective connexin channel inhibitors. Indeed, many of the compounds used to block these channels have also been shown to target other proteins, including pannexins, leading to unwanted, non-specific effects. Second, it is difficult to discriminate between connexin hemichannels and gap junctions as hemichannels are sensitive to most gap junction channel blockers. Furthermore, connexin knockout or connexin knockdown allow targeting a specific connexin isoform; however, as they act at the expression level, they influence hemichannels and gap junctions formed by this connexin equally, making them inappropriate tools to determine the role of hemichannels *in vivo*. In addition, connexin knockout models often suffer from profound tissue malfunctioning, leading to early death [Giaume and Theis, 2010]. Below, we describe advantages and disadvantages of several classes of compounds used in the connexin field. These compounds include trivalent cations, quinines, fenamates, alcohols, etc.

The best characterized connexin blocker substances are those derived from Glycyrrhetic acid (GA). GA is a lipophilic aglycone of the saponin glycyrrhizic acid, obtained from the

liquorice root *Glycyrrhizia glabra*, and can exist in the α or β stereoisomer ($18\alpha/\beta$ -GA). Carbenoxolone (Cbx) a.k.a. 18β -GA- 3β -O-hemisuccinate, is a synthetic derivative of 18β -GA. All three compounds inhibit gap junction intercellular communication [Davidson and Baumgarten, 1988; Goldberg et al., 1996; Guan et al., 1996; Taylor et al., 1998] and prevent connexin hemichannel opening as well [Contreras et al., 2003; Eskandari et al., 2002]. In practice, Cbx has not only been proven valid in cell cultures but also in brain and spinal cord slices where it abolishes hemichannel opening and cell-cell coupling [Kang et al., 2008; Karpuk et al., 2011; Meme et al., 2009; O'Carroll et al., 2008; Stridh et al., 2008], and *in vivo* where it suppresses epileptiform activity [Szente et al., 2002]. The mode of action of GA and its derivatives is not known up to date. Connexin dephosphorylation and remodeling of plaques have been suggested [Goldberg et al., 1996; Guan et al., 1996].

The anti-malarial drugs quinine, mefloquine and ilimaquinone seem to block connexin channels in a connexin subtype-dependent manner. Oppositely, most connexin hemichannels were activated by quinines by a yet unknown mechanism [Ripps et al., 2004; Saez et al., 2005; Srinivas et al., 2005]. Fenamates, cyclooxygenase-inhibiting, non-steroidal anti-inflammatory agents like flufenamic (FFA) and niflumic acid (NFA), uncouple gap junctions and block connexin hemichannels [Braet et al., 2003a; Bruzzone et al., 2005; Gomes et al., 2005; Salameh and Dhein, 2005], likely by decreasing P_o [Eskandari et al., 2002]. Finally, the long-chain alcohols heptanol and octanol are classically used to inhibit connexin channels. They have been shown to reduce gap junction conductance and to suppress connexin hemichannel currents [Eskandari et al., 2002; Romanov et al., 2007; Takens-Kwak et al., 1992]. At the basis of alcohol-induced uncoupling lays the ability of aliphatic alcohols to increase plasma membrane lipid bilayer fluidity [Salameh and Dhein, 2005; Takens-Kwak et al., 1992]. Indeed, the plasma membrane containing gap junctions is highly enriched in cholesterol, providing structural rigidity to anchor clusters of apposed gap junctions [Malewicz et al., 1990; Segretain and Falk, 2004]. Arguing against this mechanism are the observations that *i*) heptanol decreased P_o of gap junction channels without reducing the number of channels or single channel conductance [Takens-Kwak et al., 1992], that *ii*) octanol inhibits only certain connexins (Cx50 but not Cx46) and *iii*) that octanol is only effective when added to the extracellular face of hemichannels [Eskandari et al., 2002]. 2-aminoethoxydiphenyl borate (2-APB), which is used normally as a membrane-permeable blocker of InsP_3 receptor channels and/or store-operated Ca^{2+} channels (see 1.3: 'Ca²⁺ homeostasis and Ca²⁺ signaling'), was found to uncouple cells as well [Harks et al., 2003a; Tao and Harris, 2007], and just a few years ago it was discovered that probenecid, an inhibitor

of the renal organic anion transporter, attenuates Panx1 hemichannel responses [Chekeni et al., 2010; Silverman et al., 2009] whereas Cx46 and Cx32E₁₄₃ hemichannel currents were left unaffected, even at concentrations that were 5 times higher [Silverman et al., 2009]. However, further characterization of this compound is required before it can be used in the field as a true pannexin-specific blocker.

For now, the best tool to distinguish between gap junctions and hemichannels and between connexin and pannexin channels are trivalent cations. La³⁺ and Gd³⁺ block connexin hemichannels but have no access to gap junction channels that are located inside the gap junction plaques [Braet et al., 2003a; Leybaert et al., 2003], they can thus be seen as ‘specific’ hemichannel blockers. Furthermore, these trivalents do not seem to have effects on Panx1-mediated currents and P2X₇R/Panx1 dye-uptake [Bruzzone et al., 2005; Pelegrin and Surprenant, 2006], which could render them connexin-specific as well (though keeping in mind effects on for instance Ca²⁺ entry channels - [Estrada et al., 2005; Hu et al., 2009; Pizzo et al., 2001]).

1.2.5.1 Connexin mimetic peptides

Connexin mimetic peptides are synthetic peptides that generally cover highly conserved, short amino acid sequences (11-13 residues) in the extracellular domains of various connexins [Evans and Leybaert, 2007]. These motifs (QPG and SHVR in EL1 and SRPTEK in EL2) were identified as important sequences involved in connexin hemichannel docking. By incorporating these conserved motifs into short sequences that are not consistently found in other connexins or cell surface proteins, a series of Gap peptides was developed that inhibit gap junctions in an isoform-selective manner (**table 3**).

<u>Name</u>	<u>Sequence</u>	<u>Target</u>	<u>Corresponding domain</u>
³² Gap27	SRPTEKTVFT	Cx32	EL2, AA 182-191
^{37,43} Gap27	SRPTEKTIFII	Cx37, Cx43	EL2, AA 201-210
⁴⁰ Gap27	SRPTEKNVFIV	Cx40	EL2, AA 199-219
⁴³ Gap26	VCYDKSFPISHVR	Cx43	EL1, AA 63-75
¹⁰ Panx1	WRQAAFVDSY	Panx1	EL1, AA 74-83

Table 3. Overview of some selected connexin/pannexin mimetic peptides. The table indicates some commonly used connexin and pannexin mimetic peptides along with their sequence, target and corresponding domain in the connexin/pannexin. Conserved motifs in EL1/2 are presented in bold.

Up until today, it is still not known exactly how these peptides work, but three working hypotheses are currently under investigation. Most focus lies on the interference of Gap peptides with the docking of two connexin hemichannels [Evans and Leybaert, 2007]. This action takes into account the rapid turnover of connexins: ‘old’ junctions are removed and newly incorporated hemichannels are targeted by mimetic peptides leading to progressive unzipping of the gap junction plaque [Berthoud et al., 2000; Evans and Leybaert, 2007]. Alternatively, it has been proposed that the peptides diffuse into the intercellular cleft, inducing the closure of pre-existing gap junction channels [Berthoud et al., 2000; Evans and Leybaert, 2007] or that they diffuse into the intercellular space, not to destabilize docking of hemichannels, but to induce a conformational change that promotes the closure of gap junction channels [Chaytor et al., 1997] (**figure 8**).

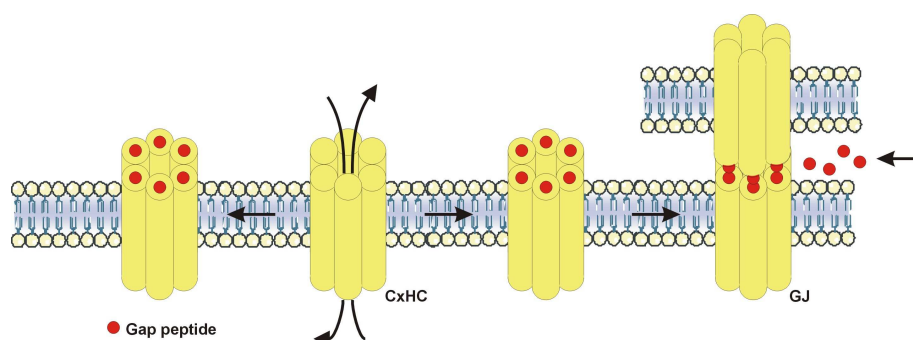


Figure 8. Proposed mechanisms of action by which connexin mimetic peptides inhibit connexin channels.

Connexin hemichannels in unapposed regions of the cell's plasma membrane open and form a bidirectional conduit between the extracellular environment and the cytosol. The connexin mimetic ‘Gap’ peptides bind to channel’s external domains causing closure. Hemichannels with bound peptide move laterally in the plasma membrane, but fail to dock with a neighboring hemichannel, thus impairing intercellular coupling/communication. Alternatively, peptides diffuse into intercellular spaces, inducing the closure of pre-existing gap junction channels. This figure was produced using Servier Medical Art.

Being originally characterized as gap junction inhibitors, mimetic peptides were also found to block connexin hemichannel responses. Leybaert and co-workers demonstrated that these peptides inhibit connexin hemichannel dye uptake and ATP release in various cell types when incubated for 30 minutes. Gap junction communication was unaffected by the peptides when incubated less than 3 hours [Leybaert et al., 2003]. Soon after this observation, many other groups confirmed that brief incubation with connexin mimetic peptides could serve to ‘specifically’ block hemichannels [Eltzschig et al., 2006; Gomes et al., 2005; Hawat et al., 2010; Pearson et al., 2005; Retamal et al., 2007b; Romanov et al., 2007; Takeuchi et al., 2006;

Wong et al., 2006]. A few older reports indicate a rapid abolishment of gap junctional coupling with an onset at 15-30 minutes after addition of the peptides [Boitano and Evans, 2000; Chaytor et al., 1997]; however, these conclusions were drawn after assessing rhythmic contractility or Ca^{2+} wave spread, not taking into account a possible contribution of connexin hemichannels in these processes (M. Bol and L. Leybaert, unpublished observations and [Cotrina et al., 1998b]). Recently, it was suggested that the distinction between hemichannels and gap junctions can also be based on their respective sensitivity to connexin mimetic peptides. When incubated for longer periods (24 h), low doses (5 μM) of an EL2 peptide only abolished dye uptake whereas 500 μM was needed to prevent dye coupling as well [O'Carroll et al., 2008].

The detailed mechanisms behind connexin hemichannel docking and, consequently, connexin hemichannel-peptide interaction, are currently unresolved. Using atomic force microscopy, Liu et al. (2006) provided the first evidence for a direct binding of $^{43}\text{Gap}26$ to EL1 of reconstituted Cx43 hemichannels [Liu et al., 2006]. However, most compelling evidence for a role of mimetic peptides as specific hemichannel blockers came from the recent observation that mimetic peptides rapidly and specifically block connexin hemichannel unitary activities [Wang et al., unpublished observations]. Similar to connexin mimetic peptides, the peptide $^{10}\text{Panx1}$ has been developed to block Panx1 currents [Wang et al., 2007] and dye uptake [Pelegriin and Surprenant, 2006].

1.3 Ca^{2+} HOMEOSTASIS AND Ca^{2+} SIGNALING

In the human body, large amounts of calcium (~99 %) are stored in bones and teeth but only a small amount is present in its free, ionized (Ca^{2+}) form that can be found in all cells [Mikoshiha et al., 2008]. High levels of these Ca^{2+} ions in the cells can be considered toxic; however, by strictly regulating $[\text{Ca}^{2+}]_i$, Ca^{2+} ions have an important second messenger function inside the cell. Transient changes in $[\text{Ca}^{2+}]_i$ are a common theme in initiating cellular processes in a variety of cells. In addition, this Ca^{2+} message can be communicated to other cells, serving as a signal between cells [Pasti et al., 1995]. For electrically non-excitabile cells such Ca^{2+} signals are the only fast (at a second time scale) system available for intra- and intercellular signaling. The importance of Ca^{2+} is emphasized by the observation that even the most primitive prokaryotes, express a variety of Ca^{2+} channels and pumps that create a Ca^{2+} gradient across the plasma membrane. This prototypic Ca^{2+} signaling system served to regulate essential bacterial functions such as movement, chemotaxis, phototaxis and sporulation. During phylogenesis the components of the first Ca^{2+} signaling toolkit became conserved while the system advanced to the most ubiquitous and versatile intracellular signaling mechanism. New sets of proteins lifted the process of Ca^{2+} signaling to a next level, allowing communication of Ca^{2+} signals between different cells in multicellular organisms. The multiplicity of messengers and channels existing today points to a highly complex signaling toolkit tuned to fulfill individual cellular needs. Ca^{2+} signaling, as we know it now, is responsible for a large variety of basic cellular functions throughout vertebrate life, from fertilization over development to death and include cell proliferation, differentiation, neurotransmitter release, secretion, synaptic plasticity, gene expression, immune responses, muscle contraction, cardiomyocyte function, endothelial permeability, apoptosis, etc. [Berridge, 1997; Case et al., 2007; Iino, 2010].

1.3.1 Ca^{2+} HOMEOSTASIS

All eukaryotic cells control their cytosolic Ca^{2+} levels through an intimate interplay between Ca^{2+} entry from the extracellular space and intracellular storage sites and Ca^{2+} extrusion out of the cells or sequestration into the stores. The free extracellular Ca^{2+} concentration is around 1.3 mM [Parfitt, 1993; Xiong and MacDonald, 1999] whereas free cytosolic Ca^{2+} concentrations in resting cells vary between 50 nM and 100 nM [Hess et al., 1989; Koenig et

al., 1989]. Free cytoplasmic Ca^{2+} represents only a small part of the total cellular Ca^{2+} as most of the intracellular Ca^{2+} is sequestered in intracellular stores to prevent a potential deleterious action. Indeed, elevated levels of cytosolic Ca^{2+} (tens of micromolars) cause aggregation of proteins and nucleic acids, affect the integrity of lipid membranes and initiate the precipitation of metabolite phosphates and are thus incompatible with life [Case et al., 2007]. Ca^{2+} is sequestered in the nuclear envelope, the Golgi apparatus, lysosome-related organelles, secretory granules and mitochondria [Dupont et al., 2007; Jardin et al., 2008; Sammels et al., 2010]. However, the ER is considered the predominant Ca^{2+} store as it contains approximately 70% of the cell's total Ca^{2+} reserve [Wood and Gillespie, 1998] which corresponds to Ca^{2+} concentrations up to 0.5 mM [Chatton et al., 1995; Meldolesi and Pozzan, 1998]. Ca^{2+} is sequestered in the ER by Ca^{2+} buffers such as calsequestrin and calreticulin which have a large capacity for Ca^{2+} ion binding [Case et al., 2007], and by Ca^{2+} sensitive chaperone proteins GRP94 (endoplasmic reticulum chaperone), GRP78 (BiP), RP60 and calnexin that are actively involved in protein processing, folding and export [Berridge, 2002]. Despite the presence of these Ca^{2+} binding proteins, there is a continuous basal leak of Ca^{2+} out of the ER that ranges from just a few tens of $\mu\text{M}/\text{min}$ up to 200 $\mu\text{M}/\text{min}$. The physiological role of this Ca^{2+} leak has not been identified thus far and neither is the leak pathway. It could contribute to the equilibrium between $[\text{Ca}^{2+}]_i$ and the Ca^{2+} concentration in the ER or serve to amplify existing Ca^{2+} signals. Different Ca^{2+} permeable, channel forming proteins have been put forward as a route for Ca^{2+} leakage, including InsP_3 receptors (InsP_3R), ryanodine receptors (RyR), transient receptor potential channels (TRP) and pannexin channels [D'Hondt et al., 2011; Ishikawa et al., 2011; Sammels et al., 2010; Vanden Abeele et al., 2006]. The sarco-endoplasmic reticulum Ca^{2+} ATPases (SERCA) continuously pump Ca^{2+} ions from the cytoplasm into the ER lumen and counteract the Ca^{2+} leak. Furthermore, the ER is a dynamic organelle, extending all over the cytoplasm and is thus in immediate contact with the plasma membrane and other intracellular Ca^{2+} stores. One example of this close apposition is the cross-talk of Ca^{2+} signals between the ER and mitochondria that appear to be important in controlling Ca^{2+} homeostasis of the cell. These organelles were first described as mere Ca^{2+} buffer sites with a capacity of about 20% of the cell's total Ca^{2+} [Wood and Gillespie, 1998]. However, in most cells at rest, mitochondria contain nearly undetectable amounts of Ca^{2+} [Rutter, 2006] which suggests that these organelles function as a Ca^{2+} sink rather than a Ca^{2+} store and as such actively contribute to the shaping of Ca^{2+} signals. This issue will be discussed further down this chapter (See 1.3.2.1: ' $[\text{Ca}^{2+}]_i$ elevation and restoration mechanisms').

1.3.2 INTRACELLULAR AND INTERCELLULAR Ca^{2+} SIGNALING

1.3.2.1 $[\text{Ca}^{2+}]_i$ elevation and restoration mechanisms

Basically, a Ca^{2+} signal is initiated when the equilibrium between cytosolic and extracellular Ca^{2+} is perturbed and the function of this intracellular Ca^{2+} increase is quite straightforward: it is meant to activate cellular processes. However, how can a simple messenger be involved in so many signal transduction pathways and yet still convey stimulus specificity within a variety of pathways? This versatility emerges from the use of an elaborate molecular repertoire of signaling components. This signaling toolkit is built up at 4 different levels and includes *i)* a stimulus that generates Ca^{2+} mobilizing molecules, *ii)* an ON mechanism that feeds Ca^{2+} into the cytoplasm, *iii)* Ca^{2+} sensitive processes and *iv)* an OFF signal that removes Ca^{2+} ions from the cytoplasm. Because many of the molecular components of the Ca^{2+} signaling toolkit have different isoforms, all with subtle different properties, each cell type will be able to exploit this large repertoire to orchestrate its cellular processes [Berridge et al., 2000] (**figure 9**).

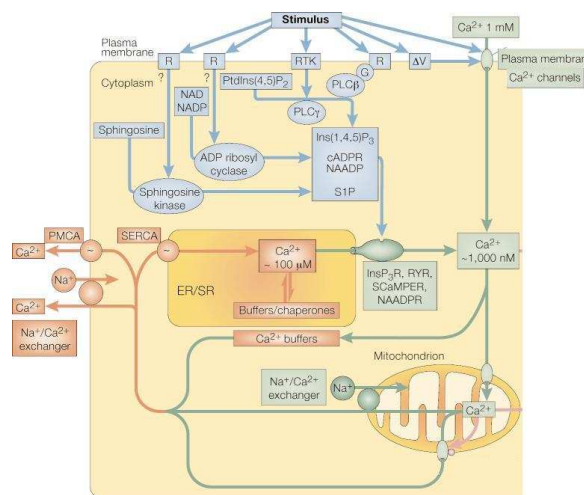


Figure 9. The Ca^{2+} signaling toolkit. Ca^{2+} -mobilizing signals (blue) are generated by stimuli acting through a variety of cell surface receptors (R), including GPCRs and receptor tyrosine kinases (RTK). The signals produced include: InsP_3 , cADPR and NAADP and S1P . ON mechanisms (green) include plasma membrane Ca^{2+} channels and intracellular Ca^{2+} channels - the InsP_3R , RyR , NAADP receptor and SCaMPEP . OFF mechanisms (red) pump Ca^{2+} out of the cytoplasm: the $\text{Na}^+/\text{Ca}^{2+}$ exchanger and PMCA pump Ca^{2+} out of the cell and SERCA pumps it back into the ER [Berridge et al., 2000].

Upon stimulation of $G\alpha_q$ protein coupled receptors (G_qPCR), $[Ca^{2+}]_i$ rises to approximately 1 μM (with the exception of Purkinje cells which can cope with Ca^{2+} levels $> 10 \mu M$ [Khodakhah and Ogden, 1993; Kuruma et al., 2003; Wang et al., 2000]). Ca^{2+} is released from the ER following the activation of a $G\alpha_q$ linked intracellular signaling cascade in the plasma membrane of the target cell with subsequent activation of phospholipase C (PLC) β , hydrolysis of phosphatidylinositol bisphosphate (PIP_2) into $InsP_3$ and diacylglycerol (DAG) and finally stimulation of $InsP_3R$ which allow the flux of Ca^{2+} out of the ER, down its electrochemical gradient [Berridge et al., 2003; Burgess et al., 1984; Streb et al., 1983]. Alternatively, PLC γ is activated following receptor protein tyrosine kinase (RPTK) dimerization. The $InsP_3R$ family contains 3 members ($InsP_3R1$, $InsP_3R2$ and $InsP_3R3$) that form rather large tetrameric channels in a homo- or heteromeric conformation. Ca^{2+} release through these channels does not only require $InsP_3$, but also Ca^{2+} ions themselves [Mak et al., 2001b]. This Ca^{2+} -induced Ca^{2+} release (CICR) further promotes $InsP_3$ -dependent Ca^{2+} release, not only on the receptor from which it was released but also from $InsP_3R$ s in its direct environment [Falcke et al., 1999]. As such, a Ca^{2+} signal that would otherwise be restricted within a few micrometers because of the limited diffusion of Ca^{2+} ions in the cytoplasm is amplified within the cell [Iino, 2010; Rottingen and Iversen, 2000].

Other Ca^{2+} releasing agents include cyclic adenosine 5'-diphosphoribose (cADPR), nicotinic acid adenine dinucleotide phosphate (NAADP) and sphingosine-1-phosphate (S1P). cADPR and Ca^{2+} were found to be the natural ligands of ryanodine receptors (RyR) that are located on the ER membrane and the nuclear envelope, and that are structurally and functionally related to the $InsP_3R$ [Barbara, 2002; Galione, 1994; Galione et al., 1998; Jardin et al., 2008]. The target receptor of NAADP has been suggested to be the two-pore channel that is present on lysosome-related acidic organelles and secretory granules [Calcraft et al., 2009; Galione et al., 2009]. The regulation of cADPR and NAADP levels inside the cell is not well understood though we know they are processed from nicotinamide adenine dinucleotide (NAD^+) by different members of the ADP-ribosyl cyclase family. One of them, CD38, is a membrane spanning glycoprotein that is responsible for the synthesis and transport of cADPR and NAADP into the cell once they are formed extracellularly [Gul et al., 2008; Schulz and Krause, 2004]. cGMP has been found to trigger cADPR formation which in turn stimulates the further production of this second messenger. In contrast, NAADP was elevated in response to cAMP signaling. Finally, S1P drives Ca^{2+} out of the ER through activation of

SCaMPER channels (sphingolipid Ca^{2+} -release mediating protein of the ER). Alternatively, polycystin-2 that is part of the TRPP-subfamily can act as a S1P-activated Ca^{2+} release channel [Bootman et al., 2002].

Because of the finite capacity of the ER and the presence of a variety of mechanisms that act to remove excessive Ca^{2+} ions from the cell, ER luminal Ca^{2+} becomes gradually depleted during ongoing stimulation. To overcome this issue, a process known as capacitative Ca^{2+} entry (CCE) is activated by the emptied store. By refilling the ER, CCE ensures that during repetitive stimulation a suitably large Ca^{2+} release from the ER remains possible (**figure 10**). CCE involves store-operated channels (SOCs) that are present in the plasma membrane but whose identity is still a matter of debate. Principally, any plasma membrane channel can be defined a SOC when it is demonstrated that channel activity is regulated by the filling state of the ER but only two types of channels have been suggested to mediate CCE. Ca^{2+} release-activated channels (CRAC) are believed to mediate the observed Ca^{2+} release-activated membrane currents (I_{CRAC}). CRACs are non-voltage sensitive channels that are highly selective for Ca^{2+} ions. Furthermore, I_{CRAC} is challenged when $[\text{Ca}^{2+}]_i$ is elevated as Ca^{2+} ions themselves inhibit the channel [Putney, 2009]. Recently it has been demonstrated that I_{CRAC} is mediated by a macromolecular complex that contains the stromal interaction molecule (STIM-1) and Orai proteins (alias CRAC modulator or CRACM) [Feske et al., 2006; Vaca, 2010]. STIM-1 is a transmembrane protein located in the ER membrane that acts as a luminal Ca^{2+} sensor. It has a single transmembrane domain with an EF-hand motif that is located in the ER lumen. Orai1 has been demonstrated to form tetrameric ion channels in the plasma membrane and to mediate I_{CRAC} . Although a pool of Orai1 is constitutively expressed in the plasma membrane, more Orai1 subunits are accumulated in the membrane upon store emptying [Salido et al., 2009]. Following ER Ca^{2+} depletion and dissociation of Ca^{2+} from STIM-1, the protein can diffuse in the ER membrane and self-associate in specialized regions where the ER meets the plasma membrane (punctae). At these sites STIM-1 induces Orai1 clustering resulting in the activation of CCE [Putney, 2009; Salido et al., 2009; Vaca, 2010]. Channels that belong to the TRP superfamily furthermore gained a lot of interest as possible SOCs. Of this superfamily, seven subfamilies (TRPC, TRPM, TRPV, TRPA, TRPP, TRPL and TRPN) are known. There is however no consensus on which TRP channel (family) contributes to CCE. Channels of the canonical (TRPC) subtype gained the highest interest concerning CCE. TRPC channels, in particular TRPC1 and TRPC4, are divalent cation channels that are known to be activated by store depletion. TRPC1 has been shown to be

involved in CCE in many cell types including astrocytes [Golovina, 2005], salivary glands [Liu et al., 2000], endothelial cells [Brough et al., 2001], smooth muscle cells [Xu and Beech, 2001] and human platelets [Rosado et al., 2002]. In addition, both STIM-1 and Orai have been shown to interact with TRP channels [Salido et al., 2009; Vaca, 2010]. The formation of this macromolecular CCE-regulating complex occurs at specialized plasma membrane domains enriched in cholesterol, named lipid rafts, and disruption of these rafts interferes with CCE [Vaca, 2010].

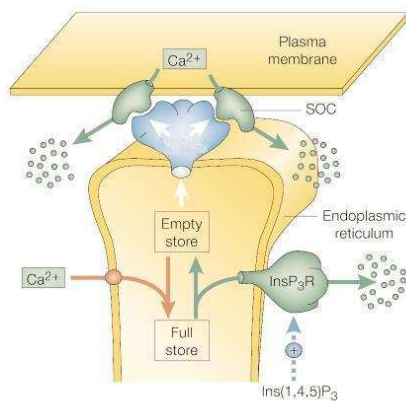


Figure 10. Capacitative Ca²⁺ entry. In response to a Ca²⁺-mobilizing signal such as InsP₃, Ca²⁺ is released from the ER. Emptying of the store is detected by a protein; most probably STIM-1, that transmits this info to the store-operated channel (SOC) to induce Ca²⁺ entry across the plasma membrane. Adapted from [Berridge et al., 2000].

After entering the cytoplasm, Ca²⁺ binds to a number of proteins to trigger various intracellular signal transduction pathways. However, prolonged elevation of cytosolic Ca²⁺ levels leads to a condition known as 'Ca²⁺ overload'. Such a condition is lethal to the cell and since Ca²⁺ cannot be metabolized, the cell needs specialized mechanisms to remove the excessive Ca²⁺ from the cytosol. This recovery is provided by the plasma membrane Ca²⁺ ATPase (PMCA) and the electrochemically driven Na⁺/Ca²⁺ exchanger, which uses the Na⁺ gradient to extrude Ca²⁺. Ca²⁺ reuptake in the ER occurs through SERCA [Heizmann and Hunziker, 1991]. In addition, mitochondria play an important role in preventing Ca²⁺ overload, as they temporarily store Ca²⁺ that is released from the ER. Mitochondria accumulate Ca²⁺ via an electrogenic uniporter powered by the inner mitochondrial membrane potential ψ_m . The *in vitro* Ca²⁺-affinity of the uniporter is rather low (EC₅₀ is 10-20 μ M) in comparison to [Ca²⁺]_i values measured during physiological responses; however, such concentrations can exist in the vicinity of ER Ca²⁺ release sites that are in the immediate surroundings of the mitochondrial uniporter. Alternatively, more recent evidence has indicated that mitochondrial Ca²⁺ uptake by the low-affinity uniporter occurs already when [Ca²⁺]_i exceeds a threshold of ~100-400 nM [Chalmers and McCarron, 2008; Colegrove

et al., 2000; Collins et al., 2001]. Ca^{2+} uptake in mitochondria is always directly pursued by a slow Ca^{2+} release that occurs through the $\text{Na}^+/\text{Ca}^{2+}$ and $\text{H}^+/\text{Ca}^{2+}$ exchangers, toward the ER on the one hand and cytosol on the other [Malli et al., 2003]. Mitochondria are also found in close relationship with plasma membrane Ca^{2+} influx channels [Lawrie et al., 1996] where they generate microdomains of low Ca^{2+} at the mouth of the entry channels, favoring an inward Ca^{2+} flux. Finally, a number of Ca^{2+} -binding proteins, such as CaM and calbindin, present in the cytosol, sequester Ca^{2+} with a high capacity [Heizmann and Hunziker, 1991].

1.3.2.2 Spatiotemporal organization of Ca^{2+} signals

A Ca^{2+} signal does not occur simply as a monotonic change in $[\text{Ca}^{2+}]_i$ following receptor stimulation. Rather, a physiological Ca^{2+} response is organized both in time and in space. At the temporal level, $[\text{Ca}^{2+}]_i$ changes may be oscillatory, appearing as repetitive Ca^{2+} spikes that result from the periodic cycling of Ca^{2+} between the cytoplasm and the internal Ca^{2+} stores. Spatial organization, on the other hand, refers to the localized nature of these signals as elementary Ca^{2+} blips or puffs and the fusion of these events into an intracellular, regenerative Ca^{2+} wave, eventually merging into a global $[\text{Ca}^{2+}]_i$ increase [Berridge, 2006; Dupont et al., 2007]. Moreover, depending on the stimulus strength, intracellular waves are not confined to the cytoplasm of one cell but spread out to neighboring cells as an intercellular Ca^{2+} wave (**figure 11**). The latter are thus defined as propagating increases in $[\text{Ca}^{2+}]_i$ that originate from a single cell and sequentially engage neighboring cells. Such waves can be repetitive as well, reflecting propagation of Ca^{2+} oscillations that originate in a single pacemaker cell. Functionally, Ca^{2+} waves allow the transmission of information, which is encoded in both the temporal and spatial pattern of the Ca^{2+} signals, coordinating the function of large groups of cells.

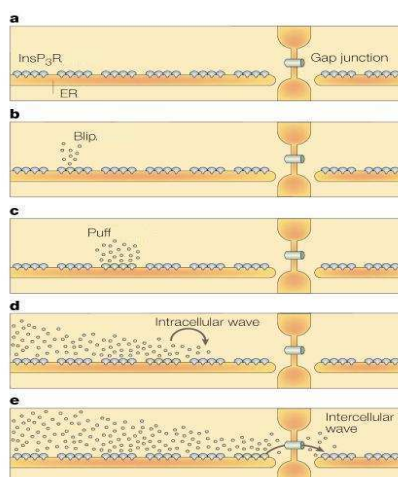


Figure 11. The spatial organization of Ca^{2+} signals. (a) InsP_3R s are distributed over the surface of the ER. (b) In response to weak stimuli, individual InsP_3R channels open to give Ca^{2+} blips. (c) At higher levels of stimulation, groups of InsP_3R s open together to produce puffs. (d) When cells are fully excitable, the elementary events depicted in (c) can excite neighboring receptors through a process of CICR to set up an intracellular wave. (e) When gap junctions connect cells, waves can travel from one cell to the next to set up an intercellular wave. Adapted from [Berridge et al., 2000].

1.3.2.2.1 Ca²⁺ oscillations

Repetitive oscillations in $[Ca^{2+}]_i$ occur over an extremely broad time interval, ranging from very rapid oscillations with a spiking frequency of 100 Hz (spike durations of < 10 ms) to frequencies of 10^{-5} Hz (1 per day) [Boulware and Marchant, 2008]. Variations in Ca^{2+} spike duration, shape and amplitude are brought about by different Ca^{2+} oscillation mechanisms [Berridge et al., 2000; De Pitta et al., 2009; Nash et al., 2001]. Frequency modulation (FM), referring to Ca^{2+} spikes with information encoded in the oscillatory frequency (**table 4**) and amplitude modulation (AM), where the $[Ca^{2+}]_i$ peak amplitudes encrypt information, are best characterized thus far; however, these are not mutually exclusive and AFM coding has also been reported [De Pitta et al., 2009]. The complexity of such Ca^{2+} signals allows to decrypt information referring to the initiating trigger and to translate this into an appropriate physiological response. In this way, the same ion can be used to orchestrate a myriad of cellular processes in the same cellular background. Another advantage of Ca^{2+} oscillations involves the protection from apoptosis and phosphate precipitation that would occur with a long-lasting, permanent $[Ca^{2+}]_i$ increase [Dupont et al., 2007].

Biological process	Oscillation period	Cell type
Cardiac cell hypertrophy	2-4 sec	cardiomyocytes
Glomerular filtration	9 sec	mesangial cells
Pulmonary hypertension	6-20 sec	smooth muscle cells
Dendritic outgrow	20 sec	cortical neurons
Gene expression (via NFAT)	5-35 sec	cardiomyocytes
Neurite outgrowth	50 sec	neuroblastoma cells
Insulin secretion	10-210 sec	pancreatic β -cells
Cell growth	3 min	cardiac progenitors
Gene expression (via c-fos, Ras or ERK)	1-10 min	endothelial, mast, HeLa cells
Interleukin production	12 min	macrophages
Fertilization	10-40 min	oocytes

Table 4: Various biological processes regulated by cytosolic Ca²⁺ oscillations. The table describes biological responses that are triggered by Ca^{2+} oscillations characterized by varying periods in different cell types. Adapted from [Uhlen and Fritz, 2010].

The molecular link between Ca^{2+} oscillations and the underlying cellular response is provided by specialized oscillation “sensors” or “frequency decoders” which translate the information that is contained in Ca^{2+} oscillations [Dupont and Goldbeter, 1998]. Typical FM-coded

signals and the corresponding specific activation of cellular functions are exemplified by CaMKII, the Ca^{2+} -dependent phosphatase calcineurin and PKC. CaMKII is maximally activated by oscillations with periods of less than 1 second whereas calcineurin, which is a vital component of NFAT-mediated gene expression, is optimally activated by slower oscillations (0.3-0.6 spikes/min) [Tomida et al., 2003]. NFAT (nuclear factor of activated T-cells) is present in the cytosol in a phosphorylated form but translocates to the nucleus when dephosphorylated (dNFAT) by calcineurin. It has been indicated that NFAT ‘stores’ the info coming from the initiating trigger because dNFAT presence can persist long after $[\text{Ca}^{2+}]_i$ has returned to baseline levels. However, this can only occur when Ca^{2+} spiking frequency exceeds the lifetime of dNFAT in the cytosol, causing a build-up of dNFAT. In practice, oscillations with frequencies of 1 spike every 1.5 to 3 minutes are fast enough but slower oscillations or sustained $[\text{Ca}^{2+}]_i$ increases are inadequate for gene expression [Tomida et al., 2003]. This was also shown in activated T-cells where gene expression could be modulated by varying the inter-spike period. Slower oscillations (with periods of > 400 sec) activated only nuclear factor κB (NF κB) but increasing the spiking frequency, activated NFAT as well [Dolmetsch et al., 1998].

CaMKII is a multifunctional serine/threonine protein kinase with broad substrate specificity. It exists as a multimeric holoenzyme with each subunit independently regulated by the $\text{Ca}^{2+}/\text{CaM}$ complex [Rosenberg et al., 2006]. Upon an increase in $[\text{Ca}^{2+}]_i$, auto-inhibition is relieved by the binding of the $\text{Ca}^{2+}/\text{CaM}$ complex. An active subunit can then phosphorylate diverse substrates, including a $\text{Ca}^{2+}/\text{CaM}$ bound subunit of the same holoenzyme. This inter-subunit, intramolecular reaction is known as ‘auto-phosphorylation’ and has two effects. First, it largely decreases the rate of dissociation of $\text{Ca}^{2+}/\text{CaM}$, which is thus ‘trapped’ by the multimeric kinase. Second, auto-phosphorylation disrupts the interaction between the auto-inhibitory domain and the catalytic site. The auto-phosphorylated subunit remains active after dissociation of $\text{Ca}^{2+}/\text{CaM}$ and is thus said to be ‘autonomous’. These events underlie the frequency decoding capacity of CaMKII. When the oscillation frequency is sufficiently high the enzyme will not completely deactivate between two successive Ca^{2+} spikes and autonomous activity will increase exponentially with frequency. With lower frequencies the accumulation of CaMKII autonomous activity is limited. In the latter case, CaM dissociates from CaMKII subunits between two Ca^{2+} spikes and auto-inhibition is restored [De Koninck and Schulman, 1998; Dupont and Goldbeter, 1998].

Of the different classes of PKCs, (conventional/classic, novel and atypic), only the Ca^{2+} -sensitive, conventional PKCs (α , βI , βII and γ) are appropriate candidates for ‘sensing’ the

spatiotemporal character of Ca^{2+} signals [Berridge et al., 2000]. Conventional PKCs contain three essential domains: an auto-inhibitory pseudosubstrate that holds PKC in an inactive state, a C1 domain that binds DAG and finally a Ca^{2+} binding domain (C2). Activation results from Ca^{2+} binding which translocates the enzyme from the cytosol to the plasma membrane and sequentially releases the pseudosubstrate domain rendering the enzyme active. DAG binding occurs with a certain delay and stabilizes PKC in the membrane [Oancea and Meyer, 1998]. In order to be able to decode spatiotemporal diversities in Ca^{2+} signals, the translocation kinetics need to be fast enough. Indeed, translocation of GFP-tagged PKC α [Reither et al., 2006; Tanimura et al., 2002] and PKC γ [Codazzi et al., 2001; Oancea and Meyer, 1998] was shown to be fast (< 250 msec) and oscillatory, in phase with the observed oscillations in $[\text{Ca}^{2+}]_i$. PKC translocation did require the elevation of $[\text{Ca}^{2+}]_i$ above a certain threshold (> 200 nM) [Oancea and Meyer, 1998; Reither et al., 2006]. Although a stable binding of PKC to the plasma membrane necessitates binding of DAG to the C1 domain, translocations with a short lifetime, which are sufficient to phosphorylate target proteins, might reflect pure Ca^{2+} -dependent, DAG-independent events [Reither et al., 2006]. When agonist concentration is low, DAG production will be limited and oscillations will have a low frequency. In this scenario, Ca^{2+} spikes induce a rapid and reversible translocation of PKC to the plasma membrane and in this finite period of unstabilized membrane binding, PKC is activated [Oancea and Meyer, 1998]. Once $[\text{Ca}^{2+}]_i$ drops, the PKC membrane tether is lost and the enzyme is inactive again. When agonist concentrations are high, DAG levels become more elevated and oscillations have a high frequency. Still, a decline in $[\text{Ca}^{2+}]_i$ can induce a dissociation from the membrane but this occurs with a delay of ~ 8 sec [Oancea and Meyer, 1998; Violin et al., 2003]. When oscillations are faster than this period, PKC activity can increase gradually. In addition to being sensitive to Ca^{2+} oscillations, PKC α translocation also followed a Ca^{2+} wave propagation pattern and was communicated along the membranes of neighboring cells, evidenced by a wave-like fluorescence reporter signal in the plasma membrane [Reither et al., 2006]. Using a C kinase activity reporter (CKAR) it was furthermore shown that not only PKC translocation/activation but also substrate phosphorylation by conventional PKCs is under the dynamic control of $[\text{Ca}^{2+}]_i$. CKAR consists of a PKC substrate sequence that is flanked by fluorophores. Normally the fluorophores are in close proximity allowing fluorescence resonance energy transfer (FRET), but phosphorylation of the substrate triggers a conformational change that dislocates the

fluorophores away from each other, causing a change in emission ratio. This change in emission ratio was oscillatory, closely following Ca^{2+} oscillations [Violin et al., 2003].

Despite years of effort, the nature of the primary oscillator responsible for Ca^{2+} oscillations is far from being clarified. One of the long-standing questions has been whether oscillations are generated by modulatory actions on the cellular Ca^{2+} release channels (InsP_3R) themselves, or whether they originate upstream in the signal transduction machinery, between ligand binding to its receptor and the activation of Ca^{2+} release. In addition, the role of Ca^{2+} influx and the involvement of Ca^{2+} stores other than the ER remain puzzling. These issues will be discussed in the following paragraphs.

Ca^{2+} oscillations based on intrinsic InsP_3 receptor properties

A bimodal regulation of InsP_3R Ca^{2+} release by $[\text{Ca}^{2+}]_i$ is most accepted as the basis of Ca^{2+} oscillations [Bezprozvanny et al., 1991; Iino, 2000; Patel et al., 1999; Zhang and Muallem, 1992]. Given that the Ca^{2+} affinity of the InsP_3R activating site is larger than that of the inhibitory site, a local increase in $[\text{Ca}^{2+}]_i$ will first induce channel opening before proceeding to channel closure. Indeed, up to a certain level $[\text{Ca}^{2+}]_i$ promotes CICR whereas $[\text{Ca}^{2+}]_i$ exceeding this threshold provides a negative feedback on InsP_3 -induced Ca^{2+} release, initiating the declining phase of the Ca^{2+} spike [Ilyin and Parker, 1994]. In such a manner, Ca^{2+} release can trigger successive cycles of activation-inhibition of InsP_3R , resulting in Ca^{2+} oscillations (**figure 12**).

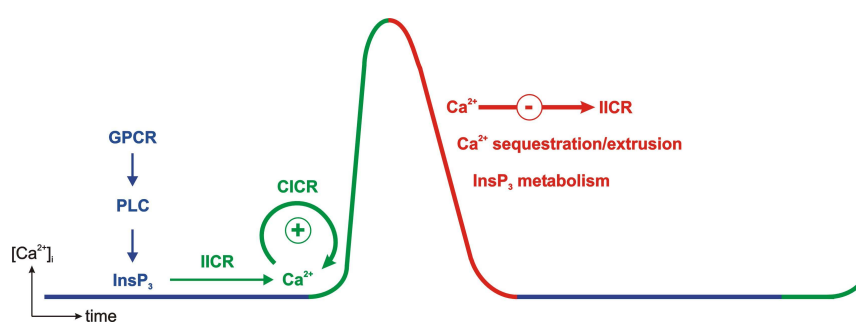


Figure 12. Diagram of basic mechanisms involved in generating an oscillatory Ca^{2+} spike. Ligand binding to a $\text{G}\alpha_q$ protein coupled receptor (GPCR) generates InsP_3 which leads to InsP_3 -induced Ca^{2+} release (IICR) that is further amplified by CICR (positive feedback), producing the steeply rising phase of the Ca^{2+} spike. Elevated $[\text{Ca}^{2+}]_i$ will inactivate IICR (negative feedback) and stimulate Ca^{2+} sequestration and extrusion. Metabolic conversion of InsP_3 to InsP_2 and InsP_4 will lower the InsP_3 concentration. Once all OFF mechanisms have restored $[\text{Ca}^{2+}]_i$ to the resting level, the cycle is ready for the next Ca^{2+} spike. Based on [Berridge et al., 1988].

A bimodal regulation has been observed for all 3 InsP₃R isoforms though unique characteristics related to their InsP₃/Ca²⁺-sensitivity are evident [Taylor and Laude, 2002]. It is fairly accepted that InsP₃R1 is regulated by cytosolic Ca²⁺ in a bimodal manner with maximal Ca²⁺ release occurring at [Ca²⁺]_i ~300 nM [Bezprozvanny et al., 1991; Tu et al., 2005a]. As for InsP₃R2 and InsP₃R3, conflicting data exist. When studied in planar lipid bilayers, both receptor types seem to lack Ca²⁺-inhibition, even when [Ca²⁺]_i approximates 100-200 μM [Hagar et al., 1998; Ramos-Franco et al., 1998], but other groups report that these receptors are negatively regulated by Ca²⁺ when studied in whole cells, and exhibit maximal responses at ~100 nM (InsP₃R3) and 150 nM (InsP₃R2) [Missiaen et al., 1998; Swatton et al., 1999; Tu et al., 2005a]. In terms of InsP₃ sensitivity, InsP₃R2 exhibits highest affinity, followed by type 1 and type 3 receptors [Miyakawa et al., 1999]. The spatiotemporal pattern of Ca²⁺ signals critically depends on the expressed set of InP₃R types. In DT40 B-cells that express all 3 InsP₃ isoforms, antigen binding causes long-lasting (> 1 h) oscillations that become highly regular when InsP₃R1 and InsP₃R3 are knocked down. In contrast, combined knockdown of receptor types 1/2 or types 2/3 results in oscillations that are irregular and rapidly fade out, indicating that InsP₃R2 is the most efficient in generating long-lasting oscillations [Miyakawa et al., 1999]. On the other hand, global increases in [Ca²⁺]_i arise when Ca²⁺ puffs reach a threshold at which CICR becomes activated and this threshold is determined by the set of InsP₃R types expressed in the cell. Cells that contain only InsP₃R3 are relatively resistant to CICR, whereas at the other extreme, cells that express both InsP₃R2 and InsP₃R3 need just a few puffs to generate a global Ca²⁺ increase. An overall downregulation of InsP₃R activity reduces puff duration, amplitude and frequency, and prevents the appearance of global [Ca²⁺]_i elevations [Tovey et al., 2001]. An additional, fundamental feature necessary to allow for oscillations is that InsP₃/Ca²⁺ activation of InsP₃R is fast whereas inhibition of Ca²⁺ release is slower. Flash photolysis of caged-InsP₃ in *Xenopus* oocytes confirmed this difference in kinetics [Parker and Ivorra, 1990].

Additional fine-tuning of InsP₃R sensitivity to [Ca²⁺]_i and the associated Ca²⁺ oscillation pattern can be brought about by cytosolic ATP [Ferris et al., 1990], that modulates the receptor's sensitivity to Ca²⁺ and InsP₃ in a bimodal manner [Betzenhauser et al., 2008; Maes et al., 2000; Mak et al., 2001a; Yule et al., 2010]. In terms of activation, InsP₃R2 appears ATP-insensitive, whereas InsP₃R1 contains a high affinity (0.1 mM) ATP modulatory site. InsP₃R3 on the other hand, requires ATP concentrations exceeding 2 mM [Miyakawa et al., 1999; Tu et al., 2005b]. InsP₃R activity is also modulated by different kinases (including

PKA, PKC, PKG, CaMKII and non-receptor tyrosine kinases) [Ferris et al., 1991; Vanderheyden et al., 2009; Yokoyama et al., 2002; Yule et al., 2010]. Whether phosphorylation potentiates or suppresses InsP₃R Ca²⁺ release is not entirely clear, but an association with InsP₃ sensitivity and oscillation parameters are evident [Giovannucci et al., 2000; Vanderheyden et al., 2009]. Repetitive phosphorylation by CaMKII appears necessary for sustained Ca²⁺ oscillations in HeLa cells. Keeping CaMKII locked in an active or inactive state precluded oscillations [Zhu et al., 1996]. Auto-phosphorylation of the InsP₃R might provide an additional sensitization/desensitization mechanism [Patterson et al., 2004]. Finally, the InsP₃R can be slowly inactivated by its own ligand, InsP₃, and this could contribute to drive Ca²⁺ oscillations. In the model proposed by Hajnoczky and Thomas (1997), InsP₃ would first stimulate ER Ca²⁺ release after which Ca²⁺ would bind the InsP₃R stimulatory binding site further potentiating Ca²⁺ release. However, at the same time, binding of Ca²⁺ to the stimulatory binding site brings the InsP₃R in a state that is susceptible to inhibition by InsP₃. Together with Ca²⁺ binding to the inhibitory site this will cause in a drop in [Ca²⁺]_i. Dissociation of Ca²⁺ from the stimulatory site would finally prevent InsP₃-induced InsP₃R inhibition after which the cycle can restart [Hajnoczky and Thomas, 1997].

Ca²⁺ oscillations that are based on intrinsic InsP₃ receptor properties are commonly regarded as Ca²⁺ oscillations that occur at fixed InsP₃ levels. Several lines of evidence derived from mathematical models support the fact that Ca²⁺ oscillations exist at constant InsP₃ levels [Atri et al., 1993; De Young and Keizer, 1992; LeBeau et al., 1999; Parker and Ivorra, 1990] and they are further backed up by experimental observations. Injection of mammalian cells with the non-metabolizable InsP₃ induces the periodic release of Ca²⁺ from intracellular stores [Berridge and Potter, 1990; Wakui et al., 1989] indicating that oscillations do not depend on fluctuating levels of [InsP₃]_i. Furthermore, Ca²⁺ oscillations can be reproduced in permeabilized cells that are kept in a solution with fixed InsP₃ amounts (100 - 200 nM) and in which only Ca²⁺ fluxes mediated by intracellular organelles remain intact [Hajnoczky and Thomas, 1997]. All the above data presume a one-pool model since Ca²⁺ release from the InsP₃-sensitive store (ER) stimulates further release from this same store. In extension, a two-pool model proposes that Ca²⁺ released from one pool amplifies Ca²⁺ release from other stores [Edwards and Pallone, 2008; Goldbeter et al., 1990; Schulz and Krause, 2004]. As such, Ca²⁺ release from the InsP₃-sensitive store could amplify Ca²⁺ release from cADPR-, NAADPH or S1P-sensitive stores or *vice versa*.

Ca²⁺ oscillations driven by InsP₃ dynamics

Models based on the bimodal regulation of InsP₃R Ca²⁺ release commonly produce fast oscillations with short periods (10-15 sec), but cannot reproduce the long inter-spike intervals that were observed experimentally. Indeed, the period of Ca²⁺ oscillations is governed by the time taken for the InsP₃R to recover from Ca²⁺-induced inhibition, which is completed in just a few seconds (or longer when InsP₃R is phosphorylated). However, Ca²⁺ oscillation periods frequently exceed 1 minute [Dupont et al., 2010]. Such longer-period oscillations can be obtained by additional regulatory mechanisms that give rise to sinusoidal changes in InsP₃ levels [Nash et al., 2001; Politi et al., 2006; Young et al., 2003]. Generally, these involve feedback actions on GTPase activity of the GPCR's Gα_q subunit and on InsP₃ production by PLC [Dupont et al., 2007; Goldberg et al., 2010; Hirose et al., 1999; Kiselyov et al., 2003] (**figure 13**).

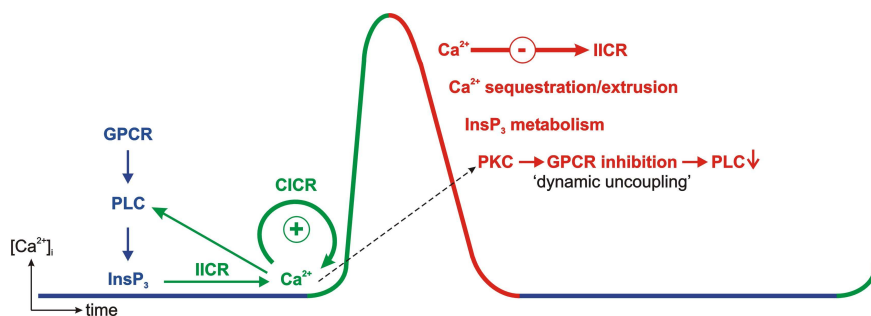


Figure 13. Additional mechanisms involved in Ca²⁺ oscillations. In addition to the mechanisms depicted in figure 12, Ca²⁺ activation of PLC may further amplify IICR. Ca²⁺, together with DAG, will also activate PKC (dotted line) suppressing GPCRs and PLC activity. Dephosphorylation of GPCRs removes this effect, preparing for the next cycle Ca²⁺ spike.

PLC activity is regulated by Ca²⁺ in a positive manner [Meyer and Stryer, 1988] amplifying the InsP₃ induced Ca²⁺ release [Tsukamoto et al., 2010]; however, which PLC subtypes are subject to Ca²⁺ activation remains questionable. All PLC isoforms at least need some Ca²⁺ for proper functioning [Rebecchi and Pentylala, 2000; Thore et al., 2005], but especially PLCδ, and in addition also PLCβ show sensitivity to [Ca²⁺]_i [Ishihara et al., 1999; Kelley et al., 2001; Kim et al., 1999]. Young and coworkers indicated that [Ca²⁺]_i up to 200 nM was able to stimulate InsP₃ production, and that a further increase in [Ca²⁺]_i had the same efficiency [Young et al., 2003]. Studies in which the GFP-linked DAG-binding domain of PKC (GFP-

C1) is transfected into astrocytes provide further insights in the Ca^{2+} regulation of PLC activity. Translocation of GFP-C1 was shown to be oscillatory, indicating the cyclical production of DAG by PLC in response to repetitive changes in $[\text{Ca}^{2+}]_i$. In addition, translocation of the whole PKC protein was found to closely follow Ca^{2+} increases and to promote Ca^{2+} oscillations by providing negative feedback on $\text{G}\alpha_q$ and PLC activity [Codazzi et al., 2001]. Such data fit the ‘dynamic uncoupling’ model, in which PKC, activated by Ca^{2+} and DAG, exerts negative feedback on the generation of InsP_3 via a reduction in stimulus strength. Ca^{2+} oscillations triggered by addition of glutamate in cells stably transfected with the metabotropic glutamate receptor mGluR5 coincided both with oscillations in $[\text{InsP}_3]_i$ and oscillatory changes in PKC localization. Translocation of PKC to the plasma membrane was furthermore correlated with a drop in the density of functional receptors. Subsequent receptor dephosphorylation led to a novel increase in $[\text{InsP}_3]_i$ resetting the cycle for the next round.

Normally, the Ca^{2+} oscillation frequency will increase with increasing stimulus strength no matter whether $[\text{InsP}_3]$ oscillates or not [Politi et al., 2006; Sneyd et al., 2006]; however, the dynamic uncoupling model is an exception to this rule. Oscillations appear like an ‘all-or-nothing’ response: once a concentration of agonist has been reached that initiates Ca^{2+} oscillations, both the frequency and amplitude are essentially insensitive to further increases in agonist concentration [Bird et al., 1993; Nash et al., 2002; Nash et al., 2001] (**figure 14A**). Instead, frequency modulation of such oscillations occurs through the interaction with positive or negative allosteric modulators of GPCRs [Bradley et al., 2009]. Modeling studies performed by Kang *et al.* indicate that the equilibrium between PLC and PKC activity determines the transition between $[\text{InsP}_3]_i$ -dependent and -independent oscillations. When these two components are out of balance, either minor, subthreshold $[\text{Ca}^{2+}]_i$ elevations (PKC > PLC) or peak-plateau patterns (PLC > PKC) will appear (**figure 14B**). Mathematical models as well experimental evidence indicate that cessation of InsP_3 turnover by introducing an InsP_3 buffer abolishes Ca^{2+} oscillations. Such a buffer would delay cytosolic InsP_3 build-up while at the same time slowing down InsP_3 degradation by the 3-kinase [Politi et al., 2006] that converts InsP_3 into the inactive inositol (1,3,4,5) tetrakisphosphate (InsP_4). This kinase is activated by Ca^{2+} as well (via CaM and CaMKII), adding an extra feedback loop; however, with this mechanism at play, InsP_3 oscillations would not trigger but rather tend to passively follow Ca^{2+} oscillations [Dupont et al., 2007; Politi et al., 2006].

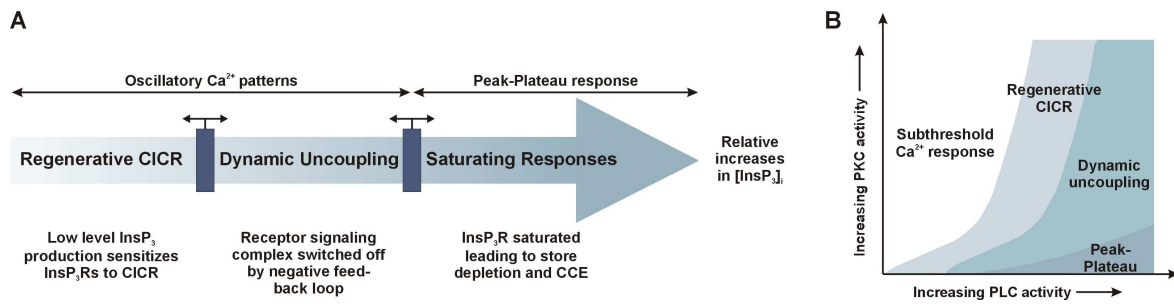


Figure 14. The InsP_3 -induced $[\text{Ca}^{2+}]_i$ signaling slide rule. (A) The large arrow indicates that there is a continuum of Ca^{2+} responses to relative increases in $[\text{InsP}_3]_i$ with three distinct types of Ca^{2+} signals. The position of the two sliders is determined by the extent of feedback inhibition on GPCR signaling or PLC activity and could vary for every receptor in each cell background. (B) GPCR signaling and PLC activity are both subject to negative feedback provided by PKC. As such, the position of the sliders is also determined by the balance between PKC and PLC activity. Adapted from [Nash et al., 2002] and [Kang and Othmer, 2007].

	Regenerative CICR	Dynamic uncoupling
Appearance	Baseline spiking	Sinusoidal oscillations
Frequency	Fast (< 1/min)	Slow (> 1/min)
Amplitude	Constant	Function of agonist concentration
Agonist	Low concentration	High concentration
PLC activity	Low	High
InsP_3 level	Low, constant	High, oscillating
Feedback	Provided by Ca^{2+}	Provided by PKC

Table 5. A comparison of the two modes of Ca^{2+} oscillations. Summary of the described features of oscillations depending on CICR only and oscillations depending on fluctuating levels of InsP_3 . Table adapted from [Kang and Othmer, 2007].

Role of Ca^{2+} entry in the Ca^{2+} oscillation mechanism

With no conclusions drawn on the primary Ca^{2+} oscillator, in addition no clear role for Ca^{2+} entry in the oscillation mechanism has been put forward. Indeed, neither the role nor the nature of Ca^{2+} entry during oscillations has been clarified. In different cell types oscillations promptly cease or gradually run down when extracellular Ca^{2+} is depleted. Others observe continued oscillations, though with a marked change in spiking frequency [Harks et al., 2003b; Jones et al., 2008; Lewis and Cahalan, 1989; Martin and Shuttleworth, 1994; Reetz and Reiser, 1996; Sacks et al., 2008]. Furthermore, treatment of parotid acinar cells or T-cells with thapsigargin, elicited Ca^{2+} oscillations that were independent of stored Ca^{2+} but relied entirely on Ca^{2+} entry and extrusion. The oscillations in $[\text{Ca}^{2+}]_i$ were consequent to

fluctuations in Ca^{2+} entry that on their turn resulted from negative feedback of Ca^{2+} itself on the entry channel [Dolmetsch and Lewis, 1994; Foskett and Wong, 1994]. Manipulation of the Ca^{2+} influx rate was found to modify the oscillation frequency: increasing extracellular Ca^{2+} levels accelerated the oscillation frequency in salivary gland cells stimulated by serotonin [Berridge, 2007]. On the other hand, oscillations could be sustained in the absence of extracellular Ca^{2+} , when blocking PMCA, but these oscillations did not give the same physiological outcome (*c-fos* expression) as the ones that occurred in the presence of Ca^{2+} entry, notwithstanding their same amplitudes and frequencies [Di Capite et al., 2009].

A Ca^{2+} spike is only possible when $[\text{Ca}^{2+}]_i$ is above the threshold necessary for activation of the InsP_3R . At the same time ER Ca^{2+} levels must be sufficiently high to provide the driving force for Ca^{2+} efflux from the store. The sum of ER Ca^{2+} and cytosolic Ca^{2+} , bound or unbound, is known as the Ca^{2+} load. Although $[\text{Ca}^{2+}]_i$ increases upon agonist stimulation, the total Ca^{2+} load will gradually decline as Ca^{2+} coming from the ER is extruded to the extracellular environment. Ca^{2+} entry thus serves to replenish lost Ca^{2+} ions and to overcome the threshold that is necessary for InsP_3R activation [Harks et al., 2003b; Martin and Shuttleworth, 1994; Sneyd et al., 2004]. Consistently, according to the luminal loading model, Ca^{2+} entry contributes to Ca^{2+} build-up in the ER to sensitize InsP_3R to low ambient InsP_3 and Ca^{2+} levels. The resulting Ca^{2+} spike is terminated by Ca^{2+} sequestration into the mitochondria and subsequently the ER. In this model, the rate of ER filling and hence the rate of Ca^{2+} influx determines the spiking frequency [Berridge, 2007].

As for the nature of Ca^{2+} entry during oscillations, different routes are possible, including CCE. When supramaximal receptor activation induces a peak-plateau type Ca^{2+} signal, the evidence for CCE, as discussed in 1.3.2.1, is fairly straightforward. However, when lower, more physiological concentrations of agonist elicit oscillations; its contribution is still a matter of debate. Theoretically, the cyclic emptying of the ER during oscillatory activity could produce an oscillating capacitative signal that replenishes the lost Ca^{2+} ions with each cycle and the rate of refilling would determine the oscillation frequency. Various data argue in favour for a role of CCE in the Ca^{2+} oscillation machinery. In primary rat hepatocytes stimulated with vasopressin, depletion of extracellular Ca^{2+} completely abolished oscillations. Gd^{3+} and 2-APB, two known CCE inhibitors, were insufficient to completely prevent Ca^{2+} oscillations but nevertheless reduced the spiking frequency. Knockdown of STIM-1, Orai1 or Orai3 had the same effect, at least indicating a partial involvement of CCE [Jones et al.,

2008]. Similar observations were made in metacholine-stimulated HEK293 cells [Bird et al., 2009; Wedel et al., 2007]. In the course of these oscillations, STIM-1 translocations and CCE occur in an oscillatory manner. Although STIM-1 is known to respond to rather large drops in the ER Ca^{2+} content, it could be so that STIM-1 responds to local drops instead of global decreases in luminal Ca^{2+} levels [Bird et al., 2009].

Yet, as reviewed by Shuttleworth (1999, 2003) there are some fundamental problems explaining a role for CCE during Ca^{2+} oscillations [Shuttleworth, 1999; Shuttleworth and Mignen, 2003]. Activation of CCE is a slow process, typified by a latency period before activation and a slow development of maximal influx. I_{CRAC} for instance, only develops after 20 to 50 seconds, which is not compatible with fast oscillations where spikes are only separated by several seconds. The second question is whether the ER is really depleted during oscillations. SERCA activity greatly exceeds PMCA activity and as a result most Ca^{2+} will be recaptured in the ER. Yet, even under these conditions it was observed that Ca^{2+} influx accompanies Ca^{2+} oscillations and changing the rate of Ca^{2+} influx affected oscillation frequency [Shuttleworth, 1999; Shuttleworth and Mignen, 2003]. In addition to CCE, it was shown that intracellular messengers like DAG, arachidonic acid, and leukotrienes, which accumulate during physiological stimulation, can activate Ca^{2+} influx through channels distinct from SOC [Bootman et al., 2002]. Arachidonate-regulated Ca^{2+} channels (ARC) represent one example of these non-SOC Ca^{2+} influx channels that are activated upon stimulation with low doses of agonist [Luo et al., 2001]. Like CRAC channels, ARC channels are highly Ca^{2+} selective, low conductance channels, formed by Orai1/3 and associate with STIM-1, the latter being located in the plasma membrane instead of the ER membrane [Mignen et al., 2007; Mignen et al., 2009]. The levels of arachidonic acid that activate ARC channels lie within the physiological range (2-8 μM) and may result from activation of phospholipase A2 (PLA2) or from DAG metabolism. Stimulation of ARC is achieved either by arachidonic acid itself (direct, fast pathway) or by arachidonic acid-derived NO (tardy, indirect pathway) [Mottola et al., 2005]. By using increasing concentrations of Orexin-A to stimulate HEK293 cells, it was shown that receptor activation promotes two independent oscillatory responses: at low nanomolar concentrations oscillations depend on ARC channels, whereas a Ca^{2+} entry-independent, repetitive Ca^{2+} discharge from the ER (the intrinsic pathway) drives oscillations with higher agonist concentrations [Peltonen et al., 2009]. Indeed, at low agonist concentrations, specific stimulation of ARC channels provides Ca^{2+} entry that, together with low levels of InsP_3 , initiates the cyclical discharge and refilling of the ER. CCE is not at play

here because stores are not sufficiently depleted to produce a capacitative signal [Mignen et al., 2001]. Finally, In *C. elegans* intestinal epithelial cells, spontaneous Ca^{2+} oscillations did not thrive on CCE as STIM-1 knockdown had no effects on the InsP_3 -driven rhythmic contractions of the intestine [Yan et al., 2006]. Instead, these oscillations involve Ca^{2+} entry via the *C. elegans* TRPM channel homologues GON-2 and GTL-1 that are subject to negative feedback of both Ca^{2+} and PIP_2 . These channels were found not to interact with STIM-1 or Orai1 and do not serve to replenish Ca^{2+} but rather to promote CICR [Xing and Strange, 2010]. Likewise, non-SOC TRP channels that are activated by OAG (a DAG analogue) have been shown to sustain Ca^{2+} oscillations in astrocytes and carbachol-stimulated HEK cells [Grimaldi et al., 2003; Wu et al., 2002]. Interference with TRPC1 channel expression or activity indicated that these channels are involved in sustaining Ca^{2+} oscillations triggered by amino acid stimulation of the Ca^{2+} -sensing receptor. These oscillations do not involve the PLC/ InsP_3 axis; instead, TRPC1 Ca^{2+} entry is activated via the small GTPase Rho and potentiated by the resulting increase in $[\text{Ca}^{2+}]_i$. Negative feedback is provided by CaM [Rey et al., 2006]. In these last two examples it can be presumed that Ca^{2+} entry itself occurs in an oscillatory manner, thus giving rise to oscillations in $[\text{Ca}^{2+}]_i$.

Other players of the Ca^{2+} oscillation machinery

Ca²⁺ extrusion and reuptake. In $\text{SERCA}^{2+/-}$ mice the oscillation frequency was reduced due to the increase in time needed for store reloading [Zhao et al., 2001]. Mathematical modeling confirmed that increased SERCA expression decreases the period length of oscillations and that reuptake in the ER itself can be rhythmic, giving rise to Ca^{2+} oscillations [Dellen et al., 2005]. In another example, expression of PMCA2a and PMCA3f, that exhibit high Ca^{2+} activation rates, could give rise to fast Ca^{2+} oscillations, whereas other PMCA isoforms, typified by a slower activation, produce slow oscillations [Caride et al., 2001].

Mitochondria. As discussed in 1.3.2.1, mitochondria function as a Ca^{2+} sink for ER-derived Ca^{2+} and this shuttling of Ca^{2+} ions between the ER and mitochondria appears to be prerequisite for the appearance of Ca^{2+} oscillations. Indeed, cytosolic Ca^{2+} oscillations are associated with periodic changes in the Ca^{2+} concentration in both the ER and mitochondria [Ishii et al., 2006]. As studies in histamine-stimulated HeLa cells reveal, the involvement of mitochondria in the oscillation mechanism probably goes like this: the initial transient after agonist application is entirely dependent on InsP_3 -mediated Ca^{2+} release from the ER but

during this phase, Ca^{2+} is rapidly sequestered in the mitochondria, blunting the maximal $[\text{Ca}^{2+}]_i$ peak. In order to fulfill this function, mitochondria are strategically located near the InsP_3R release channels (~10 nm - [Csordas et al., 2006]) where they are exposed to a local $[\text{Ca}^{2+}]_i$ that exceeds bulk values in the cytosol. By accumulating Ca^{2+} , they create a very low local $[\text{Ca}^{2+}]_i$ at the InsP_3R mouth which promotes Ca^{2+} release and prevents negative feedback [Chalmers and McCarron, 2008; Ishii et al., 2006]. Ca^{2+} released from the mitochondria will sensitize the InsP_3R initiating the regenerative release of Ca^{2+} from the ER that is taken up by the mitochondria again. Interfering with either mitochondrial Ca^{2+} uptake or release abolished the oscillations, altogether indicating the pivotal role of mitochondria in the generation of Ca^{2+} oscillations [Ishii et al., 2006]. Modeling studies indicate that mitochondria also contribute to maintain the spike amplitude at a constant level when increasing the spiking frequency. When mitochondria are omitted from the model, amplitudes vary tremendously. In addition, mitochondria prolong the period of oscillations [Marhl et al., 1998]. Oppositely, inhibition of mitochondrial Ca^{2+} uptake, by uncoupling the electron transport chain, decreased the oscillation frequency in dorsal root ganglion neurons. However, the authors attributed this effect to a diminished level of ATP that is necessary for SERCA activity [Jackson and Thayer, 2006]. Finally, it was shown that mitochondrial reactive oxygen species (ROS) production aids in the oscillatory process by sensitizing InsP_3 -mediated Ca^{2+} release. When cells were treated with antioxidants, Ca^{2+} oscillations were abolished [Camello-Almaraz et al., 2006].

1.3.2.2 Propagation of Ca^{2+} signals

In multicellular organisms, intracellular Ca^{2+} waves are usually not restricted to one cell but propagate to adjacent cells as an intercellular Ca^{2+} wave. Intercellular Ca^{2+} waves have been identified in many cell types where they spread with a velocity of 10-40 $\mu\text{m}/\text{sec}$, depending on the nature and strength of the initiating trigger [Dupont et al., 2007; Iino, 2010; Leybaert and Sanderson, In Press]. During the last decade, intercellular Ca^{2+} waves were also observed *in vivo* (in astrocytes), propagating with a slightly lower velocity (8-10 $\mu\text{m}/\text{sec}$) [Tian et al., 2006]. Two mechanisms support cell-to-cell communication of Ca^{2+} signals. The first mechanism involves the diffusion of InsP_3 or Ca^{2+} itself through gap junction channels [Boitano et al., 1992] (**figure 15**). Mechanical stimulation of tracheal airway epithelial cells elicited an intercellular Ca^{2+} wave that was blocked by the gap junction uncoupler halothane [Sanderson et al., 1990] and by connexin mimetic peptides [Boitano and Evans, 2000],

highlighting the involvement of gap junctions. These waves were also present when no Ca^{2+} was added to the cells' extracellular environment indicating that Ca^{2+} must come from intracellular stores and that therefore, InsP_3 must be implicated [Sanderson et al., 1990]. InsP_3 is a soluble, low-molecular weight molecule (486 Da) that easily diffuses through gap junction channels (see 1.2.2: 'Permeability and pore selectivity of connexin channels'). The high Ca^{2+} buffering capacity of the cytoplasm slows down the diffusion of Ca^{2+} ions so that the movement of intercellular Ca^{2+} waves across the cell border is more likely to be dependent on the diffusion of InsP_3 through the channels. Indeed, the diffusion constant of Ca^{2+} is ~15 times smaller than that of InsP_3 (~20 $\mu\text{m}^2/\text{sec}$ versus ~300 $\mu\text{m}^2/\text{sec}$). InsP_3 that diffuses through the gap junctions is subject to a small delay (0.5-1 sec) corresponding to the diffusion time in the gap junction [Sanderson et al., 1990], and can only elicit a Ca^{2+} increase in the adjacent cell when it reaches a minimal threshold (~10-30 nM) that is necessary to trigger CICR [Goldberg et al., 2010; Rottingen and Iversen, 2000]. Moreover, the occurrence of intercellular Ca^{2+} waves seems to rely on the proper localization of ER/ InsP_3 Rs and InsP_3 -metabolizing enzymes. In the vessel wall for instance, InsP_3 moves unidirectionally across myoendothelial junctions from smooth muscle cells to endothelial cells. Such unidirectional Ca^{2+} communication is due to the selective localization of the ER and the type 1 InsP_3 R in the immediate surroundings of the endothelial gap junction channels. In smooth muscle cells, no InsP_3 Rs reside close to the gap junctions; instead, elevated levels of 5-phosphatase in the vicinity of gap junctions degrade endothelium-derived InsP_3 before it can activate InsP_3 Rs that lay further away from the gap junction plaque. The latter data also imply that InsP_3 must be produced near the gap junction channel mouth in order to avoid degradation before it can be passed on to endothelial cells [Isakson, 2008]. Finally, gap junction-dependent waves imply a gradient of InsP_3 across the cytoplasm of neighboring cells that decreases with increasing distance to the initiation site [Strahonja-Packard and Sanderson, 1999]. Such an InsP_3 gradient was also shown to initiate Ca^{2+} oscillations when passing by in a cell culture. The cell's Ca^{2+} response was dependent on the distance from the origin of the wave, with InsP_3 levels too high (closest to origin) or too low (farthest away from origin) failing to produce oscillations. In addition, within the zone of oscillating cells, the oscillation features changed with distance [Strahonja-Packard and Sanderson, 1999]. The potency of triggering Ca^{2+} oscillations in the aftermath of an intercellular Ca^{2+} wave is furthermore dependent on the connexin expressed. Expression of Cx43 or Cx46 in HeLa cells nearly abolished UTP-triggered Ca^{2+} oscillations whereas the presence of Cx45 promoted repetitive Ca^{2+} spiking, as was seen in the parental HeLa cells that do not express connexins. Conceivably, the greater

ability of Cx43 and Cx46 gap junctions to allow for diffusion of a small signaling molecule like InsP_3 , accounts for this effect [Lin et al., 2004]. Finally, cADPR (541 Da) was found to diffuse through gap junctions and propagate Ca^{2+} signals between lens epithelial cells. However, incubation with a PLC inhibitor prevented intercellular Ca^{2+} waves indicating that cADPR-mediated waves still depend on InsP_3 [Churchill and Louis, 1998].

The second mechanism for Ca^{2+} wave propagation between cells is based on paracrine signaling and involves the release of a Ca^{2+} mobilizing messenger that diffuses into the extracellular space, binds to its receptors on neighboring cells and activates downstream signaling cascades that lead to an increase of $[\text{Ca}^{2+}]_i$ in the target cell [Hassinger et al., 1996] (**figure 15**). Whereas gap junction propagated intercellular waves appear to follow a convoluted path, paracrine waves are expected to propagate in a more homogenous, circular manner although heterogeneities in receptor density might render the propagation route more complex. The first evidence for the involvement of an extracellular messenger came from the observation that an intercellular Ca^{2+} wave triggered by mechanical stimulation of astrocyte cultures was able to cross a cell-free zone ($< 120 \mu\text{m}$ in width). These waves could furthermore be abolished by perfusion of the bathing medium [Hassinger et al., 1996]. The existence of paracrine Ca^{2+} signaling was further emphasized by the observation that addition of astrocyte conditioned medium to a separate culture dish was sufficient to trigger intercellular Ca^{2+} waves [Guthrie et al., 1999]. In most cases, the Ca^{2+} mobilizing messenger was identified as ATP, but other messengers like glutamate, NAD^+ , NO, or InsP_3 and Ca^{2+} themselves, have also been suggested [Bruzzone et al., 2001b; Franco et al., 2001; Gossman and Zhao, 2008; Hofer et al., 2000; Pasti et al., 2001]. These messengers can be released from the cells via multiple routes including secretory vesicles ('regulated' exocytosis), connexin/pannexin hemichannels, P2X_7 receptor channels, cystic fibrosis transmembrane regulator, multidrug resistance (MDR) transporters, voltage-gated or volume-regulated anion channels, maxi-anion channels and the maitoxin-activated pore [Evanko et al., 2004; Faria et al., 2009; Hisadome et al., 2002; Liu et al., 2008a; Praetorius and Leipziger, 2009; Schwiebert and Zsembery, 2003; Suadicani et al., 2006; Takeuchi et al., 2006; Zhao et al., 2010]. Connexin hemichannels stepped into the field after the observation by Cotrina et al. (1998) that although inter-astrocytic Ca^{2+} waves were independent of gap junctions, travelling through cell-free zones, they still required the expression of connexins. Inhibition of the waves by purinoceptor inhibitors or by the ectonucleotidase apyrase suggested that ATP was the extracellular messenger involved, and that it was released by connexin hemichannels

[Cotrina et al., 1998b]. This was confirmed later in other glial cultures [Braet et al., 2003b; Stout and Charles, 2003; Stout et al., 2002] as well as in endothelium from cornea, pulmonary artery or kidney [Gomes et al., 2006; Moerenhout et al., 2001; Toma et al., 2008]. Paracrine intercellular Ca^{2+} communication was also observed in cochlear epithelium *in situ* where it was entirely dependent on the expression of Cx26 and Cx30 [Anselmi et al., 2008]. Latest evidence indicates that ATP is released as point source bursts from a selective number of cells that display hemichannel responses. These clouds of ATP extend radially, 3 to 4 cell rows away from the pacemaker cells [Arcuino et al., 2002]. Glutamate-dependent signaling was shown in mechanically stimulated astrocyte cultures. The resulting intercellular Ca^{2+} waves were accompanied by a radially expanding wave of glutamate release that travelled at the same speed as the Ca^{2+} wave (26 $\mu\text{m}/\text{sec}$) [Innocenti et al., 2000]. The mechanism of glutamate release from astrocytes has been shown to be exocytotic [Pasti et al., 2001] or hemichannel-mediated [Ye et al., 2003]. Although NAD^+ is not a true Ca^{2+} mobilizing messenger but is converted to the RyR agonist cADPR, it has been shown to mediate the propagation of intercellular Ca^{2+} waves in 3T3 fibroblasts and glia. NAD^+ is transported out of the cell by Cx43 hemichannels and is converted into cADPR that is taken up again by CD38. As such, cADPR can elevate $[\text{Ca}^{2+}]_i$ in neighboring cells [Bruzzone et al., 2001b; Franco et al., 2001]. In addition, NAD^+ has also been shown to produce Ca^{2+} oscillations by acting in an autocrine manner in glial cells and to be responsible for Ca^{2+} -sensitive glutamate release that is used for communication with neurons [Verderio et al., 2001a]. To prevent apoptotic Ca^{2+} levels, Ca^{2+} itself feeds back to the hemichannels (via PKC) to limit further NAD^+ release [Bruzzone et al., 2001a; Bruzzone et al., 2001b]. The release of InsP_3 through hemichannels was only revealed recently and needs further characterization [Gossman and Zhao, 2008] but its paracrine role is at least supported by the identification of InsP_3R at the plasma membrane: cell-surface biotinylation studies estimate that 5-14% of the total cellular InsP_3R resides at this location [Patterson et al., 2004].

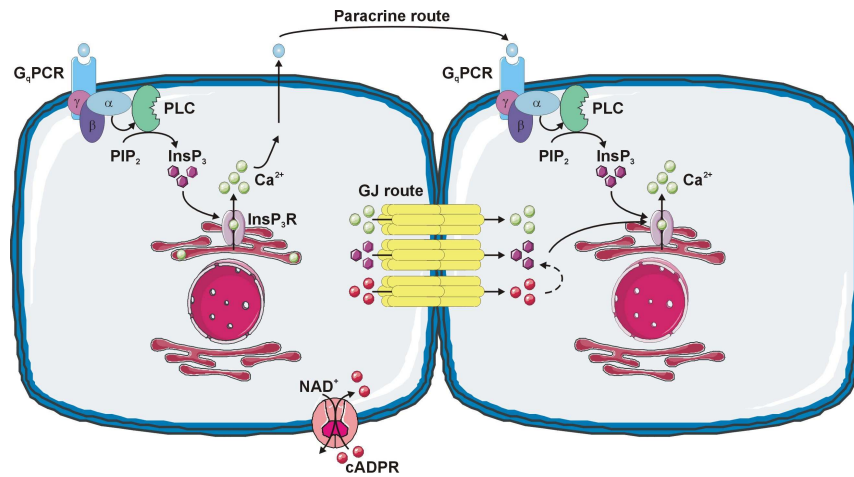


Figure 15. Intercellular Ca^{2+} wave propagation routes. Intercellular Ca^{2+} waves are supported by two routes, a direct one involving gap junctions, and an indirect one involving the release of a paracrine messenger. InsP_3 , cADPR and Ca^{2+} itself could diffuse through gap junctions and elicit an increase in $[\text{Ca}^{2+}]_i$ in the adjacent cell. With paracrine signaling, a Ca^{2+} mobilizing messenger is released into the extracellular environment via multiple possible mechanisms. It diffuses in the extracellular space and binds to its corresponding receptor on the neighboring cell. For details on the nature of the paracrine messenger and its mode of release, we refer the reader to the text. This figure was produced using Servier Medical Art.

Intercellular Ca^{2+} waves that rely on a gradient of intracellular InsP_3 or a gradient of an extracellular released messenger are expected to propagate over a limited distance due to messenger metabolism; however, Ca^{2+} is able to potentiate InsP_3 production and/or messenger release (known as regeneration) so that intercellular waves propagate perpetually, at least in theory. In reality though, intercellular waves rely on a combination of passive and self-sustained mechanisms and will eventually fade out [Dupont et al., 2007]. Regeneration of InsP_3 depends on its Ca^{2+} -triggered synthesis by PLC [Dupont et al., 2007] and most messenger release pathways can be self-sustained as well. As we described in 1.2.3.2.3, connexin hemichannel responses depend on $[\text{Ca}^{2+}]_i$. In addition, regulated exocytosis uses the SNARE protein complex that contains a Ca^{2+} sensor protein (synaptotagmin) [Malarkey and Parpura, 2008] rendering it sensitive to changes in $[\text{Ca}^{2+}]_i$ [Kreft et al., 2004; Pangrsic et al., 2007]. Exocytosis of glutamate from astrocytes was dependent on $[\text{Ca}^{2+}]_i$ that had to exceed 550 nM [Pasti et al., 2001]. ATP release from smooth muscle cells through MDR transporters was reduced when cells were treated with inhibitors of the Ca^{2+} signaling cascade or when intracellular Ca^{2+} was chelated [Sun et al., 2010]. For the other release mechanisms, the role of $[\text{Ca}^{2+}]_i$ is less clear but regenerative ATP-induced ATP release can also occur independent of changes in $[\text{Ca}^{2+}]_i$, purely relying on activation of P2X_7 purinoceptors and release through

these same receptors [Anderson et al., 2004]. Paracrine cell-cell communication in taste bud cells was found dependent on Panx1 hemichannel ATP release with the activation of Panx1 hemichannels triggered by an ATP-induced increase in $[Ca^{2+}]_i$ [Huang et al., 2007]. Especially for ATP a regenerative mechanism is of utmost importance as ATP is degraded rapidly by ectonucleotidases.

The two routes of Ca^{2+} wave propagation need not to be mutually exclusive. In most cases intercellular waves are sustained synergistically by the gap junctional and paracrine mechanism with one of them as the dominant mechanism, depending on the cell type involved [Charles et al., 1991; Goldberg et al., 2010; Isakson et al., 2001; Paemeleire et al., 2000; Scemes and Giaume, 2006]. In the cochlear epithelium it was shown that in the cell row adjacent to the stimulated cell, $[Ca^{2+}]_i$ increases in a gap junction dependent manner whereas $[Ca^{2+}]_i$ in cells lying further away from the trigger zone are affected by paracrine mechanisms [Anselmi et al., 2008]. In addition it was found that the mode of propagation can adapt itself depending on the presence of connexins. In spinal cord astrocytes (expressing Cx43) the gap junction pathway seems to overrule the paracrine mechanism, but when connexins are absent (KO cells), the receptor repertoire of the cells changes and the paracrine route takes over [Scemes et al., 2000]. Furthermore, work with cornea endothelium indicated that both pathways influence each other. Inhibition of paracrine signaling alone reduced the wave's active area ~90 % but inhibiting gap junctions alone reduced the active area about 60 %. The authors ascribe these, at first sight conflicting results to a mutual influence of paracrine signaling on the gap junctional pathway and *vice versa*. Obviously, both pathways share common messengers and so blocking gap junctions would result in lower $InsP_3$ and Ca^{2+} levels in adjacent cells with reduced ATP release as a result [Gomes et al., 2006].

In 1.2 we described that increasing $[Ca^{2+}]_i$, either to physiological or non-physiological levels, closes gap junction channels, leaving a major issue to solve: if elevated levels of $[Ca^{2+}]_i$ uncouple gap junction channels, how then is it possible that gap junctions mediate the propagation of intercellular Ca^{2+} waves? A possible explanation might be found in the varying inhibitory $[Ca^{2+}]_i$ that have been reported (1.2.3.2.3), although it is not clear why such variation exists between different cell types. Furthermore, the measured $[Ca^{2+}]_i$ usually reflects a global value whereas the actual concentration at the mouth of the gap junction can be quite different. Finally, the time frame in which $[Ca^{2+}]_i$ is elevated might determine the extent of Ca^{2+} -inhibition. Indeed, Ca^{2+} -gating of gap junctions is a rather slow process

(minutes), especially at near physiological $[Ca^{2+}]_i$ [Lazrak and Peracchia, 1993], while intercellular Ca^{2+} waves propagate much faster (20-300 $\mu m^2/sec$). When pancreatic acinar cells were stimulated with acetylcholine, gap junctional currents were inhibited minutes after the observation of the initial Ca^{2+} transient, when $[Ca^{2+}]_i$ had reached a plateau phase, due to CCE [Chanson et al., 1999]. In support, Churchill and colleagues (2001) indicated that an intercellular Ca^{2+} wave brought about by ATP or mechanical stimulation was unable to inhibit dye coupling when transiently passing through adjacent cells. Gap junctional communication was only reduced minutes after the Ca^{2+} wave had passed by and is believed to be achieved by the activation of kinases. In contrast, a sustained increase elicited by application of ionophore, reduced cell coupling within tens of seconds. Importantly, the magnitudes of the $[Ca^{2+}]_i$ elevation in all experimental approaches were in the same range (± 550 nM) [Churchill et al., 2001].

1.4 ENDOTHELIAL Ca^{2+} DYNAMICS AND BLOOD-BRAIN BARRIER FUNCTION

1.4.1 THE BLOOD-BRAIN BARRIER

The term blood-brain barrier (BBB) refers to the structurally and functionally unique microvasculature of the central nervous system (CNS). It is a highly selective lipophilic barrier between the systemic blood circulation and the brain tissue and plays an essential role in brain homeostasis, which is crucial for normal neuronal and glial activity and function. Reliable electrical signaling in the brain requires a strict composition of the ionic microenvironment around synapses and axons, which is maintained by the BBB. The BBB also prevents exo- or endogenous toxins from entering the brain and separates peripheral and central neurotransmitter pools. Indeed, nearly all neurotransmitters are polar molecules and have a very limited permeability through the barrier. In addition, regions of the brain that are rich in synapses have a high metabolic rate and thus a high level of blood flow. It would be counter-productive and economically unfavourable if a neurotransmitter were to be immediately washed away by the circulation. Thanks to the BBB, neurotransmitters are retained in the local interstitial fluid to be recycled by local reuptake mechanisms [Abbott et al., 2010; Bradbury, 1993].

The vertebrate barrier is formed by brain microvessel endothelial cells, mostly in capillaries but also extending, although less documented to what extent, in arteriolar and venular direction [Abbott et al., 2006; Bechmann et al., 2006]. In pre- and post capillary segments, where endothelial BBB characteristics are less pronounced, the barrier function is aided by phagocytic scavenging in the vessel wall and perivascular spaces [Bechmann et al., 2006; Ge et al., 2005]. The BBB is absent from circumventricular organs which require significant cross-talk between the brain and peripheral blood, e.g. for the secretion of hormones to blood or for monitoring of blood composition (for instance the blood glucose concentration) [Ballabh et al., 2004].

1.4.1.1 The blood-brain barrier from a historical point of view

More than a century ago (1885), the German immunologist Paul Ehrlich initiated BBB research after the incidental observation that vital aniline dyes stained nearly all organs with

the exception of the CNS. Ehrlich ascribed this effect to lower binding affinities of the CNS tissue for these dyes. This theory was later abandoned as ferrocyanide was lethal at low doses when injected directly into the CNS, but when systemically injected, 100-fold higher doses were required to obtain the same effect. Based on these observations, Lewandowski introduced the term 'Bluthirnschranke' or 'blood-brain barrier'. Around the same time (1909), Ehrlich's pupil Goldman provided evidence that the staining of the CNS was possible when dyes were injected into the ventricular system. Despite continuous research on this topic, it was only in the late 1960s, with the development of electron microscopy, that the site of the mammalian BBB could be determined. The inability of horseradish peroxidase (HRP), a 40 kDa glycoprotein, to diffuse into the brain tissue was caused by a continuous belt of tight junctions between brain capillary endothelial cells. They further characterized the lack of pinocytotic vesicles in these endothelial cells (See [Bechmann et al., 2006] and [Ribatti et al., 2006] and references therein).

1.4.1.2 Blood-brain barrier anatomy

The endothelial cells of the BBB function as gatekeepers, controlling the passage of blood molecules and cells across the vessel wall. Small gaseous or lipophilic molecules like O₂, CO₂, ethanol, caffeine and nicotine can freely diffuse over the BBB whereas the paracellular passage of polar and lipid-insoluble molecules is generally restricted by a junctional complex that connects adjacent endothelial cells in a zipper-like manner and that contains tight junctions, adherens junctions and gap junctions [Dejana et al., 2001] (**figure 16**). This intricate network of interendothelial junctions constitutes the physical BBB.

1.4.1.2.1 Tight junctions

Tight junctions or *zonulae occludentes* are domains of occluded intercellular clefts that in freeze-fracture replicas form an elaborate complex of parallel, anastomosing intramembranous horizontal strands of proteins arranged as a series of multiple barriers. They polarize the cell (fence function) and restrict the passage of water, ions and molecules (gate function) [Ek et al., 2006; Ribatti et al., 2006]. By limiting the movement of ions and charged molecules between the blood and the brain a high transendothelial electrical resistance (TEER) can be measured in the brain capillaries. Electrical resistance measured in frog pial

capillaries amounts $1900 \Omega \cdot \text{cm}^2$ whereas values measured in rat cerebral capillaries are in the range of $3000 \Omega \cdot \text{cm}^2$ [Bradbury, 1993]. In comparison, peripheral microvessels have values 100 times smaller. Tight junctions appear already present between endothelial cells of the very first vascular sprouts that invade the neural tube. Although these early vessels display an enlarged diameter and irregular shape, the absence of plasma proteins in the brain interstitium as well as the impermeability of 3 kDa biotin-dextran suggests that paracellular diffusion is restricted and that junctions are sufficiently well developed to exclude these proteins and markers from the fetal brain parenchyma [Ek et al., 2006; Saunders et al., 2008]. However, rat embryos do show a low TEER and can therefore be regarded as immature [Wolburg and Lippoldt, 2002]. Further maturation of the barrier arises from progressive changes in the tight junction morphology which is initiated by interactions between endothelial cells and their surrounding partners (see 1.4.1.3: ‘The neurovascular unit’) [Ek et al., 2006; Engelhardt, 2003; Saunders et al., 2008; Saunders et al., 1999].

Tight junctions are composed of 3 transmembrane proteins: claudins, occludin and proteins of the junctional adhesion molecule family (JAM). Claudins are a family of transmembrane proteins (20-24 kDa) of which more than 24 different isoforms are identified [Furuse et al., 1999]. Claudin-3, -5 and -12 appear to constitute the backbone of the tight junctional barrier [Lippoldt et al., 2000; Nitta et al., 2003; Wolburg and Lippoldt, 2002], but claudin -2, -11, and -18 have been identified as well [Cardoso et al., 2010]. Tight junctions always consist of homophilic interactions and the restricted cell-specificity of claudins possibly indicates selective cell-cell recognition and/or specific functional properties of the cells [Dejana et al., 2009]. Occludin was the first transmembrane tight junction protein discovered [Furuse et al., 1993] but it seems not necessary for the formation of tight junctions as such [Saitou et al., 2000]. Well-developed networks of tight junction strands were observed in occludin^{-/-} animals [Saitou et al., 2000]. Rather, its expression is correlated with tight junction sealing as it increases electrical resistance [Davies, 2002; McCarthy et al., 1996]. Furthermore, occludin itself cannot constitute organized strands but is instead incorporated into claudin-based strands [Furuse et al., 1998]. Strong occludin expression, like in the epithelium, is only observed in BBB endothelium whereas only trace amounts are observed in endothelial cells of peripheral tissue (aorta). Still, these peripheral cells show well-formed tight junctions, albeit with lower TEER [Hirase et al., 1997]. Mature BBB endothelial cells thus use occludin to regulate rather than to establish their barrier properties. The JAM family consists of various members (JAM-1/A, JAM-2/B and JAM-3/C) that mediate homo- and heterophilic

interactions in the tight junctional region, establishing the early attachment of adjacent cell membranes [Ebnet et al., 2004; Martin-Padura et al., 1998]. First- and second-order cytoplasmic adaptor proteins are associated with the transmembrane components and act as scaffolds for the cytoskeletal and signaling molecules. ZO (zonula occludens) proteins are the prototypic example of a first-order adaptor protein. ZO-1, -2 and -3 are members of the MAGUK family (membrane associated guanylate kinases) that are characterized by an N-terminal array of protein binding domains that include the Src Homology domain (SH3), the guanylate cyclase (GUK) domain and the PDZ (post synaptic density protein-drosophila disc large tumor suppressor-zonula occludens) domain. These domains play an important role in signal transduction and in anchoring the tight junction proteins to the cytoskeleton, either via direct interaction with actin [Itoh et al., 1997] or indirectly via binding to second-order adaptor proteins [Itoh et al., 1991]. This association is not only important for stabilization of the junctions, but also for the dynamic regulation of junction opening and closure [Dejana, 2004].

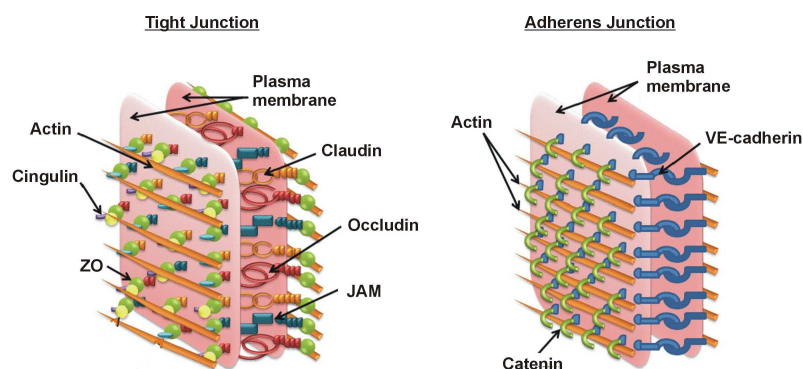


Figure 16. Endothelial junctions in the BBB. Tight and adherens junctions seal the intercellular gap between endothelial cells, restricting paracellular movement of solutes from blood to brain. These junctions consist of specialized transmembrane and adaptor proteins. The main building blocks of tight junctions are claudin, occludin and JAM that are linked to the actin cytoskeleton via first order (ZO) and second order (cingulin) adaptor proteins. Adherens junctions contain the transmembrane cadherins and cytosolic catenins. Figure adapted from [Cardoso et al., 2010].

1.4.1.2.2 Adherens junctions

Adherens junctions are formed at the early stages of cell-cell contact and are eventually followed by the formation of tight junctions [Dejana, 2004]. Adherens junctions are composed of transmembrane cadherins, which form homotypic adhesive complexes with

neighbouring cells in an extracellular Ca^{2+} -dependent manner [Baumgartner et al., 2000; Vestweber, 2000]. Endothelial cells of the BBB express the specific vascular endothelial (VE) cadherin which is not present in other cell types, and a small background of neural (N) cadherin. N-cadherin does not localize to interendothelial adherens junctions but rather recruits other cell types to the endothelial cell [Komarova and Malik, 2010]. VE-cadherins are linked to actin by the cytoplasmic α , β - and p120-catenin and are additionally linked to the major endothelial intermediate filament protein vimentin by plakoglobin (γ -catenin) and desmoplakin [Shasby et al., 2002]. The latter were also shown to be expressed in primary brain capillary endothelial cells [Fischer and Kissel, 2001; Shibata et al., 2005].

In addition to this physical BBB, endothelial cells also provide a metabolic and enzymatic barrier. The former consists of a strictly regulated ensemble of transporters expressed on both the luminal and abluminal endothelial membrane. These highly specific transport mechanisms are responsible for uptake of essential hydrophilic nutrients like glucose (GLUT-1) and amino acids (A-, L-, EAA-transporters etc.). Larger molecules like insulin, leptin and iron transferrin require receptor-mediated endocytosis to reach the brain tissue. Lipophilic compounds that freely cross plasma membranes, theoretically, easily invade the brain parenchyma. However, the entry of these molecules is counteracted by a second line of defence that contains extrusion pumps. These pumps belong to the superfamily of ATP-binding cassette proteins, consuming plenty of energy; therefore, the BBB endothelium is highly enriched in mitochondria [Cardoso et al., 2010; Persidsky et al., 2006]. Many of the BBB extrusion pumps are classified as MDR proteins with the major MDR in the BBB being MDR1 or P-glycoprotein (P-gp). P-gp recognizes and extrudes a highly diverse set of compounds but thus far, the only common structural denominator is that all of the transported compounds are lipophilic or at least amphipathic in nature [Schinkel, 1999]. Another level of protection is provided by the enzymatic barrier which is responsible for metabolic conversion of lipophilics that could otherwise 'sneak' through the BBB, adversely affecting neuronal functions. These enzymes include γ -glutamyl-transpeptidase, alkaline phosphatase, hydrolases, aromatic decarboxylase, glutathione-S-transferase, cytochrome P450 and UDP-glucuronosyltransferases [Ge et al., 2005; Ghersi-Egea et al., 1995; Persidsky et al., 2006].

1.4.1.3 The neurovascular unit

During the last 2 decades, the concept of the BBB has evolved from one of a mere endothelial barrier (described in 1.4.1.2) to a more integrative view in which the BBB is regarded a modulatory interface between the blood and the brain. The BBB in this extended form describes a number of processes that take place in the neurovascular unit, a functional unit composed of the capillary endothelium and its basement membrane, and herewith associated astrocytes, pericytes and neurons [Lok et al., 2007. Abbott, 2006 #641] (**figure 17**).

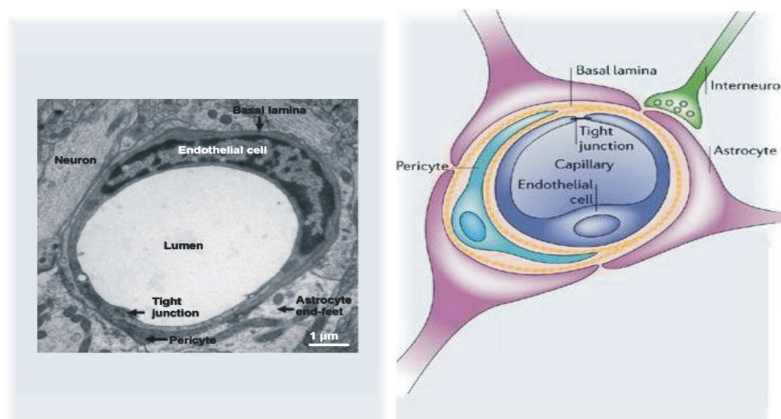


Figure 17. The neurovascular unit. Electron microscopy image and schematic diagram of the neurovascular unit. Capillary endothelial cells are surrounded by pericytes, which share the basement membrane (or basal lamina) and astrocytic endfeet. Neurones run close to the capillaries and influence the endothelium using astrocytes as intermediate players. Adapted from [Weiss et al., 2009] and [Abbott et al., 2006].

Astrocytic projections, termed endfeet, almost completely surround the brain capillaries, though direct contact between these structures and the endothelium is hindered by the endothelial basement membrane (or basal lamina) that consists of collagen type IV, elastin, fibrillin, fibronectin, laminins and heparan sulphate proteoglycans [Weiss et al., 2009]. The barrier protecting the brain changed phylogenetically from a glial (invertebrates and elasmobranchs) to an endothelial (higher vertebrates) one [Abbott, 1991; Engelhardt, 2003], indicating that astrocytic endfeet by themselves can exert some barrier function. Yet in vertebrates, capillary endothelium took over the role as the primary boundary because neural tissue became more and more complex and required more efficient ways of maintaining ionic homeostasis, delivering nutrients and removing waste products [Abbott, 2005; Bundgaard and Abbott, 2008]. In these higher vertebrates, astrocytes still display some barrier features (like expression of MDR proteins [Berezowski et al., 2004]), but they mainly fulfill a supporting

role for the BBB. Early evidence supporting this matter came from grafting experiments in which brain vessels growing into peripheral tissue grafts became less tight whereas leaky vessels became more restrictive when grafted into brain tissue [Bauer and Bauer, 2000]. Nowadays, astrocytes are known to increase tightness of the barrier [Boveri et al., 2005], to upregulate γ -glutamyl-transpeptidase activity [Garcia et al., 2004] and to stimulate the expression of several transport systems including P-gp [Berezowski et al., 2004; Boveri et al., 2005], GLUT-1 and amino acid carriers [Abbott, 2002]. The BBB-enhancing molecules secreted from astrocytes include transforming growth factor β (TGF β), glial cell-derived neurotrophic factor (GDNF), angiopoietin-1 (Ang-1) and basic fibroblast growth factor (bFGF) [Abbott, 2002; Garcia et al., 2004; Igarashi et al., 1999; Utsumi et al., 2000].

Although astrocytes are necessary for BBB maintenance, they are probably not sufficient to induce a proper barrier. Indeed, some BBB characteristics are present very early during development, even before astrocytes have differentiated. In rodents, neurogenesis (E11-17), rather than gliogenesis (E17) coincides with the invasion of early blood vessels into the neural tube (E10-11) [Saunders et al., 2008; Saunders et al., 1999]. Therefore, neurons or pericytes are more likely candidates to induce tight junction formation whereas astrocytes might be involved in their further maturation. Indeed, gliogenesis does coincide with dramatic alterations in tight junction complexity [Kniesel et al., 1996]. Subsequent to these observations, the research focus has shifted to pericytes which are present near capillaries even in the earliest stages of development. They display a dendritic morphology with several cytoplasmic processes wrapping around the vessel wall [Hirase et al., 2004]. Pericytes cover brain capillaries by ~22-32% (~1:3) and this degree of pericyte coverage appears to correlate with the degree of tightness of the interendothelial junctions. Indeed, outside the CNS, pericyte coverage of endothelial cells varies from 1:10 (lung) to 1:100 (skeletal muscle) [Shepro and Morel, 1993]. Pericytes are embedded in the endothelial basement membrane of which they synthesize most elements (including collagen, fibronectin, laminins and proteoglycans) [Cardoso et al., 2010; Shepro and Morel, 1993]. Thanks to this configuration, pericytes, unlike astrocytes, are in direct contact with endothelial cells and gap junctional communication between these two cell types has been reported [Larson et al., 1987; Mogensen et al., 2011]. Pericytes regulate vessel growth and development, as well as tight junction formation and P-gp function via secretion of growth factors such as TGF β , Ang-1, platelet-derived growth factor B (PDGF-B) and bFGF [Berezowski et al., 2004; Dohgu et al.,

2005; Hellstrom et al., 2001; Hellstrom et al., 1999; Hori et al., 2004; Lai and Kuo, 2005; Nakagawa et al., 2007; Ramsauer et al., 2002; Shepro and Morel, 1993]. In addition, pericytes may be involved in the immune response, as they seem to function as macrophages [Kamouchi et al., 2004; Thomas, 1999]. Furthermore, since capillaries in the brain have no smooth muscle cells, pericytes may fulfill their task. This is further proven by observations that they express actin and myosin, just like arterial smooth muscle cells. Contractile responses of pericytes may be important in the maintenance of the BBB. *In vitro*, it has been shown that pericytes can contract under the influence of the Ca^{2+} ionophores [Kamouchi et al., 2004].

1.4.2 Ca^{2+} AS A MAJOR DETERMINANT OF BBB FUNCTION

It is since long known that Ca^{2+} ions play an important role in controlling the function of the BBB. BBB functioning is indeed disturbed when $[\text{Ca}^{2+}]_e$ is decreased and/or $[\text{Ca}^{2+}]_i$ is increased. Decreased $[\text{Ca}^{2+}]_e$ leads to disruption of cell-cell and cell-matrix adhesive interactions [Wilhelm et al., 2007]. The Ca^{2+} -dependency of VE-cadherin interaction is characterized by a K_d that approximates the normal $[\text{Ca}^{2+}]_e$ concentration, therefore small changes in $[\text{Ca}^{2+}]_e$ in the intercellular cleft would already be sufficient for dynamic regulation of interendothelial contacts [Baumgartner et al., 2000; Vestweber, 2000]. Such discrete, local changes could result from the opening of SOC channels that reside at the site of the junctions. However, structural changes in cadherins are not the only mechanism at play. In aortic endothelial cells it was shown that low $[\text{Ca}^{2+}]_e$ conditions trigger a relatively fast and reversible, PKC-dependent endocytosis of cadherin that coincides with rounding of cells and the formation of intracellular gaps [Alexander et al., 1998]. In intestinal epithelium, tight junction proteins occludin and JAM-1 were endocytosed as well [Ivanov et al., 2004a]. Still, it remains to be determined whether disruption of adherens junctions is sufficient to induce alterations in BBB permeability. Indeed, the dissociation of VE-cadherin from cell-cell contacts does not always result in acute changes of barrier properties, even when $[\text{Ca}^{2+}]_e$ is reduced to zero. Tight junctions might compensate for the loss in VE-cadherin [Baumgartner et al., 2000]. Furthermore, disconnection of tight junctions, secondary to the effects on adherens junctions, appears to be rather slow: in cerebral microvessels and immortalized BBB endothelium, disruption of tight junctions only emerged 60-150 minutes after treatment with Ca^{2+} -free solution [Nagy et al., 1985; Wilhelm et al., 2007]. On the other hand, a drop in

TEER due to relocalization of occludin, ZO-1 and actin/myosin was already observed after 5 minutes in Caco-2 epithelial cells [Ivanov et al., 2004b; Ma et al., 2000; Ma et al., 2010]. Finally, it was shown that lowering of $[Ca^{2+}]_e$ leads to a fast and simultaneous endocytosis of the entire junctional complex (adherens and tight junctions) [Ivanov et al., 2004b].

With regard to acute $[Ca^{2+}]_i$ -dependent BBB alterations, most of the current knowledge derives from work with vasoactive inflammatory agents or ischemic conditions applied to endothelial cell layers either *in vitro* or *in vivo*. Many of these substances, including thrombin, histamine, bradykinin, etc. share the ability to trigger a substantial increase in $[Ca^{2+}]_i$ in endothelial cells thereby activating Ca^{2+} -sensitive signaling pathways. Preventing an increase in $[Ca^{2+}]_i$ protects BBB function in many experimental scenarios. Hence, $[Ca^{2+}]_i$ was identified as a major regulator of BBB function [Abbott, 1991; Abbott, 1998; Abbott, 2000; Brown and O'Neil, 2009]. Three decades ago, research on the role of Ca^{2+} in BBB function was initiated by Søren-Peter Olesen who published a series of reports highlighting that an increase in $[Ca^{2+}]_i$ in endothelial cells is an important determinant of BBB function. In a first *in vivo* study, it was found that intravenously administered serotonin had a rapid and dose-dependent permeability-increasing effect in pial microvessels of the frog brain, as evidenced by a drop in electrical resistance of the vascular wall. Preventing Ca^{2+} -entry inhibited the effect of serotonin [Olesen, 1985]. Evaluating different second messenger systems, Olesen found that only a rise in $[Ca^{2+}]_i$, elicited by Ca^{2+} ionophores, was able to decrease resistance in pial microvessels, but not cyclic nucleotides [Olesen, 1987]. Comparing a variety of agents with different origin and chemical classes like serotonin, epinephrine, bradykinin, substance P, etc., Olesen concluded that all agents that stimulated changes in permeability had the common characteristic of increasing $[Ca^{2+}]_i$. Moreover, the time course and magnitude of BBB changes elicited by these receptor agonists was almost identical for the different compounds and very comparable with changes brought about by the ionophores: barrier permeability changed within 1-2 sec, rapidly evolved to a maximum and subsequently recovered over 5-15 minutes [Olesen, 1989]. In the years that followed, the role of Ca^{2+} as an important second messenger involved in barrier function was further emphasized for different vasoactive and inflammatory agents. In different BBB models it was furthermore shown that an increase in $[Ca^{2+}]_i$ also mediates BBB hyperpermeability in response to ischemia (hypoxia and/or aglycemia), contributing as a major factor to subsequent brain dysfunction. Hypoxia transiently elevates endothelial $[Ca^{2+}]_i$, however, the source of Ca^{2+} , entry or intracellular stores, is still a matter of debate. Blockers of different classes of Ca^{2+} -permeable channels (L-

type Ca^{2+} channels or TRP channels) have been demonstrated to impede the increase in $[\text{Ca}^{2+}]_i$ [Brown and Davis, 2002]. Obviously, because ischemic conditions are associated with energy depletion, ATP-dependent Ca^{2+} extrusion mechanisms such as PMCA and SERCA will be impaired, adding their part to the $[\text{Ca}^{2+}]_i$ disturbance [Kimura et al., 2000; Sandoval and Witt, 2008]. Additionally, various released factors may contribute to the increase in $[\text{Ca}^{2+}]_i$, including bradykinin, histamine, lysophosphatidic acid (LPA), thrombin, glutamate and platelet-activating factor [Sandoval and Witt, 2008]. The next paragraphs will consider some of these substances in more detail, highlighting their biological outcome and their contribution to understanding endothelial $[\text{Ca}^{2+}]_i$ regulation. Particular attention will also be devoted to viral, bacterial and leukocyte passage over the BBB which has also brought up interesting insights on endothelial $[\text{Ca}^{2+}]_i$ regulation and its relation to BBB functioning.

1.4.2.1 Bradykinin

In accordance with the Olesen data, bradykinin was shown to increase endothelial permeability both *in vitro* [Easton and Abbott, 2002; Hurst and Clark, 1998; Revest et al., 1991] and *in vivo* [Butt, 1995; Sarker et al., 1998], when applied topically to the exposed brain surface or injected intravenously. Bradykinin is present in healthy brain tissue at nanomolar concentrations but it can increase locally up to 1 μM following brain trauma and ischemia [Abbott, 2000; Mayhan, 2001]. Furthermore, RMP7 (labradimil), a stable analogue of bradykinin used clinically to increase barrier permeability and improve drug access to brain tumors, mimics bradykinin in its capability to increase $[\text{Ca}^{2+}]_i$ [Doctrow et al., 1994]. In an ECV304/C6 cell culture BBB model, bradykinin (1 μM) induced a peak-plateau $[\text{Ca}^{2+}]_i$ signal [Easton and Abbott, 2002], consistent with CCE. Bradykinin has been characterized as a potent activator of TRPC channels in the bEnd3 cell line. Here, Ca^{2+} entry was blocked by the TRPC channel blockers but not by TRPV channel inhibitors. Furthermore, these blocking agents also reduced the thrombin-mediated permeability increase to ^{14}C -sucrose [Brown et al., 2008]. In *in vivo* studies, topical application of bradykinin to the brain surface increased the permeability of pial vessels to LY, however, this response cannot be ascribed to TRP channels as it was (in contrast to the *in vitro* obtained data) unaffected by TRP channel blockers [Sarker et al., 2000]. In line with Easton and Abbott [Easton and Abbott, 2002], the authors did find a role for PLA2 and arachidonic acid metabolism and subsequent free radical formation. They hypothesized that Ca^{2+} entry occurs through pores formed in the plasma

membrane by free radical-mediated lipid peroxidation [Sarker et al., 2000]. An alternative explanation is that arachidonic acid acts via ARC channels [Shuttleworth, 2009]. In addition to arachidonic acid metabolism and the formation of ROS, Sarker *et al.* [Sarker and Fraser, 2002] also identified a role for guanylyl cyclase (GC), cyclic guanosine monophosphate (cGMP) and protein kinase G (PKG). Blocking of PKG inhibited the permeability response to bradykinin. Neither inhibitors of nitric oxide synthase (NOS) nor blockers of soluble GC (sGC) had an effect on the bradykinin-mediated response. Bradykinin thus leads to the production of cGMP in a sGC-independent manner. One alternative mechanism is the particulate GC (pGC) that can be inhibited by leukotriene D₄. Indeed, leukotriene D₄ prevented the actions of bradykinin and the following pathway was suggested: application of bradykinin, via the metabolism of arachidonic acid and free radical formation, leads to sites of lipid peroxidation. At these sites, Ca²⁺ can flow into the cell, but several substances can also leave the cell. It is suggested that one of these stimulates the natriuretic receptor with subsequent activation of pGC [Sarker and Fraser, 2002]. A role for NOS and cGMP was also evaluated for histamine and LPA [Sarker and Fraser, 2002; Sarker et al., 2010]. LPA production is associated with Alzheimer's disease, multiple sclerosis and ischemia and may activate mast cells with subsequent discharge of histamine.

1.4.2.2 LPA and histamine

Like bradykinin, both LPA and histamine increase [Ca²⁺]_i in BBB endothelial cells [Li et al., 1999; Sarker et al., 1998; Sarker and Fraser, 2002; Sarker et al., 2010]. Despite the potency of LPA to release histamine from mast cells, application of LPA increased the permeability of pial venules in a histamine-independent manner, suggesting that the observed effect was intrinsic to LPA itself. The LPA receptor 1 activates different G-proteins, including G α_q , G α_i and G α_{12} and thus triggers the activation of both PLC and PLA2. Downstream, these pathways activate respectively NOS/sGC, and ROS/pGC signaling, the former being dependent on a Ca²⁺ increase, the latter resulting in Ca²⁺ entry. The endothelial response to LPA was not influenced by the NOS inhibition or ROS scavenging. However, combining these two treatments completely abolished the LPA-induced permeability increase, indicating that the two pathways are equally important [Sarker et al., 2010]. Histamine increased the permeability of pial microvessels to Lucifer Yellow through a H₂ receptor-mediated mechanism. Blockage of Ca²⁺ entry transformed the normally sustained increase in

permeability into a permeability increase that was limited in time (20 sec), indicating that possibly, CCE was contributing [Sarker et al., 1998]. Moreover, histamine was found to increase $[Ca^{2+}]_i$ in primary cultures of human cerebral microvascular endothelial cells. Low concentrations (25 μ M) triggered a Ca^{2+} transient, whereas higher concentrations (100 μ M) induced a Ca^{2+} peak followed by a plateau. The plateau phase was blocked in the presence of the TRP channel blockers or by depolarizing the cells (which reduces the driving force for Ca^{2+} entry) [Li et al., 1999].

1.4.2.3 Thrombin

Thrombin is another agent that has been extensively used while exploring endothelial permeability regulation. Thrombin is a ligand of the $G\alpha_q$ -protein coupled receptor PAR1 that is expressed in BBB endothelium and that induces an increase in $[Ca^{2+}]_i$ upon binding of thrombin [Bartha et al., 2000; Kim et al., 2004]. Depletion of extracellular Ca^{2+} reduced, but not totally abolished, the thrombin-induced Ca^{2+} increase, indicating that both Ca^{2+} entry and mobilization from the ER are involved [Bartha et al., 2000]. Activation of PAR1 by thrombin or PAR1 activating peptide (PAR1AP) caused an increase in $[Ca^{2+}]_i$ in primary human brain microvascular endothelial cells, however, the pattern of Ca^{2+} increase was different for both activators. Thrombin caused a rapid increase in $[Ca^{2+}]_i$ that swiftly returned to baseline, whereas the response to PAR1AP was more prolonged. The Ca^{2+} signals in response to both thrombin and PAR1AP were prevented by blocking PLC and SERCA or by depletion of extracellular Ca^{2+} , indicating the involvement of both $InsP_3$ sensitive stores and Ca^{2+} influx. La^{3+} , a broad spectrum Ca^{2+} channel blocker that inhibits CCE was without effect on the increase in $[Ca^{2+}]_i$ elicited by PAR1AP but abolished that triggered by thrombin. Remarkably, thrombin induced a strong decrease in the TEER, whereas PAR1AP did not have such effect on this parameter [Kim et al., 2004]. These data point to the recruitment of different Ca^{2+} pools by thrombin and PAR1AP which, interestingly, result in distinct functional effects on barrier permeability.

1.4.2.4 Glutamate

Glutamate, the brain's most abundant excitatory neurotransmitter, seems to contribute to the effects of hypoxia-induced BBB disruption. During hypoxia, glutamate levels dramatically

increase in the extracellular environment (from a few μM to even 1 mM) and it has been demonstrated that glutamate reduces the TEER over monolayers of porcine, rat, human or bovine brain microvessel endothelial cells. Although it was published initially that BBB endothelial cells do not express receptors for glutamate [Morley et al., 1998], the ionotropic NMDA receptor was later found to be present in these cells and inhibition of the NMDA receptor, significantly prevented the decrease in TEER [Andras et al., 2007; Kuhlmann et al., 2008; Kuhlmann et al., 2009; Sharp et al., 2003]. The NMDA receptor is permeable to Na^+ , K^+ and Ca^{2+} ($\text{Ca}^{2+} \gg \text{Na}^+$ and K^+) and Ca^{2+} entry likely contributes to the endothelial permeability changes [Kuhlmann et al., 2009]. NMDA activation by glutamate induces oxidative stress [Sharp et al., 2005]. Indeed, activation of the NMDA receptor induced an elevation in $[\text{Ca}^{2+}]_i$ that leads to mitochondrial ROS formation and increased permeability [Kuhlmann et al., 2008; Sharp et al., 2003; Sharp et al., 2005]. The production of ROS appeared insensitive to inhibition of InsP_3R , excluding a role for InsP_3 , but sensitive to ryanodine which specifically blocks RyR-dependent Ca^{2+} release from the ER [Kuhlmann et al., 2009]. AMPA/kainate receptors and mGluRs may also play a role in barrier dysfunction [Andras et al., 2007; Collard et al., 2002]. Glutamate released by polymorphonuclear leukocytes in conditions of inflammation, increases the permeability to macromolecules via activation of mGluRs and this contributes to BBB disruption in the hypoxic brain. The involvement of $\text{G}\alpha_q$ -coupled mGluRs was confirmed but other mGluRs, linked to the inhibition of adenylyl cyclase (AC), contribute as well [Collard et al., 2002].

1.4.2.5 Vascular endothelial growth factor

One of the best known genes that are induced during hypoxia is the *VEGF* gene that encodes the vascular endothelial growth factor (VEGF), or vascular permeability factor [Schoch et al., 2002]. In the brain, the growth factor is released by tumor cells [Criscuolo et al., 1989; Lee et al., 2003] or by astrocytes and endothelial cells in ischemic conditions [Davis et al., 2010; Fischer et al., 1999; Lee et al., 2002]. At the same time, expression of VEGF receptors on the endothelial membrane is upregulated [Lee et al., 2002]. VEGF is known to bind 2 tyrosine kinase receptors: VEGFR1 (flt1) and VEGFR2 (flk1/KDR) [Vogel et al., 2007] of which VEGFR2 is most abundant in the brain [Davis et al., 2010]; yet, using porcine brain microvascular endothelium, Vogel et al. (2007) have indicated that it is mainly VEGFR1 that mediates VEGF's permeability increasing effects [Vogel et al., 2007]. Dimerization and

autophosphorylation of either receptor results in tyrosine phosphorylation of PLC γ with subsequent Ca²⁺ release from the ER [Fischer et al., 2009; Spyridopoulos et al., 2002]. Ca²⁺ entry as well contributes to the VEGF-triggered Ca²⁺ transient [Criscuolo et al., 1989]. In human brain microvascular endothelial cells VEGF increased the permeability to metastatic tumor cells [Lee et al., 2003] and neutrophils [Lee et al., 2002] whereas in porcine brain microvessels permeability to inulin was increased [Fischer et al., 2009]. These events could be counteracted either by chelation of intracellular Ca²⁺ ions or by inhibition of PLC γ .

1.4.2.6 BBB permeation by pathogens and leukocytes

[Ca²⁺]_i has also been implicated in bacterial/viral and leukocyte invasion of brain microvessel endothelial cells. For instance, HIV-1 associated encephalitis and dementia are characterized with BBB impairment mediated by the HIV-1 envelope glycoprotein gp120 [Kanmogne et al., 2007] or by the soluble factor Tat that is released from infected cells [Andras et al., 2005]. Gp120 increased [Ca²⁺]_i through a CCR5/CXCR4 GPCR mediated mechanism, causing a drop in TEER accompanied with an enhanced monocyte migration in primary human brain microvascular endothelial cells [Kanmogne et al., 2007]. Neonatal gram-negative bacillary meningitis is caused by invasion of *Escherichia coli* K1 into the CNS. In order to pass the BBB, *E. coli* first penetrates BBB endothelial cells and this is guided by an increase in [Ca²⁺]_i, mediated by the *E. coli* protein FimH1, a key determinant for binding and invasion that interacts with the CD48 receptor [Khan et al., 2007; Kim et al., 2008]. Both inhibition of Ca²⁺ entry/release and chelation of intracellular Ca²⁺ reduced the invasion of *E. coli* indicating that Ca²⁺, originating from the ER and/or extracellular environment, contributes to the *E. coli* invasion of brain microvascular cells [Kim et al., 2008]. Ca²⁺-dependency was furthermore found for *Borrelia burgdorferi*, the thick-bourn pathogen that causes Lyme disease [Grab et al., 2009b; Grab et al., 2005] and for different subspecies of *Trypanosoma brucei*, which cause human African trypanosomiasis, commonly known as sleeping sickness [Grab et al., 2009a; Nikolskaia et al., 2006] or *Trypanosoma cruzi*, the major mediator of Chagas disease [Burleigh and Andrews, 1998]. Preventing an increase in [Ca²⁺]_i in human brain microvascular endothelial cells reduced the traversal of spirochetes and trypanosomes. Furthermore, pathogen cross-over was always accompanied by a drop in TEER. The pathogens most likely do not directly lead to an increase in [Ca²⁺]_i but activate PARs. *T. brucei* secrete proteases of which brucipain appears necessary for crossing the BBB whereas

B. burgdorferi uses the host's own fibrinolytic system. Brucipain or host cell-derived matrix-metalloproteinases (MMP's) and plasmin activate PARs after which Ca^{2+} -dependent pathways are activated [Grab et al., 2009a; Grab et al., 2009b; Grab et al., 2005; Nikolskaia et al., 2006]. This is supported by the observations that *i*) inhibition of cysteine proteases inhibited invasion and abolished pathogen-induced $[\text{Ca}^{2+}]_i$ elevation and that *ii*) trypanosome-conditioned medium was sufficient to cause a sustained increase in $[\text{Ca}^{2+}]_i$ [Nikolskaia et al., 2006].

Leukocyte migration over the BBB endothelium involves their activation and rolling along the surface of the endothelial cells, and attachment to the cell surface through binding with various adhesion molecules. Leukocytes interact for instance with ICAM-1 (intercellular adhesion molecule or CD54) through the integrins LFA1 (CD11a/CD18) and MAC-1 (CD11b/CD18). ICAM-1 is expressed at low level in the healthy BBB endothelium, but its expression is elevated in multiple sclerosis, Alzheimer's, stroke or trauma. These adhesion molecules are not merely docking sites for leukocytes, but rather function as signal integrators that guide the extravasation of leukocytes over the BBB [Greenwood et al., 2002]. In the immortalized BBB models RBE4 and GP8, ICAM-1 crosslinking induced strong tyrosine phosphorylation of $\text{PLC}\gamma_1$ that was obvious after 1 minute and remained elevated 20 to 30 minutes before declining again [Etienne-Manneville et al., 2000]. An increase in InsP_3 levels and an elevation of $[\text{Ca}^{2+}]_i$ coincided with the increase in PLC phosphorylation. Using human umbilical vein endothelial cells, Carman and coworkers have indicated that these ICAM1-triggered endothelial Ca^{2+} signals serve to induce formation of a 'transmigratory cup' that assists leukocytes in crossing the endothelial monolayer [Carman et al., 2003; Carman and Springer, 2004]. These mechanisms were also observed in microvascular endothelium from the skin and lung [Carman et al., 2007] but it remains to be determined if the same is true in BBB endothelium.

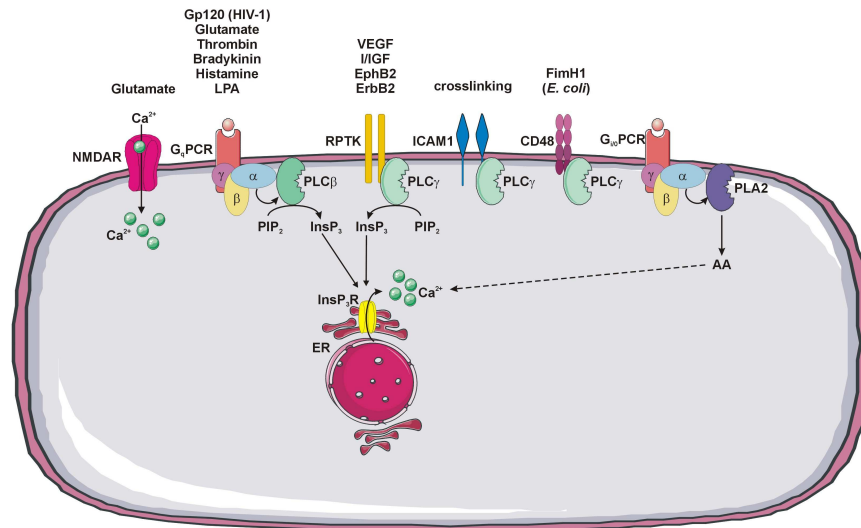


Figure 18. Overview of various classes of membrane receptors involved in generating $[Ca^{2+}]_i$ elevation in BBB endothelial cells. Most receptors, including G_q PCR, RPTK and the CD48 antigen receptor result in the activation of $PLC\beta$ or $PLC\gamma$, generating $InsP_3$ followed by Ca^{2+} release from the ER. Furthermore, $PLC\gamma$ is activated following ICAM-1 crosslinking. Glutamate may, in addition to activating metabotropic responses via G_q PCR, also trigger Ca^{2+} entry via its Ca^{2+} permeable ionotropic NMDA receptor. Activation of PLA2 and the formation of AA results in an elevated $[Ca^{2+}]_i$ according to pathways described in the text. This figure was produced using Servier Medical Art.

From the data presented above, we can conclude that many substances increase $[Ca^{2+}]_i$ in BBB endothelium, all with an increased accessibility of the BBB as a result. Hereby, Ca^{2+} is derived from different sources, be it from intracellular stores or from the extracellular environment. It appears that the addressed source varies for different triggers and gives a distinct outcome on paracellular permeability. It remains to be determined which pathways claim superiority; however, most likely different sources and pathways will contribute giving a specialized response for every permeability-increasing agent. In addition, it comes forward from the data described that different signaling pathways are activated downstream of a $[Ca^{2+}]_i$ elevation. In the following section we will further communicate on these pathways as well as on their potential targets.

1.4.2.7 Ca^{2+} dependent pathways converge on tight junction proteins and the actin cytoskeleton

Downstream of Ca^{2+} the major targets affected in the process of barrier dysfunction are the interendothelial junctions and the actin cytoskeleton. The balance between the intercellular

tethering forces at the site of the junctional complex on the one hand and the opposing contractile state of the cytoskeleton on the other hand is crucial in the maintenance of the BBB and signaling pathways disturbing this equilibrium result in an enhanced barrier permeability. Changes in adhesive properties of tight junctions and adherens junctions are largely correlated with alterations in their phosphorylation state [Stamatovic et al., 2008]. Furthermore, several lines of evidence suggest that remodeling of adherens junctions and/or tight junctions is accompanied by a reorganization of the perijunctional F-actin belt and disorganization of the actin microfilaments, resulting in the disappearance of these junctions from areas of cell-cell contact [Ivanov et al., 2005]. Importantly, an increase in endothelial paracellular permeability requires a coordinated response. Contraction of one cell would merely passively extend neighboring cells rather than to form the desired paracellular gaps [Demer et al., 1993]. Hypothetically, gap junctional intercellular communication could be involved in this coordinated response.

Crawford et al. (1996) showed that hypoxia, as well as post-hypoxic reoxygenation induces profound alterations of actin organization in aortic endothelial cells, a response that requires intact coupling of superoxide producing pathways with tyrosine kinase pathways [Crawford et al., 1996]. Mark and Davis (2002) also showed that increased paracellular permeability, caused by hypoxic stress, was correlated with an increase in actin expression and the appearance of actin stress fibers in bovine cerebral microvasculature [Mark and Davis, 2002]. Forty-eight hours of hypoxia strongly increased the permeability to ^{14}C -sucrose across monolayer cultures of bovine brain microvascular endothelial cells, whereas 24 hours of hypoxia was without effect. When the hypoxic conditions were combined with glucose deprivation (more closely mimicking ischemia), 3 hours of oxygen and glucose deprivation were sufficient to increase permeability. L-type Ca^{2+} channel block prevented the increase in permeability to ^{14}C -sucrose induced by either hypoxia or hypoxia/aglycemia, whereas TRP channel inhibition only blocked permeability changes induced by hypoxia/aglycemia [Abbruscato and Davis, 1999; Brown and Davis, 2005; Brown et al., 2004]. Furthermore, hypoxia/aglycemia in bovine, human and porcine BBB endothelial cells was accompanied by the collapse of VE-cadherin, ZO-1, ZO-2 and occludin [Brown and Davis, 2005; Fischer et al., 2004; Lee et al., 2003] and is possibly mediated by VEGF-triggered Ca^{2+} signals [Fischer et al., 2004]. In bovine BBB endothelium, inhibition of TRP channels prevented the redistribution of occludin, but it had no influence on the diffuse pattern of actin in the cytoplasm. Disappearance of the F-actin belt thus appeared not to be induced by Ca^{2+} entry.

However, actin polymerization could also be prevented simply by the absence of glucose and thus energy [Brown and Davis, 2005]. Oppositely, TRP channel mediated Ca^{2+} entry following traumatic brain injury was responsible for the formation of stress fibers [Berrout et al., 2011]. Finally, it was shown that stimulation of the NMDA receptor in rat brain microvascular cells results in tyrosine phosphorylation and redistribution of occludin with a subsequent decrease in TEER. In contrast, inhibition of AMPA/kainate receptors rescued occludin from a decreased phosphorylation on threonine residues. The equilibrium between phosphorylated serine/threonine residues and phosphorylated tyrosine residues on occludin thus determines its function and hence permeability [Andras et al., 2007].

The cortical actin cytoskeleton forms a belt just beneath the plasma membrane and is associated with the motor protein myosin II. When the regulatory myosin light chain (MLC), associated with myosin II, is phosphorylated, actin-myosin interactions lead to increased contractility of the actin cytoskeleton and enhanced stress fiber formation. The level of MLC phosphorylation is strictly regulated by two distinct pathways: the non-muscle MLC kinase (MLCK) pathway which phosphorylates MLC on Thr¹⁸ and Ser¹⁹ in a Ca^{2+} -dependent manner [Garcia et al., 1995; Goekeler and Wysolmerski, 1995; Verin et al., 1998] and the MLC phosphatase (MLCP) pathway that drives dephosphorylation of MLC. Despite the suggestion that actin polymerization and stress fiber formation do not occur during hypoxic/aglycemic conditions due to energy shortage, it was described that MLC phosphorylation contributes to BBB dysfunction during stroke. In bovine brain microvascular endothelial cells subjected to hypoxia followed by reoxygenation, TEER decreased within 30 minutes after hypoxia onset and did not recover during reoxygenation. Hypoxia also increased the level of phosphorylated MLC. Both effects were completely inhibited by the MLCK blocker ML-7, as well as by chelating $[\text{Ca}^{2+}]_i$ and by inhibition of NAD(P)H oxidase that generates superoxide upon activation by Ca^{2+} . In addition, glutamate was shown to activate MLCK in a Ca^{2+} - and NAD(P)H-dependent manner [Kuhlmann et al., 2008]. An increase in phosphorylated MLC with subsequent brain edema was also observed in the rat two-(cortical) vein occlusion stroke model. The authors concluded that the signaling cascade starts with an increase in $[\text{Ca}^{2+}]_i$ which enhances the generation of ROS by NAD(P)H oxidase. The resulting oxidative stress then activates MLCK leading to the formation of stress fibers [Kuhlmann et al., 2007]. Hicks et al. confirmed these data using the immortalized mouse cell line bEnd3 and demonstrated that it is Ca^{2+} entry via TRPC channels that activates MLCK [Hicks et al., 2010]. MLC phosphorylation occurred 15 minutes after the onset of hypoxia and declined again after 30

minutes. In contrast, measurable, reproducible increases in permeability to ^{14}C -sucrose were evident only after 6 hours. These data highlight the importance of MLC phosphorylation in the initial phase following hypoxia. Furthermore, ZO-1 relocalized from cell-cell contacts to the cytoplasm subsequent to TRP channel Ca^{2+} entry and MLCK activation [Hicks et al., 2010]. In addition, the authors found subcellular redistribution of moesin, a protein involved in the anchorage of the cytoskeleton to the plasma membrane, and of the vasodilator-stimulated phosphoprotein (VASP) which is an actin-binding protein negatively regulating actin polymerization [Hicks et al., 2010]. Unfortunately, the authors did not study the role of $[\text{Ca}^{2+}]_i$ changes and TRPC channels in VASP and moesin redistribution, yet others do observe VASP dephosphorylation following a glutamate-induced increase in $[\text{Ca}^{2+}]_i$ [Collard et al., 2002]. Proteins of the Ena/VASP family have emerged as regulators of actin assembly in a variety of cell types. These proteins localize to areas of dynamic actin reorganization such as cell-cell contacts and stress fibers. In addition, they bind directly to F- and G-actin and profilin, an actin monomer-binding protein that links the microfilament system to signal transduction pathways, suggesting that they could directly regulate actin dynamics [Krause et al., 2003; Reinhard et al., 1995]. Dephosphorylation inactivates VASP which then promotes actin polymerization, stress fiber formation, endothelial cell contraction and disruption of the BBB. Furthermore, phosphorylated VASP co-immunoprecipitates with the tight junction protein ZO-1 [Comerford et al., 2002]. It has also been shown that VASP is able to physically bind vinculin [Sporbert et al., 1999], a component of the adherens junction, and as such provides a link between the cytoskeleton and the junctional complex. Latest evidence from *Vasp*^{-/-} mice indicates that VASP is not much involved in BBB permeability under basal conditions but that its presence significantly reduces BBB leakage of Evans Blue in ischemic conditions [Kraft et al., 2010].

Alterations in the cytoskeleton have also been associated with alcohol-mediated BBB disruption. Exposure to ethanol or its metabolite, acetaldehyde, caused a gradual decrease in TEER and an increase in monocyte migration over a monolayer of bovine brain microvascular endothelial cells. In addition, the authors found small paracellular gap formation between the endothelial cells, indicating cytoskeletal rearrangements. At the molecular level, ethanol increased the expression of MLCK as well as the level of phosphorylated MLC. These events were inhibited by 4-MP, an inhibitor of the ethanol metabolizing enzymes cytochrome P450-2E1 and alcohol dehydrogenase. MLCK was also implicated in the phosphorylation and relocalization of the tight junction proteins occludin

and claudin-5 while overall, the total level of both proteins decreased. For ZO-1, the total content remained unchanged, but in analogy to occludin and claudin-5, the authors found increased phosphorylation and rearrangement of the protein. Finally, the antioxidant uric acid prevented the effects of ethanol on TEER and on MLC phosphorylation, indicating a role for ROS [Haorah et al., 2005]. Indeed, all the effects described above could be mimicked by treatment with donors of NO, superoxide or peroxynitrite [Haorah et al., 2005]. Further work on human brain microvascular cells indicated that ethanol, acetaldehyde and ROS donors upregulated the expression of InsP₃R type 1. Ethanol and acetaldehyde furthermore led to a biphasic increase in [Ca²⁺]_i and the propagation of Ca²⁺ waves between adjacent endothelial cells. The ethanol-, acetaldehyde- or ROS-induced effects on the total level of MLCK, the phosphorylation of MLC and tight junction proteins and the effects on TEER and monocyte migration, were partially prevented by blocking InsP₃R [Haorah et al., 2007a]. These data support the involvement of InsP₃-mediated Ca²⁺ signaling in BBB modulation in parallel with Ca²⁺-independent mechanisms. Finally, pretreatment of human brain microvessel endothelial cells with ML-7 reduced the invasion of *E. coli* into the cells [Kim et al., 2008]. In addition, the effect of the viral protein gp120, mediated by substance P secretion from the endothelial cells and activation of the substance P receptor NK1, proceeds via an increase in [Ca²⁺]_i and a reduced expression of ZO-1 and claudin-5 [Lu et al., 2008]. These data indicate that effects on both the cytoskeleton and junctional complex mediate BBB permeability changes in response to pathogens.

ROS (NO, H₂O₂, superoxide) and ethanol have also been shown to be potent activators of the MAPK and the RPTK signaling pathway. MAPK include the extracellular signal-regulated kinases (ERK1/2 or p44/42 MAPK), c-jun NH₂-terminal kinase (JNK) and p38 kinase. H₂O₂ probably activates GPCR via oxidation of sulfhydryl groups, leading to activation of PLC. On the other hand, H₂O₂ might directly act on PLC. In either case, oxidative stress induced by application of H₂O₂ [Fischer et al., 2005] or by the ROS donor DMNQ [Krizbai et al., 2005] induced a decrease in TEER and hyperpermeability to inulin which was prevented by chelating [Ca²⁺]_i or by blocking InsP₃R. Downstream of Ca²⁺, CaM, with subsequent activation of ERK1/2 appeared important in mediating the effect of H₂O₂ and hypoxia/ischemia. Morphologically, alterations in ZO-1, ZO-2 and occludin localization were found [Fischer et al., 2005; Krizbai et al., 2005]. In GP8, a rat brain endothelial cell line, monocyte migration was enhanced by superoxide. Downstream of superoxide, PLC was activated with a subsequent increase in InsP₃ and [Ca²⁺]_i, ultimately leading to a

reorganization of tight junction proteins and the actin cytoskeleton [Van der Goes et al., 2001]. ROS also activate the RPTKs vascular endothelial growth factor receptor (VEGFR), insulin/insulin-like growth factor receptor (I/IGF-1R), EphrinB2 receptor (EphB2R) and epidermal growth factor receptor (ErbB2R) and two non-receptor PTKs: c-Src kinase and focal adhesion kinase (FAK) [Haorah et al., 2008]. An increase in PTK activity was furthermore accompanied by a diminished activity of protein tyrosine phosphatase. PTKs mediate phosphorylation of occludin, claudin-5 and ZO-1 at tyrosine residues and lead to the activation of MMP-1 and MMP-9 in parallel with a decrease in tissue inhibitor of MMP (TIMP) activity. The increase in MMP activity was reflected in the degradation of collagen IV, an essential component of the basement membrane [Haorah et al., 2007a; Haorah et al., 2007b; Haorah et al., 2008]. MMPs comprise a family of zinc dependent endopeptidases that have a wide array of targets in the CNS. Expression of MMPs in healthy brain is very low, but during stroke or inflammation MMP activity is upregulated leading to detrimental effects on the BBB. MMPs have been described to increase permeability through degradation of the endothelial basal lamina and downregulation of tight junction proteins [Jin et al., 2010]. Little is known on the role of $[Ca^{2+}]_i$ with respect to MMP activity. It was shown recently by Wu et al. (2009) that astrocytic expression of the gelatinase MMP-9, which contributes largely to BBB disruption, is upregulated by $IL1\beta$ in a Ca^{2+} -dependent manner. $IL1\beta$ activates the production of $InsP_3$ and subsequent Ca^{2+} mobilization from the ER. Downstream of Ca^{2+} , CaM and CaMKII are activated, instigating phosphorylation of JNK and c-Jun [Wu et al., 2009]. Additionally, MMP's might potentiate Ca^{2+} entry through the NMDA receptor in ischemic conditions [Jin et al., 2010]. Whether these links between MMPs and Ca^{2+} also exist in BBB endothelial cells has to be determined still.

This section further emphasizes the participation of Ca^{2+} during episodes of increased BBB permeability and indicates that a myriad of signaling pathways can be activated downstream. Most, if not all, of these pathways converge on the interendothelial junctions and the actin cytoskeleton that, together, are responsible for the normally low paracellular permeability of the BBB. As different agents may act in concert during inflammation or ischemia, it is most likely that different BBB constituents will be targeted in parallel, ultimately leading to gap formation between adjacent endothelial cells and brain edema. **Figure 19** gives an overview of Ca^{2+} -activated signaling cascades that lead to BBB dysfunction.

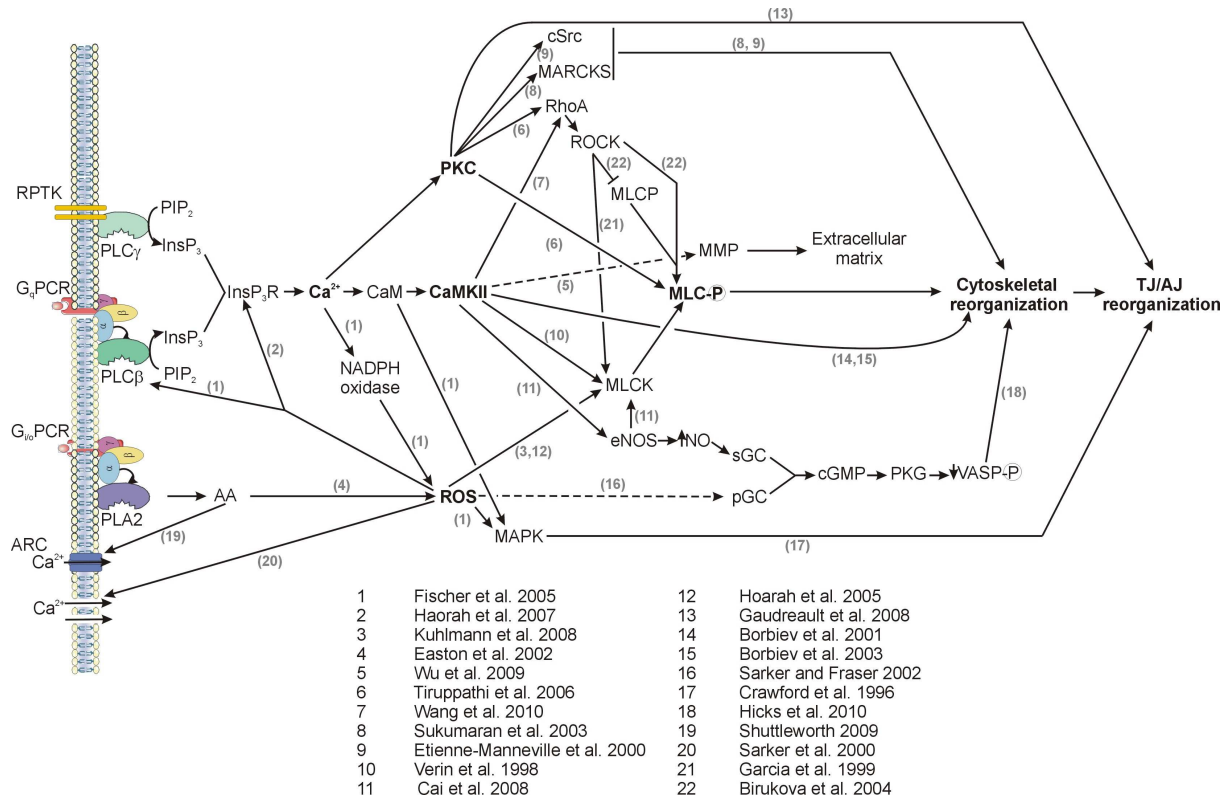


Figure 19. Summary scheme of major links between Ca^{2+} signaling and altered BBB function. Key signaling molecules are represented in bold. The link to increased paracellular permeability, acting via the actin cytoskeleton and adherens/tight junction components, is currently best understood. Details of the various signaling cascades are discussed in the text. Dotted arrows represent indirect actions. The numbers between brackets refer to the reference list at the bottom. Only key references have been added. For additional citations, the reader is referred to the text. This figure was produced using Servier Medical Art.

1.4.3 SPATIOTEMPORAL ORGANIZATION OF Ca^{2+} SIGNALS AND BBB FUNCTION

1.4.3.1 Brain microvessel endothelial cells display Ca^{2+} oscillation and intercellular Ca^{2+} wave activity

Several authors have reported Ca^{2+} oscillations and/or intercellular Ca^{2+} waves in endothelial cells of various organs. For example, intercellular Ca^{2+} waves were identified in primary endothelial cells of porcine coronary artery branches [Domenighetti et al., 1998], bovine aorta [Demer et al., 1993], or cornea [D'Hondt et al., 2007a] and in a renal glomerular capillary endothelial cell line [Toma et al., 2008] following bradykinin exposure or mechanical

stimulation. Oscillations were observed in primary endothelial cells from human pulmonary artery [Mauban et al., 2006], in rat lung arterioles *in situ* [Kerem et al., 2010], primary ovine uterus endothelial cells [Yi et al., 2010], a human aorta endothelial cell line [Hu and Ziegelstein, 2000] and in rat urether arterioles *in situ* [Burdyga et al., 2003] induced by histamine, mechanical stimulation, ATP or hypoxia/reoxygenation.

Ca²⁺ oscillations in BBB endothelia occur in response to BK, ATP and histamine [Revest et al., 1991] and were observed following hypoxia, subarachnoid hemorrhage, infection and lymphocyte migration. Brown et al. (2004) illustrated that hypoxic conditions, with or without glucose deprivation, applied to cultures of primary bovine brain microvascular endothelial cells increased their permeability to ¹⁴C-sucrose and increased [Ca²⁺]_i in a (slow) oscillatory manner. [Ca²⁺]_i displayed three separate peaks that all returned to baseline within the first hour and increased two more times, once at 4 hours and once at 6 hours after induction of hypoxia. Furthermore, addition of a Ca²⁺ ionophore failed to increase permeability, indicating that inducing a single [Ca²⁺]_i spike was not sufficient to increase the permeability [Brown et al., 2004]. Other researchers have reported a shift in the potency of BBB endothelial cells to respond to a certain trigger following hypoxia: in normoxic conditions, cerebral microvascular endothelial cells responded to extracellular ATP with oscillatory [Ca²⁺]_i changes. Ca²⁺ transients only occurred when ATP was above the threshold concentration of 0.3 μM and the oscillation frequency increased with elevated ATP concentration. The oscillations appeared to be sustained by the PLC-InsP₃-Ca²⁺ axis. When cells were exposed to hypoxia/reoxygenation, the threshold for initiating a Ca²⁺ transient was shifted to a concentration of 1 μM ATP and oscillations only occurred above 30 μM ATP. The possible underlying mechanisms are diminished Ca²⁺ levels in the ER caused by inappropriate SERCA function or diminished CCE. Reoxygenation-induced production of superoxide has been proposed as a molecular pathway underlying these observations [Kimura et al., 2000]. Ca²⁺ oscillations in primary human brain endothelial cells have also been observed following the rupture of cerebral aneurysms leading to subarachnoid hemorrhage (SAH) and leakage of bloody cerebrospinal fluid (CSF) in the brain tissue [Scharbrodt et al., 2009]. The oscillations, that depended on InsP₃R activation, appeared after approximately 1 minute and persisted at least until 1 hour after the addition of SAH-CSF that was collected from patients, to the endothelial cells. The cells oscillated at a frequency of 0.3 per minute which is in the correct range for activation of the inflammatory transcription factor NFκB. The oscillations also initiated cell shrinkage which, according to the authors, indicates activation of the contractile

machinery. The actual factors present in the SAH-CSF samples that may cause such changes in endothelial $[Ca^{2+}]_i$ were not investigated. Finally, oscillations in human brain microvascular endothelial cells were observed following infection with *T. brucei* and ICAM-1 crosslinking. *T. brucei* secrete proteases of which brucipain appears necessary for crossing the BBB. Brucipain or host cell-derived MMP's and plasmin activate PARs after which Ca^{2+} signals are initiated. Inhibition of cysteine proteases inhibited invasion and abolished pathogen-induced Ca^{2+} oscillations. [Grab et al., 2009a; Grab et al., 2009b; Grab et al., 2005; Nikolskaia et al., 2006]. ICAM-1 crosslinking resulted in Ca^{2+} oscillations continuing over a period of at least 10 minutes [Etienne-Manneville et al., 2000]. In immortalized endothelial cells derived from rat brain microvessels (RBE4 and GP8/3.9), intercellular Ca^{2+} waves were elicited by mechanical stimulation or photoliberation of caged $InsP_3$ [Vandamme et al., 2004].

Application of focussed ultrasound following administration of microbubbles caused Ca^{2+} waves in the mouse BBB cell line bEnd3 [Park et al., 2010]. Communication of $[Ca^{2+}]_i$ increases was also observed upon mechanical stimulation of rat brain capillary endothelial cells but this was only evident when these cells were passaged, not in their primary cultures [Paemeleire et al., 1999]. In contrast, intercellular Ca^{2+} wave propagation was identified in primary human brain microvessel endothelial cells following application of ethanol or acetaldehyde. When the same cells were exposed to ATP, both intercellular Ca^{2+} waves and Ca^{2+} oscillations were observed [Haorah et al., 2007a]. Whether these waves are supported by the gap junction or the paracrine route is not clarified. In terms of connexin expression, vascular endothelial cells throughout the body express Cx37, Cx40 and Cx43 with variability in abundance, depending on the vessel type and the position in the vascular tree: Cx37 and Cx40 are widely distributed in large vessel endothelial cells, whereas Cx43 is strongly expressed in regions of turbulent flow [Bruzzone et al., 1993; Gabriels and Paul, 1998; Haefliger et al., 2004]. There is no doubt about the presence of gap junctions in brain endothelia, but it is less well established which connexin subtypes are being expressed, especially at the level of brain capillaries forming the BBB. It is more or less accepted that brain endothelium expresses Cx37 and 40 [Little et al., 1995; Nagasawa et al., 2006; Traub et al., 1998]. Cx43 expression was demonstrated in freshly isolated capillary and microvascular endothelial cells of bovine, rat, mouse and porcine brain [Larson et al., 1990; Little et al., 1995; Nagasawa et al., 2006; Theis et al., 2001; Wilson et al., 2008] but this could not be confirmed in brain slices [Simard et al., 2003].

As we described in 1.3, the information contained in the Ca^{2+} oscillations are integrated by specialized sensor proteins like CaMKII and PKC. These proteins have also been implicated in the regulation of BBB permeability. As stated before, NOS mediates increased endothelial permeability, and H_2O_2 and bradykinin, which are known to cause endothelial hyperpermeability, have been shown to upregulate endothelial NOS via CaMKII [Cai et al., 2008]. Additionally, different components of the cytoskeleton like filamin and actin filaments are targets of CaMKII-dependent pathways [Cai et al., 2008] (**figure 19**). Borbiev et al. demonstrated that in bovine pulmonary artery endothelial cells CaMKII was activated following application of thrombin or ionomycin. KN93, a specific CaMKII inhibitor, blocked the associated increase in permeability to Evans blue-albumin and the decline in TEER. CaMKII was shown to mediate phosphorylation and translocation of filamin, a protein that provides an anchorage for filamentous actin to the plasma membrane [Borbiev et al., 2001]. In addition, CaMKII phosphorylates caldesmon, a protein involved in myosin ATPase activity, leading to stress fiber formation [Borbiev et al., 2003]. CaMKII seems also involved in thrombin-induced dysfunction of an endothelial barrier formed by human umbilical vein endothelial cells. Although both low (2.5nM) and high (50 nM) concentrations of thrombin caused a comparable increase in CaMKII activity, silencing of CaMKII δ prevented a decrease in TEER brought about by 2.5 nM thrombin whereas it had no effect on the TEER decrease induced by 50 nM thrombin. Ca^{2+} oscillations were observed with 2.5 nM thrombin whereas higher concentrations of thrombin gave a sustained increase in $[\text{Ca}^{2+}]_i$ [Brown et al., 2004]. Downstream of CaMKII, RhoA and ROCK were activated. Targets of ROCK involve MLC [Birukova et al., 2004], MLCP [Birukova et al., 2004], MLCK [Garcia et al., 1999] and proteins of the junctional complex [Wang et al., 2010]. In addition, MLCK contains a consensus site for CaMKII phosphorylation [Verin et al., 1998] which can directly activate MLCK giving rise to stress fibers. In BBB endothelium, CaMKII activity was confirmed [Balla et al., 2002; Chi et al., 2010; Deli et al., 1993] and *E. coli* infection of human brain microvascular endothelial cells was found to be dependent on CaMKII. The *E. coli* membrane protein IbeA binds to and phosphorylates vimentin, which is translocated to plasma membrane rafts. Both vimentin phosphorylation and *E. coli* invasion were blocked in the presence of KN93. Vimentin phosphorylation and clustering was furthermore found in neighboring, non-infected cells [Chi et al., 2010]. The latter result combined with the finding that Ca^{2+} and CaMKII are important, could indicate a role for intercellular Ca^{2+} waves that may help in communicating CaMKII activation to non-infected cells. Unfortunately though, $[\text{Ca}^{2+}]_i$ dynamics during *E. coli* infection were not investigated in this study.

Compared to CaMKII, the knowledge on the role of PKC in endothelial hyperpermeability is far more extended. PKC mainly exerts its effects on permeability via its actions on the junctional complex. Indeed, tight junction proteins are phosphoproteins whose function is regulated by their phosphorylation status and PKC-dependent phosphorylation of adherens junction components (VE-cadherin, p120) has also been observed [Gaudreault et al., 2008; Konstantoulaki et al., 2003; Sukumaran and Prasadarao, 2003; Tiruppathi et al., 2006]. In addition, PKC affects the phosphorylation status of MLC, either by direct phosphorylation of MLC or via activation of RhoA with subsequent inhibition of MLCP [Mehta et al., 2001; Tiruppathi et al., 2006] (**figure 19**). There is no consensus yet on whether PKC either protects against or enhances barrier dysfunction. The reason for this shortcoming may be related to the use of different species, diverse triggers and the existence of various PKC classes and isoforms, which are not always further specified. The distinct roles of PKC isoforms might furthermore be explained by their different subcellular localization [Kim et al., 2010]. From the data presented here it emerges that the Ca^{2+} (oscillation) sensitive, conventional PKCs act to disrupt the BBB whereas novel and atypical PKCs counteract this event. Conventional (α , βI , βII , γ), novel (μ , ϵ , η , δ , θ) and atypic (ζ , λ) PKCs were found to be present in primary or immortalized brain microvessel endothelial cells [Bruckener et al., 2003; Fleegal et al., 2005; Kim et al., 2010; Qiu et al., 2010; Stamatovic et al., 2006; Yang et al., 2006] and PKC activity was shown to be increased under ischemic conditions [Fleegal et al., 2005; Kim et al., 2010; Yang et al., 2006]. In hypoxic rat brain microvascular endothelial cells, expression of different classes/isoforms of PKC was shown to be elevated and incubation with chelerythrine, a broad spectrum PKC blocker, inhibited the increased permeability to sucrose. Only PKC βII and PKC γ expression was enhanced both *in vitro* and *in vivo*, indicating that these conventional PKCs likely mediate the observed effects on endothelial barrier permeability to sucrose [Fleegal et al., 2005]. Unfortunately, the targets of PKC were not identified. In ischemic bovine brain capillary endothelial cells, PKC α and PKC βI were increased with no detection of PKC βII . PKC γ was furthermore inactivated [Yang et al., 2006]. PKC βII was activated in ischemic mouse bEnd3 cells and this was associated with an increased TEER and the loss of ZO-1 and occludin from the plasma membrane. These effects were reduced when blocking PKC βII or when a dominant negative form of PKC βII was overexpressed. From work on coronary endothelium it is known that PKC βII colocalizes with VE-cadherin and phosphorylates junctional proteins inducing an increase in permeability [Gaudreault et al., 2008]. In contrast, PKC δ , which belongs to the novel class of PKCs and

which was found predominantly in the cytoplasm [Gaudreault et al., 2008], was activated in ischemia but was found to play a protective role: in the presence of rottlerin, a PKC δ inhibitor, or a dominant negative form of PKC δ , ischemia induced a decrease in TEER and relocalization of ZO-1 and occludin away from the plasma membrane was intensified [Kim et al., 2010]. In rat brains exposed to electromagnetic fields, PKC β II activation preceded the observed ZO-1 relocalization and the accompanying increase in permeability to albumin [Qiu et al., 2010]. The chemokine monocyte chemoattractant protein 1 (MCP1 or CCL2) was shown to activate PKC α which was correlated with an enhanced phosphorylation of tight junction proteins occludin, claudin-5, ZO-1 and ZO-2, and an increased permeability to inulin in mouse brain microvascular endothelial cells. However, despite the fact that PKC α is a conditional, Ca²⁺- and DAG-dependent kinase, the cytokine MCP-1 increased its activity via RhoA [Stamatovic et al., 2006]. PKC α has also been described to be involved in viral and bacterial invasion. Binding of the HIV-1 protein gp120 to the endothelial membrane increased [Ca²⁺]_i and activation of different PKCs, which was most evident for PKC β II. The associated alterations in TEER, permeability and monocyte migration were blocked by PKC inhibitors that specifically act at the Ca²⁺ binding site of PKC, further emphasizing a role for [Ca²⁺]_i. Inhibitors targeting the DAG binding site were ineffective in blocking changes in permeability [Kanmogne et al., 2007]. Looking back at the activation mechanism for PKC, the latter could indicate a role for small and rapid changes in PKC activity following Ca²⁺ oscillations where DAG does not come into play yet. Sukumaran and Prasadarao provide evidence that PKC α is stimulated via phosphoinositide 3-kinase (PI3K) and FAK at the bacterial entry site when cells are challenged with *E. coli* [Sukumaran and Prasadarao, 2002]. Downstream from PKC α , myristoylated alanine-rich protein kinase C substrate (MARCKS) is activated. This protein binds and cross-links actin filaments in a CaM-dependent manner, allowing cytoskeletal rearrangements. Moreover, PKC α mediated a decrease in the interaction between β -catenin and VE-cadherin provoking a disruption of the junctional complex which was reflected by a drop in TEER and increased permeability to HRP [Sukumaran and Prasadarao, 2003]. The events described here occur only at the entry site of the pathogen and enable endocytosis. In contrast to the data described above, Brückener et al. (2003) found a protective role of PKC in porcine brain capillary endothelial cells where treatment with broad spectrum PKC inhibitors enhanced pertussis toxin-induced hyperpermeability to HRP. Phorbol esters, which are known to activate PKC, blocked the increase in permeability [Bruckener et al., 2003]. The involved PKC isoform was not investigated in this study though.

Only a few reports indicate the combined involvement of Ca^{2+} oscillations and PKC activation. Oscillations were associated with PKC activation in endothelial cells infected with *T. brucei* and inhibition of PKC by calphostin C prevented invasion of trypanosomes [Nikolskaia et al., 2006]. ICAM-1 crosslinking-induced Ca^{2+} oscillations enhanced the activity of PKC with subsequent activation of the c-Src kinase. c-Src has many targets amongst which cortactin, FAK, paxillin and p130^{Cas} that regulate cell-matrix adhesion and cytoskeletal rearrangements. Preventing a Ca^{2+} increase or downregulation of PKC decreased the amount of phosphorylated cortactin, FAK and paxillin. These actions equally inhibited the migration of lymphocytes across endothelial monolayers [Etienne-Manneville et al., 2000].

This impressive amount of existing data demonstrates the role of $[\text{Ca}^{2+}]_i$ in influencing BBB function as probed from permeability measurements and TEER. It is clear that $[\text{Ca}^{2+}]_i$ has an established role in increasing the paracellular permeability and the available detailed molecular analysis allows to construct an idea on how Ca^{2+} might exert this effect, acting on junctional proteins, their associated scaffold molecules and the actin cytoskeleton. However, knowledge on the role of endothelial Ca^{2+} oscillations and waves in the regulation of BBB permeability is lagging far behind, notwithstanding their importance in other organ systems.

Chapter 2

Aim of the study

Work of our research group elucidated a crucial role of $[Ca^{2+}]_i$ in the regulation of connexin hemichannel activity. Photoreleasing $InsP_3$ in a single cell resulted in a Ca^{2+} transient that triggered the release of ATP which could be inhibited by αGA and by brief (30 minutes) exposure to the connexin mimetic peptide $^{43}Gap26$ [Braet et al., 2003b]. An accompanying paper indicated that such short incubations were found to prevent connexin hemichannel dye uptake but not gap junctional dye coupling [Leybaert et al., 2003]. Further characterization of the influence of $[Ca^{2+}]_i$ on Cx32 hemichannel responses indicated that ATP release decreased with increasing amounts of photolytically released Ca^{2+} [De Vuyst et al., 2006]. Similarly, addition of Ca^{2+} ionophore stimulated connexin hemichannel responses only when the ionophore concentration was in the appropriate range. Based on these data we concluded that Cx32 hemichannel responses depend on $[Ca^{2+}]_i$ in a bell-shaped manner, with a peak at ~500 nM [De Vuyst et al., 2006], and this was later confirmed for Cx43 in ATP release/dye uptake studies [De Vuyst et al., 2009] as well as in electrophysiological measurements (unpublished data Wang N. and Leybaert L.). Connexin hemichannel opening occurs via Ca^{2+} -CaM signaling [De Vuyst et al., 2009] whereas closure with high $[Ca^{2+}]_i$ involves actomyosin [Ponsaerts et al., 2010].

The initial objective of the present doctoral work was to **elucidate a role for connexin hemichannels in the Ca^{2+} oscillation machinery**. Indeed, as described in the introduction, Ca^{2+} oscillations largely depend on positive and negative feedback actions at different regulatory levels. Being sensitive to $[Ca^{2+}]_i$ in a bimodal manner, connexin hemichannels, like $InsP_3Rs$, could well contribute to Ca^{2+} oscillations. Connexin hemichannels can function as an entry route as well as a release pathway and we thus aimed to investigate *i*) the role of Ca^{2+} entry and ATP release in the oscillation mechanism and *ii*) a **functional link for hemichannel-supported Ca^{2+} oscillations**. Previous work in our group has illustrated a contribution of connexin hemichannels in intercellular Ca^{2+} waves in BBB endothelial cells [Braet et al., 2003b; Leybaert et al., 2003; Vandamme et al., 2004]. While brain microvascular endothelia display oscillatory and intercellular Ca^{2+} wave activity (see introduction), the spatiotemporal organization of Ca^{2+} signals has, to the best of our knowledge, never been studied with respect to their effect on BBB function. It is generally accepted nowadays that dynamic **Ca^{2+} signals encode (oscillations) and spread (waves) information referring to the initiating trigger and we further aimed to determine their outcome on BBB function in more detail**. Currently, limited tools exist to increase BBB permeability and no tools exist to counteract a BBB permeability increase that is often

associated with brain disease. Overall, our ultimate goal at the start of this study was to find novel targets for modulating BBB function, be it to increase its permeability for therapeutic purposes or to limit its permeability to prevent progression of brain disease.

Chapter 3

Results

3.1 CONNEXIN CHANNELS PROVIDE A TARGET TO MANIPULATE BRAIN ENDOTHELIAL CALCIUM DYNAMICS AND BLOOD BRAIN BARRIER PERMEABILITY

This section is based on the following reference: Marijke De Bock, Maxime Culot, Nan Wang, Mélissa Bol, Elke Decrock, Elke De Vuyst, Anaëlle da Costa, Ine Dauwe, Mathieu Vinken, Alexander M. Simon, Vera Rogiers, Gaspard De Ley, W. Howard Evans, Geert Bultynck, Geneviève Dupont, Romeo Cecchelli and Luc Leybaert. Connexin channels provide a target to manipulate brain endothelial calcium dynamics and blood brain barrier permeability. *J Cereb Blood Flow Metab* 2011 Sep; 31 (9): 1942-57

The rationale for the onset of this study comes from two major observations: *i*) a limited number of reports point towards a possible involvement of connexin hemichannels in Ca^{2+} oscillations (see 3.1.1), and *ii*) Ca^{2+} oscillations have been described in BBB endothelia (see 1.4.3.1), yet their effect on BBB permeability remains largely unknown. This section outlines our results concerning the role of connexin hemichannels in endothelial Ca^{2+} oscillations and their functional impact on BBB permeability.

ABSTRACT

The cytoplasmic Ca^{2+} concentration ($[\text{Ca}^{2+}]_i$) is an important factor determining the functional state of blood-brain barrier (BBB) endothelial cells but little is known on the effect of dynamic $[\text{Ca}^{2+}]_i$ changes on BBB function. We applied different agonists that trigger Ca^{2+} oscillations and determined the involvement of connexin channels and subsequent effects on endothelial permeability in immortalized and primary brain endothelial cells. The inflammatory peptide bradykinin (BK) triggered Ca^{2+} oscillations and increased endothelial permeability. The latter was prevented by buffering $[\text{Ca}^{2+}]_i$ with BAPTA indicating that Ca^{2+} oscillations are crucial in the permeability changes. BK-triggered Ca^{2+} oscillations were inhibited by interfering with connexin channels, making use of carbenoxolone, Gap27, a peptide blocker of connexin channels, and Cx37/43 knockdown. Gap27 inhibition of the oscillations was rapid (within minutes) and work with connexin hemichannel-permeable dyes indicated hemichannel opening and purinergic signaling in response to stimulation with BK. Moreover, Gap27 inhibited the BK-triggered endothelial permeability increase in *in vitro* and *in vivo* experiments. By contrast, Ca^{2+} oscillations provoked by exposure to ATP were not affected by carbenoxolone or Gap27 and ATP did not disturb endothelial permeability. We conclude that interfering with endothelial connexin hemichannels is a novel approach to limiting BBB permeability alterations.

3.1.1 INTRODUCTION

The blood brain barrier (BBB) is a highly selective lipophilic barrier between the systemic blood circulation and the brain tissue and plays an essential role in brain homeostasis, which is crucial for normal neuronal activity and brain function. The BBB is formed by brain capillary endothelial cells that are characterized by an extremely low rate of transcytosis and form a restrictive barrier to paracellular diffusion due to the absence of fenestrations and the presence of a complex structure of tight junctions [Zlokovic, 2008]. During neuroinflammation and stroke, BBB endothelial cells lose their barrier properties, leading to uncontrolled passage of ions, proteins and water that culminates in disturbed neural tissue functioning and edema. The detailed signal-transduction pathways leading to BBB alterations, including increased permeability of the endothelial layer, are complex and not fully understood, but it is well appreciated that an increase in the cytosolic Ca^{2+} concentration ($[\text{Ca}^{2+}]_i$) takes a central stage in this process [Abbott, 2000]. Bradykinin (BK), a nonapeptide derived from the kinin-kallikrein system, is a typical inflammatory messenger that triggers a BBB permeability increase both *in vitro* [Easton and Abbott, 2002; Hurst and Clark, 1998] and *in vivo* [Sarker et al., 2000]. Genetic knockout of the G-protein coupled BK receptor-1 or pharmacological interference with this receptor protects mice against BBB permeability increases and brain edema following stroke [Austin et al., 2009] and brain trauma [Raslan et al., 2010]. $[\text{Ca}^{2+}]_i$ was identified as the major second messenger mediating the downstream effects of BK [Easton and Abbott, 2002; Olesen, 1989]. RMP7, a stable analogue of BK used clinically to increase barrier permeability to drugs, mimics BK in its capability to increase $[\text{Ca}^{2+}]_i$ [Doctrow et al., 1994]. Investigations on BK-triggered $[\text{Ca}^{2+}]_i$ changes have been limited to studies that focus on the initial $[\text{Ca}^{2+}]_i$ transient provoked by exposing endothelial cells to BK. However, it is unlikely that a single short-lived $[\text{Ca}^{2+}]_i$ elevation would be sufficient to induce longer-lived BBB alterations. Ongoing repetitive $[\text{Ca}^{2+}]_i$ spike activity, i.e. Ca^{2+} oscillations, are more likely to result in prolonged alterations in BBB function. Ca^{2+} oscillations have been demonstrated in BBB endothelial cells, in response to ATP [Haorah et al., 2007a], hypoxia [Brown et al., 2004], endothelial-leukocyte interactions [Etienne-Manneville et al., 2000] or invasion of bacteria [Nikolskaia et al., 2006] but little is known on their effect on BBB function. BK has been demonstrated to trigger Ca^{2+} oscillations in endothelia from various vascular beds and species [Carter et al., 1991; Laskey et al., 1992; Sage et al., 1989] but it is not known whether this is also the case in BBB endothelium.

A starting point for the present study was the observation by Kawano et al. that in human mesenchymal stem cells, Ca^{2+} oscillations are linked to connexin hemichannels [Kawano et al., 2006], which are unapposed hexameric plasma membrane channels not engaged into gap junctions. The linkage factor was that ATP, released via hemichannels, activates P2Y_1 receptors and subsequently stimulates $\text{PLC}\beta$ with activation of InsP_3 signaling that lies at the basis of Ca^{2+} oscillations [Dupont et al., 2007]. A second link, provided by Verma et al., demonstrated inhibition of Ca^{2+} oscillations in cardiomyocytes and other cells by connexin mimetic peptides, which are peptides composed of a short sequence of the connexin protein, the building block of hemichannels and gap junctions [Verma et al., 2009]. Finally, Nagasawa et al. provided evidence, in a porcine BBB model, that endothelial connexins are associated with tight junction proteins and that inhibition of gap junctions inhibited barrier function [Nagasawa et al., 2006].

The aim of the present work was to investigate the role of connexin channels in endothelial Ca^{2+} oscillations and BBB function, and to determine whether these channels can be used as a target to prevent BBB alterations. We used ATP and BK as inducers of Ca^{2+} oscillations and assessed their effect on endothelial permeability as a parameter of BBB function. Interestingly, we found that interfering with connexin channels by using carbenoxolone, siRNA silencing of endothelial connexins (Cx37 and Cx43), and Gap27, a peptide identical to a sequence on the second extracellular loop of Cx37 and Cx43, inhibited Ca^{2+} oscillations triggered by BK but not those triggered by ATP. Endothelial permeability measurements *in vitro* demonstrated that the BK-triggered permeability increase was inhibited by Gap27 and this was further confirmed by *in vivo* BBB permeability measurements. Collectively, these data suggest that the connexin channel linkage of BK-triggered Ca^{2+} oscillations, which is absent in ATP-triggered oscillations, plays a role in influencing BBB permeability. Further work with connexin channel-permeable dyes indicated that BK exposure induced the opening of connexin hemichannels and that Gap27 inhibition of the oscillations was related to inhibition of hemichannels. These results demonstrate that connexin channel-linked Ca^{2+} oscillations are involved in controlling BBB permeability and that interfering with endothelial connexins is a novel approach to limit BBB permeability increases.

3.1.2 MATERIALS AND METHODS

3.1.2.1 Cell culture

RBE4 (rat brain endothelial) cells were kindly provided by Dr. F. Roux (Neurotech, Evry, France). Cells (up to passage 25) were grown on collagen-coated recipients (rat-tail collagen, Roche Diagnostics, Vilvoorde, Belgium) and maintained in alpha-MEM/Ham's F10 (1:1) supplemented with 10 % fetal calf serum (FCS), 2 mmol/L glutamine, 300 µg/ml G-418 (Gibco, Invitrogen, Merelbeke, Belgium) and 1 ng/ml human recombinant basic fibroblast growth factor (bFGF - Roche Diagnostics) at 37 °C and 5 % CO₂. Bovine brain capillary endothelial cells (BCECs) were grown in a non-contact co-culture with rat mixed glial cells as described previously [Cecchelli et al., 1999]. Glial cells were isolated from Sprague Dawley rat cerebral cortex at postnatal day 3, according to the procedure described by [Descamps et al., 2003]. Briefly, meninges were removed and brain tissue was gently forced through a nylon sieve. Glial cell cultures were obtained by seeding the cells on 6-well plates at 10⁵ cells in DMEM supplemented with 10 % FCS. Immunostainings showed that these cultures contained ~76 % GFAP positive cells (astrocytes), ~18 % ED-1 positive cells (microglia) and ~6 % O4 positive cells (oligodendrocytes). Three weeks after seeding, glial cultures were ready for use in co-culture experiments. BCECs, seeded onto rat-tail collagen-coated polycarbonate filter inserts (Millicell-PC, 3 µm pore size, 30 mm diameter, Millipore Corporation, Molsheim, France) were placed into 6-well plates containing the glial cells. BCEC and glia were grown together for another 12 days after which BBB features fully developed. During this period, cells were kept in DMEM supplemented with 10 % newborn calf serum, 10 % horse serum, 2 mmol/L L-glutamine, 50 µg/ml gentamycin and 1 ng/ml bFGF. HeLa cells (kindly provided by Dr. Klaus Willecke, Universität Bonn, Germany) and C6-glioma cells (kind gift of Dr. Christian C. Naus, University of British Columbia, Canada) were maintained in DMEM and DMEM/Ham's F12 (1:1) respectively, supplemented with 10 % FCS and 2 mmol/L glutamine.

3.1.2.2 Chemicals and reagents

Adenosine 5' triphosphate (ATP), 2-(methylthio)-ATP (2-MeS-ATP), ARL-67156, apyrase grade VI and VII, bradykinin, carbenoxolone, ethylene glycol-bis-(β-aminoethyl ether)-*N,N,N',N'*-tetraacetic acid (EGTA), paraformaldehyde, pyridoxal phosphate-6-azo(benzene-

2,4-disulfonic acid) tetrasodium salt (PPADS), probenecid and suramin were purchased from Sigma-Aldrich (Bornem, Belgium). 1,2-bis-(2-aminophenoxy)-ethane-*N,N,N',N'*-tetraacetic acid acetoxymethyl ester (BAPTA-AM), calcein-AM, 5-carboxyfluorescein diacetate acetoxymethyl ester (5-CFDA-AM), 3 kDa dextran fluorescein (lysine-fixable), 10-kDa dextran Texas Red, fluo3-AM, Hoechst 33342, lucifer yellow, pluronic[®] acid F-127 and propidium iodide were from Molecular Probes (Invitrogen). *D-myio*-inositol 1,4,5-trisphosphate, P⁴⁽⁵⁾-1-(2-nitrophenyl)ethyl ester ('caged-InsP₃') was from Calbiochem. The Gap27 peptide (SRPTEKTIFII - position 201–210 in both Cx37 and Cx43) and scrambled Gap27 (Gap27^{Scr}, TFEPIRISITK) were synthesized by Thermo Fisher Scientific (Ulm, Germany) at > 80 % purity.

3.1.2.3 Ca²⁺ imaging

RBE4 cells were seeded onto 9.2 cm² petridishes (TPP, Novolab) and experiments were performed at confluency. RBE4 monolayers were loaded with a mixture of 10 μmol/L fluo3-AM, 1 mmol/L probenecid and 0.01 % pluronic acid in HBSS-Hepes (in mmol/L: 0.95 CaCl₂; 0.81 MgSO₄; 13 NaCl; 0.18 Na₂HPO₄; 5.36 KCl; 0.44 KH₂PO₄; 5.55 D-glucose and 25 Hepes) during 1 h at room temperature (RT). BCECs on filter inserts and were placed in Petri dishes with HBSS-Hepes/probenecid containing fluo3-AM (10 μmol/L) and pluronic acid (0.01 %). The same solution was added to the filter insert. After 1 h, petridishes (RBE4) or filter inserts (BCECs) were washed and cells were left for an additional 30 min at RT in HBSS-Hepes/probenecid to allow for de-esterification. Cells were thereafter transferred to an inverted epifluorescence microscope (Eclipse TE 300, Nikon Belux), equipped with a heating stage to maintain the cells at ~27 °C. A superfusion system allowed changing the bath solution within ~1 min (bath volume ~1 mL). Superfusion was switched off during the registration of oscillatory activity. Images were taken every second with a x 40 water immersion objective (NA 0.8) and an electron multiplying CCD camera (Quantem 512SC, Photometrics, Tucson, AZ, USA). We used a Lambda DG-4 filterswitch (Sutter Instrument Company, Novato, CA, USA) to deliver excitation at 482 nm and captured emitted light via a 505 nm long-pass dichroic mirror and a 535 nm bandpass-filter (35 nm bandwidth). Recordings and analysis were done with custom-developed QuantEMframes and Fluoframes software written in Microsoft Visual C++ 6.0. Ca²⁺ oscillations were counted in a 10 min observation period and

were defined as at least two transient Ca^{2+} changes subsequent to the initial Ca^{2+} transient in a single cell, minimally 10 % above baseline fluo3-fluorescence.

3.1.2.4 Caged-InsP₃ loading and photoliberation

C6-glioma cells were loaded with caged-InsP₃ by electroporation, as described before [Decrock et al., 2009]. Briefly, cells, grown to confluency, were rinsed with a low-conductivity electroporation buffer and placed on the microscope stage. Thereafter, a small volume (10 μl) of caged-InsP₃ (200 $\mu\text{mol/L}$) and 10 kDa dextran texas red (100 $\mu\text{mol/L}$, added to visualize the electroporation zone), dissolved in electroporation buffer was added to a parallel wire Pt-Ir-electrode, positioned 400 μm above the cells. Electroporation was performed with 50 kHz bipolar pulses, at a field strength of 1000 V/cm, applied as 15 trains of 10 pulses of 2 ms duration each. After electroporation, cells were washed with HBSS-Hepes, left 5 min to recover and finally loaded with fluo3-AM. Photoliberation of InsP₃ was done by spot (20 μm diameter) illumination with 1 kHz pulsed UV light (349 nm UV laser Explorer, Spectra-Physics, Newport, Utrecht, Netherlands) applied during 20 ms (20 pulses of 90 μJ energy measured at the entrance of the microscope epifluorescence tube).

3.1.2.5 Gap junction dye coupling studies

Dye coupling via gap junctions was determined making use of fluorescence recovery after photobleaching (FRAP). Endothelial cultures were grown confluent on 9.2 cm^2 petridishes (TPP) and were loaded with the gap junction permeable fluorescent dye 5-CFDA-AM (532 Da, 10 $\mu\text{mol/L}$) in HBSS-Hepes/probenecid for 1 h at RT. Following de-esterification, cells were transferred to a custom-made video-rate confocal laser scanning microscope with a x40 water immersion objective (CFI Plan Fluor) and a 488 nm laser excitation source (Cyan CW Laser, 488 nm - 100 mW, Newport Spectra-Physics, Utrecht, The Netherlands). After 1 min of recording, the cell in the middle of the field was photobleached by spot exposure (1 s) to increased power of the 488 nm laser and fluorescence recovery, caused by dye influx from neighboring non-bleached cells, was recorded during an additional 5 min period. The fluorescence recovery trace was then analyzed for the recovery of the signal expressed relative to the starting level before photobleaching.

3.1.2.6 Hemichannel assays

Hemichannel opening was investigated by the uptake or release of fluorescent hemichannel-permeable dyes. We used calcein (623 Da) to study dye release and propidium iodide (PI, 668 Da), lucifer yellow (LY, 457 Da) or 3 kDa dextran fluorescein (DF) to investigate dye uptake. The latter was used as a hemichannel-impermeable control probe [Li et al., 1996]. Calcein release is based on the efflux of the preloaded dye via hemichannels. For calcein release studies, subconfluent cultures of RBE4, grown on glass coverslips, were preloaded with 50 $\mu\text{mol/L}$ calcein-AM in HBSS-hepes/probenecid for 1 h at RT. Subsequently, the remaining calcein-AM was removed; cells were left to de-esterify an additional 30 min at RT in HBSS-Hepes/probenecid and were then transferred to an inverted epifluorescence microscope. For analysis, we measured the decrease in calcein fluorescence as a function of time. The first 5 min baseline leakage in HBSS-Hepes/probenecid (control) was measured. Thereafter, the trigger solution was added and efflux of calcein was further evaluated during 5 min. Gap27 was either preincubated during 1 h or added together with trigger for an additional 5 min in superfusion experiments. The slope of the curve, calculated by linear regression, was used as a parameter describing the loss of dye in time. Calcein efflux in the presence of trigger is presented as % of control. For dye uptake, cells were seeded onto four-well plates (Nunc brand products, Novolab) at a density of 50 000 cells/ml and used the next day. Cultures were rinsed twice and incubated during 10 min with propidium iodide (PI, 2 mmol/L), Lucifer Yellow (LY, 25 mmol/L) or 3 kDa dextran fluorescein (DF, 100 $\mu\text{mol/L}$) added to the trigger solution. Pictures were acquired with a Nikon TE300 epifluorescence microscope, x10 objective (Plan APO, NA 0.45) and Nikon DS-5M camera (Nikon Belux). In each culture, 9 snap-shot images were taken. The number of dye-positive cells in each image was counted using ImageJ (<http://rsb.info.nih.gov/ij>) after application of a threshold corresponding to the upper level of the background signal. Dye uptake is expressed as the percentage of dye-positive cells relative to the total number of cells counted with Hoechst staining ($22,000 \pm 900$ cells/cm²).

3.1.2.7 Cell death studies

Cell death was assessed by examining PI uptake into the cells. Cell cultures were exposed to PI (30 $\mu\text{mol/L}$) and Hoechst (10 $\mu\text{g/mL}$) for 10 min. The number of dead cells showing PI-staining was expressed as the percentage of dye-positive cells relative to the total number of cells

counted from the Hoechst staining. Note that PI was also used for dye uptake studies which needed much higher concentrations (see ‘Hemichannel assays’).

3.1.2.8 *In vitro* endothelial permeability

In vitro endothelial permeability was measured as described previously [Cecchelli et al., 1999]. Filter inserts containing confluent BCEC monolayers were separated from the glial cells, washed with HBSS-Hepes and added to a six-well plate with each well containing 2.5 ml HBSS-Hepes (lower compartment). The filter insert (upper compartment) was filled with 1.5 ml HBSS-Hepes containing 50 $\mu\text{mol/L}$ LY (457 Da) or 3 kDa DF (20 $\mu\text{mol/L}$) as a transport marker. At 15, 30, 45 and 60 min the filters were transferred to a new well (**figure 24A**) and samples were taken from each lower compartment. The temperature was kept at 37 °C. Aliquots were also taken from the upper compartment, at the beginning and end of the experiment. The cleared volume was determined by dividing the fluorescence in the lower compartment at each time point by the concentration in the upper compartment and was plotted versus time. The slope of this curve, calculated by linear regression, corresponds to the permeability-surface (PS) product and subtracting the PS product of an empty, coated filter gives the PS product of the endothelial monolayer. Subsequent division by the surface area of the filter membrane (4.2 cm²) yields the permeability coefficient Pe. The inhibitory agents and vehicles used in this study were all without effect on the permeability.

3.1.2.9 *In vivo* BBB permeability

Male Wistar rats (200-250 g) and FVB mice (20-22 g) were treated according to the European Ethics Committee guidelines and the study protocol was approved by the university animal experiment ethical committee. The animals were housed under controlled environmental conditions with *ad libitum* access to food and water and were randomly assigned to treatment (‘control’, ‘BK’, ‘BK + Gap27’ or ‘BK + Gap27^{Scr}’). On the same day, rats were anesthetized with sodium pentobarbital (100 mg/kg, I.P.) and a catheter (PE 50) was placed in the femoral vein. Control rats received 3 kDa DF (30 mg/kg, I.V.), ‘BK rats’ received 3 kDa DF in combination with BK (150 $\mu\text{g/kg}$, I.V.) and in ‘BK + Gap27’ or ‘BK + Gap27^{Scr}’ rats 3 kDa DF was administered along with BK (150 $\mu\text{g/kg}$, I.V.) and Gap27 or Gap27^{Scr} respectively (both 25 mg/kg, I.V.). All solutions were allowed to circulate during 30 min. Subsequently, the

animals were transcardially perfused, first with PBS and in second instance with 4% paraformaldehyde to fix the tissue. Immediately after isolation, the brain was sliced into thick (± 2 mm) coronal sections using a vibrating microtome (VibrosliceTM 725M, Campden instruments Ltd., Loughborough, UK). The area from which sections were made was located between 4.7 mm anterior and 7.3 mm posterior to the bregma. Brain sections were visualized using a GeneFlash system (Syngene, Cambridge, UK) equipped with a UV light source, a 410-510 nm conversion screen, CCD camera, f/1.2 8-48 mm zoom lens and an emission bandpass filter to detect fluorescence (550-600 nm). The signal intensity was determined using ImageJ software. For each section, fluorescence intensity was determined in 10 zones, all located in the cortex which was identified by comparison of visible light images with a rat brain atlas. Background fluorescence was measured just outside the coronal sections and was subtracted from the fluorescence in the measurements points.

3.1.2.10 siRNA treatment

RBE4 cells were seeded on 9.2 cm² dishes at 27 000 cells/cm² and transfected the following day with 50 nmol/L siGENOME ON-TARGETplus SMARTpool siRNA using Dharmafect1 lipid reagent (Dharmacon, Thermo Fisher Scientific). The siRNA pool used was a mix of 4 different duplexes directed against the Cx37 gene *gja4* and the Cx43 gene *gja1* (rat). On day 3, culture medium was refreshed and on day 4, cells were used for experiments. Transfection efficiency was 51 ± 2.0 % (n=16) on day 3, as determined with the fluorescent indicator siGLO. Control conditions were untreated cultures, Mock treated cultures (lipid reagent alone) and a negative control consisting of cultures transfected with a pool of 4 duplexes that have minimal targeting of known rat genes (ON-TARGETplus siCONTROL non-targeting pool - Dharmacon). Western blotting demonstrated that siRNA pools targeting Cx37 and Cx43 reduced the expression of their respective target in RBE4 cells, but there were cross-reactions from the Cx43 siRNA on Cx37 expression and *vice versa* (caused either by coordinated regulation of Cx37 and Cx43 expression or true cross-activation of the applied siRNAs). We therefore combined the two siRNA treatments to knockdown both Cx37 and Cx43. siRNA treatment of BCECs was not possible as the procedure by itself caused increased permeability of the endothelial cell layer.

3.1.2.11 Electrophoresis and western blotting

For western blots, cells were seeded in 75 cm² falcons or 9.2 cm² dishes (siRNA-treated cells). Total RBE4 lysates were extracted with RIPA buffer, BCEC filters were scraped in ice-cold PBS containing protease inhibitor cocktail (Roche Diagnostics). Protein concentration was determined using the Biorad DC protein assay kit (BioRad, Nazareth, Belgium) and absorbance was measured with a 590 nm long-pass filter. The lysate was separated by electrophoresis over a 10 % SDS-polyacrylamide gel and transferred to a nitrocellulose membrane (Amersham, Buckinghamshire, UK). Membranes were subsequently blocked with TBS containing 5 % non-fat milk and 0.1 % Tween20. Following the blocking, blots were probed with rabbit anti-Cx43 antibody (Sigma-Aldrich), rabbit anti-Cx40 antibody (alpha-diagnostic international, Brussels, Belgium), rabbit anti-Cx37 antibody (gift of A.M. Simon; [Simon et al., 2006]), rabbit anti-P2X₇ antibody (Alomone Labs, Jerusalem, Israel) and rabbit anti- β -tubulin antibody (Abcam, Cambridge, UK) as a loading control. Membranes were subsequently incubated with an alkaline phosphatase-conjugated goat anti-rabbit IgG antibody (Sigma-Aldrich) and detection was done using the nitro-blue-tetrazolium/5-bromo-4-chloro-3-indolyl-phosphate reagent (NBT/BCIP kit, Zymed, Invitrogen). Quantification was done by drawing a rectangular window around the concerned connexin band and determining the signal intensity using ImageJ. Background correction was done by the same procedure applied to nitrocellulose membranes where protein was absent.

3.1.2.12 Polymerase chain reaction

Cells were grown to confluence on 75 cm² falcons, scraped in ice-cold PBS and the resulting pellet was put at -80 °C. Total RNA was isolated using the RNeasy Plus mini kit (Qiagen, Venlo, Netherlands). Reverse transcription was performed by the iScript cDNA synthesis kit (BioRad) and cDNA was amplified using the Taq DNA polymerase kit (Invitrogen). Primers were: Panx1 forward 5'-TTCTTCCCCTACATCCTGCT-3' and reverse 5'-GGTCCATCTCTCAGGTCCAA-3'; GAPDH (internal control) forward 5'-ACCACAGTCCATGCCATCAC-3' and reverse 5'-TCCACCACCCTGTTGCTGTA-3' (all synthesized by Invitrogen). The PCR protocol contained 35 cycles of 94 °C (45 sec), 50 °C (1 min) and 72 °C (1 min), preceded by 4 min 94 °C and followed by 5 min 72 °C. As a negative

control, a sample lacking reverse transcriptase (RT-) was used. The PCR end-products were separated on a 2 % agarose gel and visualized with ethidium bromide (Invitrogen).

3.1.2.13 Immunofluorescence

Immunostaining of BCECs was performed with the following primary antibodies: rabbit anti-occludin, mouse anti-vimentin and rabbit anti-ZO-1 (all from Zymed Laboratories Inc., Invitrogen). Rhodamine-phalloidine (Molecular Probes, Invitrogen) was used for F-actin labelling. Following fixation with 4 % paraformaldehyde, cells were permeabilized with 0.1 % Triton X-100 or ice-cold acetone (vimentin staining). Cells were then preincubated for 30 min in 10 % goat serum before addition of primary antibodies (diluted in 2 % normal goat serum). After washing, secondary antibody conjugated to Alexa-568 or Alexa-488 (Molecular Probes, Invitrogen) was added and filter sections were mounted in Mowiol containing DABCO (Sigma-Aldrich).

3.1.2.14 Statistical analysis

Data are expressed as mean \pm S.E.M. with n giving the number of independent experiments. Multiple groups were compared by one-way ANOVA and a Bonferroni post-test, making use of Graphpad Instat software. Two groups were compared with an unpaired student's t-test and two-tail p-value. Results were considered statistically significant when $p < 0.05$ (one symbol for $p < 0.05$, two for $p < 0.01$ and three for $p < 0.001$).

3.1.3 RESULTS

3.1.3.1 BK triggers Ca^{2+} oscillations that involve connexin hemichannel opening and purinergic signaling

Exposure of confluent RBE4 cell cultures to BK in the range of 50 nmol/L to 1 $\mu\text{mol/L}$ typically elicited a transient $[\text{Ca}^{2+}]_i$ increase, followed by repetitive $[\text{Ca}^{2+}]_i$ spikes or oscillations. Occasionally, the initial $[\text{Ca}^{2+}]_i$ transient was absent (**figure 20A**). **Figure 20B** depicts the number of oscillating cells and the oscillation-frequency, which did not change markedly with the BK concentration. At 0.5 $\mu\text{mol/L}$ (the concentration used in subsequent

experiments) the frequency averaged 10 ± 0.5 $[Ca^{2+}]_i$ transients per 10 min (n=5), comparable to the BK-triggered oscillation-frequency in other cell types [De Blasio et al., 2004b]. There was no apparent synchronization of oscillatory activity between neighboring, oscillating cells. Baseline measurements in vehicle-treated RBE4 cultures showed that 1.8 ± 0.9 % of the cells were spontaneously oscillating at an average frequency of 2.3 ± 0.2 spikes per 10 min (n=6; percentage of oscillating cells significantly lower than following BK stimulation for all concentrations applied; $p < 0.01$). BK exposure of long term cultivated, primary bovine BCECs kept in co-culture with glial cells (see Materials and methods) gave a similar $[Ca^{2+}]_i$ response pattern as in RBE4, with an initial transient followed by oscillatory activity. Here, baseline conditions showed 5.3 ± 1.8 % of the cells spontaneously oscillating (n=3; significantly lower than after BK stimulation for all concentrations applied; $p < 0.05$). Interestingly, oscillations in response to $0.5 \mu\text{mol/L}$ BK were significantly less frequent when BCECs were cultured on membrane inserts without mixed glial cells in the bottom dish (~25 % of the cells oscillating *versus* ~65 % with glial cells present during co-culture, **figure 20C,D**).

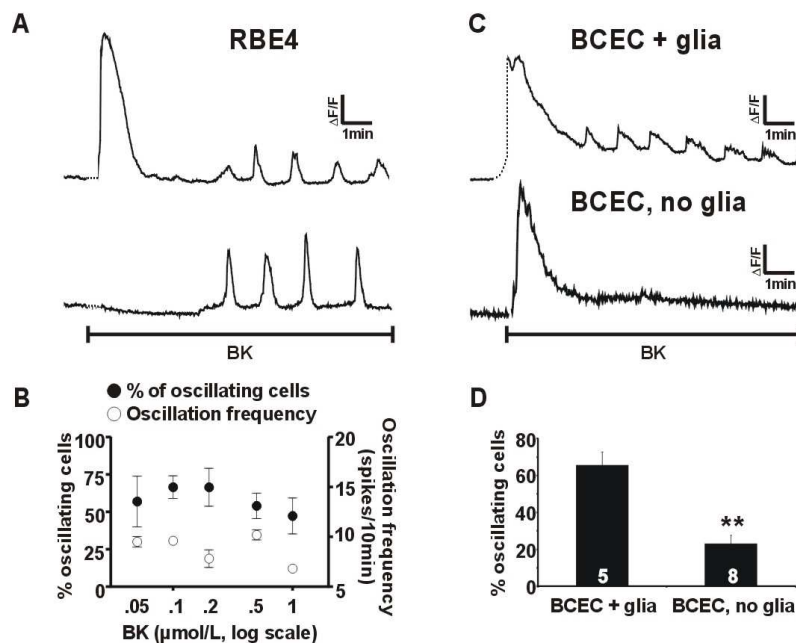
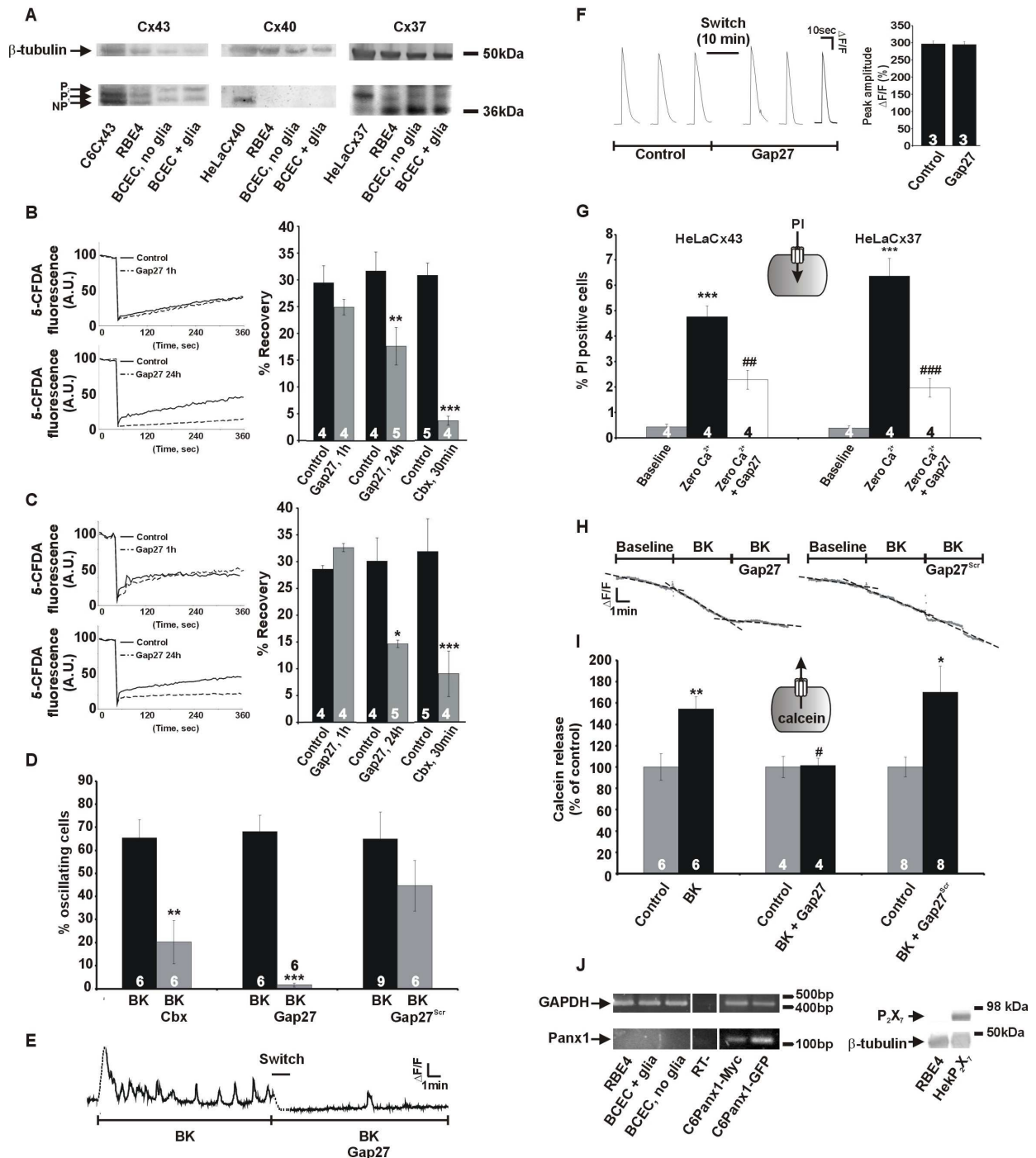


Figure 20. BK elicits Ca^{2+} oscillations. (A) Example traces of Ca^{2+} oscillations in selected RBE4 cells (from 2 different confluent cultures) triggered by $0.5 \mu\text{mol/L}$ BK. (B) The percentage of oscillating cells (●, left ordinate) and the oscillation-frequency (○, right ordinate) for various BK concentrations. (C) Example traces of Ca^{2+} oscillations triggered by $0.5 \mu\text{mol/L}$ BK in BCEC cells on membrane inserts grown in the presence (+ glia) or absence (no glia) of mixed glial cells in the bottom dish. (D) Summary data of the percentage of oscillating cells in BCECs grown with or without glia, stimulated with $0.5 \mu\text{mol/L}$ BK.

Previous work in various cell types has suggested that Ca^{2+} oscillations can be suppressed by interfering with connexin hemichannels [Kawano et al., 2006; Verma et al., 2009]. We tested the effect of two types of blockers: carbenoxolone, a general connexin channel blocker [Giaume and Theis, 2010], and connexin mimetic peptides [Evans et al., 2006]. The action of the mimetic peptides may depend on the connexin isoforms being present [Evans et al., 2006] and we first checked connexin expression in the cells used. Western blot analysis showed Cx37 and Cx43 expression in RBE4 and BCECs (**figure 21A**) with no discernable Cx40 signal. The Cx40 signal was also absent in RT-PCR experiments on the two cell types (data not shown). Connexin expression was not different between the 'BCEC + glia' and 'BCEC, no glia' conditions, indicating that the strong reduction of Ca^{2+} oscillations in 'BCEC, no glia' is not caused by changes in connexin expression.

Gap27 is a peptide identical to a short sequence in the second extracellular loop of both Cx37 and Cx43; this peptide has been demonstrated to inhibit connexin hemichannel-mediated ATP release and dye uptake upon short (minutes) exposure [Braet et al., 2003a; Eltzschig et al., 2006; Evans et al., 2006] while longer exposures (several hours) also affect gap junctions [Braet et al., 2003a; Decrock et al., 2009]. **Figure 21B,C** demonstrate that 1 h exposure to Gap27 (200 $\mu\text{mol/L}$) did not impair gap junctional dye coupling in RBE4 and BCEC cultures measured with FRAP, while 24 h incubations indeed inhibited junctional coupling. Gap27 (200 $\mu\text{mol/L}$, 1 h pre-incubation) and the non-specific connexin channel inhibitor carbenoxolone (Cbx, 25 $\mu\text{mol/L}$, 30 min) strongly reduced the number of cells displaying Ca^{2+} oscillations in response to BK exposure, whereas scrambled Gap27 (Gap27^{Scr}) had no effect (**figure 21D**). The Gap27 effect on oscillations in individual cells occurred rapidly, within minutes after introducing the peptide in the bath solution (**figure 21E**).

Ca^{2+} oscillations are driven by the concerted action of InsP_3 and Ca^{2+} on InsP_3 receptors [Dupont et al., 2007] and we tested whether Gap27 influenced this signaling pathway. We performed these experiments in C6-glioma cells that have a low endogenous connexin expression to avoid interference of Gap27 with connexin channels. Stepwise increases of intracellular InsP_3 in these cells, brought about by photoliberation of InsP_3 , triggered transient $[\text{Ca}^{2+}]_i$ changes that were not influenced by Gap27 (**figure 21F**). As a consequence, in RBE4, inhibition of oscillations by Gap27 was not caused by influencing InsP_3 -triggered Ca^{2+} release and we further explored the involvement of connexin hemichannels in BK-triggered oscillations.



We used the hemichannel-permeable dye PI (668 Da, charge +2) in dye uptake studies and calcein (623 Da, charge -4, preloaded into the cells) in dye release experiments in order to document hemichannel opening. Experiments on Cx37- or Cx43-expressing HeLa cells indicated that Gap27 inhibited dye uptake in both cell lines with similar potency (**figure 21G**), as expected from the sequence homology of the Gap27 domain in Cx37 and 43. Exposure of RBE4 cells to BK (0.5 μ mol/L, 10 min) triggered PI uptake (data not shown) and calcein

release that was inhibited by Gap27 but not affected by Gap27^{Scr} (**figure 21H,I**). A contribution of Panx1 hemichannels or P2X₇ receptor channels as alternative pathways for dye uptake was excluded based on the absence of mRNA and protein expression respectively (**figure 21J**).

Figure 21. Connexin channels are involved in BK-triggered Ca²⁺ oscillations. (A) Western blot analysis for Cx37, Cx40 and Cx43 in RBE4 and BCEC cells. Cx43 and Cx37 were present whereas Cx40 was not detected. C6Cx43, HeLaCx40 and HeLaCx37 were positive controls; β -tubulin was a loading control. (B) Gap junctional dye coupling studied with fluorescence recovery after photobleaching (FRAP) in RBE4 cultures. Gap27 (200 μ mol/L) did not influence dye coupling (quantified from fluorescence recovery) after 1 h incubation but inhibited coupling following 24 h incubation. The general connexin channel blocker carbenoxolone (Cbx, 25 μ mol/L) was used as a positive control. Star signs compare to control. (C) Similar observations were made in BCECs. (D) In RBE4 cells, Ca²⁺ oscillations elicited by 0.5 μ mol/L BK were inhibited by Cbx (25 μ mol/L, 30 min) and Gap27 (200 μ mol/L, 1 h) but not by Gap27^{Scr} (200 μ mol/L, 1 h). Stars compare to BK. (E) Example trace illustrating rapid block of BK-induced Ca²⁺ oscillations after adding Gap27 ('switch', 1 min duration). (F) Gap27 does not disturb InsP₃-Ca²⁺ signaling. Example traces of [Ca²⁺]_i transients triggered by photoactivation of InsP₃ in C6-glioma cells under control conditions and in the presence of Gap27 (200 μ mol/L, 10 min). The bar chart at the right summarizes the results of these experiments: Gap27 had no influence on the peak amplitude of InsP₃-induced [Ca²⁺]_i changes. (G) Experiment demonstrating that Gap27 inhibited PI uptake in HeLa cells expressing Cx37 (HeLaCx37) and in HeLaCx43. Hemichannel opening was stimulated by exposure of the cells to zero extracellular Ca²⁺ solution and the percentage of PI-positive cells was determined. Stars compare to Baseline; number signs compare to zero Ca²⁺. (H) Exposure of RBE4 cells pre-loaded with calcein (ester loading) to BK (0.5 μ mol/L) stimulated the loss of calcein from the cells and this was rapidly inhibited by Gap27 (200 μ mol/L) but not by Gap27^{Scr}. The dashed lines represent linear fits of the 3 trace sections. (I) Summary data of experiments as illustrated in panel H, demonstrating inhibition of calcein release by Gap27 but not by Gap27^{Scr}. Stars compare to control; number sign compares to BK. (J) PCR demonstrating absence of Panx1 mRNA in RBE4 and BCEC. C6-Panx1-Myc and C6-Panx-GFP are positive controls; RT- is a negative control; GAPDH is an internal control. The western blot shown right demonstrates absence of P2X₇ in RBE4; HEK-P2X₇ is a positive control.

We next applied siRNA technology to silence the two connexin isoforms (Cx37/Cx43) and verified the effect on Ca²⁺ oscillations. Treatment of RBE4 cells with siRNA directed against Cx37/Cx43 reduced the expression of both connexins by ~1/3 (**figure 22A**) and approximately halved the number of oscillating cells during BK exposure (**figure 22B**). siRNA treatment did not influence cell death (0.2 \pm 0.1 % PI-positive cells *versus* 0.3 \pm 0.1 % in untreated cells, n=6).

Connexin hemichannel opening results in ATP release [Kang et al., 2008] and we tested whether extracellular ATP played a role in the oscillations. The number of RBE4 cells displaying BK-triggered Ca^{2+} oscillations was strongly reduced by apyrase VI/VII (5 U/ml, 30 min pre-incubation), an enzyme mix that hydrolyzes ATP to AMP, or the two broad spectrum P2 receptor antagonists suramin (200 $\mu\text{mol/L}$, 30 min pre-incubation) and PPADS (75 $\mu\text{mol/L}$, 30 min pre-incubation) (**figure 22C**). Interestingly, when RBE4 cells were exposed to BK and ATP together (both 0.5 $\mu\text{mol/L}$), the oscillations disappeared in ~55% of the cells (**figure 22C**). We tested lower concentrations of ATP (0.1 and 0.05 $\mu\text{mol/L}$) co-applied with 0.5 $\mu\text{mol/L}$ BK and this gave an equally strong (and equally significant) inhibition as 0.5 $\mu\text{mol/L}$. In addition, hemichannel PI uptake studies demonstrated less PI-positive cells when ATP was co-administered with BK (both at 0.5 $\mu\text{mol/L}$) as compared to BK alone (**figure 22D**).

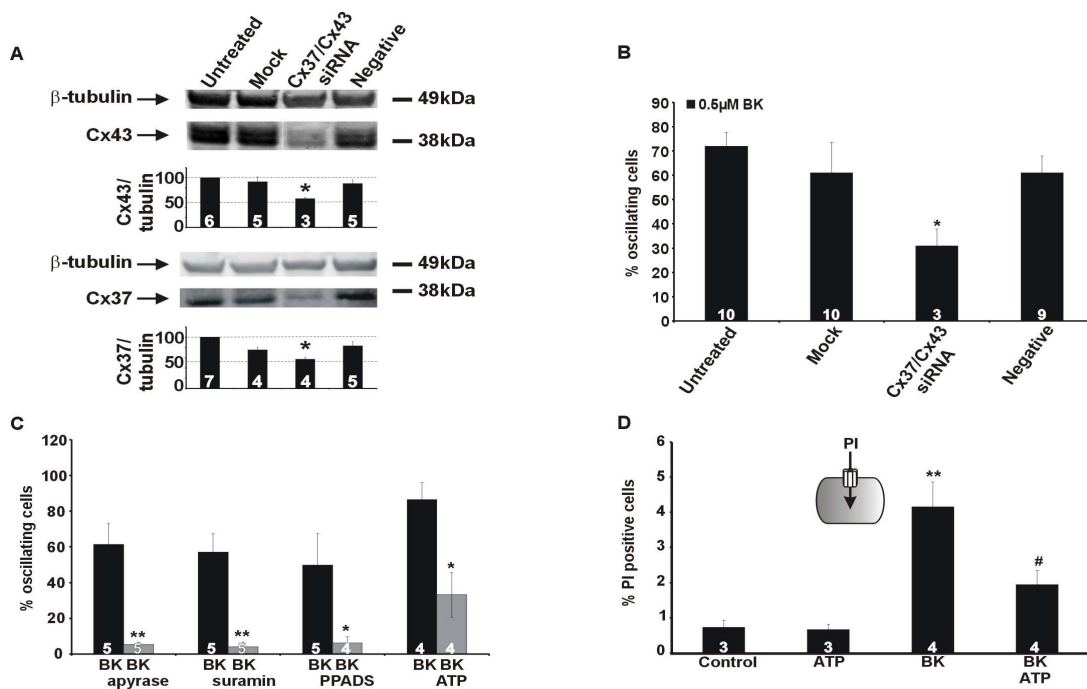


Figure 22. Effect of Cx37/43 gene silencing and contribution of purinergic signaling in BK-triggered Ca^{2+} oscillations. (A) siRNA suppression of Cx37 and Cx43 in RBE4, demonstrating significantly reduced expression to ~2/3 of the negative control signal (star symbol compares to negative control). (B) Cx37/Cx43 knockdown in RBE4 approximately halved the number of oscillating cells (star compares to negative control). (C) BK-triggered Ca^{2+} oscillations were strongly reduced by apyrase VI/VII (5 U/ml, 30 min), suramin (200 $\mu\text{mol/L}$, 30 min) or PPADS (75 $\mu\text{mol/L}$, 30 min). Co-exposure of BK together with ATP (0.5 $\mu\text{mol/L}$) resulted in significantly reduced oscillatory activity. Stars compare to BK. (D) PI dye uptake in RBE4 cells demonstrating that BK (0.5 $\mu\text{mol/L}$) triggered an increase in the number of PI-positive cells whereas ATP (0.5 $\mu\text{mol/L}$) had no effect. Including ATP (0.5 $\mu\text{mol/L}$) together with BK inhibited the BK-triggered increase in dye uptake. Stars compare to Control; number signs compare to BK.

3.1.3.2 ATP triggers Ca^{2+} oscillations that are not associated with hemichannel opening

Exposing RBE4 or BCECs (co-cultured with glial cells) to ATP (25 nmol/L to 1 $\mu\text{mol/L}$) triggered Ca^{2+} oscillations (**figure 23A**) and the oscillation-frequency increased with ATP concentration (from 6 to 11 Ca^{2+} transients/10 min, **figure 23B**). The amplitudes of ATP-triggered oscillations (0.5 $\mu\text{mol/L}$) were smaller than those triggered by BK in RBE4 cells but they were equal in BCECs (co-cultured with glial cells), the cell system in which *in vitro*-permeability measurements were made (see below) (**figure 23C**). As observed with BK, ATP-triggered oscillatory activity (0.5 $\mu\text{mol/L}$) was significantly suppressed when glial cells were absent during co-culture (2.8 ± 2.4 % oscillating cells compared to 63.0 ± 18.3 % with glial cells present during co-culture, $n=7$). Importantly, hemichannel PI uptake studies in RBE4 cells demonstrated no hemichannel opening in response to ATP (**figure 22D**) and ATP-induced oscillations were not influenced by Cbx and Gap27 (**figure 23D**), indicating an oscillation mechanism that is distinct from BK-triggered oscillations.

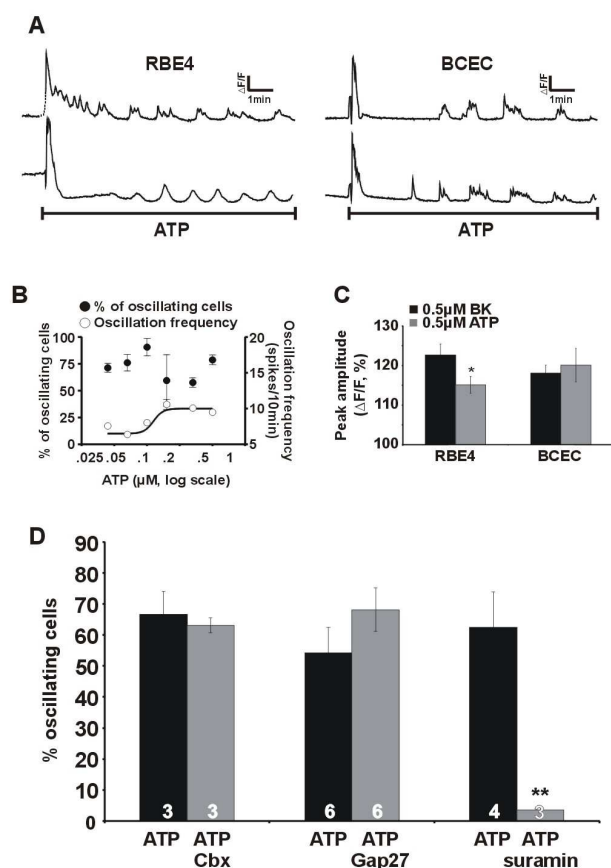


Figure 23. ATP elicits Ca^{2+} oscillations that are not influenced by connexin channel blockers. (A) Example traces demonstrating Ca^{2+} oscillations triggered by 0.5 $\mu\text{mol/L}$ ATP in selected RBE4 and BCEC cells. (B) Percentage of oscillating cells (●, left ordinate) and oscillation-frequency (○, right ordinate) for various ATP concentrations. (C) Comparison of the peak-amplitudes of Ca^{2+} oscillations obtained with BK and ATP. The amplitudes were slightly (but significantly) different in RBE4 but not different in BCECs, the cells used for endothelial permeability measurements presented in figure 24. (D) ATP-induced Ca^{2+} oscillations disappeared with suramin (200 $\mu\text{mol/L}$, 30 min) but were not influenced by Cbx (25 $\mu\text{mol/L}$, 30 min) and Gap27 (200 $\mu\text{mol/L}$, 1 h). Stars compare to the neighboring black bar.

3.1.3.3 BK, but not ATP, increases BCEC permeability in a $[Ca^{2+}]_i$ -dependent and Gap27-inhibitable manner

We tested the effect of BK and ATP on the permeability of BCECs grown on filter membranes in the presence of glial cells [Cecchelli et al., 1999]. Exposure to BK (0.5 $\mu\text{mol/L}$, present during the 60 min duration of the permeability assay) increased the endothelial permeability measured with lucifer yellow (LY). Treatment with BK did not have any effect on BCEC cell death ($0.5 \pm 0.2\%$ and $0.8 \pm 0.3\%$ PI-positive cells in untreated and BK-treated cultures respectively, $n=5$). Pre-loading of the BCECs with the Ca^{2+} buffer BAPTA (BAPTA-AM ester-loading, 5 $\mu\text{mol/L}$, 1 h), to restrain the induced $[Ca^{2+}]_i$ changes, or incubation of the cells with Gap27 (200 $\mu\text{mol/L}$, 30 min pre-incubation and present during the permeability assay) prevented the permeability increase brought about by BK (**figure 24B-D**). In contrast to BK, ATP (0.5 $\mu\text{mol/L}$) had no influence on endothelial permeability (**figure 24E**), which is in line with observations in other endothelia where ATP has no effect on permeability [Jacobson et al., 2006]. Applying higher ATP concentrations (5 $\mu\text{mol/L}$) or the more potent P2Y receptor agonist 2-MeS-ATP (0.5 $\mu\text{mol/L}$), as well as combining ATP exposure with ARL-67156 (100 $\mu\text{mol/L}$) to inhibit ATP degradation by ecto-ATPases were all without effect on endothelial permeability (data not shown).

We further probed the BK-triggered permeability increase with 3 kDa DF instead of LY (457 Da) as a reporter dye, in order to obtain information on the permeability profile. The BK-triggered permeability increase (expressed as fold increase) was very similar when assessed with these two dyes, as illustrated in **Table 6**. Because the results of experiments presented in figures 21H,I and 22D suggest connexin hemichannel opening upon BK-exposure, we tested the possibility that hemichannel opening at both sides of the endothelial plasma membrane creates a transcellular passageway for reporter dyes. We therefore applied LY and 3 kDa DF in hemichannel dye uptake experiments. These experiments showed that BK-triggered dye uptake in RBE4 cells was very different with the two probes, displaying no significant dye uptake of 3 kDa DF and an almost three-fold increase (compared to control) when probed with LY (**Table 6**). These distinct permeation profiles for increased endothelial permeability *versus* hemichannel opening indicate that hemichannels do not contribute as a direct, transcellular pathway to increased endothelial permeability as measured with the 3 kDa DF probe.

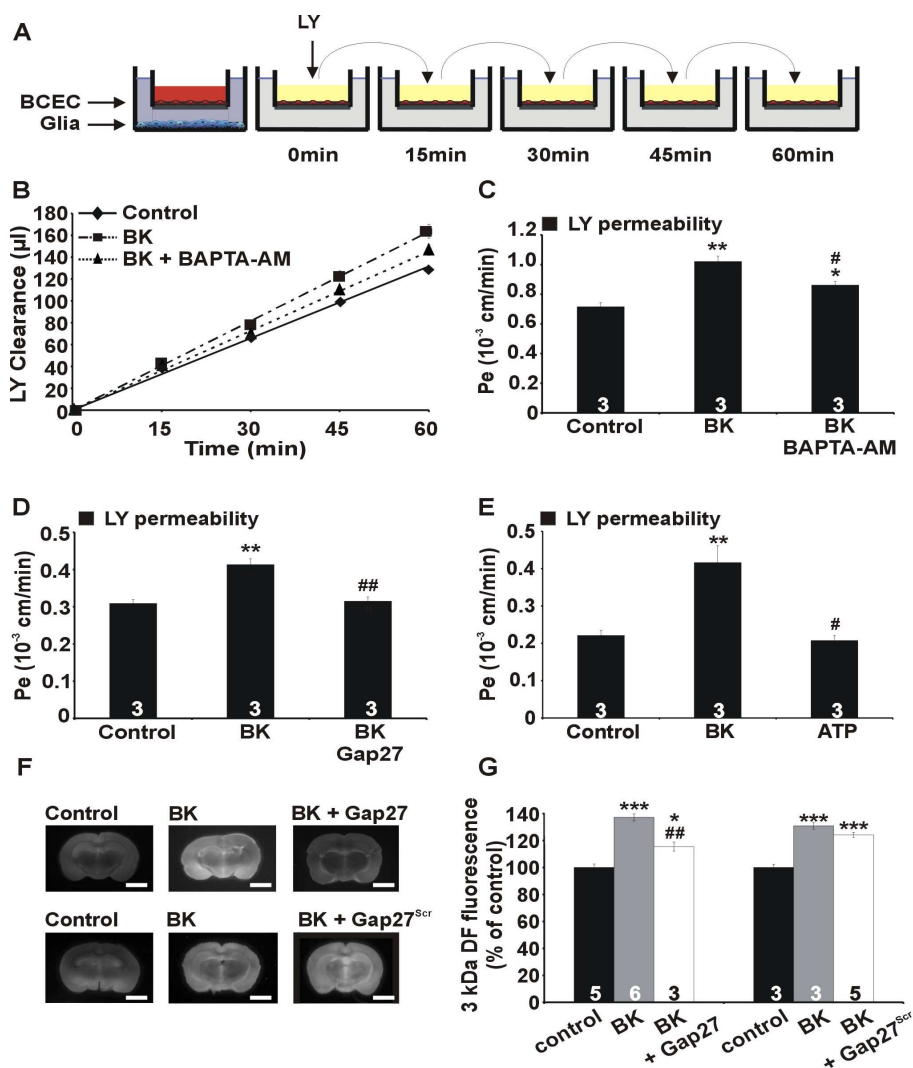


Figure 24. Effects of BK and ATP on endothelial permeability. (A) *In vitro* permeability measurements. BCECs were grown on membrane inserts in non-contact co-culture with glial cells at the bottom of the well. Membrane inserts were then placed in a new well and the fluorescent marker lucifer yellow (LY) was added. (B) Example curves for LY clearance from which the permeability coefficient P_e was calculated. BK (0.5 $\mu\text{mol/L}$) was added in the upper compartment; BAPTA-AM loading (1 h) was done with 5 $\mu\text{mol/L}$ in the upper compartment, in a well without glia. (C) Summary data of experiments as illustrated in panel B. BK (0.5 $\mu\text{mol/L}$) significantly increased the permeability to LY and this effect was inhibited by pre-loading BCECs with BAPTA-AM. (D) The BK-triggered permeability-increase was significantly reduced by Gap27 (200 $\mu\text{mol/L}$, 1 h pre-incubation in upper and lower compartment without glia, and present during the permeability assay). (E) ATP (0.5 $\mu\text{mol/L}$, upper compartment) did not influence endothelial permeability, in contrast to BK. (F) *In vivo* BBB permeability measurements. Coronal brain sections demonstrating that BK (150 $\mu\text{g/kg}$ I.V.) increased the leakage of 3 kDa dextran fluorescein (DF) in the neural tissue determined 30 min after BK/3 kDa DF injection. Administration of BK/3 kDa DF together with Gap27 (25 mg/kg) decreased the tissue leakage of the fluorescent marker while Gap27^{Scr} had no effect. Scale bar represents 0.5 cm. (G). Summary data of experiments as illustrated in panel F. The fluorescence intensity was measured in 10 analysis points in the cortical zones. Gap27 significantly reduced 3 kDa DF leakage while Gap27^{Scr} had no effect. Stars compare to Control; number signs compare to BK.

	<u>Endothelial permeability</u>	<u>Hemichannel dye uptake</u>
LY	1.5 ± 0.6	2.8 ± 0.7
3 kDa DF	1.5 ± 0.2	0.5 ± 0.4

Table 6. Overview of BK-triggered changes in *in vitro*-measured BCEC permeability and hemichannel dye uptake in RBE4. Numbers report the fold increase of dye passage/uptake provoked by 0.5 $\mu\text{mol/L}$ BK and expressed relative to control (n =3 for all).

In a next step, we investigated whether Gap27 was able to limit BBB permeability changes induced by BK *in vivo*. BK was injected intravenously (150 $\mu\text{g/kg}$) together with 3 kDa DF (30 mg/kg) as a marker for endothelial permeability. Thirty minutes later, the animals were sacrificed and coronal brain slices were cut. These experiments showed an enhanced fluorescence signal as quantified in the cortical regions, demonstrating increased leakage of reporter dye from the vascular lumen into the tissue, both in rats and in mice. When the same experiment was performed with Gap27 (25 mg/kg, corresponding to ~ 200 $\mu\text{mol/L}$ assuming the blood compartment as the distribution volume) co-administered together with BK/3 kDa DF, the cortical fluorescence signal was significantly suppressed (for rat data, see **figure 24F,G**), replicating the observations in the *in vitro* BBB model. In rats treated with Gap27^{Scr} (25 mg/kg), the BK-triggered permeability-increase was not different from rats treated with BK alone. Thus, in addition to inhibiting BK-triggered Ca^{2+} oscillations, Gap27 also inhibits the BK-triggered elevation of endothelial permeability *in vitro* and *in vivo*.

3.1.3.4 Effects of BK and Gap27 treatment on tight junction and cytoskeletal proteins

In a last step, we verified in BCECs whether BK exposure was associated with alterations in the organization of tight junction and cytoskeletal proteins. We did not observe any modifications in immunocytochemical stainings of occludin or ZO-1 and in phalloidin-stained F-actin (**figure 25A**) following exposure to BK (0.5 $\mu\text{mol/L}$, 1 h). We did, however, observe changes in the organization of the intermediate filament vimentin, with thickening, clustering and stretching of the fibers as compared to untreated control cells. These BK-triggered alterations were absent in cells exposed to BK + Gap27 (200 $\mu\text{mol/L}$, 1 h) or to ATP (0.5 $\mu\text{mol/L}$, 1 h) (**figure 25A**).

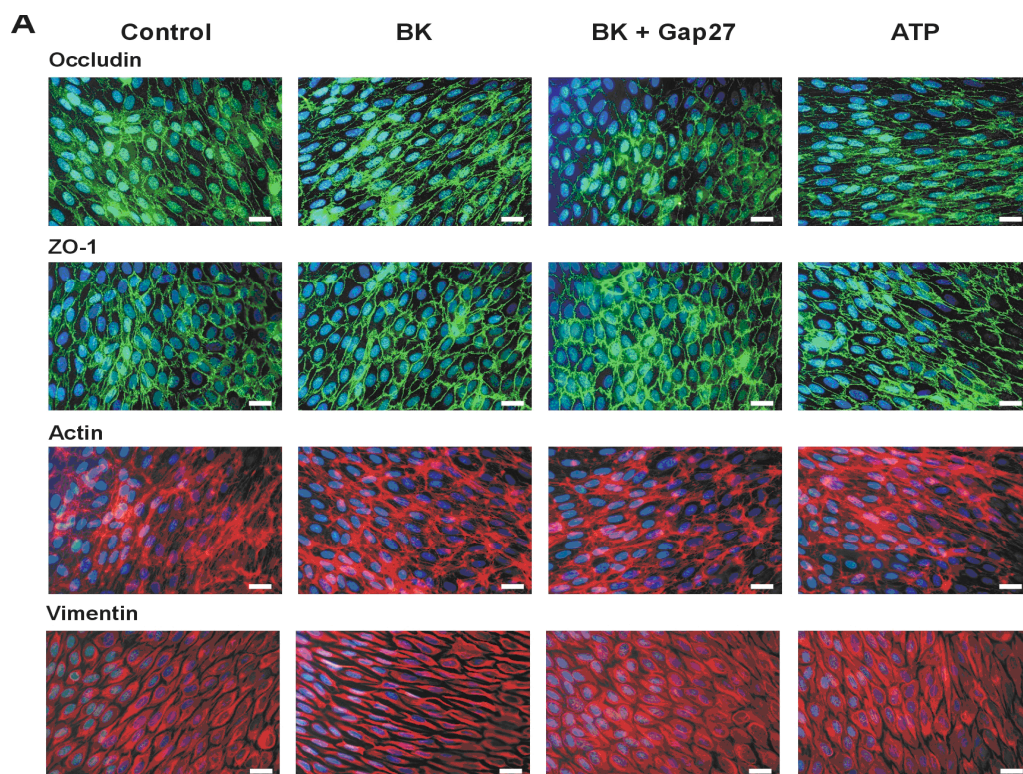


Figure 25A. Alterations at the level of tight junctions and cytoskeletal proteins. Representative images of occludin, ZO-1, F-actin and vimentin staining in BCEC under the various experimental conditions indicated. Vimentin filaments appeared more condense and stretched after BK exposure (0.5 $\mu\text{mol/L}$, 1 h) and this was not observed with BK + Gap27 (200 $\mu\text{mol/L}$, 1 h) or ATP (0.5 $\mu\text{mol/L}$, 1 h). The data shown are representative for 4 different experiments (scale bar is 25 μm).

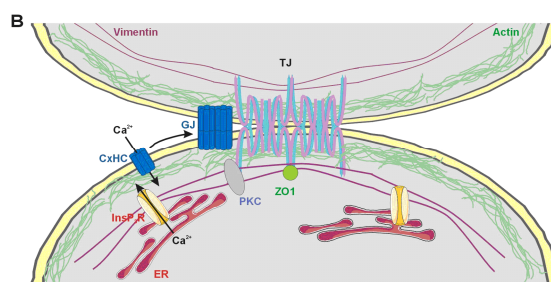


Figure 25B. Summary scheme. Summary scheme sketching a possible scenario for hemichannel involvement in BK-triggered BBB permeability increases. Endothelial junctions are zipper-like structures containing tight junctions (TJ) and gap junctions (GJ). Connexin hemichannels (CxHC) are transported to the plasma membrane and diffuse laterally (arrow) to become incorporated into gap junctions. Tight junctions, cytoskeletal proteins, InsP₃ receptors, PKC, gap junctions and hemichannels are all in close association at the nexus. InsP₃ receptors (InsP₃R) form the basis of Ca²⁺ oscillations. BK-triggered oscillations are associated with hemichannel opening while those triggered by ATP do not activate the hemichannel pathway (for unknown reasons). Hemichannel opening results in Ca²⁺ entry thereby affecting tight junction/cytoskeletal proteins directly or via intermediate signaling steps involving PKC. This figure was produced using Servier Medical Art.

3.1.4 DISCUSSION

The present work demonstrates that BK induces endothelial Ca^{2+} oscillations that are inhibited by interfering with connexin channel function, making use of Cbx, Gap27 peptide or Cx37/43 knockdown. BK triggered an increase of *in vitro*-measured endothelial permeability, which was dependent on endothelial $[\text{Ca}^{2+}]_i$ changes and was counteracted by inhibiting Ca^{2+} oscillations with Gap27. Moreover, Gap27 also inhibited BK-triggered BBB permeability elevation *in vivo*. ATP-triggered oscillations were not influenced by interfering with connexin channels and ATP did not alter *in vitro*-measured endothelial permeability. The rapid effect of Gap27 on BK-triggered oscillations, its inhibition of hemichannel dye uptake/release before having any effect on gap junctions, and the BK-stimulation of dye uptake/release all point to hemichannel involvement in the BK-triggered oscillations. Collectively, these data suggest that the connexin channel-linkage of BK-triggered Ca^{2+} oscillations which is absent in ATP-triggered oscillations, plays a role in influencing BBB permeability. Thus, Gap27 can be used to disrupt connexin channel-linked oscillations, thereby preventing BBB permeability changes.

BK is a well known permeability-increasing substance in brain endothelium [Abbott, 2000; Sarker et al., 2000]. Binding to its corresponding receptors produces the second messenger InsP_3 that triggers Ca^{2+} release from the endoplasmic reticulum (ER) [Easton and Abbott, 2002]. Several downstream signals and targets further contribute to the effects of BK on brain endothelial permeability, including free radical formation [Easton and Abbott, 2002; Sarker et al., 2000], activation of Ca^{2+} - or ATP-sensitive potassium channels [Ningaraj et al., 2003], activation of VEGF receptors [Thuringer et al., 2002] and alterations in junctional proteins [Easton and Abbott, 2002; Liu et al., 2008b]. InsP_3 , ER-located InsP_3 receptors and subsequent Ca^{2+} release are the necessary and sufficient ingredients to generate Ca^{2+} oscillations [Dupont et al., 2007]. Brain endothelial cells have been reported to display Ca^{2+} oscillations in response to various stimuli and conditions, including ATP [Haorah et al., 2007a], hypoxia [Brown et al., 2004], subarachnoid hemorrhage [Scharbrodt et al., 2009], infection [Nikolskaia et al., 2006] and lymphocyte migration [Etienne-Manneville et al., 2000]. However, at present, the role of Ca^{2+} oscillations in brain endothelial function is not clear.

The inhibition of BK-triggered Ca^{2+} oscillations by Cbx, Gap27 and Cx37/43 knockdown demonstrates that interfering with connexin channels affects the oscillatory activity. The data

obtained from dye uptake/dye release experiments, Cx37/43 silencing and Gap27 peptide, all point to involvement of unapposed connexin hemichannels. Gap27 is known to inhibit gap junctions but we show here that one hour exposure to the peptide has no effect on gap junctional coupling, in line with previous work in other cell types [Decrock et al., 2009; Evans et al., 2006]. Instead, hemichannel dye uptake/release was strongly inhibited by the peptide and recent single-channel electrophysiological studies indicate that Gap27 inhibits unitary currents through Cx37 and Cx43 hemichannels with a time-constant of 2-4 min (Wang et al., unpublished observations). This appears to be confirmed in the results depicted in figure 21E demonstrating rapid disappearance of oscillations upon addition of Gap27 and figure 21H illustrating fast-onset effects on the slope of calcein release. Side effects of Gap27 on other targets, like the $\text{InsP}_3\text{-Ca}^{2+}$ signaling-axis that forms the basis of the $[\text{Ca}^{2+}]_i$ oscillation machinery [Dupont et al., 2007], were excluded based on InsP_3 photoliberation experiments in C6-glioma cells. A contribution of hemichannels composed of Panx1 was excluded based on the absence of Panx1 mRNA.

Connexin hemichannels form a release pathway for ATP [Kang et al., 2008] and purinergic signaling was involved in BK-triggered oscillations, as apyrase, suramin and PPADS all suppressed the oscillations. The contribution of purinergic signaling in BK-triggered oscillations is likely to be autocrine because a paracrine contribution would be associated with time- or phase-related $[\text{Ca}^{2+}]_i$ changes in surrounding cells, which was not observed. Connexin hemichannels also form a pathway for Ca^{2+} entry into the cell [Schalper et al., 2010; Verma et al., 2009], which is necessary for sustained Ca^{2+} oscillations [Berridge, 2007]. In addition to forming a Ca^{2+} entry pathway, connexin hemichannels are also activated by $[\text{Ca}^{2+}]_i$ changes [De Vuyst et al., 2006; Ponsaerts et al., 2010]. Thus, hemichannels are expected to open with each oscillatory $[\text{Ca}^{2+}]_i$ spike, thereby opening a Ca^{2+} entry pathway. In addition, every $[\text{Ca}^{2+}]_i$ spike will be associated with ATP release via hemichannels, with subsequent autocrine activation of P2Y receptors (P_2Y_1 and P_2Y_2) [Albert et al., 1997] and increased generation of InsP_3 . This will result in repetitive increases in InsP_3 concentration that are known to support Ca^{2+} oscillations [Nash et al., 2001]. Inhibiting connexin hemichannels with Gap27 may thus disrupt the BK-triggered oscillations by limiting Ca^{2+} entry and InsP_3 generation, two fundamental modulators of Ca^{2+} oscillations. Ca^{2+} oscillations triggered by ATP were, on the other hand, not influenced by Cbx and Gap27, which is in line with the observation that ATP did not trigger PI uptake and hemichannel opening. The BK-triggered oscillations thus involve hemichannel opening while those triggered by ATP do not activate this pathway. Moreover,

the simultaneous activation of two distinct oscillation mechanisms by co-applying BK and ATP reduced the number of oscillating cells and prevented hemichannel opening, adding further evidence that hemichannel opening contributes to the oscillations.

Connexin proteins are transported via the ER and Golgi apparatus to the plasma membrane, where they appear as hexameric hemichannels. Plasma membrane hemichannels can diffuse laterally on their way to becoming incorporated into gap junction plaques [Laird, 2006] which are located at the nexus between endothelial cells, together with the tight junctional proteins [Lum et al., 1999]. InsP₃ receptors and PKC, which is a possible intermediate effector between [Ca²⁺]_i and endothelial permeability changes, are also situated at the nexus [Colosetti et al., 2003; Stamatovic et al., 2006] (**figure 25B**). Taken together, we speculate that the hemichannel Ca²⁺ entry/purinergic signaling pathway activated by BK is located close to the nexus and may be well positioned to result in spatially restricted [Ca²⁺]_i changes at the very place where they are needed to influence the tight junction proteins and to alter the paracellular permeability. We found evidence for BK-induced changes at the level of vimentin fibers, without accompanying effects on occludin, ZO-1 or F-actin organization. These BK-triggered alterations were absent with Gap27 treatment and were not observed with ATP. At present, it is not clear how [Ca²⁺]_i changes would affect vimentin organization but there is some evidence that [Ca²⁺]_i is involved in endothelin-1-induced vimentin reorganization [Chen et al., 2003] and that vimentin signaling plays a role in *E. coli* invasion of brain endothelial cells [Chi et al., 2010]. In addition to affecting paracellular permeability, BK has also been reported to favor the transcellular route [Jungmann et al., 2008] by increasing endocytosis whereby the fusion of endocytotic vesicles may lead to the formation of ‘transcellular channels’ [Neal and Michel, 1995]. An alternative formed by the opening of connexin hemichannels in the luminal and abluminal endothelial membranes is possible (**Table 6**) but is limited to below 1.5 kDa molecules as expected from the permeability properties of these channels [Kondo et al., 2000; Li et al., 1996]. Finally, it needs to be stressed that BBB permeability *in vivo* is regulated not only by the endothelium in close cooperation with astrocytes [Boveri et al., 2005] but also by pericytes [Bell et al., 2010] and neurons, i.e. by the cells forming the neurovascular unit [Neuwelt et al., 2011; Zlokovic, 2008]. At present, we do not know whether these cells have any influence on connexin channel functioning and/or endothelial Ca²⁺ oscillations. The findings presented in this paper indicate that glial cells are necessary for BK- and ATP-triggered endothelial Ca²⁺ oscillations.

In conclusion, this work shows that Gap27 inhibits BK-triggered Ca^{2+} oscillations and endothelial permeability changes, thereby bringing up a novel connexin-related pathway that may be exploited to limit BBB permeability increases under pathological conditions like brain ischemia and trauma. In contrast to inhibiting gap junctions, which results in a loss of barrier function [Nagasawa et al., 2006] inhibition of hemichannels appears to preserve barrier function.

3.2 LOW EXTRACELLULAR Ca^{2+} CONDITIONS INDUCE AN INCREASE IN BRAIN ENDOTHELIAL PERMEABILITY THAT IS LARGELY MEDIATED BY TRIGGERING INTERCELLULAR Ca^{2+} WAVES

This section corresponds to the following reference: Marijke De Bock, Maxime Culot, Nan Wang, Anaëlle da Costa, Elke Decrock, Mélissa Bol, Geert Bultynck, Romeo Cecchelli and Luc Leybaert. Low extracellular Ca^{2+} conditions induce an increase in brain endothelial permeability by triggering intercellular Ca^{2+} waves. Revised manuscript submitted to Brain Research.

In the previous section we presented evidence for a contribution of connexin hemichannels to Ca^{2+} oscillations and BBB permeability. Here, we aimed to investigate the effect of a second form of Ca^{2+} dynamics, namely intercellular Ca^{2+} waves (ICWs), on endothelial permeability. The propagation of ICWs largely relies on gap junctions with an additional component consisting of paracrine communication whereby hemichannels have been implicated. In the work that follows, we hypothesize that ICWs coordinate Ca^{2+} signals between adjacent endothelial cells, and thereby, resort a stronger effect on endothelial permeability.

ABSTRACT

The intracellular calcium concentration ($[\text{Ca}^{2+}]_i$) is an important factor determining the permeability of endothelial barriers including the blood-brain barrier (BBB). However, nothing is known concerning the effect of spatially propagated intercellular Ca^{2+} waves (ICWs). The propagation of ICWs relies in large part on connexins and the channels formed by connexins that are present in endothelia. We hypothesized that ICWs may result in a strong disturbance of endothelial function, because the $[\text{Ca}^{2+}]_i$ changes are coordinated and involve multiple cells. Thus, we aimed to investigate the effect of ICWs on endothelial permeability. ICW activity was triggered in immortalized and long term cultivated primary brain endothelial cells by lowering the extracellular Ca^{2+} concentration. Low extracellular Ca^{2+} increased the endothelial permeability and this was significantly suppressed by buffering $[\text{Ca}^{2+}]_i$ with BAPTA-AM, indicating a central role of $[\text{Ca}^{2+}]_i$ changes. The endothelial permeability increase was furthermore inhibited by the connexin channel blocking peptide Gap27, which also blocked the ICWs, and by inhibiting protein kinase C (PKC), Ca^{2+} /calmodulin-dependent kinase II (CaMKII) and actomyosin contraction. We compared these observations with the $[\text{Ca}^{2+}]_i$ changes and permeability alterations provoked by the inflammatory agent bradykinin (BK), which triggers oscillatory $[\text{Ca}^{2+}]_i$ changes without wave activity. BK-associated $[\text{Ca}^{2+}]_i$ changes

and the endothelial permeability increase were significantly smaller than those associated with ICWs, and the permeability increase was not influenced by inhibition of PKC, CaMKII or actomyosin contraction. We conclude that ICWs significantly increase endothelial permeability and therefore, the connexins that underlie wave propagation form an interesting target to limit BBB alterations.

3.2.1 INTRODUCTION

The endothelium that lines the blood vessels does not merely form a static vascular wall but strictly controls the interchange of fluids and nutrients between blood and tissue at the level of capillaries, which in the brain form a low-permeability barrier, the blood-brain barrier (BBB). This endothelial barrier is formed by mutual interactions with astrocytes that are in close contact with the endothelium via perivascular endfeet [Abbott et al., 2006]. This results in an extremely well-sealed tight junctional network that restricts the paracellular diffusion across the endothelium, whereas transcellular pinocytosis is nearly absent. In several brain disorders such as Alzheimer's disease, stroke, and epilepsy the BBB loses its ability to restrict passage, causing uncontrolled diffusion across the endothelium, edema, and loss of appropriate tissue functioning [Neuwelt et al., 2011; Zlokovic, 2008].

It is generally accepted that an increase in the endothelial intracellular Ca^{2+} concentration ($[\text{Ca}^{2+}]_i$) plays a key role in BBB dysfunction [Abbott, 2000] and we recently reported that oscillations in brain endothelial $[\text{Ca}^{2+}]_i$, brought about by stimulation of the cells with bradykinin (BK), increased the BBB permeability while Ca^{2+} oscillations triggered by ATP did not influence BBB permeability [De Bock et al., 2011]. The BK-triggered Ca^{2+} oscillations and BBB alterations were dependent on unapposed connexin hemichannels, i.e. hemichannels not incorporated into gap junctions. In addition to Ca^{2+} oscillations which occur in the temporal domain, Ca^{2+} dynamics can also take place in the spatiotemporal domain, allowing the transmission of $[\text{Ca}^{2+}]_i$ changes from cell to cell as intercellular Ca^{2+} waves (ICWs). Because ICWs involve spatially propagating $[\text{Ca}^{2+}]_i$ changes we hypothesized that ICWs in BBB endothelial cells amplify BBB alterations and have stronger functional implications than non-coordinated $[\text{Ca}^{2+}]_i$ changes. Currently, nothing is known about the effect of spatiotemporal organization of $[\text{Ca}^{2+}]_i$ changes on endothelial barrier function and we here aimed to investigate the effect of ICWs on endothelial permeability.

ICWs are based on Ca^{2+} signal communication between cells via diffusion of the intracellular Ca^{2+} -mobilizing messenger inositol trisphosphate (InsP_3) via gap junction channels [Leybaert and Sanderson, in press]. The latter are dodecamers of connexin (Cx) subunits and endothelial cells, including those from brain microvessels, typically express Cx37 and Cx40 [Little et al., 1995; Nagasawa et al., 2006; Traub et al., 1998], sometimes adjoined by Cx43, depending on the species [Larson et al., 1990; Little et al., 1995; Nagasawa et al., 2006; Theis et al., 2001; Wilson et al., 2008]. The gap junctional pathway of ICW propagation combines with paracrine purinergic signaling, which involves the release of ATP via various proposed mechanisms including connexin hemichannels [Arcuino et al., 2002; Braet et al., 2003a; Braet et al., 2003b; Eltzschig et al., 2006; Evans et al., 2006; Gomes et al., 2006; Kang et al., 2008; Leybaert and Sanderson, In Press]. ATP acts on metabotropic P2 receptors, stimulating InsP_3 synthesis and mobilizing Ca^{2+} from the endoplasmic reticulum (ER) resulting in $[\text{Ca}^{2+}]_i$ elevation in surrounding cells. ICWs have been demonstrated in endothelia of various origins [Demer et al., 1993; D'Hondt et al., 2007a; Domenighetti et al., 1998; Parthasarathi et al., 2006; Toma et al., 2008] and wave propagation seems to rely on the two communication pathways, at least in bovine corneal endothelial cells [Gomes et al., 2006] and in immortalized brain endothelial cells (RBE4, SV-ARBEC) [Braet et al., 2003b].

Exposure to low extracellular Ca^{2+} conditions is known to trigger ICWs in glial cells [Arcuino et al., 2002; Stout and Charles, 2003; Torres et al., 2012]. This kind of stimulation is relevant as a lowering of extracellular Ca^{2+} is known to accompany stroke [Kristian et al., 1993] and epilepsy [Vezzani et al., 1988]. Recent work in hippocampal brain slices has demonstrated that neuronal activation is accompanied by decreased extracellular Ca^{2+} that results in the opening of connexin hemichannels in astrocytes, triggering ATP release and ICWs that influence local surrounding interneurons [Torres et al., 2012]. Here, we utilized this stimulus to trigger ICWs in BBB endothelial cells and to determine the effect of this spatiotemporal form of endothelial Ca^{2+} dynamics on BBB permeability. Upon low extracellular Ca^{2+} exposure, we observed a strong increase in endothelial permeability that was highly dependent on changes in $[\text{Ca}^{2+}]_i$. Suppression of ICWs by inhibiting hemichannels and gap junctions with the connexin channel blocker Gap27 reduced the increase in endothelial permeability. Inhibition of PKC, CaMKII or actomyosin signaling downstream of $[\text{Ca}^{2+}]_i$ changes also strongly suppressed the endothelial permeability increase. By contrast, BK, that triggers Ca^{2+} oscillations and no ICWs, led to a much smaller endothelial permeability increase that was characterized by $[\text{Ca}^{2+}]_i$ dynamics of smaller amplitude and was not

counteracted by inhibiting the contractile machinery or PKC- and CaMKII activity. Taken together, our data suggest that ICWs more potently influence endothelial permeability than those triggered by Ca^{2+} oscillations. At present, no tools are available to limit a BBB permeability increase which is a common aspect of many brain diseases. The involvement of $[\text{Ca}^{2+}]_i$ and connexin channels that are at the basis of ICWs brings up interesting targets for the development of new approaches to limit BBB alterations.

3.2.2 MATERIALS AND METHODS

3.2.2.1 Cell culture

RBE4 cells were kindly provided by Dr. F. Roux (Neurotech, Evry, France). Cells (up to passage 25) were grown on collagen-coated recipients (rat-tail collagen, Roche Diagnostics, Vilvoorde, Belgium) and maintained in alpha-MEM/Ham's F10 (1:1) supplemented with 10 % fetal calf serum, 2 mM glutamine, 300 $\mu\text{g}/\text{ml}$ G-418 (Gibco, Invitrogen, Merelbeke, Belgium) and 1 ng/ml human recombinant basic fibroblast growth factor (bFGF - Roche Diagnostics) at 37 °C and 5 % CO_2 . BCECs were grown in a non-contact co-culture with rat glial cells as described previously [Cecchelli et al., 1999]. Glial cells were isolated from Sprague Dawley rat cerebral cortex and cultured for 3 weeks. At the end of this stabilization period, BCEC, seeded onto rat-tail collagen-coated polycarbonate filter inserts (Millicell-PC, 3 μm pore size, 30 mm diameter, Millipore Corporation, Molsheim, France) were placed into 6-well plates containing the glial cells. BCEC and glia were grown together for another 12 days during which BBB features fully develop. In this phase, cells were kept in DMEM supplemented with 10 % newborn calf serum, 10 % horse serum, 2 mM L-glutamine, 50 $\mu\text{g}/\text{ml}$ gentamycin and 1 ng/ml bFGF. The HeLaCx37, HeLaCx40 cells (kindly provided by Dr Klaus Willecke, Universität Bonn, Germany) and C6Cx43 cells (kind gift of Dr Christian C Naus, University of British Columbia, Canada), which were used as positive controls in western blotting experiments, were maintained in DMEM and DMEM/Ham's F12 (1:1), respectively, supplemented with 10% fetal calf serum and 2 mM glutamine.

3.2.2.2 Chemicals and reagents

1,2-bis-(2-aminophenoxy)-ethane-*N,N,N',N'*-tetraacetic acid acetoxy methyl ester (BAPTA-AM), 3kDa dextran fluorescein, fluo3-AM, lucifer yellow, pluronic[®] acid F-127 and

propidium iodide (PI) were from Molecular probes (Invitrogen). Bradykinin, chelerythrine chloride, ethylene glycol-bis-(β -aminoethyl ether)-*N,N,N',N'*-tetraacetic acid (EGTA), KN62, probenecid and (-)-blebbistatin were purchased from Sigma-Aldrich (Bornem, Belgium). The Gap27 peptide (SRPTEKTIFII) was synthesized by Thermo Fisher Scientific (Ulm, Germany) at > 80 % purity.

3.2.2.3 Ca²⁺ imaging

RBE4 cells were seeded onto 9.2 cm² petridishes (TPP, Novolab, Geraardsbergen, Belgium) and experiments were performed at confluency. RBE4 monolayers were loaded with a mixture of 10 μ M fluo3-AM, 1 mM probenecid and 0.01 % pluronic acid in HBSS-Hepes (0.95 mM CaCl₂; 0.81 mM MgSO₄; 137 mM NaCl; 0.18 mM Na₂HPO₄; 5.36 mM KCl; 0.44 mM KH₂PO₄; 5.55 mM D-glucose and 25 mM Hepes) during 1 h at room temperature (RT). BCEC on filter inserts were removed from the glial cells and were placed in petridishes with HBSS-Hepes/probenecid containing fluo3-AM (10 μ M) and pluronic acid (0.01 %). The same solution was added to the filter insert. After 1 h, petridishes (RBE4) or filter inserts (BCEC) were washed and cells were left for an additional 30 min at RT in HBSS-Hepes/probenecid to allow for de-esterification. Cells were thereafter transferred to an inverted epifluorescence microscope (Eclipse TE 300, Nikon Belux, Brussels, Belgium), equipped with a heating stage to maintain the cells at ~ 27 °C. A superfusion system allowed changing the bath solution within ~ 1 min (bath volume ~ 1 mL). Superfusion was switched off during the registration of wave/oscillatory activity. Images were taken every second with a x 40 water immersion objective (NA 0.8) and an electron multiplying CCD camera (Quantem 512SC, Photometrics, Tucson, AZ, USA). We used a Lambda DG-4 filterswitch (Sutter Instrument Company, Novato, CA, USA) to deliver excitation at 482 nm and captured emitted light via a 505 nm long-pass dichroic mirror and a 535 nm bandpass-filter (35 nm bandwidth). Recordings and analysis were done with custom-developed QuantEMframes and Fluoframes software written in Microsoft Visual C++ 6.0. An ICW was defined as a minimally 10 % increase in fluo3 fluorescence starting in one cell and propagating to at least two surrounding cells. The surface area of an ICW was determined from the area of cells displaying an above threshold (≥ 10 %) fluorescence change. Wave events were counted in a 10 min observation period. Ca²⁺ oscillations were defined as at least two transient [Ca²⁺]_i changes (≥ 10 % fluo-3 fluorescence change) after the BK-triggered Ca²⁺ transient.

3.2.2.4 Endothelial transport studies

Endothelial permeability was measured as described previously [Cecchelli et al., 1999]. Filter inserts containing confluent BCEC monolayers were separated from the glial cells, washed with HBSS-Hepes and added to a six-well plate with each well containing 2.5 ml HBSS-Hepes (lower compartment). The filter insert (upper compartment) was filled with 1.5 ml HBSS-Hepes containing 50 μ M LY (457 Da) or 3kDa DF (20 μ M) as a transport marker. At 15, 30, 45 and 60 min the filters were transferred to a new well and samples were then taken from each lower compartment. The temperature was kept at 37 °C. Aliquots were also taken from the upper compartment at the beginning and the end of the experiment. The cleared volume was determined by dividing the fluorescence in the lower compartment at each time point by the concentration in the upper compartment and was plotted versus time. The slope of this curve, calculated by linear regression, corresponds to the permeability-surface (PS) product and subtracting the PS product of an empty, coated filter gives the PS product of the endothelial monolayer. Subsequent division by the surface area of the filter membrane (4.2 cm²) yields the permeability coefficient Pe. The vehicles used throughout this study were all without effect on the permeability.

3.2.2.5 Hemichannel assays

Hemichannel opening was investigated by dye uptake and ATP release. Dye uptake is based on the entry of a low (< 1.5 kDa) molecular weight dye like propidium iodide (PI - 668 Da) via connexin hemichannels. RBE4 cells were seeded onto four-well plates (Nunc brand products, Novolab) at a density of 50 000 cells/ml and used the next day. Cultures were rinsed twice and incubated during 10 min with 2 mM PI added to the trigger solution. Pictures were acquired with a Nikon TE300 epifluorescence microscope, a x 10 objective (Plan APO, NA 0.45) and a Nikon DS-5M camera (Nikon Belux). In each culture, 9 snap-shot images were taken. The number of dye-positive cells in each image was counted using ImageJ (<http://rsb.info.nih.gov/ij>) after application of a threshold corresponding to the upper level of the background signal. Dye uptake is expressed as the percentage of dye-positive cells relative to the total number of cells counted with Hoechst staining (22 000 \pm 900 cells/cm²). For ATP measurements, cells were seeded at 75 000 cells/ml in 24-multiwell plates (Falcon) and experiments were performed the next day. The cells were exposed during 2.5 min to the trigger after which 75 μ l luciferin/luciferase ATP assay-mix (Sigma-Aldrich) diluted 1:5 in

HBSS-Hepes was added. Luminescence was measured with a Victor-3 plate-reader (type 1420 multilabel counter, Perkin Elmer, Brussels, Belgium). ATP release was expressed as a percentage relative to 100 % signal recorded in cultures exposed to vehicle.

3.2.2.6 Electrophoresis and western blotting

For western blots, RBE4 cells were seeded in 75 cm² falcons and lysates were extracted with RIPA buffer. BCEC filters were scraped in ice-cold PBS containing protease inhibitor cocktail (Roche Diagnostics). Protein concentration was determined using the Biorad DC protein assay kit (BioRad, Nazareth, Belgium) and absorbance was measured with a 590 nm long-pass filter. The lysate was separated by electrophoresis over a 10 % SDS-polyacrylamide gel and transferred to a nitrocellulose membrane (Amersham, Buckinghamshire, UK). Membranes were subsequently blocked with TBS containing 5 % non-fat milk and 0.1 % Tween20. Following blocking, blots were probed with rabbit anti-Cx43 antibody (Sigma-Aldrich), rabbit anti-Cx40 antibody (alpha-diagnostic international, Brussels, Belgium), rabbit anti-Cx37 antibody (alpha-diagnostic international) and rabbit anti- β -tubulin antibody (Abcam, Cambridge, UK) as a loading control. Membranes were subsequently incubated with an alkaline phosphatase-conjugated goat anti-rabbit IgG antibody (Sigma-Aldrich) and detection was done using the nitro-blue-tetrazolium/5-bromo-4-chloro-3-indolyl-phosphate reagent (NBT/BCIP kit, Zymed, Invitrogen).

3.2.2.7 Statistical analysis

Data are expressed as mean \pm S.E.M. with n giving the number of independent experiments. Multiple groups were compared by one-way ANOVA and a Bonferroni post-test, making use of Graphpad InStat software. Two groups were compared with an unpaired student's t-test and two-tail p-value. Results were considered statistically significant when $p < 0.05$ (one symbol for $p < 0.05$, two for $p < 0.01$ and three for $p < 0.001$).

3.2.3 RESULTS

3.2.3.1 Low extracellular Ca^{2+} induces intercellular Ca^{2+} waves in brain endothelial cells

Reduction of the extracellular Ca^{2+} concentration has been shown previously to trigger ICWs in glial cells [Arcuino et al., 2002; Zanotti and Charles, 1997]. We applied various low Ca^{2+} solutions (**figure 26A**) to confluent RBE4 monolayers and found that Ca^{2+} -free ($\sim 10 \mu\text{M}$ Ca^{2+}) and Ca^{2+} -free + EGTA ($\sim 1 \text{ nM}$ Ca^{2+}) were most potent in triggering ICW events, giving ~ 4 waves in a 10 min observation period (**figure 26B-D**).

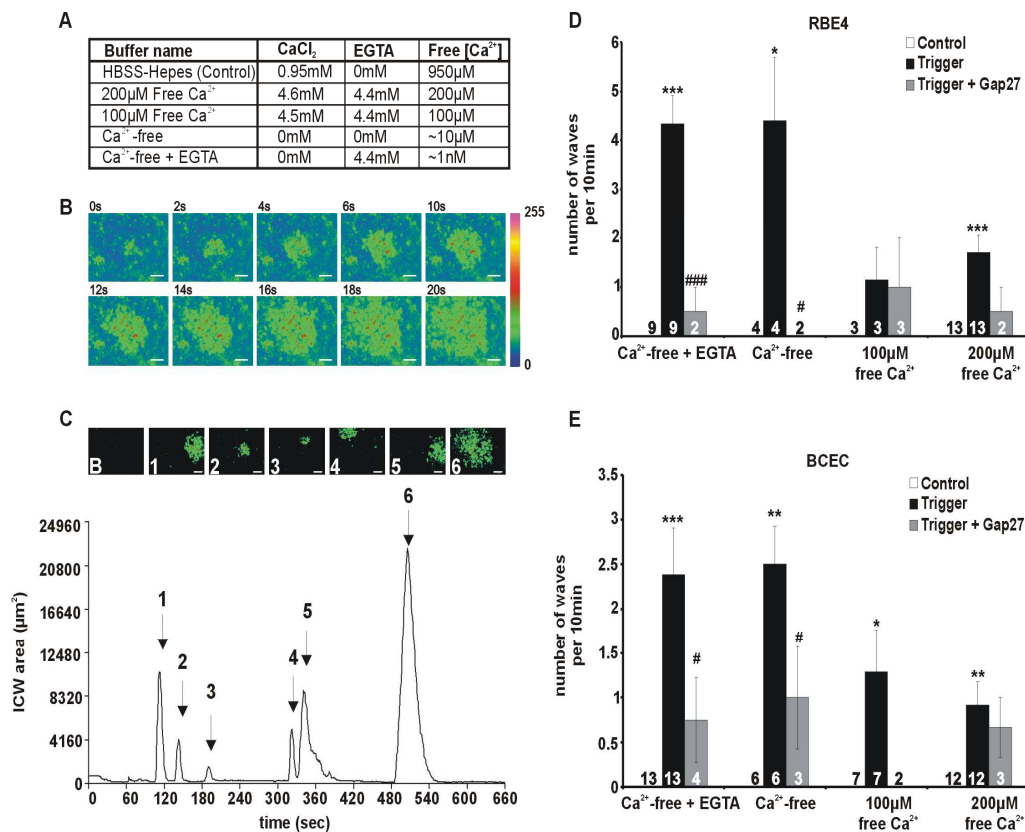


Figure 26. Intercellular Ca^{2+} waves (ICWs) in RBE4 and BCEC. (A) Composition of the low extracellular Ca^{2+} solutions. (B) Examples showing an ICW in a confluent RBE4 culture exposed to ' Ca^{2+} -free + EGTA' (scale bar: 50 μm). (C) Time plot illustrating multiple ICWs in response to Ca^{2+} -free + EGTA. The ordinate expresses the surface area of above threshold $[\text{Ca}^{2+}]_i$ changes. Vertical arrows point to individual ICW events counted from such plots. Numbers on the graph correspond to the ICWs exemplified above (B signifies baseline). (D) The ICW activity decreased with increasing extracellular Ca^{2+} concentration and was suppressed by Gap27 (200 μM , 2 h). The numbers printed in the bars represent 'n'. (E) ICW activity in BCECs showed a similar dependency on extracellular Ca^{2+} and the waves were also inhibited by Gap27. Stars: statistical significance compared to control; number signs: significance compared to the corresponding trigger.

Oscillatory $[Ca^{2+}]_i$ activity was observed in a limited number of cells with these two solutions (3-5 cells on a total of 65 ± 3 cells in view; $n = 10$). BCECs also responded to low extracellular $[Ca^{2+}]$ with wave activity (**figure 26E**) without any discernible accompanying oscillatory $[Ca^{2+}]_i$ activity.

ICWs rely in large part on connexin channels [Boitano and Evans, 2000; Sanderson et al., 1990] and we first checked which connexins are present in RBE4 and BCEC cells. In accordance with earlier work [De Bock et al., 2011] both immortalized and long term cultivated primary cells expressed Cx37 and Cx43 but not Cx40 (**figure 27A**).

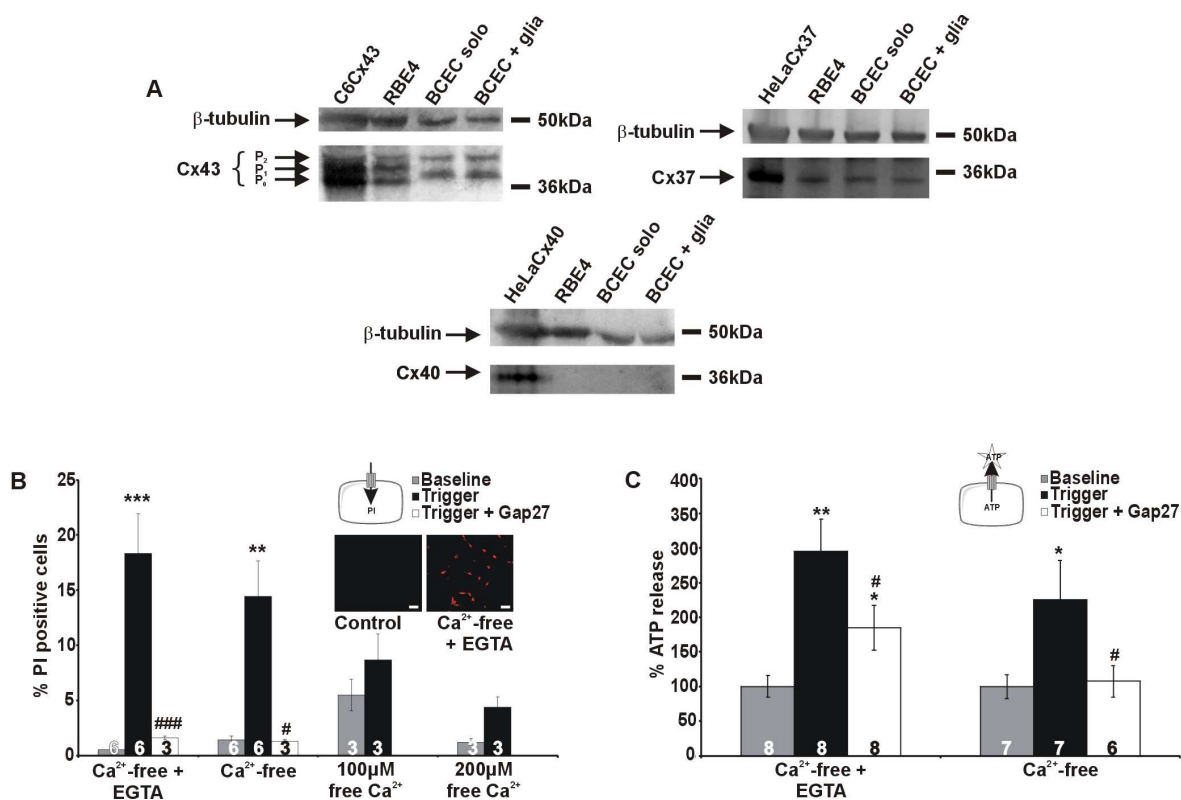


Figure 27. Connexin expression and hemichannel responses in brain endothelial cells. (A) Western blot analysis for Cx37, Cx40 and Cx43 in RBE4 cells and BCEC reveals the presence of Cx37 and Cx43 but not of Cx40. HeLaCx37, HeLaCx40 and C6Cx43 were used as respective positive controls. β -tubulin was used a loading control. (B) Low extracellular Ca^{2+} conditions triggered significant PI uptake in RBE4 cells that decreased with increasing extracellular Ca^{2+} concentration and was strongly inhibited by Gap27 (200 μ M, 2 h). Inset shows example images (scale bar is 50 μ m). (C) Ca^{2+} -free conditions triggered ATP release from RBE4 cells, which was reduced by Gap27 (200 μ M, 2 h). Stars: statistical significance compared to baseline; number signs: significance compared to the corresponding trigger.

Gap27 is a peptide identical to a short sequence in the second extracellular loop of Cx37 and Cx43 that inhibits ICWs by blocking both gap junctions and hemichannels [Braet et al., 2003a; Braet et al., 2003b]. This peptide (200 μM , 2 h) significantly suppressed ICWs triggered by exposure to Ca^{2+} -free and Ca^{2+} -free + EGTA extracellular conditions in RBE4 cells and BCECs (**figure 26D,E**). Gap27 also significantly inhibited connexin hemichannel opening as concluded from dye uptake and ATP release experiments triggered by exposure of the cells to low extracellular Ca^{2+} solutions (**Figure 27B, C**). Therefore, ICWs are likely suppressed by abolishing ICW initiation, where hemichannels may play a prominent role [Arcuino et al., 2002], and ICW propagation that is mediated by gap junctions and hemichannel-mediated ATP release and paracrine purinergic signaling [Leybaert and Sanderson, In Press].

3.2.3.2 BAPTA-AM and Gap27 inhibit endothelial permeability-increases induced by low extracellular $[\text{Ca}^{2+}]$

Lowering extracellular Ca^{2+} can increase endothelial permeability by disrupting extracellular Ca^{2+} -dependent VE-cadherin interactions in the junctional complex [Baumgartner et al., 2000; Vestweber, 2000]. To study the effect of ICWs on endothelial permeability, we screened the different low extracellular $[\text{Ca}^{2+}]$ solutions listed in figure 26A to find a condition that would minimize such direct effects. Ca^{2+} -free + EGTA solution drastically increased the endothelial permeability but Ca^{2+} -free solution had a milder permeability-increasing effect, as determined from the transport of lucifer yellow (LY, molecular weight 457 Da) over confluent BCEC monolayers on filter membranes (**figure 28A**). When the permeability elevation triggered by exposure to Ca^{2+} -free solution was measured with a dextran fluorescein (DF) tracer of higher molecular weight (3 kDa DF), we found similar results: a 4.7 ± 2.2 ($n = 3$) fold permeability increase for 3 kDa DF compared to 4.5 ± 2.3 fold ($n = 3$) for LY. All subsequent experiments were done with LY as a permeability tracer. Pretreatment of BCECs with BAPTA-AM (5 μM , 1 h) to restrain the induced $[\text{Ca}^{2+}]_i$ changes, largely prevented the permeability-increase triggered by exposure to Ca^{2+} -free solution (**figure 28B,C**). This indicates that the permeability-increase is not caused by lowering extracellular $[\text{Ca}^{2+}]$ *per se* but results from $[\text{Ca}^{2+}]_i$ changes associated with the ICW. Pretreatment of BCECs with Gap27 (200 μM , 2 h) to inhibit ICW activity, significantly inhibited the Ca^{2+} -free-induced permeability-increase

(**figure 28D**). Neither BAPTA-AM preloading nor treatment with Gap27 influenced endothelial permeability under control conditions, without the low Ca^{2+} trigger (**Figure 28F**).

3.2.3.3 PKC, CaMKII and cytoskeletal involvement in endothelial permeability-increases induced by low extracellular $[\text{Ca}^{2+}]$

Various signaling cascades may be activated downstream of ICWs: conventional protein kinase C (PKC) and calmodulin-dependent kinase II (CaMKII) are kinases that can be readily activated by Ca^{2+} [De Koninck and Schulman, 1998; Dupont and Goldbeter, 1998; Oancea and Meyer, 1998; Reither et al., 2006]. These kinases activate various targets, ultimately leading to endothelial cell contraction, cell-cell junction remodeling and an increase in endothelial permeability [Borbiev et al., 2003; Brown et al., 2004; Chi et al., 2010; Fleegal et al., 2005; Gaudreault et al., 2008; Konstantoulaki et al., 2003; Qiu et al., 2010; Sukumaran and Prasadarao, 2003; Tiruppathi et al., 2006]. Inhibiting PKC with chelerythrine (250 nM, 1 h) or CaMKII with KN62 (1 μM , 1 h) significantly reduced the permeability increase triggered by exposure to Ca^{2+} -free solution (**figure 28E**). To identify a role for cytoskeletal rearrangements and activation of the contractile machinery, we used (-)-blebbistatin, an inhibitor of myosin ATPase. Pretreatment with (-)-blebbistatin (5 μM , 30 min) strongly limited the increase in endothelial permeability elicited by Ca^{2+} -free solution (**figure 28E**). None of these inhibitory compounds had any significant effect on endothelial permeability under control conditions without trigger (**Figure 28F**). Thus, the Ca^{2+} -free-induced ICWs are associated with endothelial cell contraction that largely contributes to the observed permeability changes.

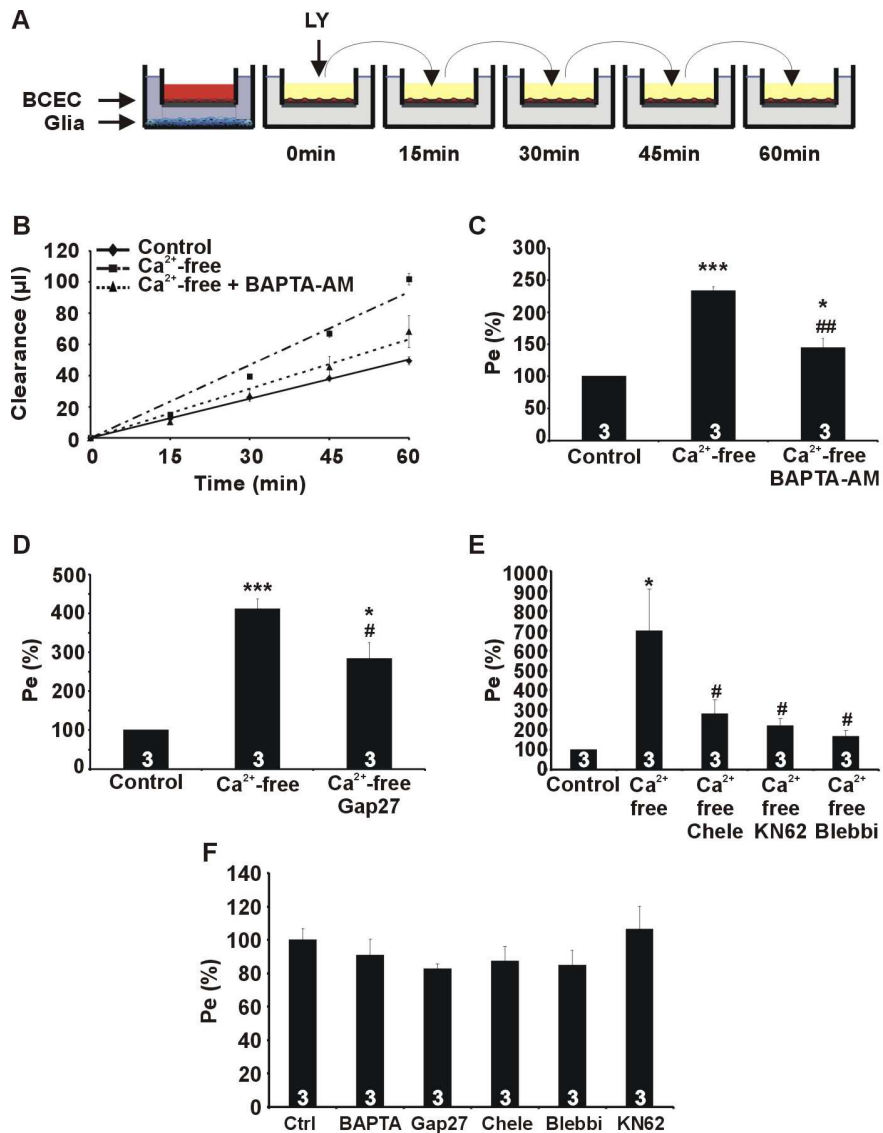


Figure 28. Effects of low extracellular Ca²⁺ on endothelial permeability. (A) Protocol for the permeability measurements. BCECs were grown on filter-inserts in a non-contact co-culture with glial cells (first well). The filter-inserts were then placed in wells without glia, transport marker was added and diffusion of the marker to the lower compartment was assessed at the time points indicated. (B) LY clearance for BCECs exposed to Ca²⁺-free solution present in the upper and lower compartment. Pe values were calculated from the slope of the clearance curve and were $0.33 \pm 0.03 \cdot 10^{-3} \text{ cm/min}$ in control (n = 9). (C) Pre-loading BCECs with BAPTA-AM (5 μM , 1 h) inhibited the permeability-increase. (D) Gap27 (200 μM , 1 h pre-incubation and 1 h present during the assay in both compartments) significantly reduced the permeability-increase for LY. (E) Exposure to the PKC inhibitor chelerythrine (chele; 250 nM, 1 h), the CaMKII inhibitor KN62 (1 μM , 1 h) or the myosin-ATPase blocker (-)-blebbistatin (blebbi; 5 μM , 30 min) strongly reduced the permeability-increase triggered by Ca²⁺-free solution (inhibitory agents applied as explained for Gap27). (F) Exposure to BAPTA-AM, Gap27, chelerythrine, (-)-blebbistatin and KN62 at the concentrations and durations indicated above did not affect endothelial permeability under control conditions with normal extracellular Ca²⁺. Stars: statistical significance compared to control; number signs: significance compared to the Ca²⁺-free condition.

3.2.3.4 Ca²⁺ oscillations triggered by bradykinin provoke a limited endothelial permeability increase that is not mediated by PKC, CaMKII or actomyosin contraction.

Bradykinin (BK) is an inflammatory agent that triggers increased endothelial permeability *in vitro* [Easton and Abbott, 2002] and *in vivo* [Sarker et al., 2000]. This agent, triggers Ca²⁺ oscillations in RBE4 and BCEC cells without causing ICWs, and increases the endothelial permeability in a [Ca²⁺]_i oscillation-dependent manner [De Bock et al., 2011]. We compared the [Ca²⁺]_i dynamics and endothelial permeability changes triggered by BK with those brought about by extracellular Ca²⁺-free conditions. **Figure 29A** shows typical traces of Ca²⁺ oscillations triggered by 0.5 μM BK in RBE4 cells and BCECs. **Table 7** summarizes the properties (and differences) of the [Ca²⁺]_i dynamics caused by Ca²⁺-free conditions (waves) and those triggered by BK (oscillations). The fraction of the cells displaying oscillatory activity was equal to the fraction of cells participating to Ca²⁺-free induced ICWs. By contrast, the amplitude of [Ca²⁺]_i changes associated with the oscillations were significantly smaller than those associated with ICWs. We further determined the effect of BK on endothelial permeability and found that the permeability increase was almost 4 times smaller than the permeability increase caused by Ca²⁺-free conditions (**Table 7**). Interestingly, unlike the Ca²⁺-free-induced endothelial permeability changes, the BK-triggered permeability increase was not influenced by inhibiting PKC, CaMKII or actomyosin contraction (**figure 29B**).

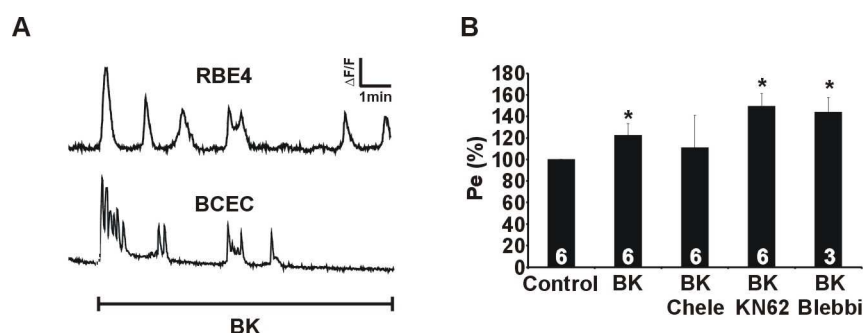


Figure 29. BK triggers Ca²⁺ oscillations and induces an endothelial permeability increase that is not influenced by PKC, CaMKII and myosin-ATPase inhibitors. (A) Example traces of Ca²⁺ oscillations in RBE4 and BCEC (0.5 μM BK). (B) Chelerythrine, KN62 and (-)-blebbistatin had no effect on the BK-triggered permeability increase (concentrations and incubation times as in figure 28E). Star sign indicates statistical significance compared to control.

Table 7. Properties of endothelial Ca²⁺ dynamics and Pe in response to Ca²⁺-free solution and BK determined over a 10 min recording period (data recorded from experiments on BCEC).

	Ca ²⁺ -free solution	BK (0.5 μM)
Pattern of endothelial Ca²⁺ dynamics	ICWs	Ca ²⁺ oscillations
Fraction of cells participating	53.9 ± 13.5 % (n = 6)	53.6 ± 11.6 % (n = 3)
Amplitude of [Ca²⁺]_i changes (ΔF/F)	34 ± 2.8 (n = 4)* (averaged over entire wave)	19.8 ± 5.1 (n = 3) (averaged over all spikes)
Pe (fold increase)	4.5 ± 2.3 (n = 3)*	1.2 ± 0.1 (n = 3)
Pe increase inhibited by		
- Chelerythrine	Yes	No
- KN62	Yes	No
- (-)-Blebbistatin	Yes	No

Stars indicate significant differences between Ca²⁺-free condition and BK (* p < 0.05)

3.2.4 DISCUSSION

The purpose of this work was to determine the effect of spatially extending [Ca²⁺]_i changes in endothelial permeability. Using low extracellular Ca²⁺ conditions which induce ICWs in confluent RBE4 and BCEC cultures, we observed a strong increase in endothelial permeability that was highly dependent on changes in [Ca²⁺]_i. Furthermore, preventing ICWs by the connexin channel blocker Gap27 reduced the increase in endothelial permeability. PKC, CaMKII and actomyosin contraction all contributed to the wave-induced permeability-increase. BK, that elicits Ca²⁺ oscillations, led to a much smaller endothelial permeability increase that was not counteracted by interference with the contractile machinery or PKC- and CaMKII activity.

Low extracellular Ca²⁺ conditions are known to trigger ICWs in glial cells [Stout and Charles, 2003] and various trigger mechanisms have been proposed [Zanotti and Charles, 1997]. Arcuino et al. (2002) reported that connexin hemichannel-mediated ATP release, activated by low extracellular Ca²⁺ conditions, acts as a point-source from trigger cells that initiate the ICW [Arcuino et al., 2002] and this has been recently confirmed in brain slices [Torres et al., 2012]. The released ATP subsequently diffuses, activates P2Y receptors on surrounding cells

and generates InsP_3 that triggers Ca^{2+} release from the ER. At the same time, InsP_3 , passing via gap junctions, contributes in a synergistic manner to ICW propagation [Anselmi et al., 2008; Suadicani et al., 2004; Toma et al., 2008]. As in glial cells, Ca^{2+} removal from the culture medium also triggers ICWs in RBE4 and BCEC. RBE4 cells and BCECs express Cx37 and Cx43 with no obvious Cx40 expression. Gap27, a peptide identical to an 11 amino acid sequence in the extracellular loops of Cx37 and Cx43, prevented the ICWs in RBE4 and BCEC cultures, as also reported for bovine corneal endothelial cells [Gomes et al., 2006] and alveolar capillary endothelial cells [Parthasarathi et al., 2006]. A 2 h incubation with Gap27, as used here, will result in combined inhibition of gap junctions and hemichannels, thereby counteracting both the initiation and propagation of ICWs [Leybaert and Sanderon, In Press].

In addition to triggering ICWs, lowering of extracellular $[\text{Ca}^{2+}]$ also induced an increase of endothelial permeability. Decreasing extracellular $[\text{Ca}^{2+}]$ to nanomolar levels (Ca^{2+} -free + EGTA) drastically increased the endothelial permeability while the effect was more moderate with a decrease to micromolar levels (Ca^{2+} -free solution). Electron and atomic force microscopy studies indicate that interendothelial junctions disconnect when Ca^{2+} is removed from the bathing medium [Nagy et al., 1985; Wilhelm et al., 2007]. Such effects likely occur secondary to the disruption of VE-cadherins, the main building blocks of adherens junctions, that are strictly dependent on the extracellular Ca^{2+} concentration [Baumgartner et al., 2000]. We here show that the endothelial permeability increase induced by extracellular Ca^{2+} -free solution is significantly counteracted by buffering $[\text{Ca}^{2+}]_i$ changes with BAPTA-AM, indicating that ICWs are a major factor in the permeability increase. However, we cannot exclude a residual contribution of direct effects of low extracellular Ca^{2+} conditions at the level of junctional proteins.

Lowering of extracellular Ca^{2+} has been reported to activate PKC [Alexander et al., 1998] and to promote actomyosin contraction, leading to the redirection of ZO-1, occludin and perijunctional actin-myosin out of the junctional complex [Ma et al., 2000]. These effects are likely to be mediated by $[\text{Ca}^{2+}]_i$ changes induced by the low extracellular Ca^{2+} condition, for example via activation of the $[\text{Ca}^{2+}]_i$ -dependent myosin light chain (MLC) kinase [Haorah et al., 2005; Luh et al., 2009]. We were unable to examine the role of MLC kinase because the MLC kinase inhibitor ML7 had intrinsic toxic effects on the BCEC cultures. Instead, we used (-)-blebbistatin, an inhibitor of the myosin-ATPase, and found that it largely prevented the increase in endothelial permeability brought about by Ca^{2+} -free solution. Additionally, we

identified a role for PKC and CaMKII, two other $[Ca^{2+}]_i$ -sensitive kinases [De Koninck and Schulman, 1998; Dupont and Goldbeter, 1998; Oancea and Meyer, 1998; Reither et al., 2006].

The Ca^{2+} -free-induced endothelial permeability increase was much larger (4.5 fold) than the one brought about by BK (1.2 fold) which only triggers Ca^{2+} oscillations without any associated wave activity [De Bock et al., 2011]. The data in table 7 indicate that the Ca^{2+} -free-induced $[Ca^{2+}]_i$ changes have a larger amplitude than those triggered by BK while the proportion of cells contributing to the $[Ca^{2+}]_i$ dynamics was not different. Thus, it is likely that the smaller BK-associated $[Ca^{2+}]_i$ changes are less efficient in activating downstream signaling leading to cytoskeletal reorganization. In line with this, the BK-triggered endothelial permeability increase was not prevented by inhibition of PKC, CaMKII or myosin-ATPase activity (figure 29B). These data corroborate earlier observations that BK does not induce rearrangements of actin fibers; we did however observe changes in vimentin fiber organization [De Bock et al., 2011]. The data above suggest that in BCECs, disturbance of vimentin fibers does not depend on PKC, CaMKII or myosin-ATPase, in contrast to the suggested role for CaMKII in human brain endothelial cells infected with *E. coli* [Chi et al., 2010]. Taken together, our data suggest that ICWs more potently influence endothelial permeability than those triggered by Ca^{2+} oscillations for a comparable cell mass contributing to these two different forms of $[Ca^{2+}]_i$ dynamics. This may be caused by the larger amplitude of $[Ca^{2+}]_i$ changes associated with ICWs, resulting in a more efficient activation of PKC, CaMKII or myosin-ATPase. It is possible that direct effects of low extracellular Ca^{2+} on tight junction proteins contribute to the larger effect of the low extracellular Ca^{2+} condition as compared to BK exposure. However, the strong inhibitory effects of interfering with intracellular signaling via PKC, CaMKII and myosin-ATPase (figure 28E) points to a crucial role of intracellular signaling rather than direct extracellular effects.

BBB endothelial cells are normally exposed to 1.25 - 1.5 mM free extracellular Ca^{2+} on the blood side and to slightly lower concentrations of ~1 mM at the brain interstitial side [Somjen, 2004; Massimini and Amzica, 2001]. Brain interstitial Ca^{2+} decreases 0.5 to 1 mM in response to neuronal stimulation [Hofer, 2005; Torres et al., 2012] and may attain very low levels (10 - 100 μ M range) under pathological conditions such as hypoglycemia, ischemia and epileptic seizures [Kristian et al., 1993; Leybaert and De Ley, 1994; Somjen et al., 1986; Vezzani et al., 1988]. As a consequence, these conditions may trigger a BBB permeability

increase that may contribute to disturbing the function of neurons and glial cells that, together with the vascular cells form the neurovascular unit [Hawkins and Davis, 2005; Neuwelt et al., 2011]. Preventing BBB impairment by inhibiting endothelial $[Ca^{2+}]_i$ changes might prove protective in such circumstances.

In conclusion, this work shows that low extracellular Ca^{2+} triggers a strong permeability increase of brain endothelium that is largely (but not exclusively) mediated by $[Ca^{2+}]_i$ changes that occur during ICW initiation and propagation. The involvement of gap junction channels and hemichannels that are at the basis of ICWs brings up novel targets for the development of new approaches that aim to limit BBB dysfunction. Importantly, there are currently no tools available to limit a BBB permeability increase which is a common aspect of many brain diseases.

3.3 CONNEXIN-43 HEMICHANNELS CONTRIBUTE TO CYTOPLASMIC Ca^{2+} OSCILLATIONS BY PROVIDING A BIMODAL Ca^{2+} -DEPENDENT Ca^{2+} ENTRY PATHWAY

This section corresponds to the following reference: Marijke De Bock, Nan Wang, Melissa Bol, Elke Decrock, Raf Ponsaerts, Geert Bultynck, Geneviève Dupont, Luc Leybaert. Connexin-43 hemichannels contribute to cytoplasmic Ca^{2+} oscillations by providing a bimodal Ca^{2+} -dependent Ca^{2+} entry pathway. *J Biol Chem* 2012 Apr; 287 (15): 12250-66

In this final section, we further explored how connexin hemichannels contribute to Ca^{2+} oscillations. We performed this work on Madine Darby Canine Kidney (MDCK) cells because these cells, like BBB endothelial cells, form a barrier characterized by a high TEER. MDCK cells are easier to culture and maintain a certain degree of barrier function in culture. In addition, these cells can be kept in culture for longer periods and do not require the additional influence of other co-cultured cells to build up a high resistance. All these characteristics make this model system more accessible than BBB endothelium. MDCK cells furthermore respond to bradykinin and ATP with oscillatory $[Ca^{2+}]_i$ changes [De Blasio et al., 2004a; Hirose et al., 1999; Violin et al., 2003] making them an appropriate tool for this follow-up study on the role of connexin hemichannels in the oscillation mechanism and the regulation of paracellular permeability. Some preliminary results not included in the submitted version, are presented in section 3.3.3.5.

ABSTRACT

Many cellular functions are driven by changes in the intracellular Ca^{2+} concentration ($[Ca^{2+}]_i$) that are highly organized in time and space. Ca^{2+} oscillations are particularly important in this respect and are based on positive and negative $[Ca^{2+}]_i$ feedback on $InsP_3$ receptors ($InsP_3Rs$). Connexin hemichannels are Ca^{2+} -permeable plasma membrane channels that are also controlled by $[Ca^{2+}]_i$. We aimed to investigate how hemichannels may contribute to Ca^{2+} oscillations. Madine Darby Canine Kidney cells expressing Cx32 and Cx43 were exposed to bradykinin (BK) or ATP to induce Ca^{2+} oscillations. BK-induced oscillations were rapidly (minutes) and reversibly inhibited by the connexin-mimetic peptides $^{32}Gap27/^{43}Gap26$, while ATP-induced oscillations were unaffected. Furthermore, these peptides inhibited the BK-triggered release of calcein, a hemichannel-permeable dye. BK-induced oscillations, but not those induced by ATP, were dependent on extracellular Ca^{2+} . Alleviating the negative

feedback of $[Ca^{2+}]_i$ on $InsP_3Rs$ using CytC inhibited BK- and ATP-induced oscillations. Cx32 and Cx43 hemichannels are activated by <500 nM $[Ca^{2+}]_i$ but inhibited by higher concentrations and CT9 peptide (last 9 amino acids of the Cx43 C-terminus) removes this high $[Ca^{2+}]_i$ inhibition. Unlike interfering with the bell-shaped dependence of $InsP_3Rs$ to $[Ca^{2+}]_i$, CT9 peptide prevented BK-induced oscillations but not those triggered by ATP. Collectively, these data indicate that connexin hemichannels contribute to BK-induced oscillations by allowing Ca^{2+} -entry during the rising phase of the Ca^{2+} spikes and by providing an OFF-mechanism during the falling phase of the spikes. Hemichannels were not sufficient to ignite oscillations by themselves; however, their contribution was crucial as hemichannel inhibition stopped the oscillations.

3.3.1 INTRODUCTION

Ca^{2+} is a universal and versatile intracellular messenger controlling a large variety of basic cellular functions that include fertilization, gene expression, cell differentiation, exocytosis, muscle contraction, cell survival and cell death [Case et al., 2007; Dupont et al., 2007]. Ca^{2+} is released from the endoplasmic reticulum (ER), the cell's major Ca^{2+} store, following activation of $G\alpha_q$ -protein coupled receptors (GPCR) on the plasma membrane with subsequent activation of phospholipase C_β (PLC_β), hydrolysis of phosphatidylinositol 4,5-bisphosphate ($PInsP_2$), and production of inositol 1,4,5-trisphosphate ($InsP_3$). Stimulation of $InsP_3$ receptors ($InsP_3Rs$) on the ER membrane triggers the release of ER Ca^{2+} , thereby increasing the cytosolic Ca^{2+} concentration ($[Ca^{2+}]_i$). $[Ca^{2+}]_i$ elevation is followed by a recovery phase that is mediated by Ca^{2+} sequestration back into the ER lumen through sarcoplasmic/endoplasmic Ca^{2+} ATPases (SERCAs) and by Ca^{2+} extrusion out of the cell through plasma membrane Ca^{2+} ATPases (PMCAs) [Berridge et al., 2003; Berridge et al., 2000]. This is followed by store-operated/capacitative Ca^{2+} entry (CCE) to replenish the ER with Ca^{2+} and attain pre-spike ER Ca^{2+} content [Putney and Bird, 2008].

Physiological Ca^{2+} signals can take the form of a single, transient elevation in $[Ca^{2+}]_i$ but may also appear as repeated $[Ca^{2+}]_i$ transients, called Ca^{2+} oscillations [Dupont et al., 2007; Uhlen and Fritz, 2010]. The simplest model of Ca^{2+} oscillations is based on positive and negative modulatory effects of Ca^{2+} on the open probability of $InsP_3R$ -channels, which display a typical bell-shaped dependence [Bezprozvanny et al., 1991; Keizer and De Young, 1992]. When $[Ca^{2+}]_i$ is below a certain threshold (~ 300 nM), Ca^{2+} potentiates $InsP_3$ -triggered Ca^{2+} -

release [Bezprozvanny et al., 1991], resulting in Ca^{2+} -induced Ca^{2+} release (CICR) [Goldbeter et al., 1990]. A further rise in $[\text{Ca}^{2+}]_i$ above this level results in negative feedback, marking the start of the decaying phase of the Ca^{2+} spike [Bezprozvanny et al., 1991]. After restoration of the ER Ca^{2+} content (by SERCA pumps and CCE) the cycle repeats to induce the next Ca^{2+} spike. An important condition for Ca^{2+} oscillations to occur is the necessity for kinetic differences between positive and negative Ca^{2+} -feedback, that means, the positive feedback action should be faster than the negative one [Keizer and De Young, 1992; Politi et al., 2006; Sneyd et al., 1995; Young et al., 2003], a condition that is fulfilled for InsP_3R -channels [Dawson, 1997; Parker and Ivorra, 1990]. Continued Ca^{2+} oscillations necessitate a slightly elevated intracellular InsP_3 concentration that sets a certain degree of Ca^{2+} excitability of InsP_3R -channels, making them sensitive to small local Ca^{2+} increases that can fire the next Ca^{2+} spike through CICR [Sneyd et al., 1995]. When the InsP_3 concentration is elevated consequent to stronger GPCR stimulation, the oscillation frequency generally increases [Hajnoczky and Thomas, 1997; Sneyd et al., 1995]. In addition, the intracellular InsP_3 concentration is not solely determined by the level of GPCR stimulation, but may also be influenced by direct or indirect feedback actions of $[\text{Ca}^{2+}]_i$ on Ca^{2+} - or PKC-sensitive PLC isoforms (δ , ζ , η or β , γ isoforms respectively) [Fukami et al., 2010; Rebecchi and Pentylala, 2000] thereby generating oscillations in the InsP_3 concentration. These InsP_3 oscillations may modulate the Ca^{2+} oscillations (by augmenting CICR [Young et al., 2003]) but may also take the lead and provide the primary driving force for the Ca^{2+} oscillations [Nash et al., 2001], depending on the GPCRs involved. Additionally, other feedback actions on the InsP_3 metabolism [Thore et al., 2004; Young et al., 2003] and on Ca^{2+} entry [Jones et al., 2008; Reetz and Reiser, 1996; Sacks et al., 2008; Shuttleworth and Mignen, 2003; Thomas et al., 1996] provide supplementary tools to modulate and shape the oscillatory signal [Dupont et al., 2010].

Evidence is accruing that connexin channels play a role in Ca^{2+} oscillations. Connexins form two kinds of channels: hemichannels and gap junction channels, the latter resulting from the head-to-head interaction of two hemichannels. Gap junction channels connect the cytoplasm of adjacent cells while unapposed hemichannels, when open, link the cytoplasm with the extracellular fluid. Both types of channels are permeable to substances with a molecular weight (MW) below 1-1.5 kDa [Alexander and Goldberg, 2003; Loewenstein, 1981]. Kawano et al. (2006) reported that octanol, a non-specific connexin-channel blocker, inhibited spontaneous Ca^{2+} oscillations in human mesenchymal stem cells [Kawano et al., 2006]. This

work suggested the opening of hemichannels, followed by ATP diffusing out of the cell and acting in an autocrine way on plasma membrane P2Y₁ receptors, thereby activating PLC β and generating InsP₃. Verma et al. (2009) reported that ⁴³Gap26 and ^{37/43}Gap27, two synthetic peptides that mimic short sequences in respectively the first and second extracellular loop of connexin-43 (Cx43), inhibited Ca²⁺ oscillations in connexin-expressing HeLa cells and in cardiac myocytes, [Verma et al., 2009]. ⁴³Gap26 and ^{37/43}Gap27 peptides are inhibitors of Cx43 gap junctions and have been reported to inhibit Cx43 hemichannels with faster kinetics [Braet et al., 2003a; Braet et al., 2003b; Evans et al., 2006; Leybaert et al., 2003]. Verma et al. (2009) proposed that Gap inhibition of Ca²⁺ oscillations was mediated by reducing Ca²⁺ entry via hemichannels thereby affecting ER Ca²⁺ release [Verma et al., 2009]. We recently reported that ^{37/43}Gap27 inhibits bradykinin (BK)-triggered Ca²⁺ oscillations in blood-brain barrier endothelial cells and thereby prevents a subsequent increase in barrier permeability [De Bock et al., 2011]. In addition to the fact that hemichannel-mediated ATP release and Ca²⁺ entry may play a role in Ca²⁺ oscillations, hemichannel opening is controlled by [Ca²⁺]_i [De Vuyst et al., 2006; De Vuyst et al., 2009; Ponsaerts et al., 2010]. Since hemichannels both influence and are influenced by [Ca²⁺]_i, we examined the mechanisms by which hemichannels contribute to Ca²⁺ oscillations. We specifically aimed to determine whether hemichannel-[Ca²⁺]_i interactions constitute a mechanism supporting oscillatory activity in a manner analogous to the InsP₃R-[Ca²⁺]_i link by using tools that selectively target either InsP₃Rs or connexin channels. We found that hemichannels contribute to InsP₃R-based oscillations by providing a Ca²⁺-entry pathway and by shutting down this Ca²⁺-entry pathway by inhibiting hemichannel activity when [Ca²⁺]_i increases above ~500 nM. This contribution of hemichannels was essential as the Gap peptides blocked the BK-induced oscillations. Hemichannels were not involved in ATP-induced Ca²⁺ oscillations indicating that they may help in shaping distinct Ca²⁺ response patterns to different agonists.

3.3.2 MATERIALS AND METHODS

3.3.2.1 Cell culture

MDCK cells (up to passage 15) and C6-glioma cells stably transfected with Cx43 (C6Cx43), Panx1 (C6Panx1) or Panx1-Myc (C6Panx1-Myc) (C6 were kindly provided by Dr. Christian C. Naus, University of British Columbia, Canada) were maintained in Dulbecco's modified Eagle medium (DMEM)/Ham's F12 (1:1) supplemented with 10 % fetal calf serum (FCS)

and 2 mM glutamine, 10 U/mL penicillin, 10 µg/mL streptomycin and 0.25 µg/mL fungizone (all from Gibco, Invitrogen, Merelbeke, Belgium) at 37 °C and 5 % CO₂. Rat brain endothelial (RBE4) cells were maintained in α-minimal essential medium (α-MEM)/Ham's F10 supplemented with 10% FCS, 2 mM L-glutamine, 300 µg/mL G-418 (Gibco, Invitrogen) and 1 ng/mL human recombinant basic fibroblast growth factor (Roche Diagnostics, Vilvoorde, Belgium). MDCK and RBE4 cells were grown on collagen-coated recipients (rat-tail collagen, Roche Diagnostics).

3.3.2.2 Chemicals and reagents

Arachidonyl trifluoromethyl ketone (AACOCF₃), 4-Bromo-A23187, adenosine 5' triphosphate (ATP), apyrase grade VI and VII, bradykinin, carbenoxolone (Cbx), Cytochrome C (CytC) from equine heart, digitonin, ethylene glycol-bis-(β-aminoethyl ether)-N,N,N',N'-tetraacetic acid (EGTA), 8-(p-Sulfophenyl)theophylline (8-SPT) and staurosporine were purchased from Sigma-Aldrich (Bornem, Belgium). 1,2-Bis(2-aminophenoxy) ethane-N,N,N',N'-tetraacetic acid tetrakis -acetoxymethyl ester (BAPTA-AM), Calcein-AM, 5-carboxyfluorescein diacetate-AM (5-CFDA-AM), 10 kDa dextran texas red (DTR), 10 kDa dextran fluorescein, D-myo-inositol 1,4,5-trisphosphate, P⁴⁽⁵⁾-1-(2-nitrophenyl)ethylester ('caged InsP₃'), fluo3-AM, fura2-AM, Hoechst 33342, Mitotracker Green FM, o-nitrophenyl-EGTA-AM ('Caged Ca²⁺'), propidium iodide (PI), RhodFF-AM and thapsigargin were from Molecular probes (Invitrogen). Xestospongine-C (XeC) and U73122 were from Tocris Bioscience (Bristol, UK). ³²Gap27 (SRPTEKTVFT, amino acids 182 to 191 in the second extracellular loop of Cx32), ⁴³Gap26 (VCYDKSFPISHVR, amino acids 64 to 76 in the first extracellular loop of Cx43), CT9 (RPRPDDLEI, last 9 amino acids of the C-terminal tail of Cx43), CT9ΔI (RPRPDDLE), the reversed CT9 peptide (CT9^{Rev}, IELDDPRPR), YGRKKRRQRRR-CT9 (Tat-CT9) and Tat-CT9^{Rev} were synthesized by LifeTein (New Jersey, USA) at > 80 % purity. The C-terminal peptide IP3RCYT, corresponding to amino acids 2621-2636 of InsP₃R1 (DNKTVTFEEHIKEEHNC) [Boehning et al., 2005] was a kind gift of Dr. Darren F. Boehning (University of Texas Medical Branch, USA).

3.3.2.3 Ca²⁺ imaging

MDCK cells were seeded onto 18 mm diameter, glass coverslips (Knittel Glaser, Novolab, Geraardsbergen, Belgium) and experiments were performed at subconfluency, the next day.

The cells were loaded with 10 μM fluo3-AM in HBSS-Hepes (1 mM CaCl_2 ; 0.81 mM MgSO_4 ; 13 mM NaCl; 0.18 mM Na_2HPO_4 ; 5.36 mM KCl; 0.44 mM KH_2PO_4 ; 5.55 mM D-glucose and 25 mM Hepes) during 1 h at room temperature (RT). After 1 h, coverslips were washed and then left for an additional 30 min at RT in HBSS-Hepes to allow for de-esterification. Cells were thereafter transferred to an inverted epifluorescence microscope (Eclipse TE 300, Nikon Belux, Brussels, Belgium), equipped with a superfusion system which allowed changing the bath solution within ~ 1 min (bath volume ~ 300 μl). Superfusion was switched off during the registration of oscillatory activity. Images were taken every second with a $\times 40$ oil-immersion objective and an electron-multiplying CCD camera (Quantem 512SC, Photometrics, Tucson, AZ, USA). We used a Lambda DG-4 filterswitch (Sutter Instrument Company, Novato, CA, USA) to deliver excitation at 482 nm and captured emitted light via a 505 nm long-pass dichroic mirror and a 535 nm bandpass-filter (35 nm bandwidth). Cells were loaded with fura2-AM (5 μM) in a similar manner. Excitation was alternated between 340 nm and 380 nm at a rate of one image pair every second. Emitted light was captured using a 430 nm long-pass dichroic mirror and a 510 nm bandpass-filter (40-nm bandwidth). Fura2 *in situ* calibration was performed in zero Ca^{2+} medium (10 mM EGTA) containing 10 μM A23187 (R_{\min}) and a saturating Ca^{2+} solution (10 mM CaCl_2) containing 40 μM digitonin (R_{\max}). $[\text{Ca}^{2+}]_i$ was calculated from $K_d \cdot Q \cdot [(R - R_{\min}) / (R_{\max} - R)]$ with R the F_{340}/F_{380} ratio, $Q = F_{\min}/F_{\max}$ at 380 nm and $K_d = 224$ nM [Grynkiewicz et al., 1985]. Mitochondrial Ca^{2+} measurements were performed with the mitochondrial Ca^{2+} indicator RhodFF as we described previously [Van Moorhem et al., 2010]. MDCK cells were loaded with RhodFF-AM (5 μM) during 1 h at RT followed by 30 min de-esterification. Imaging was performed in a similar manner as Fluo3 imaging but with excitation at 556 nm and long-pass filtering at 590 nm. A punctuate distribution that matches the distribution of Mitotracker confirmed the mitochondrial localization of the dye (**figure 30**). Recordings and analysis were done with custom-developed QuantEMframes and Fluoframes software written in Microsoft Visual C++ 6.0. Oscillatory activity was recorded in a 10 min observation window and only Ca^{2+} spikes minimally 10 % above baseline were considered in the analysis. To calculate the percentage of oscillating cells, an oscillating cell was defined as a cell displaying at least 2 Ca^{2+} spikes subsequent to the initial spike. The percentage of cells oscillating was calculated relative to the total number of cells in view. The oscillation frequency is the average frequency of all cells in view, including non-oscillating cells.

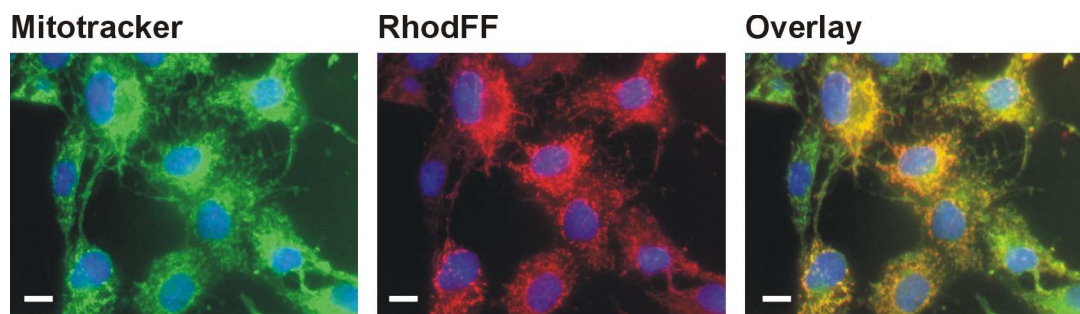


Figure 30. Mitochondrial localization of RhodFF. Representative images of RhodFF-loaded MDCK cells counterstained with Mitotracker Green and nuclear Hoechst staining. The images show a punctate RhodFF distribution that matches the distribution of Mitotracker. Scalebar is 10 μm .

3.3.2.4 Electroporation loading

MDCK cells were loaded with CytC or CT peptides by electroporation. Cells, seeded the day before the experiment, were rinsed with a low-conductivity electroporation buffer and placed on the microscope stage. Thereafter, a small volume (10 μl) of CytC (3 μM)/DTR (100 μM) or CT9 peptide (300 μM)/PI (12 μM), dissolved in electroporation buffer was added to a parallel wire Pt-Ir-electrode, positioned 400 μm above the cells. DTR (10 kDa) or PI (668 Da) have MW's approaching that of CytC (12 kDa) or CT9 (1 kDa) respectively and were added to visualize the electroporated cells. In experiments using the Ca^{2+} dye RhodFF, we visualized the CytC-loaded zone with 10 kDa dextran fluorescein. The IP3RCYT peptide (15 μM) was added to the CytC (3 μM) solution (see above) 30 min prior to electroporation to allow for interaction. Electroporation was performed following fluo3-AM loading with 50 kHz bipolar pulses, at a field strength of 1000 V/cm, applied as 15 trains of 10 pulses of 2 ms duration each [De Vuyst et al., 2008; Decrock et al., 2009]. Electroporation did not result in loss of fluo3/fura2/RhodFF from the cells.

3.3.2.5 Caged compound loading and photoliberation

Cells, seeded on coverslips the day before the experiment, were electroporated with cell-impermeant, caged InsP_3 (30 μM) and DTR (100 μM) as described above. Caged Ca^{2+} was loaded into the cells by ester-loading, similar to the Ca^{2+} -sensitive dyes. Thereafter, the coverslips were transferred to an inverted epifluorescence microscope. Photoliberation of InsP_3 was done by spot (20 μm diameter) illumination with 1 kHz pulsed UV light (349 nm UV laser Explorer, Spectra-Physics, Newport, Utrecht, Netherlands) applied during 20 ms (20

pulses of 90 μJ energy measured at the entrance of the microscope epifluorescence tube). For uncaging of Ca^{2+} we applied UV illumination with different flash durations.

3.3.2.6 Hemichannel assays

Hemichannel opening was investigated by calcein (623 Da) release which is based on the efflux of the preloaded dye via open hemichannels [Anselmi et al., 2008]. Subconfluent cultures of MDCK, grown on glass coverslips (18 mm diameter), were preloaded with 50 μM calcein-AM in HBSS-hepes for 1 h at RT. Subsequently, the remaining calcein-AM was removed; cells were left for an additional 30 min at RT in HBSS-Hepes to allow the AM ester to de-esterify and were then transferred to the stage of an inverted epifluorescence microscope. For analysis, we measured the decrease in calcein fluorescence in function of time. The first 5 min, baseline leakage in HBSS-Hepes was measured (control), thereafter, the trigger solution was added and efflux of calcein was further evaluated. The slope of the curve, calculated by linear regression, was used as a parameter describing the loss of dye in time. Calcein efflux in the presence of trigger is presented as % of control.

3.3.2.7 Gap junction dye coupling studies

Dye coupling via gap junctions was determined making use of fluorescence recovery after photobleaching (FRAP). MDCK cultures were grown to confluence on 9.2 cm^2 petridishes (TPP) and were loaded with the gap junction permeable fluorescent dye 5-CFDA-AM (532 Da, 10 μM) in HBSS-Hepes for 1 h at RT. Following de-esterification, cells were transferred to a custom-made video-rate confocal laser scanning microscope with a x40 water immersion objective (CFI Plan Fluor) and a 488 nm laser excitation source (Cyan CW Laser, 488 nm - 100 mW, Newport Spectra-Physics, Utrecht, The Netherlands). After 1 min of recording, the cell in the middle of the field was photobleached by spot exposure (1 s) to increased power of the 488 nm laser and fluorescence recovery, caused by dye influx from neighboring non-bleached cells, was recorded during an additional 5 min period. The fluorescence recovery trace was then analyzed for the recovery of the signal expressed relative to the starting level before photobleaching.

3.3.2.8 Ectonucleotidase activity

Ectonucleotidase activity was assessed by measuring the breakdown of ATP added to the cells via the decline of luciferin/luciferase luminescence in the medium above the cells. MDCK and RBE4 cells were seeded at a density of 40,000 cells/cm² in 24-well plates. ATP (100 μM), together with an ATP bioluminescent assay mix (luciferin/luciferase, 625 fold dilution, Sigma-Aldrich), was prepared in ATP assay mix dilution buffer (Sigma-Aldrich). Photon flux was counted using a multilabel counter (Victor-3, type 1420, Perkin-Elmer, Brussels, Belgium). The time constant (τ) of the exponential luminescence decay was used as a parameter to express ectonucleotidase activity.

3.3.2.9 Apoptosis assay

Annexin V staining detects the flip-flop of phosphatidylserine toward the outer plasma membrane leaflet that occurs during apoptosis. Following electroporation with 10 kDa DTR (100 μM) and CytC (3 μM), cells were rinsed with PBS and incubated for 15 min (RT) with Annexin V-FITC (1:50; Roche Diagnostics) and Hoechst 33342 (2 μg/ml) in Annexin V buffer (140 mM NaCl, 5 mM CaCl₂, 10 mM HEPES, pH 7.4). The cultures were subsequently washed with PBS and transferred to a Nikon TE300 epifluorescence microscope, equipped with a x 10 objective (Plan Apo, NA 0.4, Nikon). Ten images inside the electroporation zone were taken and Annexin V-positive cells were counted. The number of apoptotic cells was expressed as the percentage of Annexin V-positive cells relative to the total number of cells (determined by Hoechst 33342 staining).

3.3.2.10 siRNA treatment

MDCK cells were seeded onto 18 mm diameter glass coverslips at a density of 20,000 cells/cm² and transfected the following day using Dharmafect1 lipid reagent (Dharmacon, Thermo Fisher Scientific). We used 2 siRNA duplexes (125 nM) directed against the canine Cx43 gene *gja1* (siCx43-1: 5'-GUUCAAGUAUGGAAUUGAA-dTdT-3' and siCx43-2: 5'-UUCAAUUCCAUACUUGAACdTdT-3'). On day 3 medium was refreshed and on day 4, cells were used for experiments. Transfection efficiency on day 3 was 52 ± 4.1 % (n = 11), as determined with the fluorescent indicator siGLO. Control conditions were untreated cultures, Mock treated cultures (lipid reagent alone) and a negative control consisting of cultures transfected with a scrambled version of siCx43-1 (siCx43-1^{Scr}: 5'-

GCGUAUAUAUGAGUAAGUAAdTdT-3'). All siRNA duplexes were synthesized and annealed by Eurogentec (Luik, Belgium) after selective designing against *Canis familiaris* and screening for off-target sequences using 'Batch RNAi selector' [Iyer et al., 2007].

3.3.2.11 Electrophoresis and Western blot analysis

For western blots, cells were seeded in 75 cm² flasks. Total MDCK lysates were extracted with RIPA buffer (25 mM Tris, 50 mM NaCl, 0.5% NP40, 0.5% deoxycholate, 0.1% SDS, 1 mM DTT, 0.055 g/mL β -glycerolphosphate, 30 μ L/mL phosphatase inhibitor cocktail and 20 μ L/mL mini EDTA-free protease inhibitor cocktail). For separation of Triton-X-100 soluble (cytosol) and insoluble (membrane) fractions, cells were harvested in 1% Triton-X-100, supplemented with 50 mM NaF and 1 mM Na₃VO₄, and centrifuged at 16,000 g for 10 min. The Triton-X-100 insoluble pellets were resuspended in 1 x Laemmli sample buffer. Protein concentration was determined using a Biorad DC protein assay (BioRad, Nazareth, Belgium) and absorbance was measured with a 590 nm long-pass filter. Lysates were separated by electrophoresis over a 10 % SDS-polyacrylamide gel and transferred to a nitrocellulose membrane (Amersham, Buckinghamshire, UK). Membranes were subsequently blocked with TBS containing 5 % non-fat milk and 0.1 % Tween20. Following blocking, blots were probed with rabbit anti-Cx43 antibody (Sigma-Aldrich), rabbit anti-Cx32 antibody (Sigma-Aldrich), rabbit anti-Cx26 antibody (Zymed, Invitrogen), rabbit anti-phosphoCx43 (pS368) (Cell Signaling Technology, Inc., Danvers, MA, USA), rabbit anti-P2X₇ antibody (Alomone Labs, Jerusalem, Israel), anti-Panx1 antibody (kind gift of Dr. Dale W. Laird, University of Western Ontario, Canada) and rabbit anti- β -tubulin antibody (Abcam, Cambridge, UK) as a loading control. Membranes were subsequently incubated with an alkaline phosphatase-conjugated goat anti-rabbit IgG antibody (Sigma-Aldrich) and detection was done using the nitro-blue-tetrazolium/5-bromo-4-chloro-3-indolyl-phosphate reagent (NBT/BCIP kit, Zymed, Invitrogen). Quantification was done by drawing a rectangular window around the concerned band and determining the signal intensity using ImageJ software. Background correction was done by the same procedure applied to nitrocellulose membranes where protein was absent.

3.3.2.12 Statistical analysis

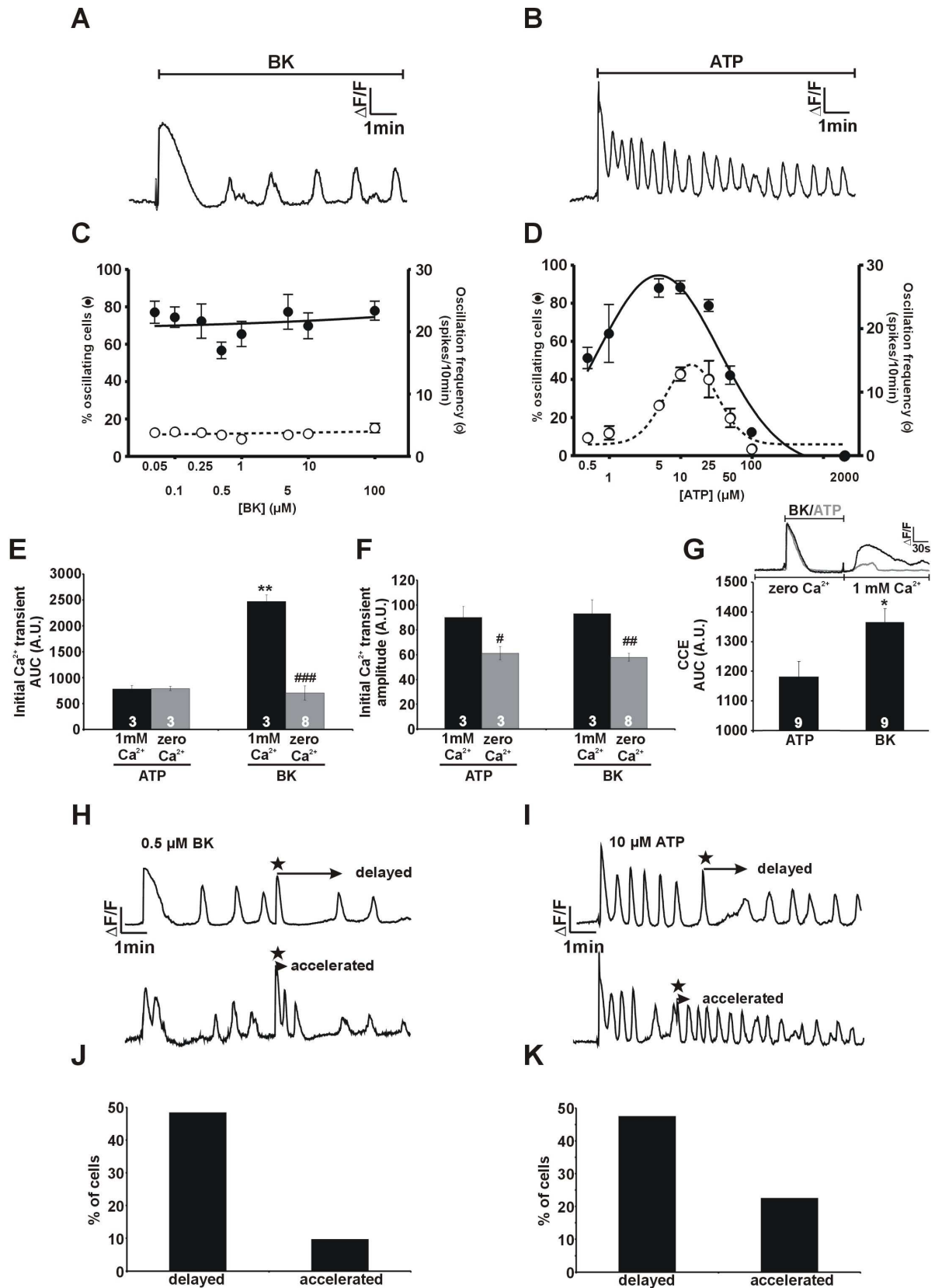
Data are expressed as mean \pm S.E.M. with n giving the number of independent experiments. Multiple groups were compared by one-way ANOVA and Bonferroni post-test, making use of

Graphpad Instat software. Two groups were compared with an unpaired student's t-test and two-tail p-value. Results were considered statistically significant when $p < 0.05$ (one symbol for $p < 0.05$, two for $p < 0.01$ and three for $p < 0.001$).

3.3.3 RESULTS

3.3.3.1 Concentration and InsP₃-dependency of BK- and ATP-induced Ca²⁺ oscillations

We first characterized BK- and ATP-induced Ca²⁺ oscillations in MDCK cells and determined the concentration-dependency of the percentage of oscillating cells and of the oscillation frequency. We used non-confluent MDCK cell cultures in order to limit the degree of gap junctional coupling. BK and ATP triggered an initial [Ca²⁺]_i transient followed by repetitive Ca²⁺ spikes (recorded over a 10 min period) with quite a different profile (**figure 31A,B**). BK concentrations ranging from 0.05 μM to 100 μM all triggered Ca²⁺ oscillations in an invariable percentage of cells (~72 %) and a similar oscillation frequency (~5 spikes/10 min, measured over all cells in view) (**figure 31C**). By contrast, oscillations triggered by ATP concentrations between 0.5 μM and 2 mM were characterized by a bell-shaped concentration-response curve for the percentage of oscillating cells and oscillation frequency (**figure 31D**). The maximum number of oscillating cells (89 ± 3.4 %; $n = 5$) and the maximal oscillation frequency (13 ± 1.1 spikes/10 min; $n = 5$) were observed with 10 μM ATP. These markedly different patterns of concentration-dependency indicate distinct oscillation mechanisms for ATP and BK. We chose 10 μM ATP (a concentration located between the two peaks depicted in figure 31D) and 0.5 μM BK (relative location within the range of concentrations tested comparable to ATP) for further analysis of differences between the oscillations triggered by these two agonists. We first determined whether the amplitude of the initial [Ca²⁺]_i transient triggered by BK (0.5 μM) or ATP (10 μM) was different but found they were very similar (650 ± 59 nM and 783 ± 110 nM respectively, $n=8$, $p > 0.05$) which suggests that the intracellular InsP₃ elevation is comparable with the two stimuli. Yet, the area under the curve (AUC) for both triggers differed markedly with BK exhibiting a much larger AUC compared to ATP (**figure 31E,F**). Because the amplitudes were not different, it follows that the BK-triggered [Ca²⁺]_i transient is longer than the one triggered by ATP (see example traces in figure 31).



The longer duration of the BK-induced $[Ca^{2+}]_i$ transient is likely to be related to Ca^{2+} entry from the extracellular space. In line with this, withdrawal of extracellular Ca^{2+} (zero extracellular Ca^{2+}) did not much affect the initial $[Ca^{2+}]_i$ transient elicited by ATP whereas it largely reduced the one triggered by BK (**figure 31E,F**). Further probing of CCE by re-introducing extracellular Ca^{2+} after the $[Ca^{2+}]_i$ transient in zero extracellular Ca^{2+} conditions showed that CCE was much larger for BK than for ATP (**figure 31G**).

Figure 31. Concentration dependency of Ca^{2+} oscillations triggered by BK and ATP. **A-B.** Representative traces demonstrating that exposure of MDCK cells to 0.5 μ M BK or 10 μ M ATP elicited Ca^{2+} oscillations. **C.** Challenging MDCK cells with different concentrations of BK gave an almost flat response curve for both the percentage of oscillating cells and the oscillation frequency. **D.** The concentration dependence of ATP-induced oscillations was bell-shaped with a maximum at \sim 10 μ M ATP. **E-F.** Comparison of the initial $[Ca^{2+}]_i$ transients (AUC and amplitude) triggered by BK (0.5 μ M) and ATP (10 μ M) under control (1 mM extracellular Ca^{2+}) and extracellular zero Ca^{2+} (no added Ca^{2+} + 1 mM EGTA) conditions. Star symbols indicate significant differences between ATP and BK; number signs compare 1 mM Ca^{2+} conditions to zero Ca^{2+} conditions. **G.** ATP- and BK transients were triggered in zero Ca^{2+} medium after which Ca^{2+} (1 mM) was re-introduced to the bathing medium. CCE (AUC) triggered in this manner was significantly larger for BK compared to ATP. **H-I.** Example traces illustrating the effect of photolytically releasing $InsP_3$ (indicated by the star symbol) on Ca^{2+} oscillations induced BK (0.5 μ M) or ATP (10 μ M). **J-K.** Bar charts summarizing the percentage of cells displaying delayed or accelerated spiking activity following photorelease of $InsP_3$.

Sneyd et al. have described a method to distinguish between oscillations characterized by a constant level of intracellular $InsP_3$ and those associated with oscillatory $InsP_3$ fluctuations, by recording the response to an applied $InsP_3$ -concentration step [Sneyd et al., 2006]. If $InsP_3$ fluctuates during the Ca^{2+} oscillations, induction of a sudden $InsP_3$ increase will introduce a delay to the next Ca^{2+} spike. The delay is caused by the fact that $InsP_3$ has to recover to a level that is again compatible with Ca^{2+} oscillations; thereafter, the oscillation frequency stabilizes again. If $InsP_3$ is constant during the Ca^{2+} oscillations, an induced $InsP_3$ elevation will temporarily increase the oscillation frequency, giving accelerated oscillations [Sneyd et al., 2006; Swann and Yu, 2008]. We performed $InsP_3$ elevation experiments with flash photolysis of caged $InsP_3$ and found that the majority of the cells (\sim 48 %) showed a delayed response for both BK- and ATP-induced oscillations (**figure 31H-K**). A smaller fraction of the cells displayed an accelerated response: \sim 10 % for BK and \sim 22 % for ATP oscillations. In the

remainder of the cells InsP_3 elevation had no effect. These data indicate that oscillations triggered by BK and ATP are similar, at least with respect to the occurrence of InsP_3 oscillations.

3.3.3.2 Connexin-channel blockers inhibit BK-induced Ca^{2+} oscillations but not those triggered by ATP

SDS-Page and Western blot analysis revealed the presence of Cx32 and Cx43 in MDCK cells, with a small background expression of Cx26. Both Cx32 and Cx43 were present in the plasma membrane whereas their presence in the cytosolic fraction was limited (**figure 32A**). MDCK cells did not express Panx1 nor P2X_7 , which is linked to Panx1 channels [Pelegrin and Surprenant, 2006] (**figure 32B,C**).

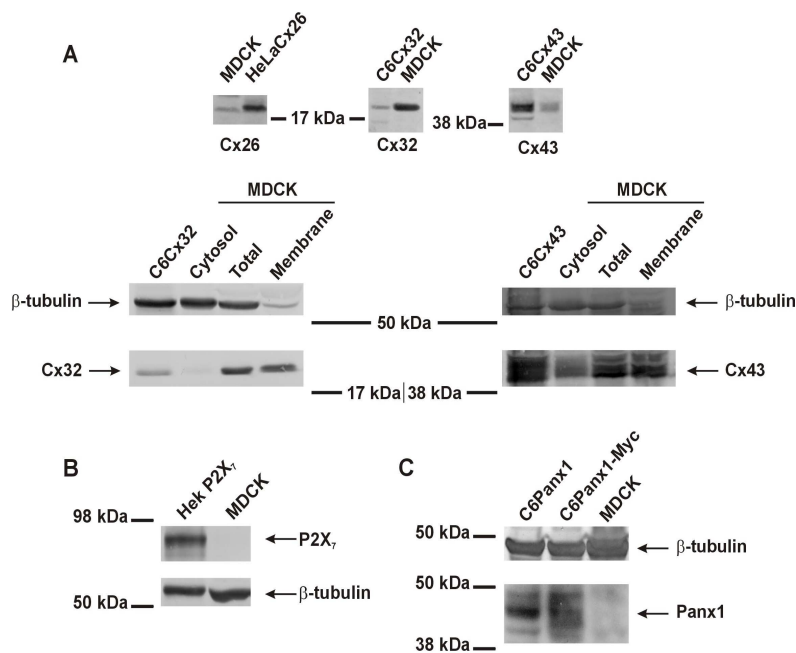


Figure 32. Connexin, pannexin and P2X_7 expression in MDCK. **A.** Western blot analysis showing expression of Cx32 and Cx43, with a small background of Cx26. Cx32 and Cx43 were mainly present in membrane fractions whereas their presence in the cytosol fraction was much lower. C6Cx32, C6Cx43 or HeLaCx26 were used as positive controls, β -tubulin was a loading control. **B.** MDCK cells do not express the purinoceptor P2X_7 . Hek cells stably transfected with P2X_7 were used as a positive control. **C.** Panx1 is not expressed in MDCK. C6 cells stably transfected with Panx1 or Panx1-Myc or used as positive controls.

When BK-triggered oscillations were elicited in the presence of the general connexin-channel blocker Cbx (25 μ M, 30 min pre-incubation and present during the 10 min observation window), the initial Ca^{2+} spike remained but the subsequent oscillations disappeared. We further applied two peptide connexin-channel inhibitors, $^{32}\text{Gap27}$ and $^{43}\text{Gap26}$ that target Cx32 and Cx43 channels respectively [De Vuyst et al., 2009; Vinken et al., 2010]. Application of $^{32}\text{Gap27}/^{43}\text{Gap26}$ ('Gap', 200 μ M, 30 min pre-incubation and present during the recording) also inhibited the Ca^{2+} oscillations, without perturbing the initial peak (**figure 33A**). $^{32}\text{Gap27}$ and $^{43}\text{Gap26}$, either separately or in an equimolar mix, reduced the percentage of oscillating cells to $\sim 1/3$ and Cbx reduced it to $\sim 1/7$ (**figure 33B**); a similar degree of inhibition was observed for the oscillation frequency (**figure 33C**). Superfusion experiments showed that inhibition by $^{32}\text{Gap27}/^{43}\text{Gap26}$ was rapid, within ~ 1 min, and that oscillations reappeared upon wash-out of the peptides (**figure 33D**). We next tested the effect of Gap peptides and Cbx on Ca^{2+} oscillations triggered by ATP (10 μ M) and found they had no effect on the percentage of oscillating cells or the oscillation frequency (**figure 33E-G**). Thus, only BK-triggered Ca^{2+} oscillations are influenced by Cbx or Gap peptides. The BK-triggered Ca^{2+} oscillations were not synchronized in neighboring cells, pointing to absence of gap junctional or other synchronizing mechanisms [Bindschadler and Sneyd, 2001; De Blasio et al., 2004b; Koizumi, 2010]. The rapid block of oscillations by Gap peptides suggests an effect at the level of hemichannels, as generally longer incubations are needed to also influence gap junctions [Braet et al., 2003b; De Bock et al., 2011; Leybaert et al., 2003]. In line with this, $^{32}\text{Gap27}/^{43}\text{Gap26}$ (200 μ M, 60 min) had no effect on gap junction dye coupling studied with fluorescence recovery after photobleaching (**figure 33H**).

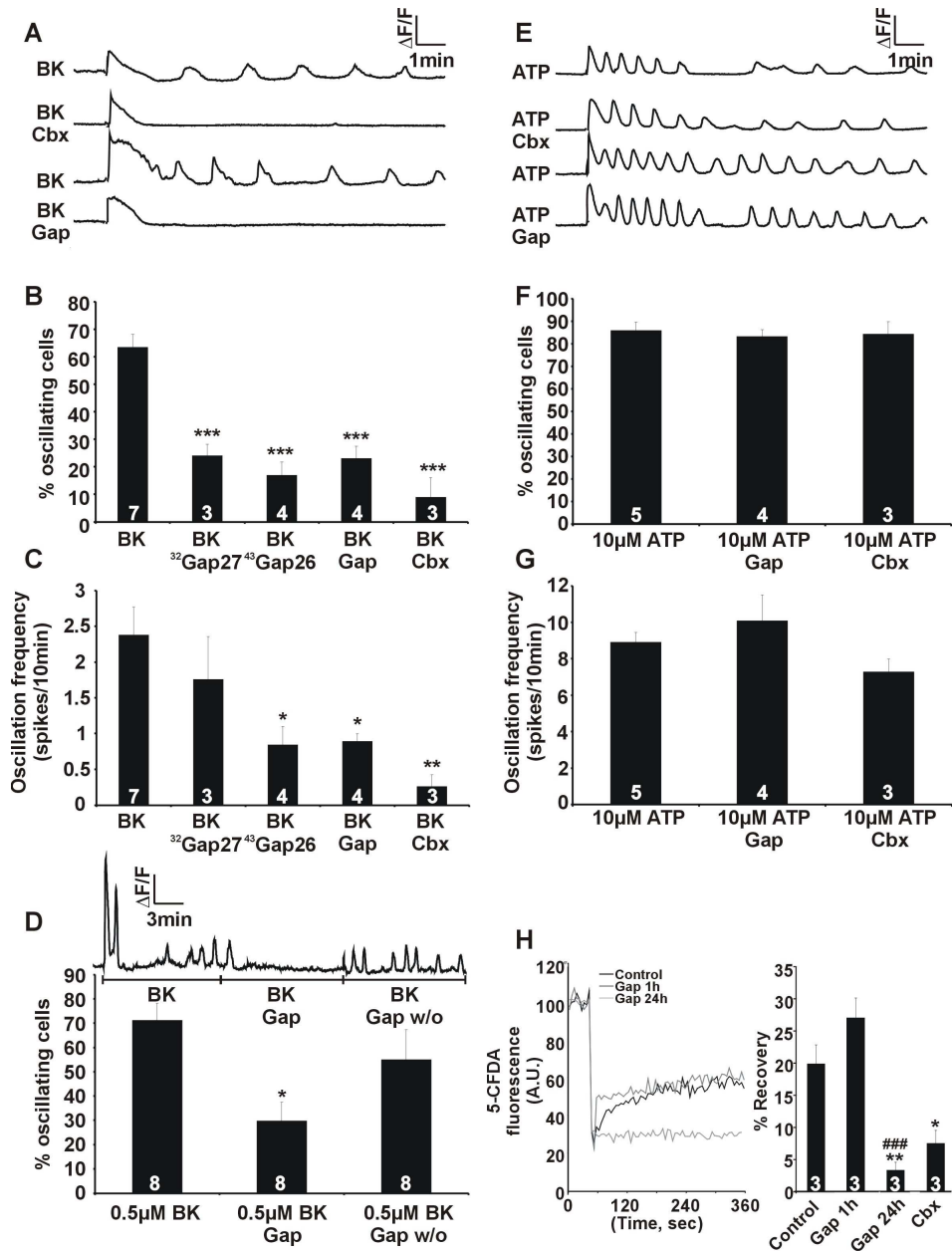


Figure 33. Gap peptides and Cbx block BK-induced Ca^{2+} oscillations. **A.** Representative traces of $[\text{Ca}^{2+}]_i$ responses to BK application ($0.5 \mu\text{M}$) illustrating that Cbx ($25 \mu\text{M}$) and $^{32}\text{Gap}27/^{43}\text{Gap}26$ (Gap, $200 \mu\text{M}$) inhibit the oscillations. **B.** Effect of Cbx and Gap peptides on the percentage of oscillating cells. **C.** Effect of Cbx and Gap peptides on oscillation frequency. Star signs compare to BK alone. **D.** Superfusion experiment illustrating that BK-triggered oscillations almost immediately disappeared after addition of the Gap peptides. Summary data of experiments are shown underneath. Star signs indicate significance compared to BK alone. **E.** Example traces of Ca^{2+} responses triggered by ATP ($10 \mu\text{M}$) illustrating absence of any effect of Cbx and Gap on the oscillations. **F.** The percentage of cells displaying oscillations in response to ATP was not altered by Cbx and Gap. **G.** The oscillation frequency with ATP stimulation was not significantly altered by Cbx and Gap. **H.** Gap junctional dye coupling was unaffected when $^{32}\text{Gap}27/^{43}\text{Gap}26$ (Gap) were incubated for 1 h but strongly declined when these peptides were present for 24 h or when the aspecific connexin-channel blocker Cbx ($25 \mu\text{M}$, 15 min) was used. Stars designate significance compared to control; number signs compare to 1 h Gap exposure.

Knock-down of Cx43 RNA showed that suppressing Cx43 expression prevented BK-triggered Ca^{2+} oscillations, in line with inhibition of oscillations by $^{43}\text{Gap26}$ added alone (without $^{32}\text{Gap27}$). Western blot analysis indicated a ~50 % reduction of Cx43 expression in cells transfected with SiCx43-1 (125 nM, 48 h) (**figure 34A**) and the number of oscillating cells in the presence of BK was reduced to a similar extent (**figure 34B,C**). SiCx43-2 was less efficient and gave proportionally less inhibition (**figure 34A,C**). Importantly, neither SiCx43-1 nor SiCx43-2 reduced Cx32 expression (data not shown); therefore, the oscillations that remain after Cx43 silencing may result from incomplete Cx43 knockdown or from the contribution of Cx32 hemichannels. Cx43-gene silencing did not influence ATP-triggered Ca^{2+} oscillations (**figure 34D,E**).

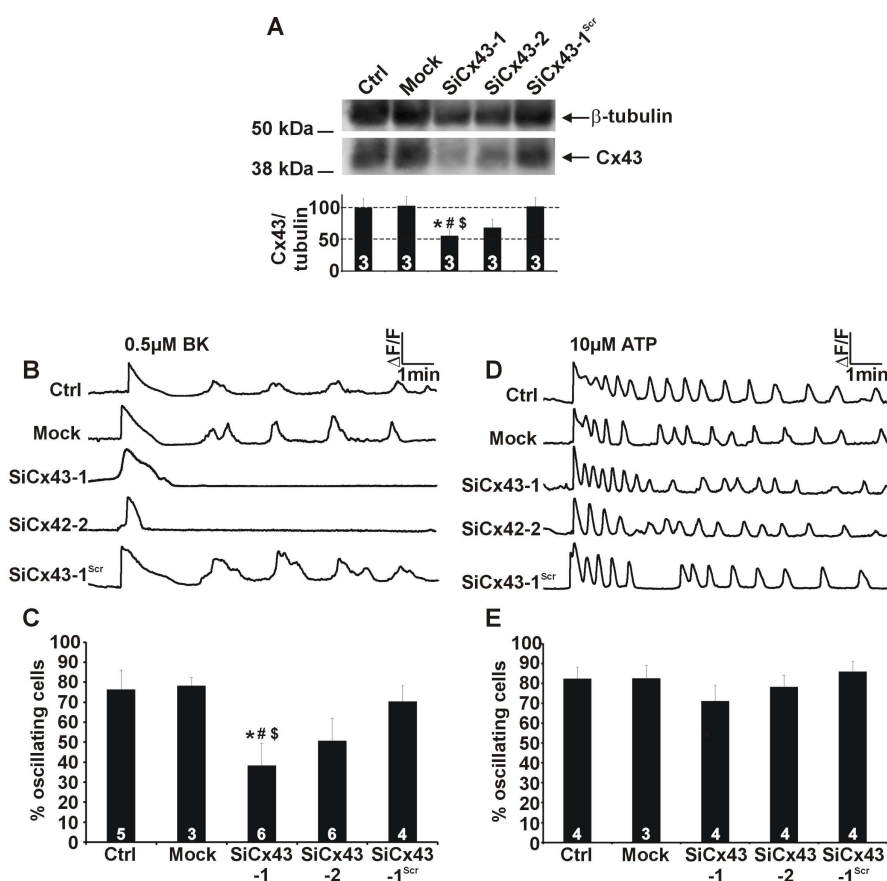


Figure 34. Effect of Cx43 gene silencing on Ca^{2+} oscillations. **A.** Silencing of Cx43 gene expression in MDCK cells demonstrating significantly reduced expression to ~50% of the control signals (star symbol compares to Ctrl, number sign compares to Mock-treated cultures and dollar sign compares to cells transfected with a scrambled sequence). **B.** Example traces of Ca^{2+} responses triggered by BK (0.5 μM) for the different treatment conditions shown in panel A. **C.** Cx43 knockdown in MDCK cells approximately halved the number of oscillating cells in the presence of 0.5 μM BK (significance signs as in panel A). **D, E.** Cx43 gene silencing did not influence Ca^{2+} oscillations triggered by 10 μM ATP.

3.3.3.3 Lowering extracellular Ca²⁺ differentially affects BK- and ATP-induced oscillations

Hemichannels may contribute to the oscillations via ATP release acting in an autocrine manner [De Bock et al., 2011; Kawano et al., 2006] or via Ca²⁺ entry [Verma et al., 2009]. We first set out to find evidence for hemichannel opening in response to BK. Exposure of cells preloaded with calcein (a hemichannel-permeable fluorescent dye with a MW of 623 Da [Anselmi et al., 2008]) to BK (0.5 μM) increased the calcein efflux rate and this effect was counteracted by ³²Gap27/⁴³Gap26 (**figure 35A**). In contrast, ATP (10 μM) did not accelerate dye efflux (**figure 35A**). BK-triggered calcein release could be furthermore reduced by buffering increases in [Ca²⁺]_i using the Ca²⁺ chelator BAPTA-AM (**figure 35B**). PLA₂ is reported to be activated by BK [Easton and Abbott, 2002; Kennedy et al., 1997] and is involved in connexin hemichannel opening [De Vuyst et al., 2009]; however, PLA₂ inhibition by AACOCF3 had no effect on the percentage of cells displaying oscillations in response to BK (63 ± 7 % oscillating cells in control vs. 65 ± 7 % oscillating cells in AACOCF3-treated cells, n = 4), further emphasizing that [Ca²⁺]_i changes are necessary for hemichannel opening. We next tested whether ATP release through open hemichannels played a role in BK-induced Ca²⁺ oscillations. We applied apyrase VI/VII (to degrade extracellular ATP), PPADS or suramin (to inhibit purinergic P2 receptors), and 8-SPT (to inhibit adenosine A1/A2_B receptors) but these agents did not significantly influence the percentage of oscillating cells or the oscillation frequency (**figure 35C,D**). We recently reported that ATP release via hemichannels was involved in BK-induced oscillations in RBE4 brain endothelial cells [De Bock et al., 2011] and we speculated that MDCK cells display a stronger ectonucleotidase activity than RBE4 cells. In line with this, we found that ATP added to the incubation solution above the cells was much faster degraded in MDCK as compared to RBE4 cell cultures (**figure 35E,F**) indicating stronger ectonucleotidase activity in MDCK cells. Thus, ATP released via BK-induced hemichannel opening likely has no downstream effects on purinergic receptors or Ca²⁺ oscillations in MDCK cells due to its rapid degradation.

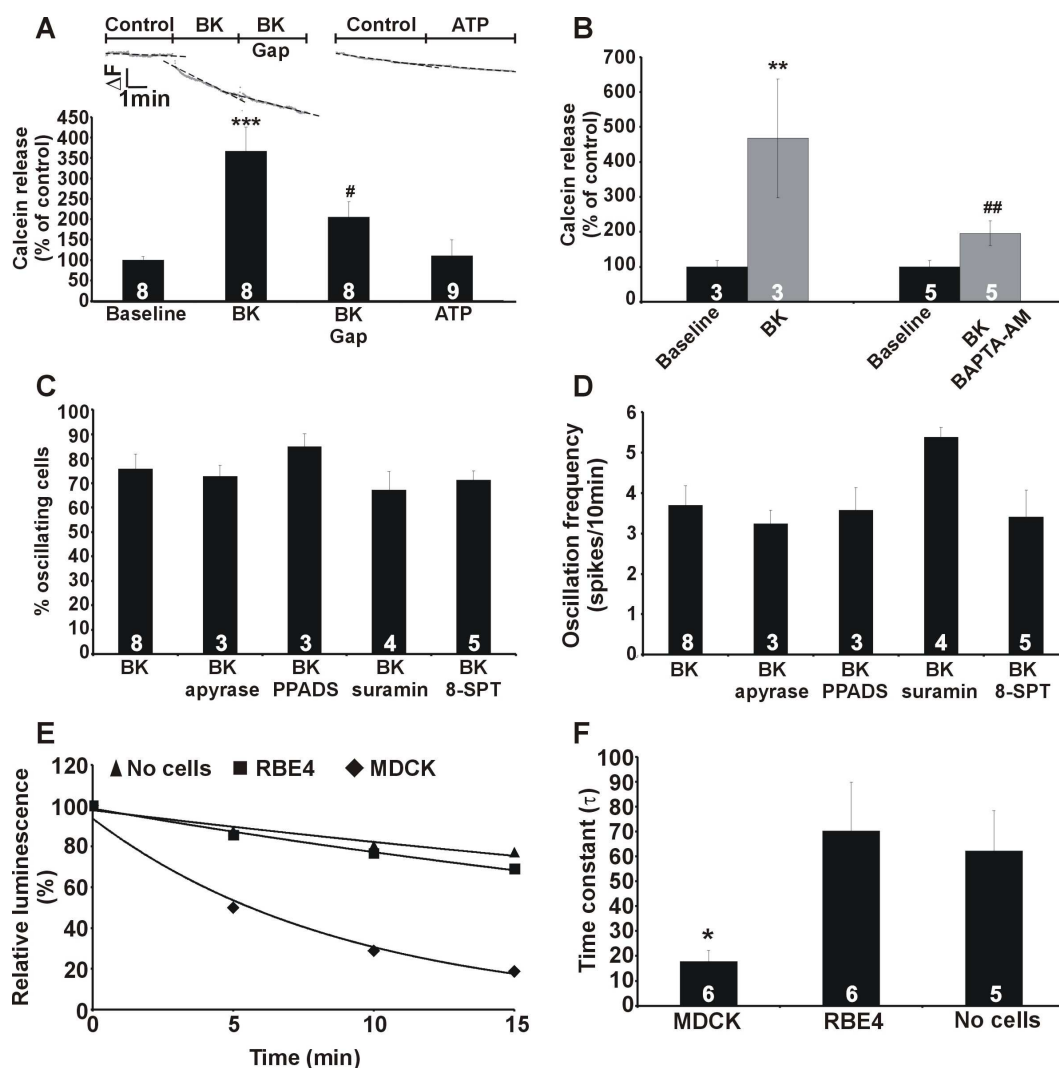


Figure 35. Calcein hemichannel studies and involvement of ATP release. **A.** BK (0.5 μ M) stimulated the rate of calcein release from MDCK cells and this was rapidly inhibited by $^{32}\text{Gap}27/^{43}\text{Gap}26$ (Gap, 200 μ M). ATP did not influence the rate of calcein release. **B.** BK-triggered calcein release was inhibited by $[\text{Ca}^{2+}]_i$ chelation with BAPTA-AM (5 μ M, 1 h pre-incubation). Asterisks indicate significance compared to baseline, number signs indicate a significant difference compared to BK-triggered calcein release. **C-D.** Apyrase (5 U/ml, 30 min pre-incubation), PPADS (75 μ M, 30 min pre-incubation), suramin (200 μ M, 30 min pre-incubation) or 8-SPT (100 μ M, 30 min pre-incubation) did not significantly influence BK-induced Ca^{2+} oscillations. **E.** Example traces illustrating the spontaneous decrease of ATP concentration after addition of exogenous ATP to the medium above the cells. In MDCK, ATP decreased much more rapidly compared to rat brain endothelial cells (RBE4) or no cells being present. **F.** Bar chart summarizing analysis of experiments shown in E. The data indicate prominent ecto-nucleotidases activity in MDCK cells.

Since ATP release does not contribute to BK-triggered Ca^{2+} oscillations in MDCK cells, we evaluated the role of Ca^{2+} entry through hemichannels. To this purpose, we decreased the driving force for Ca^{2+} entry by lowering the extracellular Ca^{2+} concentration. The latter may result in hemichannel opening [Gomez-Hernandez et al., 2003; Thimm et al., 2005; Ye et al.,

2003], compromising the interpretation of the intended experiments. However, concentrations below ~ 0.2 mM are reported to open hemichannels [Stridh et al., 2008], thus, we applied 0.5 mM instead of the normal extracellular Ca^{2+} concentration of 1 mM. Calcein-release experiments confirmed that exposure of MDCK cells to 0.5 mM extracellular Ca^{2+} did not trigger hemichannel opening, while a further reduction of extracellular Ca^{2+} to 0.2 mM or the subnanomolar range indeed provoked the opening of hemichannels (**figure 36A,B**).

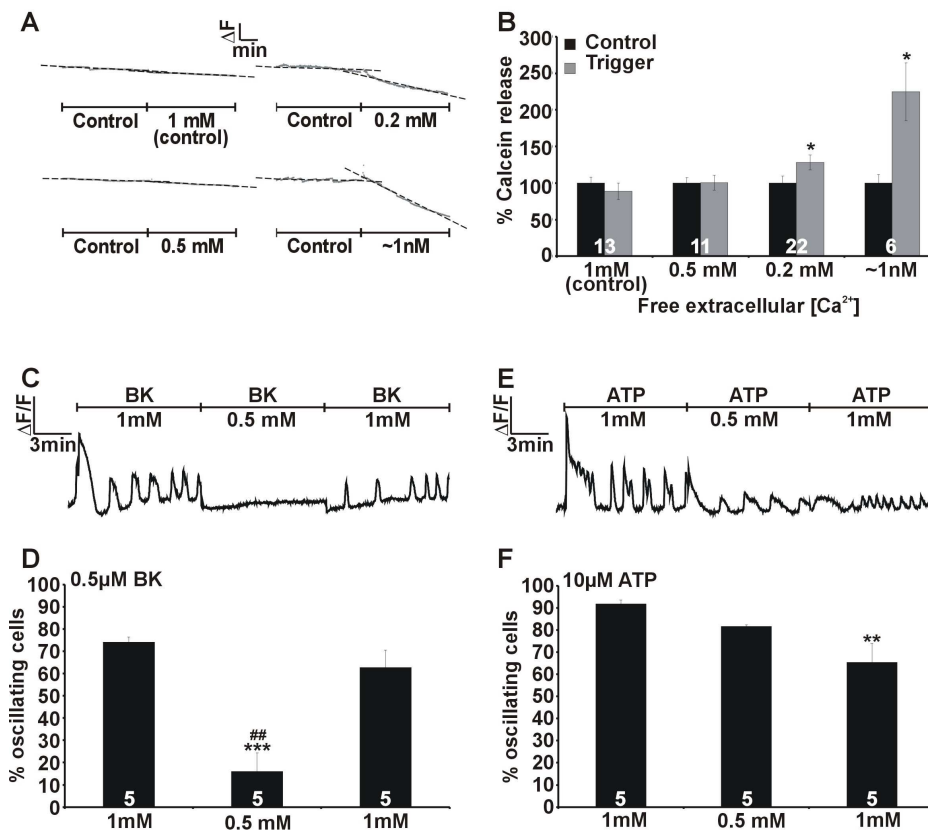


Figure 36. Depletion of extracellular Ca^{2+} inhibits BK-induced Ca^{2+} oscillations. **A.** Applying 0.5 mM Ca^{2+} solution did not trigger calcein release in MDCK cells, whereas 0.2 mM or ~ 1 nM free extracellular Ca^{2+} solutions did. **B.** Bar chart summarizing the effect of low extracellular Ca^{2+} on calcein release. * indicates a significant difference from the corresponding control. **C.** Switching to 0.5 mM extracellular Ca^{2+} during BK-induced Ca^{2+} oscillations immediately interrupted the oscillations and the effect was reversible upon switching to normal extracellular Ca^{2+} . **D.** Low extracellular Ca^{2+} (0.5 mM) strongly reduced the number of oscillating cells. **E-F.** Low extracellular Ca^{2+} (0.5 mM) had no effect on ATP-induced oscillations. * significantly different from 0.5 μM BK before Ca^{2+} depletion, # significantly different from oscillations following restoration of extracellular Ca^{2+} .

Application of 0.5 mM extracellular Ca^{2+} during BK-exposure interrupted the Ca^{2+} oscillations and re-addition of normal extracellular Ca^{2+} restored the oscillations (**figure**

36C). The number of oscillating cells was strongly reduced by 0.5 mM extracellular Ca^{2+} (**figure 36D**). Interestingly, Ca^{2+} oscillations induced by ATP decreased in amplitude but were not suppressed by switching to 0.5 mM extracellular Ca^{2+} and the percentage of oscillating cells was not significantly altered (**figure 36E,F**). Thus, BK-induced oscillations are dependent on extracellular Ca^{2+} , indicating a contribution of CCE or Ca^{2+} entry via hemichannels to the oscillation mechanism. Importantly, hemichannels did not contribute to CCE as $^{32}\text{Gap27}/^{43}\text{Gap26}$, added during re-introduction of extracellular Ca^{2+} in an experiment as shown in figure 31G, did not influence CCE after BK stimulation (data not shown).

3.3.3.4 ATP-induced Ca^{2+} oscillations are inhibited by CytC while BK-induced oscillations are inhibited by both CytC and Cx43-targeting CT9 peptide

A critical and essential factor in the generation of Ca^{2+} oscillations is the presence of positive and negative feedback actions [Hajnoczky and Thomas, 1997; Politi et al., 2006; Young et al., 2003]. In the classical scheme of InsP_3 -triggered Ca^{2+} oscillations, this feedback acts at InsP_3Rs , with low $[\text{Ca}^{2+}]_i$ stimulating ER Ca^{2+} release and higher concentrations being inhibitory [Bezprozvanny et al., 1991] (**figure 37B**). Based on dye uptake and ATP release studies, hemichannels composed of Cx32 and Cx43 have also been demonstrated to display a bell-shaped $[\text{Ca}^{2+}]_i$ -dependency for opening [De Vuyst et al., 2006; De Vuyst et al., 2009] (**figure 37D**). There is an interesting set of tools available to influence the bell-shaped Ca^{2+} -dependency of InsP_3Rs and hemichannels. Negative feedback of Ca^{2+} on InsP_3Rs can be alleviated by CytC [Boehning et al., 2003] (**figure 37A,B**). In fact, this is an important mechanism contributing to apoptotic cell death because CytC-binding to the InsP_3 receptor removes the brake on ER Ca^{2+} release, resulting in Ca^{2+} accumulation in mitochondria that amplifies CytC release in a vicious circle [Boehning et al., 2004; Pacher and Hajnoczky, 2001; Szalai et al., 1999]. Inhibiting the declining phase of InsP_3R activity is expected to disrupt oscillations because of the essential role of negative feedback as an OFF-signal in the oscillation cycle.

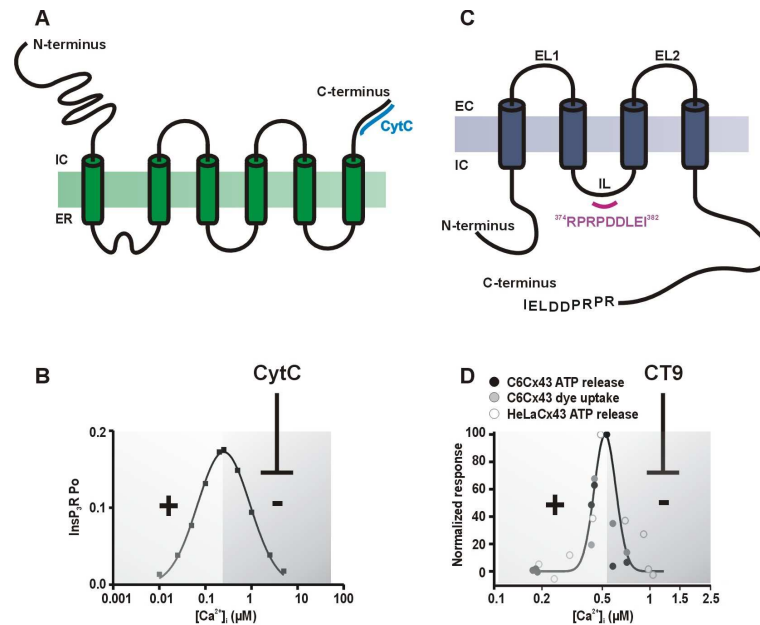


Figure 37. CytC and CT9 influence InsP_3Rs and connexin hemichannels respectively. **A.** CytC binds to the C-terminal domain of InsP_3R . **B.** InsP_3Rs have a bell-shaped $[\text{Ca}^{2+}]_i$ -dependence of the open probability (P_o) with below 250 nM concentrations potentiating InsP_3R opening and higher concentrations acting inhibitory. The bell-shaped dose response curve is derived from parameters and equations described in [Tu et al., 2005a] for InsP_3R type 1. CytC binds to InsP_3R and removes the inhibitory effects of high $[\text{Ca}^{2+}]_i$ on InsP_3R open probability. **C.** CT9 peptide is composed of the last 9 amino acids of the Cx43 C-terminus and interacts with a sequence on the intracellular loop (IL). **D.** Ca^{2+} activation of hemichannels composed of Cx43 are characterized by a bell-shaped $[\text{Ca}^{2+}]_i$ -dependence (hemichannel ATP release and dye uptake studies, derived from data in [De Vuyst et al., 2009]). CT9 peptide removes the declining phase at $[\text{Ca}^{2+}]_i$ above 500 nM [Ponsaerts et al., 2010].

We recently reported that a synthetic peptide composed of the last 10 amino acids of the C-terminal (CT) tail of Cx43 prevented the inhibitory phase of the bell-shaped $[\text{Ca}^{2+}]_i$ -dependency of hemichannel opening [Ponsaerts et al., 2010] (**figure 37C,D**). If this bell-shaped $[\text{Ca}^{2+}]_i$ -dependency contributes as a hemichannel-related mechanism in the oscillations, it is expected (similar as for the InsP_3R) that such CT peptide would inhibit the oscillations by removing the OFF-signal. We used CytC and CT9 peptide (last 9 amino acids of the Cx43 CT) to selectively interfere with the negative feedback of Ca^{2+} on InsP_3Rs and connexin hemichannels respectively, and examined their effect on the BK-induced Ca^{2+} oscillations. CytC binds to InsP_3R type 1 and 3 [Boehning et al., 2003] which are both present in MDCK cells [Colosetti et al., 2003]. CT9 and CytC are plasma membrane-impermeable and we used *in situ* electroporation to load these substances into the cells without disturbing cell function or viability [De Vuyst et al., 2008; Decrock et al., 2009]. To identify the cells loaded with these agents, we included the fluorescent markers DTR/DF and PI that have

MWs in the range of CytC (~12 kDa) and CT9 (~1 kDa) respectively. Electroporation loading allows analysis of the Ca^{2+} oscillations in loaded as well as non-loaded (control) cells (**figure 38A,F**). After applying BK (0.5 μM), cells loaded with CytC (~1 μM intracellular concentration) displayed significantly less oscillatory activity as compared to control cells in the same culture and as compared to cells loaded with vehicle-only (**figure 38B,C**). The decreased oscillations were not caused by apoptosis (triggered by CytC) as CytC exposure was short (10 min) and annexin V staining to detect early apoptotic cells was negative (data not shown). We further applied the IP3RCYT peptide that corresponds to the CytC-binding residues of the $\text{InsP}_3\text{R1}$ (located on the C-terminus), thereby preventing the binding of CytC to InsP_3R [Boehning et al., 2005; Monaco et al., 2012]. Inclusion of the IP3RCYT peptide (~5 μM intracellular concentration) prevented the CytC-mediated decrease in percentage of cells displaying Ca^{2+} oscillations (**figure 38C**). To further document the involvement of InsP_3 signaling in BK-triggered oscillations, we tested inhibition of PLC with U73122, inhibition of InsP_3Rs with xestospongin C (XeC) and pre-emptying of thapsigargin-sensitive Ca^{2+} stores; all these conditions suppressed BK-triggered oscillations, as expected (**figure 38E**). Loading cells with CytC did not affect the AUC (**figure 38D**) or peak amplitude (not shown) of the initial $[\text{Ca}^{2+}]_i$ transient triggered by BK under zero extracellular Ca^{2+} conditions, indicating no effect of CytC on the Ca^{2+} dynamics associated with the initial $[\text{Ca}^{2+}]_i$ transient triggered by BK. However, addition of thapsigargin after BK stimulation (still under zero extracellular Ca^{2+} conditions) released less Ca^{2+} from CytC-loaded cells than from control cells (**figure 38D**). Hence, Ca^{2+} store emptying was more complete with CytC and this substance thus potentiates BK-triggered ER Ca^{2+} release. This effect of CytC is in line with its expected action as a stimulator of InsP_3Rs , which is the result of a lack of InsP_3R inhibition by high $[\text{Ca}^{2+}]_i$ [Boehning et al., 2005]. Because CytC did not influence the amplitude of the $[\text{Ca}^{2+}]_i$ transient, we anticipated that the larger ER Ca^{2+} release flux was more effectively taken up by mitochondria. Accordingly, we found that the mitochondrial Ca^{2+} response (measured with RhodFF) after BK stimulation was larger in CytC loaded cells as compared to control (**figure 38D**). When cells were loaded with the Cx43-targeting CT9 peptide (last 9 amino acids of the Cx43 CT; ~100 μM intracellular concentration), BK-induced oscillations were significantly inhibited compared to non-loaded control cells in the same culture and to cells loaded with vehicle-only (**figure 38G,H**). By contrast, CT9^{Rev} peptide (reversed sequence) did not affect the number of oscillating cells (**figure 38H**).

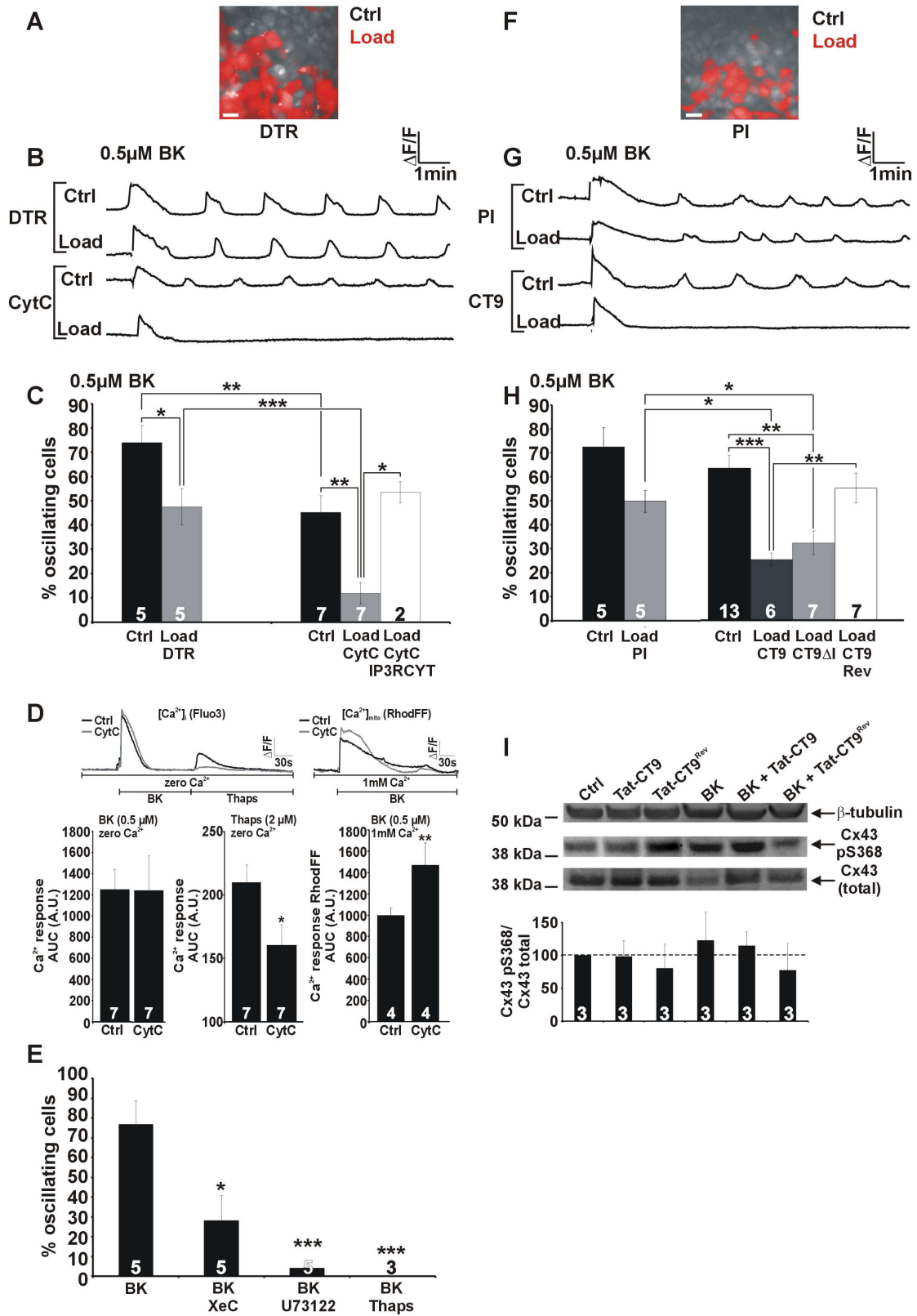


Figure 38. CytC and CT9 inhibit BK-induced Ca^{2+} oscillations. **A.** Cells were loaded with CytC or with vehicle only (DTR) by *in situ* electroporation. Loaded cells are in red ('Load') and non-loaded cells are gray ('Ctrl'). Scalebar is 25 μm . **B.** Representative traces of CytC loaded cells ('Load') and control cells ('Ctrl'). Parallel experiments were done with the cells loaded with vehicle only (DTR). **C.** Average data of experiments as illustrated in the previous panel. The loading procedure resulted, by itself, in some suppressive effect on the oscillations (percentage of oscillating cells). CytC strongly reduced the oscillations and co-loading together with IP3RCYT peptide removed the inhibitory effect of CytC. Star signs indicate a significant difference between the bars indicated. **D.** CytC did not affect the initial $[\text{Ca}^{2+}]_i$ transient triggered by 0.5 μM BK (2 min in zero Ca^{2+} medium). Subsequent addition of thapsigargin (2 μM , 3 min, in zero Ca^{2+} medium) liberated less Ca^{2+} from intracellular stores in CytC-loaded cells compared to their controls, indicating more complete store emptying. Mitochondrial Ca^{2+} uptake was larger in cells containing CytC (mitochondrial Ca^{2+} concentration, $[\text{Ca}^{2+}]_{\text{mito}}$, was measured with RhodFF). **E.** Pre-treatment with XeC (10 μM , 1 h), U73122 (10 μM , 1h) and thapsigargin (2 μM , 10 min) reduced the number of oscillating cells triggered by BK. **F.** Cells were loaded with CT9 or with vehicle only (PI, similar to panel A). **G.** Representative traces of loaded and control cells. **H.** CT9 peptide and CT9 ΔI peptide significantly reduced the percentage of oscillating cells, in contrast to CT9^{Rev}. Significant differences indicated as explained in panel C. **I.** Western blot analysis for Cx43-specific phosphorylated S368 and total levels of Cx43 in control cells and cells treated with Tat-CT or Tat-CT^{Rev} (100 μM , 30 min) in the presence or absence of BK (0.5 μM). β -tubulin was used as a loading control. The bar chart summarizes data derived from different western blots.

Cx43's last isoleucine residue is essential for interaction with the scaffolding protein ZO-1 [Giepmans and Moolenaar, 1998] and CT9 peptide is thus expected to bind to ZO-1 and prevent Cx43/ZO-1 binding [Hunter et al., 2005; Ponsaerts et al., 2010]. To investigate whether Ca^{2+} oscillations are suppressed by dissociation of the Cx43/ZO-1 complex we used a peptide similar to CT9 which is lacking the last isoleucine residue (CT9 ΔI). This peptide does not disrupt Cx43/ZO-1 interaction [Ponsaerts et al., 2010] but was equally potent in inhibiting BK-triggered Ca^{2+} oscillations (**figure 38H**). Therefore, the CT9-induced block of Ca^{2+} oscillations is not likely to be caused by altering Cx43/ZO-1 interactions.

As observed for CytC, the AUC or peak amplitude of the first $[\text{Ca}^{2+}]_i$ increase were not influenced by CT9 or CT9 ΔI , indicating that the InsP_3 production and initial InsP_3R responses were not affected by these treatments. In addition, baseline $[\text{Ca}^{2+}]_i$ was not affected by CytC or CT9: 58 ± 5 nM for CytC and 56 ± 4 nM for CT9, compared to 57 ± 5 nM for control ($n = 4$). Calcein release was not different in CT9- or CytC-loaded cells from their controls outside the loading zone (88 ± 8 % and 107 ± 31 % respectively vs. 100 % in control, $n = 3$),

indicating that CT9 and CytC by themselves do not trigger hemichannel opening. Recently, O'Quinn et al. (2011) showed that the CT9 peptide triggers a PKC-mediated phosphorylation of the Cx43 S368 consensus site in cardiomyocytes [O'Quinn et al., 2011] but we could not observe such an effect when MDCK cells were treated with cell-permeable Tat-CT9 peptide (**figure 38I**).

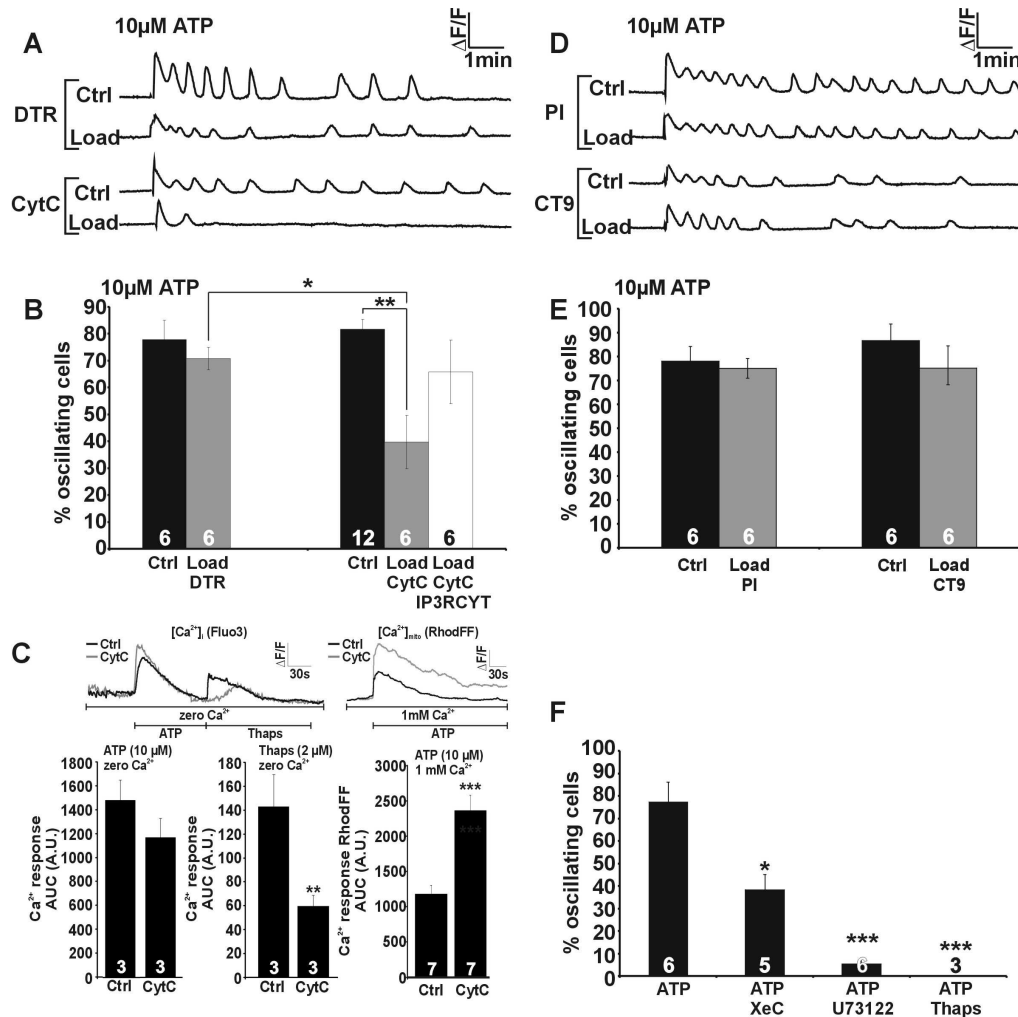


Figure 39. ATP-induced Ca²⁺ oscillations are inhibited by CytC but not by CT9 peptide. Experiments as in figure 38 but now performed with ATP as the oscillation inducing stimulus. **A.** Example traces of vehicle/CytC loaded cells and their controls. **B.** CytC inhibited the oscillatory activity and this effect was suppressed by co-loading with IP3RCYT peptide. **C.** Less Ca²⁺ was liberated from intracellular stores in the presence of CytC, indicating more complete store emptying; accordingly, mitochondrial Ca²⁺ uptake was larger. **D.** Representative traces of vehicle/CT9 loaded cells. **E.** CT9 peptide had no effect on ATP-triggered oscillations. **F.** XeC, U73122 and thapsigargin inhibited ATP-triggered oscillations. Significance symbols as defined in figure 38.

We next tested CytC and CT9 peptide on Ca^{2+} oscillations elicited by ATP (**figure 39**) and found that CytC acted inhibitory and inclusion of IP3RCYT peptide removed the inhibition. Again, Ca^{2+} store emptying was more complete and mitochondrial Ca^{2+} response was larger with CytC (**figure 39C**). Also, inhibition of PLC and InsP_3R as well as pre-emptying of thapsigargin-sensitive Ca^{2+} stores suppressed oscillatory activity (**figure 39F**). Importantly, CT9 peptide had no effect on ATP-induced Ca^{2+} oscillations. These experiments indicate that ATP-induced oscillations rely on InsP_3Rs while those induced by BK rely on both InsP_3Rs and hemichannels.

We further tested whether hemichannels were sufficient as a mechanism to obtain oscillations without a contribution of InsP_3Rs . Hemichannel opening can be triggered by $[\text{Ca}^{2+}]_i$ elevation without increasing InsP_3 and thus without activating InsP_3Rs and InsP_3R -based oscillations. $[\text{Ca}^{2+}]_i$ elevation triggered by photolytic release of Ca^{2+} did not trigger Ca^{2+} oscillations ($n = 4$), indicating that hemichannels are not sufficient as an oscillatory mechanism and InsP_3Rs are the dominant mechanism leading to oscillations.

3.3.3.5 BK triggers TEER changes that can be inhibited by BAPTA-AM and carbenoxolone

MDCK cells are derived from the kidney's collecting duct epithelium that is characterized by an extremely tight barrier, with TEER values exceeding $1000 \Omega \cdot \text{cm}^2$ like in the BBB [Butt et al., 1990; Garberg et al., 2005]. MDCK cells are therefore considered to be an appropriate cell model to study effects on TEER. TEER changes were measured in MDCK cells, grown to confluence on collagen-coated filter inserts. After 2-3 weeks, when baseline TEER had stabilized, culture medium was removed and filters were rinsed with HBSS-Hepes. At time points 0, 5, 10, 15, 30, 45 and 60 min TEER was measured using two Ag/AgCl electrodes positioned on either side of the filter insert and connected to a Millicell-ERS Volt-Ohm meter (Millipore). TEER values are the result of the following formula: $\text{TEER} = (\text{TEER}_a - \text{TEER}_b) \times A$, whereby TEER_a is the measured TEER and TEER_b is the TEER measured over a coated filter without cells (blank). 'A' is the surface of the filter insert (4.2 cm^2). The time constant of the exponential TEER decay was used as a parameter to express effects in TEER.

Preliminary data indicate that BK induces a decrease in TEER across a monolayer of MDCK cells. Like BK-triggered changes in endothelial permeability (see 3.1), this decrease in TEER could be reduced by preloading cells with BAPTA-AM or by exposing the cells to the connexin channel blocker Cbx (**figure 40**).

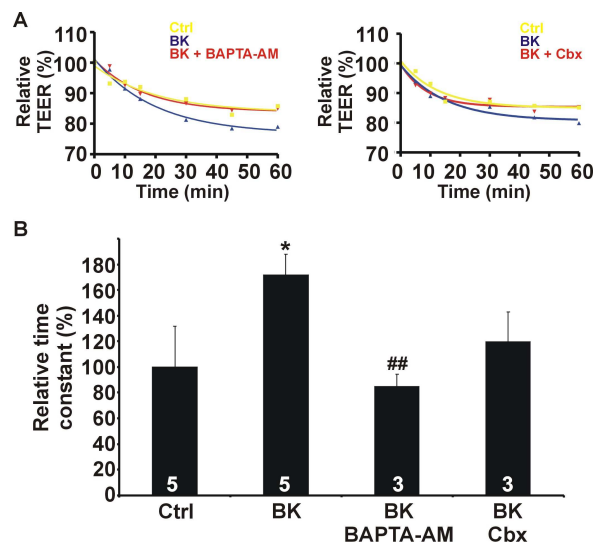


Figure 40. Effects of BK on TEER in a MDCK cell monolayer. (A) Relative TEER changes in MDCK cells over time, triggered by BK (0.5 μM). TEER values at the start (0 min) are $305.5 \pm 20.9 \Omega \cdot \text{cm}^2$. (B) Pre-loading cells with BAPTA-AM (5 μM , 1h) inhibited the decrease in TEER. Exposure to the connexin channel blocker Cbx (25 μM , 30 min pre-incubation) reduced the TEER decrease brought about by BK. Stars signs: significance compared to Ctrl; number signs: significance compared to BK.

3.3.4 DISCUSSION

The present data demonstrate that BK- and ATP-induced Ca^{2+} oscillations display distinct properties in MDCK cells. Oscillations induced by BK (i) showed a flat concentration dependence of frequency and percentage of responding cells, (ii) were inhibited by Cbx, Gap peptides and Cx43 gene silencing, (iii) disappeared when extracellular Ca^{2+} was lowered and (iv) were inhibited by CytC and CT9 peptide. By contrast, ATP-induced oscillations (i) showed a bell-shaped ATP concentration dependency, (ii) were not influenced by Cbx, Gap peptides or Cx43 silencing, (iii) were not abolished by lowering extracellular Ca^{2+} and (iv) were inhibited by CytC but not by CT9 peptide. Several data point to the involvement of hemichannels: (i) BK potentiated calcein dye release while ATP did not, (ii) BK-triggered calcein release was rapidly (~ 1 min) inhibited by Gap peptides while 60 min incubation with these peptides had no effect on dye coupling and (iii) BK-induced Ca^{2+} oscillations were

inhibited by CT9 peptide that removes the Ca^{2+} -inhibition of Cx43 hemichannels but not by CT9^{rev} peptide. The fact that the oscillations were not synchronized between cells furthermore argues against a contribution of gap junctions.

ATP-induced Ca^{2+} oscillations displayed a bell-shaped concentration dependency. An S-shaped concentration dependency is more typical [Bergner and Sanderson, 2002; Berridge et al., 1988; Parker and Ivorra, 1990; Tai et al., 2001] but it is well known that oscillations can only occur in a limited range of InsP_3 concentrations so the disappearance of the oscillations at high ATP concentration may well result from too high an intracellular InsP_3 level [Davis et al., 1999; Rottingen et al., 1997; Sneyd et al., 2006]. BK-induced oscillations had a flat concentration dependency, a finding also reported by others [Carter et al., 1991; De Blasio et al., 2004a; Sage et al., 1989]. Despite the importance of encoding the strength of agonist stimulation in the frequency of oscillations, it is not uncommon that spiking frequencies are independent of agonist concentration. According to the 'dynamic desensitization mechanism', that occurs upon stimulation of mGluR5 [Nash et al., 2002] or the M_3 muscarinic receptor [Bird et al., 1993], elevated levels of $[\text{Ca}^{2+}]_i$ and DAG activate PKC that phosphorylates and desensitizes the receptor, thereby limiting InsP_3 production and stabilizing the oscillation frequency. BK does activate PKC [Boarder and Challiss, 1992] and PKC phosphorylation consensus sites in BK receptors have been identified [Willars et al., 1999], but further studies are required to determine whether dynamic desensitization is involved here.

Ca^{2+} oscillations were previously found to be inhibited by octanol, palmitoleic acid and $18\alpha\text{GA}$ [Kawano et al., 2006], by antibodies directed against connexins and by Gap peptides [De Bock et al., 2011; Verma et al., 2009], all known blockers of connexin channels. Conversely, stimulating hemichannel responses with the anti-arrhythmic peptide AAP10 [Clarke et al., 2009] has been reported to induce Ca^{2+} oscillations [Zhang et al., 2007]. Ca^{2+} oscillations triggered by BK were inhibited by $^{32}\text{Gap}27/^{43}\text{Gap}26$ peptides within 1 min, as reported by others [Romanov et al., 2007], and the Gap peptides did not influence the initial $[\text{Ca}^{2+}]_i$ transient triggered by BK. The latter indicates that the InsP_3 -triggered Ca^{2+} release was not influenced by the Gap peptides, which is in accordance with our observation that these peptides do not influence $[\text{Ca}^{2+}]_i$ transients triggered by photolytic release of InsP_3 [De Bock et al., 2011]. BK potentiated calcein dye efflux from MDCK cells, indicating hemichannel opening. This opening is likely caused by the elevation of $[\text{Ca}^{2+}]_i$ to values in the 500 nM range that are appropriate for activation of Cx32 and Cx43 hemichannels [De Vuyst et al., 2006; De Vuyst et al., 2009]. BK-triggered calcein efflux was rapidly inhibited by the Gap

peptides, in line with previous experimental work [De Bock et al., 2011] and complemented by recent single-channel electrophysiological studies that indicate Gap peptide-inhibition of unitary currents through Cx43 hemichannels with a time constant in the order of minutes (unpublished observation Wang N. and Leybaert L.). The contribution of hemichannel opening to the Ca^{2+} oscillations appeared to be related to Ca^{2+} entry, as indicated by the low extracellular Ca^{2+} experiments, and was not related to hemichannel ATP release. We cannot exclude hemichannel ATP release, but our results indicate rapid ATP degradation at the surface of MDCK cells, lowering its concentration below the threshold for purinergic receptor activation. A role for hemichannels as a non-selective Ca^{2+} -entry route has been postulated under varying circumstances including alkalinization (Cx43, [Schalper et al., 2010]) and metabolic inhibition (Cx32, [Sanchez et al., 2009] and Cx43, [Shintani-Ishida et al., 2007]). Ca^{2+} entry contributes to reloading of ER Ca^{2+} stores and the entry rate can influence the inter-spike interval and thus the oscillation frequency [Shuttleworth, 1999]. At low agonist concentrations, hardly any Ca^{2+} is lost from the ER [Martin and Shuttleworth, 1994] and Ca^{2+} entry may, under those circumstances, act to sensitize the InsP_3R to produce a regenerative Ca^{2+} spike [Shuttleworth and Thompson, 1996] or exert positive feedback on PLC-mediated InsP_3 production [Meyer and Stryer, 1988; Thore et al., 2004]. The present study shows that Ca^{2+} entry, related to CCE or as a consequence of hemichannel opening (or a combination of both), is more prominent with BK than with ATP as a stimulus.

Ca^{2+} -mediated feedback actions residing at different levels of the Ca^{2+} -signaling cascade (GPCR, InsP_3R or PLC), lie at the basis of Ca^{2+} oscillations [Jones et al., 2008; Nash et al., 2001; Reetz and Reiser, 1996; Shuttleworth and Mignen, 2003; Sneyd et al., 1995; Thomas et al. 1996; Thore et al., 2004]. Ca^{2+} activation of hemichannel-dye uptake and ATP release is, like the InsP_3R open probability, characterized by a bell-shaped $[\text{Ca}^{2+}]_i$ -response curve ([De Vuyst et al., 2006; De Vuyst et al., 2009] and figure 37D), and recent evidence shows that unitary currents through Cx43 hemichannels display a similar bimodal $[\text{Ca}^{2+}]_i$ -dependency (unpublished observation Wang N. and Leybaert L.). This bimodal $[\text{Ca}^{2+}]_i$ -dependence may introduce additional positive and negative feedback that contributes to the Ca^{2+} oscillations. Thus, we used CT9 peptide that overcomes Cx43 hemichannel inhibition at high $[\text{Ca}^{2+}]_i$ without influencing hemichannel activity at lower $[\text{Ca}^{2+}]_i$ [Ponsaerts et al., 2010]. Ca^{2+} -dependent activation of hemichannels has been proposed to involve binding of the C-terminal tail to the intracellular loop of Cx43. Conversely, hemichannel inhibition at high $[\text{Ca}^{2+}]_i$ is mediated by Ca^{2+} -activation of actomyosin that disrupts the loop/tail interaction. Addition of

CT9 peptide will substitute for the disrupted C-terminal tail binding, by interacting with the cytoplasmic loop and thereby preventing high $[Ca^{2+}]_i$ inhibition of hemichannels [Ponsaerts et al., 2010]. Here, we show that CT9 but not the reversed sequence, inhibits Ca^{2+} oscillations induced by BK. CT9 inhibition of BK-induced oscillations is mediated by an effect on Cx43 but not on Cx32. Unfortunately, a CT9 analogue for Cx32 is not yet available. Both Cx43 and Cx32 appear to be essential in the BK-triggered Ca^{2+} oscillations, as interfering with each of these connexins individually prevented the oscillations. This is in line with the fact that hemichannels composed of Cx32 have, like those composed of Cx43, also a bell-shaped $[Ca^{2+}]_i$ dependence.

Mathematical modeling has demonstrated that positive and negative feedback on voltage-gated Ca^{2+} entry is by itself sufficient to generate Ca^{2+} oscillations [Fioretti et al., 2005]. In contrast, the present experiments show that a forced $[Ca^{2+}]_i$ change does not induce Ca^{2+} oscillations, indicating that the Ca^{2+} -sensitive and Ca^{2+} -entry mediating hemichannels are not sufficient as an oscillation mechanism. Consistent with this is the observation that BK-triggered Ca^{2+} oscillations largely rely on $InsP_3Rs$ (**figure 38**). CytC removes $InsP_3R$ inactivation at high $[Ca^{2+}]_i$, giving increased ER Ca^{2+} release leading to a gradually increasing $[Ca^{2+}]_i$, mitochondrial Ca^{2+} overload and apoptosis [Boehning et al., 2003]. We did not observe $[Ca^{2+}]_i$ elevation following CytC application but this is probably related to the relatively short (10 min) time window used to record Ca^{2+} oscillations. Additionally, high $[Ca^{2+}]_i$ inhibition of $InsP_3Rs$ is not the only OFF mechanism mediating $[Ca^{2+}]_i$ restoration to resting level: Ca^{2+} pumps like SERCA and PMCA, which are not affected by CytC [Boehning et al., 2003], will ensure proper maintenance of normal $[Ca^{2+}]_i$ within the 10 min time frame of our recordings. Importantly, our data are the first demonstration in intact cells that CytC promotes ER Ca^{2+} release, supporting its proposed action as an antagonist of high $[Ca^{2+}]_i$ inhibition of $InsP_3Rs$ [Boehning et al., 2005]. CytC also stimulated mitochondrial Ca^{2+} uptake but this may be a direct consequence of the increased ER Ca^{2+} release.

Interestingly, ATP-induced oscillations were also inhibited by CytC but not by CT9 peptide, indicating that these oscillations thrive exclusively on $InsP_3$ -based mechanisms. Thus, BK-triggered oscillations are based on $InsP_3Rs$ with an additional hemichannel component. Because hemichannels can be activated by moderate (< 500 nM) $[Ca^{2+}]_i$ elevation, we hypothesize these channels open with each Ca^{2+} spike and contribute with Ca^{2+} entry during the rising phase. When the spike amplitude rises above 500 nM, hemichannels close again and

contribute with an OFF mechanism that adds to the OFF mechanism of InsP₃R channels. The fact that hemichannels are by themselves not sufficient to mediate oscillations probably results from a slower kinetics for opening than for closing. Previous work has indeed suggested that hemichannel activation by Ca²⁺ is characterized by several intermediate signaling steps pointing to slow activation kinetics [De Vuyst et al., 2009]. A point of notice is that the duration of the primary Ca²⁺ peak was different for both triggers: ~40 sec for 0.5 μM BK and 15 sec for 10 μM ATP (see example traces in figure 31). Preliminary modeling using the activation kinetics of hemichannel opening presented in [De Vuyst et al., 2006; De Vuyst et al., 2009] indeed indicates that a [Ca²⁺]_i rise of 40 sec (BK) can trigger the opening of twice as much hemichannels compared to a peak that lasts only 15 sec (ATP). Additionally, the Ca²⁺ spikes of BK-triggered oscillations were generally of longer duration than those triggered by ATP (see example traces in figure 31) making it possible that these Ca²⁺ transients were more efficient to induce hemichannel opening. We speculate that the more prominent contribution of CCE with BK stimulation is more effective in triggering hemichannel opening because it occurs more localized and in close proximity of the hemichannels in the plasma membrane.

Our experiments indicate that hemichannels actively contribute to BK-induced Ca²⁺ oscillations by providing a Ca²⁺-entry pathway characterized by a bimodal [Ca²⁺]_i-dependency. This contribution is crucial as inhibition of this pathway blocks the oscillations. Several compounds like the InsP₃R inhibitor 2-APB used to explore the mechanism of Ca²⁺ oscillations [Maruyama et al., 1997] are known to inhibit connexin hemichannels [Tao and Harris, 2007]. Additionally, the non-selective Ca²⁺ channel blocker La³⁺ has frequently been used to investigate Ca²⁺ entry during Ca²⁺ oscillations, also in cells that express connexins [Estrada et al., 2005; Hu et al., 2009; Pizzo et al., 2001], but these trivalent ions also inhibit hemichannels [Braet et al., 2003a; Contreras et al., 2003; Retamal et al., 2007a]. In conclusion, connexin hemichannels may contribute to Ca²⁺ oscillations in connexin expressing cells. Interestingly, connexin expressing cells may also display hemichannel-independent Ca²⁺ oscillations, as exemplified here with ATP. This differential contribution of hemichannels to Ca²⁺ oscillations may result in distinct downstream response patterns to this fundamental cell signal, as recently observed in brain endothelial cells [De Bock et al., 2011].

Chapter 4

General discussion & perspectives

4.1 CONNEXIN HEMICHANNELS CONTRIBUTE TO BK-TRIGGERED Ca^{2+} OSCILLATIONS

Ca^{2+} is an allround messenger controlling a large variety of basic cellular functions that include fertilization, gene expression, cell differentiation, exocytosis, muscle contraction, cell survival and cell death [Case et al., 2007; Dupont et al., 2007]. Ca^{2+} ions are released into the cytosol from intracellular Ca^{2+} storage organelles like the ER, while at the same time extracellular Ca^{2+} ions enter the cytosol through plasma membrane channels altogether creating a ' Ca^{2+} signal'. Ca^{2+} signals are usually not mere one-time events but are typified by a spatiotemporal organization with the temporal aspect referring to the repetitive character of Ca^{2+} oscillations. Oscillations are believed to result from positive and negative feedback actions of Ca^{2+} on InsP_3R -mediated Ca^{2+} release [Bezprozvanny et al., 1991; Hajnoczky and Thomas, 1997] and additional feedback at higher levels such as InsP_3 metabolism and GPCR activity [Nash et al., 2001; Politi et al., 2006; Young et al., 2003]. Evidence is also available that Ca^{2+} entry may further contribute to shaping the oscillatory signal [Jones et al., 2008; Nash et al., 2001; Reetz and Reiser, 1996; Shuttleworth and Mignen, 2003; Sneyd et al., 1995; Thomas et al., 1996; Thore et al., 2004].

Several studies have commented on the pivotal role of $[\text{Ca}^{2+}]_i$ in the regulation of connexin hemichannels [Braet et al., 2003b; Cotrina et al., 1998b; Pearson et al., 2005; Schalper et al., 2008]. $[\text{Ca}^{2+}]_i$ influences connexin hemichannels in a bimodal manner with modest $[\text{Ca}^{2+}]_i$ increases (< 500 nM) promoting and higher $[\text{Ca}^{2+}]_i$ preventing hemichannel opening [De Vuyst et al., 2006; De Vuyst et al., 2009; Ponsaerts et al., 2010]. The experimental work performed in this thesis indicates that $[\text{Ca}^{2+}]_i$ regulation of connexin hemichannel opening may influence Ca^{2+} oscillations. We started this work based on observations of others that interfering with connexin channels influences Ca^{2+} oscillations. Mouse glial cells for instance display spontaneous Ca^{2+} oscillations that disappear when Cx43 gene expression is silenced. Treatment with apyrase or suramin had the same effect as Cx43 knockout, indicating that ATP likely controls the oscillations in an autocrine manner [Scemes et al., 2003]. Kawano et al. (2006) reported that $18\alpha\text{GA}$ and octanol inhibit spontaneous Ca^{2+} oscillations in human mesenchymal stem cells. This work further argues in favor of hemichannel opening, diffusive ATP release and autocrine actions on plasma membrane P2Y_1 receptors [Kawano et al., 2006]. Accordingly, spontaneous Ca^{2+} oscillations in neural precursor cells depend on

autocrine purinergic signaling and are prevented by the gap junction blockers Cbx and meclofenamic acid and by the hemichannel blockers La^{3+} and Gd^{3+} [Liu et al., 2010b]. Connexin mimetic peptides have also been shown to inhibit both spontaneous and agonist-triggered Ca^{2+} oscillations in connexin-expressing HeLa cells and cardiomyocytes [Verma et al., 2009]. The authors found that peptide inhibition of Ca^{2+} oscillations is mediated by reducing Ca^{2+} entry via hemichannels thereby affecting ER Ca^{2+} release. The same was observed when using antibodies directed at Cx43 ELs. Inhibition of Ca^{2+} entry by connexin channel blockers was also suggested to be responsible for elimination of ATP-triggered oscillations in uterine artery endothelial cells [Yi et al., 2010]. Recently, Berra-Romani et al. (2011) have proposed a role for connexin hemichannels in Ca^{2+} oscillations that are initiated by endothelial cell injury. These authors suggest that hemichannel opening causes not only entry of Ca^{2+} but also of Na^+ . This will stimulate the $\text{Na}^+/\text{Ca}^{2+}$ exchanger to work in the reversed mode, thereby contributing to Ca^{2+} entry and Ca^{2+} oscillations [Berra-Romani et al., 2011]. Finally, stimulating hemichannel responses with the anti-arrhythmic peptide AAP10 [Clarke et al., 2009] enhances Ca^{2+} oscillations in ventricular myocytes [Zhang et al., 2007], and aconitine, a toxic alkaloid from the plant *Aconitium napellus* that induces dephosphorylation of Cx43, led to altered Ca^{2+} oscillation patterns [Zhang et al., 2007].

Our work in RBE4 brain endothelial cells and MDCK renal epithelial cells shows that Ca^{2+} oscillations triggered by BK were suppressed by the connexin channel inhibitor carbenoxolone, connexin silencing or short-term (1-60 min) exposure to connexin mimetic peptides. Gap junction dye coupling was not affected by this short-term exposure to connexin mimetic peptide, pointing to inhibition of connexin hemichannels. Furthermore, BK promoted connexin hemichannel opening as concluded from dye release/uptake assays, and this likely results from Ca^{2+} release out of InsP_3 -sensitive stores [Easton and Abbott, 2002; Jan et al., 1998] that results in $[\text{Ca}^{2+}]_i$ elevation in the 500 nM range which is optimal for Cx32 and Cx43 hemichannel opening [De Vuyst et al., 2006; De Vuyst et al., 2009]. Thus, work with the Gap peptides reveals a role for connexin hemichannel opening in the Ca^{2+} oscillation mechanism but does not allow drawing any conclusions on the role of negative feedback of Ca^{2+} on hemichannels. We recently reported that a peptide mimicking the last 9 amino acids of the Cx43 C-terminal domain (CT9) removes the inhibition of hemichannels by high $[\text{Ca}^{2+}]_i$, resulting in hemichannel opening over a wide range (up to 1 μM) of physiological $[\text{Ca}^{2+}]_i$ [Ponsaerts et al., 2010]. The CT9 peptide strongly suppressed BK-triggered oscillations in MDCK cells, demonstrating that Ca^{2+} oscillations are not only influenced by hemichannel

opening but also by hemichannel closure with high $[Ca^{2+}]_i$. In fact, the bimodal regulation of hemichannel opening by $[Ca^{2+}]_i$ is highly similar to the dependency of $InsP_3Rs$ on $[Ca^{2+}]_i$ and we wondered whether cyclical opening and closing of hemichannels would be sufficient to cause Ca^{2+} oscillations in its own right. To test this hypothesis, hemichannel opening was triggered by photolytically releasing Ca^{2+} from a caged precursor, resulting in a $[Ca^{2+}]_i$ elevation that is independent of $InsP_3Rs$. However, $[Ca^{2+}]_i$ elevations induced in this way were not able to trigger Ca^{2+} oscillations, indicating that connexin hemichannels are not sufficient as a mechanism to drive Ca^{2+} oscillations. Oscillations elicited by BK were also abolished by inhibition of PLC and $InsP_3R$, by pre-emptying of thapsigargin-sensitive Ca^{2+} stores and by CytC, a molecule that interrupts high $[Ca^{2+}]_i$ inhibition of the $InsP_3R$ [Boehning et al., 2003]. Altogether this indicates that activation of $InsP_3R$ -mediated Ca^{2+} release is the dominant mechanism leading to BK-triggered oscillations and that hemichannels add an extra level of modulation. Similar conclusions on the fundamental role of $InsP_3Rs$ were drawn from spontaneous hemichannel-dependent Ca^{2+} oscillations in neural precursor cells [Liu et al., 2010b] and endothelial cells [Berra-Romani et al., 2011].

In a next step we sought to further define the contribution of hemichannels to the Ca^{2+} oscillation machinery. Connexin hemichannels form a bidirectional passageway across the plasma membrane allowing both Ca^{2+} entry and release of messenger molecules such as ATP, and either of these could be involved in the Ca^{2+} oscillation mechanism. Inspired by the fact that intercellular Ca^{2+} wave propagation in RBE4 cells depends on hemichannel-mediated ATP release [Braet et al., 2003b; Leybaert et al., 2003; Vandamme et al., 2004] we investigated the role of extracellular ATP in the Ca^{2+} oscillations. In RBE4 cells, BK-triggered oscillations almost completely disappeared when extracellular ATP was degraded by apyrases or when purinoceptor activation was prevented. The contribution of purinergic signaling in BK-triggered oscillations was likely to be autocrine because a paracrine contribution would be associated with time- or phase-related $[Ca^{2+}]_i$ changes in surrounding cells which was not observed. Oppositely, in MDCK cells, there was no contribution of purinergic signaling which created an opportunity to investigate the contribution of Ca^{2+} entry via hemichannels, under conditions not obscured by additional hemichannel-mediated ATP release. BK-triggered Ca^{2+} oscillations were interrupted by low (0.5 mM) extracellular Ca^{2+} conditions, indicating that Ca^{2+} entry supports the Ca^{2+} oscillations. Connexin hemichannels have been reported to act as a non-selective Ca^{2+} entry route activated by alkalization [Schalper et al., 2010], metabolic inhibition [Sanchez et al., 2009; Shintani-Ishida et al.,

2007], or injury to endothelial cells from excised rat aorta [Berra-Romani et al., 2008]. We cannot fully exclude a contribution of ATP release in experiments with MDCK cells, but our results indicate a strong and rapid ATP degradation at the surface of these cells that was not observed in RBE4 cells. Such degradation would reduce extracellular ATP levels below the threshold required for purinergic receptor activation. Adenosine, ATP's main degradation product, didn't contribute to the oscillations either. The results obtained with MDCK cells indicate that, by inference, connexin hemichannel Ca^{2+} entry may also contribute to Ca^{2+} oscillations in RBE4 cells, as a mechanism that adds to hemichannel-mediated ATP release. Ca^{2+} entry contributes to replenishment of ER Ca^{2+} (CCE) whereby the entry rate can influence the inter-spike interval and thus the oscillation frequency [Shuttleworth, 1999]. However, at low agonist concentrations, hardly any Ca^{2+} is lost from the ER and CCE is not observed [Martin and Shuttleworth, 1994]. We further indicate that connexin hemichannels contribute to the Ca^{2+} oscillation mechanism; yet they do not contribute to CCE. Under those circumstances, Ca^{2+} entry may act to sensitize the InsP_3R to produce a regenerative Ca^{2+} spike [Shuttleworth and Thompson, 1996] or exert positive feedback on InsP_3 production [Meyer and Stryer, 1988; Thore et al., 2004]. **Figure 41** summarizes the contribution of connexin hemichannels to the Ca^{2+} oscillations as a supplemental mechanism to the InsP_3R -based oscillations (see figures 12 and 13).

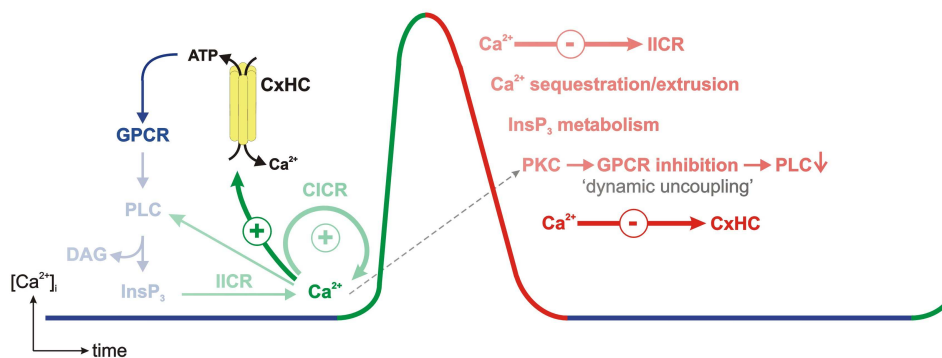


Figure 41. Diagram summarizing the proposed contribution of connexin hemichannels to InsP_3R -based Ca^{2+} oscillations. Connexin hemichannel opening by moderate $[\text{Ca}^{2+}]_i$ elevation results in Ca^{2+} entry, accompanied by ATP release (positive feedback). ATP acts on $\text{G}\alpha_q$ protein coupled receptors at the cell surface thereby enhancing InsP_3 production, while Ca^{2+} entry via hemichannels contributes to the rising phase of the Ca^{2+} transient. When $[\text{Ca}^{2+}]_i$ rises above 500 nM, connexin hemichannels close (negative feedback) and this contributes to restoration of resting $[\text{Ca}^{2+}]_i$. The system is then ready for a subsequent Ca^{2+} spike cycle. For an explanation of the shaded mechanisms we refer to figure 12 and 13.

Importantly, we show that not all agonist-induced oscillations involve connexin hemichannels. ATP-triggered oscillations were solely dependent on InsP₃-based mechanisms as they persisted after addition of Cbx, connexin mimetic peptides, CT9 peptide or Cx43 silencing, and they continued in low (0.5 mM) extracellular Ca²⁺ conditions. In line with this, ATP did not act as a trigger for connexin hemichannel opening as indicated by the absence of effect on dye uptake/release. If [Ca²⁺]_i changes authorize both connexin hemichannel opening and Ca²⁺ oscillations triggered by BK, the questions rises as to why ATP is not able to recruit hemichannels in the process of Ca²⁺ oscillations? The different nature of the initial Ca²⁺ transient triggered by both agonists may lie at the basis of these differences. The amplitudes of the initial Ca²⁺ transients elicited by ATP (10 μM) and BK (0.5 μM) were not significantly different, but the duration of the transients varied considerably (~40 sec for BK and ~15 sec for ATP in MDCK cells). For ATP, the initial Ca²⁺ transient was essentially dependent on InsP₃-triggered Ca²⁺ release with only a minor contribution of Ca²⁺ entry. For BK, the primary Ca²⁺ transient was more dependent on extracellular Ca²⁺ as a consequence of a larger contribution of CCE as compared to ATP. It is possible that the longer duration is more effective in triggering hemichannel opening. In addition, the localization of the Ca²⁺ signal may be decisive for hemichannel activation. BK might be more effective in triggering opening because it triggers CCE that occurs more close to the plasma membrane. For gap junctions, regulation by CCE has been shown to be more effective than a global [Ca²⁺]_i increase [Dakin et al., 2005], but for hemichannels this is mere speculation and further proof is needed. Thus, we hypothesize that hemichannels open in response to CCE, which is more prominent for BK than for ATP. In the following two sections we will discuss the different effects of ATP and BK on endothelial permeability as well as why connexin hemichannel involvement in BK-triggered Ca²⁺ oscillations is more likely to influence endothelial permeability.

4.2 CA²⁺ DYNAMICS MODULATE BBB PERMEABILITY IN CONCERT WITH OTHER SIGNALING CASCADES

The presence of oscillatory and wave activity in brain microvascular endothelia (see 1.4.3.1) indicates that the essential components of the cellular and intercellular Ca²⁺ signaling toolbox are present in these cells; however, to the best of our knowledge, the spatiotemporal organization of Ca²⁺ signals has not yet been studied with respect to their effect on BBB

function. Work with MDCK cells has suggested that BK induces synchronized Ca^{2+} oscillations as well as rhythmic changes in TEER that exhibited the same periodicity. Inhibition of gap junctions resulted in a decreased synchrony of oscillations and suppressed changes in resistance. Thus, cyclical changes in resistance are likely to result directly from coordinated Ca^{2+} signals [De Blasio et al., 2004b]. At the start of this work, this was the first and only evidence available for a linkage between Ca^{2+} oscillations and the permeability of cell monolayers. In 3.1 and 3.2 we provided evidence for a relation between Ca^{2+} dynamics and endothelial permeability, and explored the molecular pathways leading to a loss of endothelial barrier function.

The effects of BK on the immortalized RBE4 cells in terms of Ca^{2+} dynamics have been outlined in section 4.1. In addition, BK- and ATP-triggered Ca^{2+} oscillations were also observed in long term cultivated primary endothelial cells. Importantly, Ca^{2+} oscillatory activity in these cells appeared to be dependent on the culture conditions: oscillations were only evident when cells were grown in co-culture with astrocytes, although the latter were not present during the actual $[\text{Ca}^{2+}]_i$ measurement. This observation suggests that astrocytes are required for differentiation of the Ca^{2+} signaling toolkit in the BBB endothelium, but presently, the signals mediating this effect are not known. The BK-triggered Ca^{2+} oscillations in BBB endothelium were associated with an increase of *in vitro*- and *in vivo*-measured endothelial permeability to tracer molecules. Furthermore, with both approaches, the permeability increase was counteracted by short incubation with Gap27. This peptide mimicks a well-conserved sequence on EL2 of Cx37 and Cx43, the two connexins expressed in BCEC.

ATP, which can be released from various cell types in the region of the vessel wall (nerve fibers, astrocytes, platelets or endothelial cells) [Abbott, 2000; Bodin and Burnstock, 1996], has been shown to increase endothelial permeability in different vascular beds [McClenahan et al., 2009; Pocock et al., 2000; Tanaka et al., 2006; Tanaka et al., 2005; Victorino et al., 2004], including BBB endothelium [Abbott, 2000; Hurst and Clark, 1998; Olesen and Crone, 1986]. However, in BCEC monolayers, ATP did not increase endothelial permeability despite triggering Ca^{2+} oscillations. In fact, ATP has been shown to enhance endothelial barrier function notwithstanding the associated $[\text{Ca}^{2+}]_i$ elevation. The purinoceptor agonists ATP, ADP and UTP all increase $[\text{Ca}^{2+}]_i$, yet they reduce endothelial permeability to albumin in porcine aortic endothelial cells in a Ca^{2+} -independent manner. ATP-stimulation also increased

intracellular cAMP and cGMP levels, but these were not responsible for the observed reduction in permeability [Noll et al., 1999]. ATP also resulted in MLCP activation which overruled the Ca^{2+} -dependent activation of MLCK [Gunduz et al., 2003; Klingenberg et al., 2004]. Activation of PLC contributed to the permeability decrease, but the signaling cascade was not explored [Noll et al., 1999]. In agreement, Kolosova et al. (2005) show that activation of $\text{G}\alpha_q$ -coupled receptors can lead to MLCP activation through yet unknown signaling steps [Kolosova et al., 2005]. Opposed to observations made in aortic endothelium, in corneal microvascular endothelial cells MLCP activation following ATP exposure was mediated by a cAMP-activated signaling cascade [Satpathy et al., 2005] and according to Jacobson et al. (2006), ATP-mediated barrier enhancement of pulmonary artery endothelial cells is due to activation of the small GTPase Rac [Jacobson et al., 2006] which is dependent on $[\text{Ca}^{2+}]_i$ [Price et al., 2003]. Rac activation leads to a peripheral translocation of the actin-binding protein cortactin causing relaxation of the actin cytoskeleton [Jacobson et al., 2006]. Alternatively, cAMP-activated PKA phosphorylates VASP, resulting in cytoskeletal relaxation. A tightening of endothelial junctions through rearrangement of ZO-1 and VE-cadherin was observed as well [Kolosova et al., 2005]. Finally, ATP reduces LPS-induced vascular leakage, providing protection against acute lung injury [Kolosova et al., 2008]. Thus, ATP triggers a $[\text{Ca}^{2+}]_i$ elevation but also activates several other signaling pathways that lead to a reduction rather than an increase of endothelial permeability.

Based on expression records and pharmacological profiles, BBB endothelial cells have been shown to express a rather large repertoire of purine receptors including P2Y_1 , P2Y_2 , P2Y_6 , P2Y_{11} and P2Y_{12} as well as P2X_4 , P2X_5 and P2X_7 [Anwar et al., 1999; Bintig et al., 2011; Simon et al., 2002; Simon et al., 2001; Webb et al., 1996]. In addition, a P2Y_1 -like receptor that stimulates the release of Ca^{2+} from thapsigargin-sensitive stores in an InsP_3 -independent manner has been reported in rat brain endothelial cells [Vigne et al., 1994]; but no further information is available on how activation of this receptor leads to Ca^{2+} release. The set of purinoceptors present on the endothelial membrane seems to be dictated by the species and can vary between immortalized and freshly prepared cells [Bintig et al., 2011; Feolde et al., 1995]. In addition, the signal transduction pathways that are activated by these receptors depend on the cellular background [Simon et al., 2002]. Generally, P2Y_1 , P2Y_2 , P2Y_6 , and P2Y_{11} all activate the $\text{G}\alpha_q$ protein while P2Y_{12} stimulates $\text{G}\alpha_i$, inhibiting adenylyl cyclase. In addition to activating the PLC- InsP_3 signaling cascade, P2Y_2 also couples to $\text{G}\alpha_i$ whereas

P2Y₁₁ has additionally been shown to stimulate G α_s [Balogh et al., 2005], the latter leading to the production of cAMP that promotes BBB function [Bruckener et al., 2003; Hurst and Clark, 1998; Ishizaki et al., 2003; Rubin et al., 1991]. Although expressed in BBB endothelium, thus far, P2X receptors, that are ligand gated ion channels, do not appear to contribute to the [Ca²⁺]_i increase induced by nucleotides [Albert et al., 1997; Bintig et al., 2011; Sipos et al., 2000] and it has to be resolved still what their function in the BBB is. We did not verify which purinoceptors are expressed in RBE4 and BCEC cells but we hypothesize that activation of P2Y₁₁ stimulates Ca²⁺ oscillations as well as the production of cAMP, thereby opposing a Ca²⁺-mediated disturbance of endothelial barrier function as described in corneal endothelium [Satpathy et al., 2005]. Other P2Y receptors might contribute to the [Ca²⁺]_i increase or might activate alternative signaling pathways leading to the strengthening of endothelial barrier function. P2Y₁₁ receptor activation with subsequent cAMP production might also be responsible for the observed suppression of BK-induced oscillations by co-applied ATP. Indeed, cAMP has been shown to inhibit Ca²⁺ oscillations in different cell systems by preventing InsP₃ formation [Abdel-Latif, 1996], by reducing the InsP₃R's sensitivity to InsP₃ [Bai and Sanderson, 2006] or by limiting Ca²⁺ entry [Vajanaphanich et al., 1995]. Importantly, cAMP also suppresses connexin hemichannel opening [Bevans and Harris, 1999] which would, by inference, hinder the BK-triggered oscillation mechanism. Taken together, intrinsic differences in the signaling cascades activated by BK and ATP may influence the effect on BBB function. In section 4.3 we will further elaborate on the specific role of connexin hemichannel opening on BBB permeability.

Ca²⁺ oscillations represent [Ca²⁺]_i changes in the temporal domain; however, [Ca²⁺]_i changes can also spatially extend as intercellular Ca²⁺ waves. Unlike the asynchronous oscillations triggered by BK, Ca²⁺ waves are coordinated [Ca²⁺]_i changes that could result in stronger BBB alterations. Intercellular Ca²⁺ waves in BBB endothelium were triggered by lowering [Ca²⁺]_e, a condition that was also associated with a large permeability increase of BCEC cultures. This permeability increase was highly dependent on [Ca²⁺]_i changes and was reduced by Gap27 that also prevented Ca²⁺ waves. A [Ca²⁺]_e reduction can have several effects on the level of the membrane as well as intracellularly, but current evidence points to hemichannel opening and ATP release as primary factors triggering intercellular Ca²⁺ waves [Anselmi et al., 2008]. Liberated ATP will act as a paracrine messenger that induces a [Ca²⁺]_i increase in neighboring cells, mediating Ca²⁺ wave propagation [Anselmi et al., 2008]. Our data indicate that low [Ca²⁺]_e conditions trigger intercellular Ca²⁺ waves that involve a similar number of

cells as compared to BK-triggered oscillations; however, the effect of low $[Ca^{2+}]_e$ on endothelial permeability is much stronger than for BK. $[Ca^{2+}]_e$ reduction may have different effects that are not related to $[Ca^{2+}]_i$ changes, for example the dissociation of VE-cadherin interactions [Baumgartner et al., 2000]. Our data indicate that the intercellular Ca^{2+} waves induced by low $[Ca^{2+}]_e$ recruit PKC and CaMKII signaling and lead to actomyosin contraction. By contrast, BK-associated Ca^{2+} oscillations did not activate PKC/CaMKII signaling and actomyosin contraction, presumably because of the lower amplitude of the $[Ca^{2+}]_i$ changes.

Our knowledge on the role of connexin channels in the function of capillaries and microvessels is still limited. In larger vessels (arteries/veins and arterioles/venules) gap junctions coordinate cell migration during angiogenesis and wound healing [Haefliger et al., 2004], and coupling of endothelial cells with smooth muscle cells via myoendothelial junctions contributes in modulating the vessel diameter that is subject to changes in blood pressure, blood flow and shear stress [Schuster et al., 2001]. Alterations in these parameters have furthermore been demonstrated to adjust connexin expression levels [Johnson and Nerem, 2007; Toubas et al., 2011]. In capillaries, connexin channels have been associated with inflammatory responses. In lung alveolar blood vessels, gap junctions mediate the bidirectional propagation of intercellular Ca^{2+} waves between capillaries and first order venules whereby at the venular level, these Ca^{2+} waves induce the expression of P-selectin, a cell-adhesion molecule that is important for leukocyte recruitment [Parthasarathi et al., 2006]. Similar results were reported for hamster cheek pouch capillaries [Veliz et al., 2008] and capillaries of the renal cortex [Toubas et al., 2011]. Importantly, connexin hemichannels were found to contribute to the inflammatory response of immortalized bEnd5 BBB cells. Treatment of these cells with LPS stimulated Cx43 hemichannel ATP release that resulted in increased expression of the Toll-like receptor 2 and potentiated the production of IL6 [Robertson et al., 2010]. Our work brings up a novel role for connexin hemichannels in the regulation of BBB function through their involvement in the Ca^{2+} oscillation machinery. In addition, gap junctions and hemichannels contribute to the propagation of intercellular Ca^{2+} waves that likely act in a synergistic manner thereby increasing their impact on BBB function. In the next section we further explore how Ca^{2+} , connexins and junctional proteins interact to alter BBB function.

4.3 THE NEXUS: WHERE CONNEXINS MEET Ca^{2+} AND JUNCTIONAL PROTEINS

Gap junction channels interact with a number of complementary components, forming a multiprotein complex termed ‘the nexus’ [Duffy et al., 2002]. Such a complex is believed to have some benefits like the targeting of connexin channels to specific cell surface domains and the spatial organization of signaling cascades giving a highly local efficiency of biological responses [Olk et al., 2009]. Connexins are associated with caveolae [Langlois et al., 2008; Liao et al., 2010; Saliez et al., 2008; Schubert et al., 2002a] which represent a specialized subset of lipid rafts, defined by small surface invaginations enriched in cholesterol and caveolin-1. They function as membrane scaffolds and are abundant in endothelial cells, including those constituting the BBB [Dodelet-Devillers et al., 2009; Isshiki and Anderson, 2003; Murata et al., 2007]. The interaction with caveolin-1 has been implicated in trafficking of connexins to the gap junctional plaque. Cx43-caveolin-1 binding involves the Cx43 C-terminal domain and takes place intracellularly, even before connexin incorporation in the plasma membrane [Langlois et al., 2008]. This would suggest that connexin hemichannels are connected to caveolin-1 and exhibit a caveolar localization; however, at present it is not known whether this linkage is associated with signaling or functional consequences. Knockdown of caveolin-1 in arteries has been associated with a severe diminution of plasma membrane-bound Cx37, Cx40 and Cx43 [Saliez et al., 2008]. Accordingly, caveolin-1 knockdown did not alter total Cx43 in the keratinocyte plasma membrane but it did lower the amount of Cx43 in caveolae which resulted in reduced gap junctional coupling [Langlois et al., 2008]. Lipid rafts/caveolae appear to be the preferred sites for Ca^{2+} entry [Murata et al., 2007] and since connexins are associated with caveolae they might well mediate Ca^{2+} entry. Ca^{2+} entry through hemichannels has thus far only been shown in HeLa cells subjected to alkalization [Schalper et al., 2010] or metabolic inhibition [Sanchez et al., 2009], and in cardiomyocytes [Shintani-Ishida et al., 2007], but a connection to caveolae was not studied. There is also evidence for a functional link between Cx43 and TRP channels, but again irrespective of their association in caveolae. In skeletal myoblasts, Cx43 expression was dependent on TRPC1-mediated Ca^{2+} entry [Meacci et al., 2010] and in the esophageal epithelium, Ca^{2+} entry via TRPV4 was shown to elicit hemichannel-mediated ATP release [Ueda et al., 2011]. In addition, there is some proof for an association of connexins with ER Ca^{2+} release: in mouse cremaster arteriole sections and freshly isolated cremasteric

endothelial cells, a close apposition of gap junction plaques and InsP₃R1 has been reported [Isakson, 2008], yet a link with lipid rafts was not investigated.

In endothelial cells, a number of molecules responsible for Ca²⁺ handling, including PMCA, GPCRs, TRP channels and ER InsP₃Rs, have been shown to be compartmentalized in caveolae [Isshiki and Anderson, 2003; Murata et al., 2007; Vaca, 2010]. Additionally, lipid rafts/caveolae have also been implicated in G α_q -mediated activation of PLC and InsP₃-triggered Ca²⁺ release [Isshiki and Anderson, 2003]. Intercellular Ca²⁺ waves triggered by BK or ATP originate in caveolin-rich regions at the plasma membrane of endothelial cells [Isshiki et al., 1998] and disruption of lipid rafts abolishes ATP-triggered intercellular Ca²⁺ waves in glial cells [Weerth et al., 2007]. There are discrepant reports about the localization of BK- and ATP receptors in lipid rafts/caveolae. The B1 and B2 BK receptors have been shown to be (at least partially) localized in caveolae under resting conditions [de Weerd and Leeb-Lundberg, 1997; Zhang et al., 2008], or to be translocated to these microdomains only in the presence of BK [Haasemann et al., 1998; Sabourin et al., 2002]. The purinergic receptors, P2Y₁, P2Y₂, P2Y₆ and P2Y₁₂, that are present in BBB endothelium, have all been shown to segregate in lipid rafts/caveolae under resting conditions [Ando et al., 2011; D'Ambrosi et al., 2007; Norambuena et al., 2008; Savi et al., 2006; Uehara and Uehara, 2011; Vial et al., 2006; Weerth et al., 2007]; however, their association with these plasma membrane microdomains varies between different cell types. For instance, P2Y₁ was shown to co-migrate with caveolin-1 in glia [Weerth et al., 2007] and smooth muscle cells [Norambuena et al., 2008] but not in human platelets [Vial et al., 2006]. P2Y₂ did not associate with caveolin-1 in smooth muscle cells [Norambuena et al., 2008] but was localized in lipid rafts in neuroblastoma cells [Ando et al., 2011]. In rat splenic sinus endothelial cells, P2Y₁, P2Y₆ and P2Y₁₂ were all localized in caveolae [Uehara and Uehara, 2011]. For the P2Y₁₁ receptor, thus far, no localization data are available.

Although the available data often contradict each other, interestingly, some suggest that a link with lipid rafts/caveolae is not essential for purinergic and B1/B2 receptor signaling [de Weerd and Leeb-Lundberg, 1997; Sabourin et al., 2002; Vial et al., 2006]. This could indicate that compartmentalization of the receptor in these raft microdomains rather serves to increase their proximity to certain effectors so that a highly specific cellular response can be obtained. A different distribution of purinergic receptors in the BBB endothelium might explain why ATP, when added to the extracellular solution, has no effect on endothelial permeability,

whereas ATP release via hemichannels is required for sustaining BK-triggered oscillations that do lead to a permeability increase.

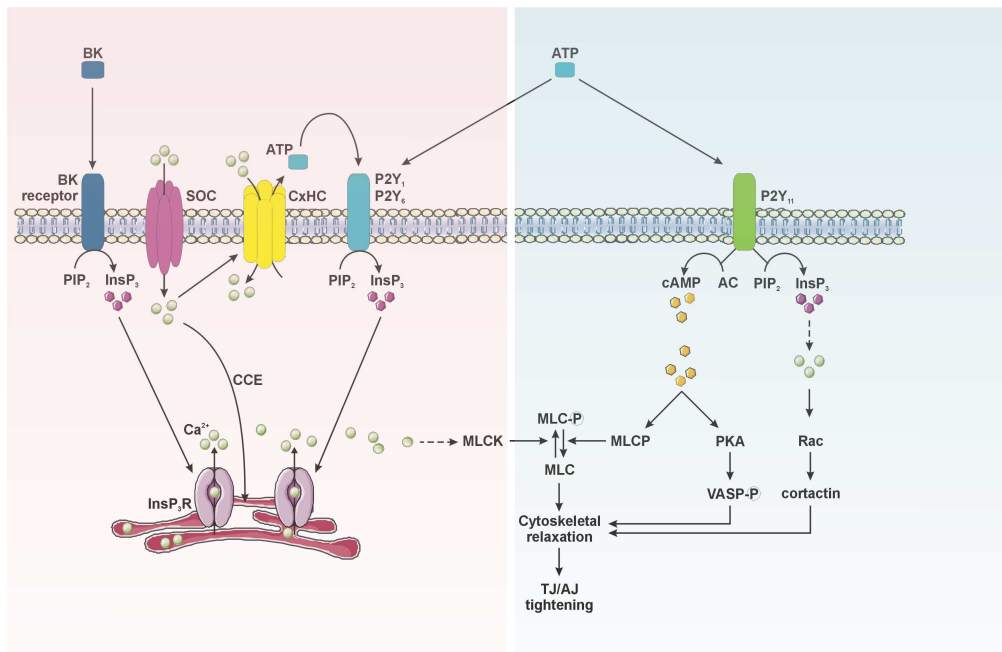


Figure 42. ATP- and BK-activated signaling cascades and their influence on BBB. Stimulation of BK $1/2$ $G\alpha_q$ -coupled receptors triggers the production of $InsP_3$ that stimulates Ca^{2+} release from the ER. Depletion of ER luminal Ca^{2+} will activate SOC channels that replenish luminal Ca^{2+} via capacitative Ca^{2+} entry (CCE). SOC channels and connexin hemichannels (CxHC) co-localize in lipid rafts, and therefore CCE can activate connexin hemichannels resulting in Ca^{2+} entry as well as ATP release. We propose that this spatially localized ATP then binds to $P2Y_1$ and/or $P2Y_6$ purinergic receptors that reside close to the connexin hemichannels. The resulting $[Ca^{2+}]_i$ increase can activate different pathways leading to increased BBB permeability (see figure 19), including the activation of MLCK (pink frame). When ATP is added exogenously to the bath solution, it activates $P2Y_{11}$ in addition to $P2Y_1$ and/or $P2Y_6$. This receptor is coupled to the production of $InsP_3$ via PLC and to the production of cAMP through activation of adenylyl cyclase (AC) and is hypothesized to localize in other signaling domains, distant from connexin hemichannels. Elevated levels of cAMP lead to the activation of MLCP and overrule the effect of Ca^{2+} on MLCK activity. Additionally, cAMP can stimulate PKA that phosphorylates VASP. ATP triggers substantially less CCE and is therefore believed not to activate connexin hemichannels (blue frame). Dotted lines represent indirect actions. This figure was produced using Servier Medical Art.

In 4.2 we describe evidence that $P2Y_{11}$ receptor activation promotes the production of cAMP, possibly counteracting Ca^{2+} -induced endothelial barrier changes. Other purinergic receptors might associate with connexins and junctional proteins in specific membrane microdomains whose purpose is to regulate BBB permeability. This hypothesis is supported by the observation that in RBE4 cells, BK-triggered Ca^{2+} oscillations are inhibited by suramin as

well as by PPADS, two purinoceptor inhibitors, whereas ATP-triggered Ca^{2+} oscillations are only sensitive to suramin, but not to PPADS (data not shown). This suggests the involvement of a different subset of purine receptors whereby P2Y_1 and/or P2Y_6 , the only BBB purinergic receptors sensitive to PPADS [Sigma-RBI], would co-localize with connexins and drive BK-triggered Ca^{2+} oscillations (**figure 42**).

Lipid rafts/caveolae are not only important for Ca^{2+} signaling and connexin trafficking, they are also implicated in regulating endothelial permeability. Caveolin-1 knockout mice present with vascular hyperpermeability [Lin et al., 2007; Schubert et al., 2002b] and electron micrographs of lung capillaries reveal defects in tight junction morphology and abnormalities in endothelial cell adhesion to the basement membrane [Schubert et al., 2002b]. Caveolin-1 was shown to interact with occludin in kidney epithelium and caveolin-1 knockdown correlated with a dissociation of occludin and ZO-1 from caveolae [Nusrat et al., 2000b]. An interaction between caveolin-1 and junctional proteins was also shown in BBB endothelium and treatment of these cells with the chemokine MCP-1 resulted in a loss of caveolin-1 with subsequent disappearance of ZO-1, occludin, VE-cadherin and β -catenin from the plasma membrane. Enhanced flux of dyes and monocytes across the endothelial monolayer were found to accompany these junctional alterations [Song et al., 2007]. Similar results were obtained when BBB endothelial cells were treated with the HIV-1 protein Tat [Zhong et al., 2008]. Additionally, ample evidence reveals a link between connexins and junctional proteins. In freeze-fracture analysis, tight junctions appear as a set of continuous, anastomosing strands whereas gap junctions present as large plaques of particles that can be found within the tight junction strand networks [Kojima et al., 2007]. In human colonic Caco-2 cells, Cx26 associates with occludin and claudin-4 [Nusrat et al., 2000a] whereas in the human airway epithelial cell line Calu-3, introduction of Cx26 potentiates expression of claudin-14 [Kojima et al., 2007]. Connexins furthermore associate with N-cadherin [Gourdie et al., 2006; Wei et al., 2005] and catenins [Derangeon et al., 2009; Duffy et al., 2002; Herve et al., 2004; Wu et al., 2003]. At the functional level, Cx32 co-localization with occludin, claudin-1 and ZO-1 strengthens the tight junctions in primary rat hepatocytes [Kojima et al., 2007]. In the blood-testis barrier that is formed by seminiferous Sertoli cells, a transient loss of Cx43 from the junctions occurs during spermiation which involves a disassembly of the junctional complex, facilitating the transit of spermatocytes to enter the tubule lumen. Cx43 re-enters the junctional complex as soon as the barrier closes up again [Li et al., 2009]. These data thus indicate that connexins can stabilize intercellular junctions and promote barrier function. This

was also confirmed in porcine BBB endothelial cells from which Cx40 and Cx43 co-immunoprecipitate with occludin, claudin-5 and ZO-1. The connexin blocker 18 β GA did not alter the expression or localization of connexins and tight junction proteins, but still, it induced a marked increase in paracellular permeability [Nagasawa et al., 2006]. Unfortunately, none of these studies have investigated whether connexin hemichannels or gap junctions were involved.

On the other hand, junctional proteins also affect connexin channel function. For instance, Cx43 interaction with ZO-1 was found to regulate the gap junction plaque size [Hunter et al., 2005; Roh and Funderburgh, 2011]. The presence of ZO-1 at the outer edges of the plaque limits the rate at which free hemichannels are added to the plaque [Hunter et al., 2005]. The area surrounding the plaque (the perinexus) contains ZO-1-bound hemichannels and may function as a specialized membrane domain for hemichannel function [Rhett et al., 2011]. In capillary cell-cell junctions that are enriched in ZO proteins, the associated connexin channels might therefore be rather of the hemichannel type than of the gap junction type. The fact that endothelial cells at the arteriolar and capillary level still display significant expression of connexins follows the possibility that these connexins are present as unapposed hemichannels. Also in support of this is that in vascular endothelial cells the gap junction plaque size as well as the extent of coupling seem to decrease with the size of the vessels [Pepper et al., 1992]. Inhibition of Cx43-ZO-1 interaction reduces low $[Ca^{2+}]_e$ -triggered dye uptake in cardiomyocytes, though this is probably not due to gating effects but to an increased incorporation of hemichannels into gap junction plaques [Rhett et al., 2011]. Further work will be necessary to reconcile these data with opposing observations in corneal endothelial cells that ZO-1 does not co-localize with Cx43 hemichannels and is not involved in gating of the channel [Ponsaerts et al., 2010]. At least in support of our own data is the observation that hemichannels transiently reside in caveolae until they are recruited to the gap junction plaque by ZO-1 binding [Laing et al., 2005]. Either way, interaction with ZO-1 is believed to provide a structural link between connexins and the actin cytoskeleton, like in tight junctions [Olk et al., 2009]. Finally, Van Zeijl et al. hypothesized that ZO-1 can target PLC β to the gap junction plaques so that ambient levels of PIP₂ are immediately sensed by Cx43 and gap junctional communication can be adapted in response to GPCR activation [van Zeijl et al., 2007] (**figure 43**).

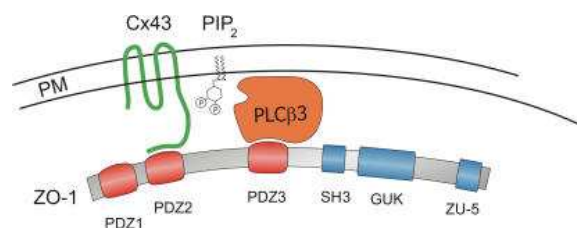


Figure 43. Schematic drawing illustrating ZO-1 as a proposed scaffold that assembles Cx43 and PLC β into a complex. The close association of Cx43 and PLC β is believed to facilitate regulation of Cx43 channel function by localized changes in PIP₂ brought about by GPCR activation. As there is no evidence for a direct binding of PIP₂ to Cx43, PIP₂ may influence (inhibit) junctional communication in an indirect manner, for example, via a Cx43-associated protein that modifies the Cx43 regulatory tail and thereby shuts off channel function. PM, plasma membrane [van Zeijl et al., 2007].

In addition to links between GPCRs, Ca²⁺ and connexins at the nexus, finally, there is evidence for a link between Ca²⁺ handling proteins and cell-cell junctions. In MDCK cells, ER-derived InsP₃R1 and InsP₃R3 can be detected in the vicinity of the cell surface where they colocalize with ZO-1 and occludin. This close proximity of InsP₃R3 and tight junction proteins places Ca²⁺ release sites at a strategic position for regulating paracellular permeability [Colosetti et al., 2003]. Most likely, intracellular Ca²⁺ ions do not directly affect junctional proteins but alter their functionality via specialized [Ca²⁺]_i sensor kinases like CaMKII and PKC, that convert information encoded in the Ca²⁺ oscillations to a specific biological response. Although we could not ascertain their engagement in the BK-triggered permeability increase, PKC and CaMKII were involved in low [Ca²⁺]_e-triggered, Ca²⁺ wave-associated barrier disruption. Interestingly, PKC has been identified in caveolae [Yang et al., 2009] and is well known to be associated with the junctional complex [Stamatovic et al., 2006]. In addition, CaMKII was found present in lipid rafts [Du et al., 2006; Suzuki et al., 2008] and to colocalize with connexins and tight junction associated, actin-binding second order adaptor molecules [Li et al., 2012]. Both PKC and CaMKII have been shown to phosphorylate proteins of the interendothelial junctions [Gaudreault et al., 2008; Kim et al., 2010; Konstantoulaki et al., 2003; Qiu et al., 2010; Stamatovic et al., 2006; Sukumaran and Prasadarao, 2003; Tirupathi et al., 2006; Wang et al., 2010]. Activation of CaMKII is well known to depend on Ca²⁺, but for PKC the situation is somewhat more complex. Low [Ca²⁺]_e-induced barrier disruption was halted by the PKC inhibitor chelerythrine which is specific for conventional and novel PKC isoforms [Herbert et al., 1990]. Both demand the activation of PLC but only conventional PKCs require an additional increase in [Ca²⁺]_i. We hypothesize that activation of Ca²⁺-sensitive, conventional PKCs increase BBB permeability whereas

novel and atypical PKCs rather seem to counteract this event (see 1.4.3.1). Both kinases have also been implicated in the regulation of actomyosin contraction [Birukova et al., 2004; Borbiev et al., 2003; Garcia et al., 1999; Mehta et al., 2001; Sukumaran and Prasadarao, 2002; Tirupathi et al., 2006; Verin et al., 1998]. Our experiments with (-)-blebbistatin suggest a role for endothelial cell contraction in the low $[Ca^{2+}]_e$ -induced permeability increase. Blebbistatin is a non-competitive inhibitor of the myosin II-ATPase that blocks myosin in an actin-detached state and thus prevents actin-myosin crosslinking [Kovacs et al., 2004]. In addition, we found evidence for BK-induced changes at the level of vimentin fibers that were absent when cells were pretreated with Gap27 or when cells were exposed to ATP. Vimentin is important for cell shape and integrity and loss or fragmentation of this intermediate filament results in cell rounding [Goldman et al., 1996]; however, not much is known in relation to the structural integrity of epi- or endothelial barriers. Both in Sertoli cells that form the blood-testis barrier, and endothelial cells, a relationship between vimentin and cell-cell junctions has been revealed [Bekheet and Stahlmann, 2009; Lee et al., 2004; Shasby et al., 2002]. Phosphorylation of vimentin in HUVEC disrupts its interaction with VE-cadherin [Shasby et al., 2002] while in pulmonary endothelial cells the collapse of vimentin fibers has been shown to facilitate cell contraction and flux of tracer dyes [Liu et al., 2010a]. Altered expression of vimentin was found in brain tissue from different CNS diseases (infarction, multiple sclerosis and Alzheimer's disease) [Yamada et al., 1992] but an endothelial localization was not confirmed. In brain microvascular endothelial cells, vimentin rearrangement has been associated with endothelin-1-triggered $[Ca^{2+}]_i$ [Chen et al., 2003] changes and bacterial activation of CaMKII [Chi et al., 2010] but no attempts were made to explain how vimentin alterations might relate to enhanced barrier permeability. Our observations demonstrate that vimentin rearrangements occur isolated without associated alterations in ZO-1, occludin or F-actin. Recently, Bekheet and Stahlman (2009) indicated a possible connection between Cx43 and vimentin in Sertoli cells as treatment with gentamycin caused a collapse of vimentin along with a decrease in plasma membrane junctional proteins and the disappearance of gap junctional plaques [Bekheet and Stahlmann, 2009]. However, detailed structural and functional links between the different components remain to be ascertained.

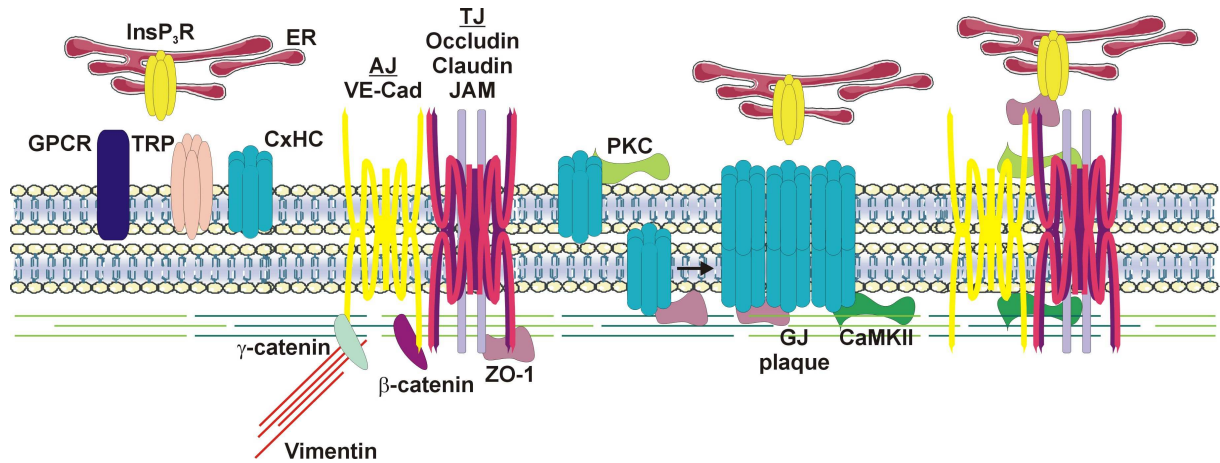


Figure 44. Connexins, Ca^{2+} handling proteins and endothelial junctions form a macromolecular complex in the plasma membrane. GPCRs, along with InsP_3R s and TRP channels have been found in caveolae. Connexins have been identified in these specialized membrane areas as well, and there is evidence for a functional link between connexin channels and both TRP channels (Ca^{2+} entry) and InsP_3R Ca^{2+} release channels. Endothelial junctions (adherens and tight junctions) are associated with caveolae were they interact with cytosolic proteins like catenins and ZO-1 that create a link to cytoskeletal (myosin and actin) and intermediate (vimentin) filaments. ZO-1 furthermore links occludin to Ca^{2+} release sites (InsP_3R) and is associated with connexins. Connexin/ZO-1 interaction has been proposed to regulate gap junction plaque size (indicated by the arrow). PKC and CaMKII, which are a Ca^{2+} sensitive kinase, associate with both connexins and junctional proteins. For references, see text. This figure was produced using Servier Medical Art.

In conclusion, BBB permeability is strictly kept low to guarantee an environment in which neurons can function optimally; however, many CNS disorders are associated with an increase in BBB permeability, either as a cause or a consequence, further aggravating tissue damage. The primary BBB is built up by the interendothelial junctions which are associated with the cytoskeleton and that restrict paracellular diffusion. Ca^{2+} is a key element in controlling BBB function and an elevation of intracellular Ca^{2+} levels is central to increased paracellular permeability, e.g. in case of inflammation or stroke. However, except for the occasional observations of Ca^{2+} oscillations and waves in BBB endothelial cells, nothing was known on the role of Ca^{2+} dynamics on BBB permeability. Our work indicates that both Ca^{2+} oscillations and intercellular waves can induce BBB impairment with Ca^{2+} waves having more profound effects on BBB permeability compared to Ca^{2+} oscillations. Importantly, our work further brings up a novel role for connexins in the modulation of BBB permeability. Available data combined with our novel findings suggest that connexins, cell-cell junctions and Ca^{2+} handling proteins all come together in a macromolecular complex that can influence endothelial permeability. In this complex connexins may have a double role; from the

literature it appears that in resting conditions they stabilize the junctional complex while the data described in this thesis indicate that in the presence of a Ca^{2+} -mobilizing agonist (p.e. bradykinin), connexin hemichannels are decisive in opening the BBB: agonists that trigger hemichannel-dependent oscillations are associated with BBB leakiness whereas those eliciting oscillations that do not require hemichannels have no impact on BBB permeability. We hypothesize that Ca^{2+} oscillations sustained by hemichannels occur in close proximity to the junctions thereby increasing endothelial permeability and compromising BBB function. Interference with hemichannel opening using connexin mimetic peptides is expected to prevent the occurrence of $[\text{Ca}^{2+}]_i$ changes in the immediate vicinity of the junctional complex. In addition, connexin mimetic peptides block gap junction channels, preventing the propagation of $[\text{Ca}^{2+}]_i$ changes to neighboring cells. Altogether, our data indicate that blocking connexin channels will protect against BBB dysfunction under pathological conditions.

4.4 FUTURE PERSPECTIVES

In addition to the hypothesis that assumes the existence of a macromolecular complex involved in the regulation of endothelial permeability, two other questions will be tackled: *i*) how do pericytes, astrocytes and microglia contribute to the process of BBB disruption, and *ii*) what is the role of connexin channels and Ca^{2+} dynamics herein?

Indeed, from our work it emerges that inflammatory mediators like bradykinin act at the level of the endothelial cells to increase BBB permeability, but we did not look beyond the endothelium. As described in 1.4.1.3, BBB endothelial cells are part of a larger complex -the neurovascular unit- that additionally encompasses astrocytes, pericytes and microglia. Astrocytic endfeet, that nearly completely ensheath the BBB endothelium, and pericytes, that share the basement membrane with endothelial cells, are at the gateway to the CNS parenchyma and are probably the first to be affected by a breakdown of the BBB. Astrocytes have indeed been shown to be activated by blood components (albumin, thrombin) that leak into the brain parenchyma following BBB disruption [Nadal et al., 1998; Shirakawa et al., 2010]. In addition, circulating inflammatory mediators like bradykinin or LPS [McKimmie and Graham, 2010; Schwaninger et al., 1999; Su et al., 2009] can trigger an astrocyte response. Alternatively, Ca^{2+} entry into the brain parenchyma could activate astrocytes or pericytes. Microglial cells are the resident macrophages of the CNS and exhibit a downgraded

phenotype in the 'resting' state; however, infection, ischemia, etc., induce microglia to acquire an activated state and to migrate to their target site [Kettenmann et al., 2011]. We anticipate that microglia become activated directly, by leakage of circulating compounds into the brain parenchyma [Hooper et al., 2005; Ryu and McLarnon, 2009; Sumi et al., 2010], or indirectly, via reactive astrocytes and/or pericytes. In either case, we believe that BBB disruption and glial cell/pericyte activation will engage in a vicious cycle with BBB impairment causing the activation of pericytes/astrocytes/microglia, this leading to further BBB dysfunction and brain damage. Finally, endothelial cells exposed to inflammatory agents secrete chemo- and cytokines [D'aversa et al., 2012; Didier et al., 2003] via which they could further signal to the bystander cells [Eugenin et al., 2001; Guo et al., 1998; Papadopoulos et al., 2000].

With respect to connexin channels, we know now that endothelial connexins contribute to BBB permeability changes, but are connexin channels in glial cells and pericytes involved as well? Connexin hemichannel opening has been observed in both astrocytes and microglia upon inflammation [Karpuk et al., 2011; Orellana et al., 2011b; Retamal et al. 2007] and this is usually correlated with a decrease in gap junctional intercellular communication. Although pericytes express Cx43 and are known to form gap junctions with adjacent pericytes as well as with endothelial cells [Kamawura et al., 2004; Larson et al., 1987; Li et al., 2003]; currently, nothing is known on the presence or absence of hemichannels in these cells. Exactly how glial or pericyte hemichannels would contribute to BBB dysfunction remains obscure, but some suggestions have been made. Hemichannel opening has been shown to be responsible for the creation of an ATP gradient that functions as a guiding signal for microglia towards the site of injury [Kim et al., 2006]; therefore, hemichannel opening in endothelial cells, astrocytes or pericytes could be important to attract microglial cells. In addition, connexin hemichannel-mediated ATP release seems to contribute to the release of cytokines [Robertson et al., 2010], though the exact mechanism is not known. Lastly, hemichannels provide a route for enhanced uptake of glucose by astrocytes, ultimately leading to excessive lactate production/release, acidosis and tissue damage [Retamal et al., 2007] that could on its turn activate microglia.

Finally, in addition to the well-known appearance of Ca^{2+} oscillations and intercellular Ca^{2+} waves in astrocytes, oscillations have also been observed in microglia and pericytes [Edwards et al., 2008; Visentin et al., 2006], and Ca^{2+} waves, depending on a paracrine, purinergic

pathway, were identified between astrocytes and microglia [Schipke et al., 2002; Verderio et al. 2001b]; however, the link between Ca^{2+} dynamics in these cells and BBB permeability (or hemichannel opening) remains undefined.

References

- Abbott N (2002): Astrocyte-endothelial interactions and blood-brain barrier permeability. *J Anat* 200:527.
- Abbott NJ (1991): Permeability and transport of glial blood-brain barriers. *Ann N Y Acad Sci* 633:378-94.
- Abbott NJ (1998): Role of intercellular calcium in regulation of brain endothelial permeability. In Partridge WM (ed): "Introduction to the Blood-Brain Barrier: Methodology and Biology." Cambridge UK: Cambridge University Press, pp 354-353.
- Abbott NJ (2000): Inflammatory mediators and modulation of blood-brain barrier permeability. *Cell Mol Neurobiol* 20:131-47.
- Abbott NJ (2005): Dynamics of CNS barriers: evolution, differentiation, and modulation. *Cell Mol Neurobiol* 25:5-23.
- Abbott NJ, Ronnback L, Hansson E (2006): Astrocyte-endothelial interactions at the blood-brain barrier. *Nat Rev Neurosci* 7: 41-53
- Abbott NJ, Patabendige AA, Dolman DE, Yusof SR, Begley DJ (2010): Structure and function of the blood-brain barrier. *Neurobiol Dis* 37:13-25.
- Abbott NJ, Ronnback L, Hansson E (2006): Astrocyte-endothelial interactions at the blood-brain barrier. *Nat Rev Neurosci* 7:41-53.
- Abbruscato TJ, Davis TP (1999): Combination of hypoxia/aglycemia compromises in vitro blood-brain barrier integrity. *J Pharmacol Exp Ther* 289:668-75.
- Abdel-Latif AA (1996): Cross talk between cyclic AMP and the polyphosphoinositide signaling cascade in iris sphincter and other nonvascular smooth muscle. *Proc Soc Exp Biol Med* 211:163-77.
- Abudara V, Jiang RG, Eyzaguirre C (2001): Acidic regulation of junction channels between glomus cells in the rat carotid body. Possible role of $[Ca^{2+}]_i$. *Brain Res* 916:50-60.
- Albert JL, Boyle JP, Roberts JA, Challiss RA, Gubby SE, Boarder MR (1997): Regulation of brain capillary endothelial cells by P2Y receptors coupled to Ca^{2+} , phospholipase C and mitogen-activated protein kinase. *Br J Pharmacol* 122:935-41.
- Alexander DB, Goldberg GS (2003): Transfer of biologically important molecules between cells through gap junction channels. *Curr Med Chem* 10:2045-58.
- Alexander JS, Jackson SA, Chaney E, Kevil CG, Haselton FR (1998): The role of cadherin endocytosis in endothelial barrier regulation: involvement of protein kinase C and actin-cadherin interactions. *Inflammation* 22:419-33.
- Allen MJ, Gemel J, Beyer EC, Lal R (2011): Atomic force microscopy of Connexin40 hemichannels reveals calcium-dependent 3D molecular topography and open-closed conformations of both the extracellular and cytoplasmic faces. *J Biol Chem*.
- Anderson CM, Bergher JP, Swanson RA (2004): ATP-induced ATP release from astrocytes. *J Neurochem* 88:246-56.
- Ando K, Obara Y, Sugama J, Kotani A, Koike N, Ohkubo S, Nakahata N (2011): P2Y2 receptor-Gq/11 signaling at lipid rafts is required for UTP-induced cell migration in NG 108-15 cells. *J Pharmacol Exp Ther* 334:809-19.
- Andras IE, Deli MA, Veszelka S, Hayashi K, Hennig B, Toborek M (2007): The NMDA and AMPA/KA receptors are involved in glutamate-induced alterations of occludin expression and phosphorylation in brain endothelial cells. *J Cereb Blood Flow Metab* 27:1431-43.
- Andras IE, Pu H, Tian J, Deli MA, Nath A, Hennig B, Toborek M (2005): Signaling mechanisms of HIV-1 Tat-induced alterations of claudin-5 expression in brain endothelial cells. *J Cereb Blood Flow Metab* 25:1159-70.
- Anselmi F, Hernandez VH, Crispino G, Seydel A, Ortolano S, Roper SD, Kessar N, Richardson W, Rickheit G, Filippov MA, Monyer H, Mammano F (2008): ATP release through connexin hemichannels and gap junction transfer of second messengers propagate Ca^{2+} signals across the inner ear. *Proc Natl Acad Sci U S A* 105:18770-5.
- Anumonwo JM, Taffet SM, Gu H, Chanson M, Moreno AP, Delmar M (2001): The carboxyl terminal domain regulates the unitary conductance and voltage dependence of connexin40 gap junction channels. *Circ Res* 88:666-73.
- Anwar Z, Albert JL, Gubby SE, Boyle JP, Roberts JA, Webb TE, Boarder MR (1999): Regulation of cyclic AMP by extracellular ATP in cultured brain capillary endothelial cells. *Br J Pharmacol* 128:465-71.
- Arcuino G, Lin JH, Takano T, Liu C, Jiang L, Gao Q, Kang J, Nedergaard M (2002): Intercellular calcium signaling mediated by point-source burst release of ATP. *Proc Natl Acad Sci U S A* 99:9840-5.
- Atri A, Amundson J, Clapham D, Sneyd J (1993): A single-pool model for intracellular calcium oscillations and waves in the *Xenopus laevis* oocyte. *Biophys J* 65:1727-39.
- Austinat M, Braeuning S, Pesquero JB, Brede M, Bader M, Stoll G, Renne T, Kleinschnitz C (2009): Blockade of bradykinin receptor B1 but not bradykinin receptor B2 provides protection from cerebral infarction and brain edema. *Stroke* 40:285-93.
- Bai Y, Sanderson MJ (2006): Airway smooth muscle relaxation results from a reduction in the frequency of Ca^{2+} oscillations induced by a cAMP-mediated inhibition of the IP3 receptor. *Respir Res* 7:34.

- Balogh J, Wihlborg AK, Isackson H, Joshi BV, Jacobson KA, Arner A, Erlinge D (2005): Phospholipase C and cAMP-dependent positive inotropic effects of ATP in mouse cardiomyocytes via P2Y₁₁-like receptors. *J Mol Cell Cardiol* 39: 223-30.
- Balla Z, Hoch B, Karczewski P, Blasig IE (2002): Calcium/calmodulin-dependent protein kinase II δ 2 and gamma isoforms regulate potassium currents of rat brain capillary endothelial cells under hypoxic conditions. *J Biol Chem* 277:21306-14.
- Ballabh P, Braun A, Nedergaard M (2004): The blood-brain barrier: an overview: structure, regulation, and clinical implications. *Neurobiol Dis* 16:1-13.
- Bao L, Samuels S, Locovei S, Macagno ER, Muller KJ, Dahl G (2007): Innexins form two types of channels. *FEBS Lett* 581:5703-8.
- Baranova A, Ivanov D, Petrash N, Pestova A, Skoblov M, Kelmanson I, Shagin D, Nazarenko S, Geraymovych E, Litvin O, Tiunova A, Born TL, Usman N, Staroverov D, Lukyanov S, Panchin Y (2004): The mammalian pannexin family is homologous to the invertebrate innexin gap junction proteins. *Genomics* 83:706-16.
- Barbara JG (2002): IP₃-dependent calcium-induced calcium release mediates bidirectional calcium waves in neurones: functional implications for synaptic plasticity. *Biochim Biophys Acta* 1600:12-8.
- Barbe MT, Monyer H, Bruzzone R (2006): Cell-cell communication beyond connexins: the pannexin channels. *Physiology (Bethesda)* 21:103-14.
- Bargiotas P, Monyer H, Schwaninger M (2009): Hemichannels in cerebral ischemia. *Curr Mol Med* 9:186-94.
- Bartha K, Domotor E, Lanza F, Adam-Vizi V, Machovich R (2000): Identification of thrombin receptors in rat brain capillary endothelial cells. *J Cereb Blood Flow Metab* 20:175-82.
- Bauer HC, Bauer H (2000): Neural induction of the blood-brain barrier: still an enigma. *Cell Mol Neurobiol* 20:13-28.
- Baumgartner W, Hinterdorfer P, Ness W, Raab A, Vestweber D, Schindler H, Drenckhahn D (2000): Cadherin interaction probed by atomic force microscopy. *Proc Natl Acad Sci U S A* 97:4005-10.
- Baux G, Simonneau M, Tauc L, Segundo JP (1978): Uncoupling of electrotonic synapses by calcium. *Proc Natl Acad Sci U S A* 75:4577-81.
- Beahm DL, Hall JE (2002): Hemichannel and junctional properties of connexin 50. *Biophys J* 82:2016-31.
- Beblo DA, Veenstra RD (1997): Monovalent cation permeation through the connexin40 gap junction channel. Cs, Rb, K, Na, Li, TEA, TMA, TBA, and effects of anions Br, Cl, F, acetate, aspartate, glutamate, and NO₃. *J Gen Physiol* 109:509-22.
- Bechmann I, Galea I, Perry VH (2006): What is the blood-brain barrier (not)? *Trends Immunol*.
- Bekheet SH, Stahlmann R (2009): Disruption of gap junctional intercellular communication by antibiotic gentamicin is associated with aberrant localization of occludin, N-cadherin, connexin 43, and vimentin in SerW3 Sertoli cells in vitro. *Environ Toxicol Pharmacol* 28:155-60.
- Bell RD, Winkler EA, Sagare AP, Singh I, LaRue B, Deane R, Zlokovic BV (2010): Pericytes control key neurovascular functions and neuronal phenotype in the adult brain and during brain aging. *Neuron* 68:409-27.
- Beltramello M, Piazza V, Bukauskas FF, Pozzan T, Mammano F (2005): Impaired permeability to Ins(1,4,5)P₃ in a mutant connexin underlies recessive hereditary deafness. *Nat Cell Biol* 7:63-9.
- Bennett MV, Contreras JE, Bukauskas FF, Saez JC (2003): New roles for astrocytes: gap junction hemichannels have something to communicate. *Trends Neurosci* 26:610-7.
- Berezowski V, Landry C, Dehouck MP, Cecchelli R, Fenart L (2004): Contribution of glial cells and pericytes to the mRNA profiles of P-glycoprotein and multidrug resistance-associated proteins in an in vitro model of the blood-brain barrier. *Brain Res* 1018:1-9.
- Bergner A, Sanderson MJ (2002): ATP stimulates Ca²⁺ oscillations and contraction in airway smooth muscle cells of mouse lung slices. *Am J Physiol Lung Cell Mol Physiol* 283:L1271-9.
- Berra-Romani R, Raqeeb A, Avelino-Cruz JE, Moccia F, Oldani A, Speroni F, Taglietti V, Tanzi F (2008): Ca²⁺ signaling in injured in situ endothelium of rat aorta. *Cell Calcium* 44:298-309.
- Berra-Romani R, Raqeeb A, Torres-Jacome J, Guzman-Silva A, Guerra G, Tanzi F, Moccia F (2011): The mechanism of injury-induced intracellular calcium concentration oscillations in the endothelium of excised rat aorta. *J Vasc Res* 49:65-76.
- Berridge MJ (1997): Elementary and global aspects of calcium signalling. *J Physiol* 499 (Pt 2):291-306.
- Berridge MJ (2002): The endoplasmic reticulum: a multifunctional signaling organelle. *Cell Calcium* 32:235-49.
- Berridge MJ (2006): Calcium microdomains: organization and function. *Cell Calcium* 40:405-12.
- Berridge MJ (2007): Inositol trisphosphate and calcium oscillations. *Biochem Soc Symp*:1-7.
- Berridge MJ, Bootman MD, Roderick HL (2003): Calcium signalling: dynamics, homeostasis and remodelling. *Nat Rev Mol Cell Biol* 4:517-29.
- Berridge MJ, Cobbold PH, Cuthbertson KS (1988): Spatial and temporal aspects of cell signalling. *Philos Trans R Soc Lond B Biol Sci* 320:325-43.
- Berridge MJ, Lipp P, Bootman MD (2000): The versatility and universality of calcium signalling. *Nat Rev Mol Cell Biol* 1:11-21.

- Berridge MJ, Potter BV (1990): Inositol trisphosphate analogues induce different oscillatory patterns in *Xenopus* oocytes. *Cell Regul* 1:675-81.
- Berrout J, Jin M, O'Neil RG (2011): Critical role of TRPP2 and TRPC1 channels in stretch-induced injury of blood-brain barrier endothelial cells. *Brain Res*.
- Berthoud VM, Beyer EC, Seul KH (2000): Peptide inhibitors of intercellular communication. *Am J Physiol Lung Cell Mol Physiol* 279:L619-22.
- Betzenhauser MJ, Wagner LE, 2nd, Iwai M, Michikawa T, Mikoshiba K, Yule DI (2008): ATP modulation of Ca^{2+} release by type-2 and type-3 inositol (1, 4, 5)-triphosphate receptors. Differing ATP sensitivities and molecular determinants of action. *J Biol Chem* 283:21579-87.
- Bevans CG, Harris AL (1999): Direct high affinity modulation of connexin channel activity by cyclic nucleotides. *J Biol Chem* 274:3720-5.
- Bevans CG, Kordel M, Rhee SK, Harris AL (1998): Isoform composition of connexin channels determines selectivity among second messengers and uncharged molecules. *J Biol Chem* 273:2808-16.
- Beyer EC, Paul DL, Goodenough DA (1987): Connexin43: a protein from rat heart homologous to a gap junction protein from liver. *J Cell Biol* 105:2621-9.
- Bezprozvany I (2009): Calcium signaling and neurodegenerative diseases. *Trends Mol Med* 15:89-100.
- Bezprozvany I, Watras J, Ehrlich BE (1991): Bell-shaped calcium-response curves of $Ins(1,4,5)P_3$ - and calcium-gated channels from endoplasmic reticulum of cerebellum. *Nature* 351:751-4.
- Bhalla-Gehi R, Penuela S, Churko JM, Shao Q, Laird DW (2010): Pannexin1 and pannexin3 delivery, cell surface dynamics, and cytoskeletal interactions. *J Biol Chem* 285:9147-60.
- Bindschadler M, Sneyd J (2001): A bifurcation analysis of two coupled calcium oscillators. *Chaos* 11:237-246.
- Bintig W, Begandt D, Schlingmann B, Gerhard L, Pangalos M, Dreyer L, Hohnjec N, Couraud PO, Romero IA, Weksler BB, Ngezahayo A (2011): Purine receptors and Ca^{2+} signalling in the human blood-brain barrier endothelial cell line hCMEC/D3. *Purinergic Signal*.
- Bird GS, Hwang SY, Smyth JT, Fukushima M, Boyles RR, Putney JW, Jr. (2009): STIM1 is a calcium sensor specialized for digital signaling. *Curr Biol* 19:1724-9.
- Bird GS, Rossier MF, Obie JF, Putney JW, Jr. (1993): Sinusoidal oscillations in intracellular calcium requiring negative feedback by protein kinase C. *J Biol Chem* 268:8425-8.
- Birukova AA, Smurova K, Birukov KG, Kaibuchi K, Garcia JG, Verin AD (2004): Role of Rho GTPases in thrombin-induced lung vascular endothelial cells barrier dysfunction. *Microvasc Res* 67:64-77.
- Boarder MR, Challiss RA (1992): Role of protein kinase C in the regulation of histamine and bradykinin stimulated inositol polyphosphate turnover in adrenal chromaffin cells. *Br J Pharmacol* 107:1140-5.
- Boassa D, Ambrosi C, Qiu F, Dahl G, Gaietta G, Sosinsky G (2007): Pannexin1 channels contain a glycosylation site that targets the hexamer to the plasma membrane. *J Biol Chem* 282:31733-43.
- Bodin P, Burnstock G (1996): ATP-stimulated release of ATP by human endothelial cells. *J Cardiovasc Pharmacol* 27:872-5.
- Boehning D, Patterson RL, Sedaghat L, Glebova NO, Kurosaki T, Snyder SH (2003): Cytochrome c binds to inositol (1,4,5) trisphosphate receptors, amplifying calcium-dependent apoptosis. *Nat Cell Biol* 5:1051-61.
- Boehning D, Patterson RL, Snyder SH (2004): Apoptosis and calcium: new roles for cytochrome c and inositol 1,4,5-trisphosphate. *Cell Cycle* 3:252-4.
- Boehning D, van Rossum DB, Patterson RL, Snyder SH (2005): A peptide inhibitor of cytochrome c/inositol 1,4,5-trisphosphate receptor binding blocks intrinsic and extrinsic cell death pathways. *Proc Natl Acad Sci U S A* 102:1466-71.
- Boitano S, Dirksen ER, Sanderson MJ (1992): Intercellular propagation of calcium waves mediated by inositol trisphosphate. *Science* 258:292-5.
- Boitano S, Evans WH (2000): Connexin mimetic peptides reversibly inhibit Ca^{2+} signaling through gap junctions in airway cells. *Am J Physiol Lung Cell Mol Physiol* 279:L623-30.
- Bootman MD, Berridge MJ, Roderick HL (2002): Calcium signalling: more messengers, more channels, more complexity. *Curr Biol* 12:R563-5.
- Borbiev T, Verin AD, Birukova A, Liu F, Crow MT, Garcia JG (2003): Role of CaM kinase II and ERK activation in thrombin-induced endothelial cell barrier dysfunction. *Am J Physiol Lung Cell Mol Physiol* 285:L43-54.
- Borbiev T, Verin AD, Shi S, Liu F, Garcia JG (2001): Regulation of endothelial cell barrier function by calcium/calmodulin-dependent protein kinase II. *Am J Physiol Lung Cell Mol Physiol* 280:L983-90.
- Boulware MJ, Marchant JS (2008): Timing in cellular Ca^{2+} signaling. *Curr Biol* 18:R769-R776.
- Boveri M, Berezowski V, Price A, Slupek S, Lenfant AM, Benaud C, Hartung T, Cecchelli R, Prieto P, Dehouck MP (2005): Induction of blood-brain barrier properties in cultured brain capillary endothelial cells: comparison between primary glial cells and C6 cell line. *Glia* 51:187-98.
- Bradbury MW (1993): The blood-brain barrier. *Exp Physiol* 78:453-72.

- Bradley SJ, Watson JM, Challiss RA (2009): Effects of positive allosteric modulators on single-cell oscillatory Ca^{2+} signaling initiated by the type 5 metabotropic glutamate receptor. *Mol Pharmacol* 76:1302-13.
- Braet K, Aspeslagh S, Vandamme W, Willecke K, Martin PE, Evans WH, Leybaert L (2003a): Pharmacological sensitivity of ATP release triggered by photoliberation of inositol-1,4,5-trisphosphate and zero extracellular calcium in brain endothelial cells. *J Cell Physiol* 197:205-13.
- Braet K, Vandamme W, Martin PE, Evans WH, Leybaert L (2003b): Photoliberating inositol-1,4,5-trisphosphate triggers ATP release that is blocked by the connexin mimetic peptide gap 26. *Cell Calcium* 33:37-48.
- Brough GH, Wu S, Cioffi D, Moore TM, Li M, Dean N, Stevens T (2001): Contribution of endogenously expressed Trp1 to a Ca^{2+} -selective, store-operated Ca^{2+} entry pathway. *Faseb J* 15:1727-38.
- Brown RC, Davis TP (2002): Calcium modulation of adherens and tight junction function: a potential mechanism for blood-brain barrier disruption after stroke. *Stroke* 33:1706-11.
- Brown RC, Davis TP (2005): Hypoxia/aglycemia alters expression of occludin and actin in brain endothelial cells. *Biochem Biophys Res Commun* 327:1114-23.
- Brown RC, Mark KS, Egleton RD, Davis TP (2004): Protection against hypoxia-induced blood-brain barrier disruption: changes in intracellular calcium. *Am J Physiol Cell Physiol* 286:C1045-52.
- Brown RC, O'Neil RG (2009): Mechanosensitive Calcium Fluxes in the Neurovascular Unit: TRP Channel Regulation of the Blood-Brain Barrier: "Mechanosensitivity of the Nervous System." Springer Netherlands, pp 321-343.
- Brown RC, Wu L, Hicks K, O'Neil R G (2008): Regulation of blood-brain barrier permeability by transient receptor potential type C and type v calcium-permeable channels. *Microcirculation* 15:359-71.
- Bruckener KE, el Baya A, Galla HJ, Schmidt MA (2003): Permeabilization in a cerebral endothelial barrier model by pertussis toxin involves the PKC effector pathway and is abolished by elevated levels of cAMP. *J Cell Sci* 116:1837-46.
- Bruzzone R, Barbe MT, Jakob NJ, Monyer H (2005): Pharmacological properties of homomeric and heteromeric pannexin hemichannels expressed in *Xenopus* oocytes. *J Neurochem* 92:1033-43.
- Bruzzone R, Haefliger JA, Gimlich RL, Paul DL (1993): Connexin40, a component of gap junctions in vascular endothelium, is restricted in its ability to interact with other connexins. *Mol Biol Cell* 4:7-20.
- Bruzzone R, Hormuzdi SG, Barbe MT, Herb A, Monyer H (2003): Pannexins, a family of gap junction proteins expressed in brain. *Proc Natl Acad Sci U S A* 100:13644-9.
- Bruzzone R, White TW, Paul DL (1996): Connections with connexins: the molecular basis of direct intercellular signaling. *Eur J Biochem* 238:1-27.
- Bruzzone S, Franco L, Guida L, Zocchi E, Contini P, Bisso A, Usai C, De Flora A (2001a): A self-restricted CD38-connexin 43 cross-talk affects NAD^{+} and cyclic ADP-ribose metabolism and regulates intracellular calcium in 3T3 fibroblasts. *J Biol Chem* 276:48300-8.
- Bruzzone S, Guida L, Zocchi E, Franco L, De Flora A (2001b): Connexin 43 hemi channels mediate Ca^{2+} -regulated transmembrane NAD^{+} fluxes in intact cells. *Faseb J* 15:10-12.
- Bukauskas FF, Bukauskiene A, Bennett MV, Verselis VK (2001): Gating properties of gap junction channels assembled from connexin43 and connexin43 fused with green fluorescent protein. *Biophys J* 81:137-52.
- Bukauskas FF, Elfgang C, Willecke K, Weingart R (1995): Biophysical properties of gap junction channels formed by mouse connexin40 in induced pairs of transfected human HeLa cells. *Biophys J* 68:2289-98.
- Bukauskas FF, Jordan K, Bukauskiene A, Bennett MV, Lampe PD, Laird DW, Verselis VK (2000): Clustering of connexin 43-enhanced green fluorescent protein gap junction channels and functional coupling in living cells. *Proc Natl Acad Sci U S A* 97:2556-61.
- Bukauskas FF, Kreuzberg MM, Rackauskas M, Bukauskiene A, Bennett MV, Verselis VK, Willecke K (2006): Properties of mouse connexin 30.2 and human connexin 31.9 hemichannels: implications for atrioventricular conduction in the heart. *Proc Natl Acad Sci U S A* 103:9726-31.
- Bukauskas FF, Verselis VK (2004): Gap junction channel gating. *Biochim Biophys Acta* 1662:42-60.
- Bundgaard M, Abbott NJ (2008): All vertebrates started out with a glial blood-brain barrier 4-500 million years ago. *Glia* 56:699-708.
- Burdyga T, Shmygol A, Eisner DA, Wray S (2003): A new technique for simultaneous and in situ measurements of Ca^{2+} signals in arteriolar smooth muscle and endothelial cells. *Cell Calcium* 34:27-33.
- Burgess GM, Godfrey PP, McKinney JS, Berridge MJ, Irvine RF, Putney JW, Jr. (1984): The second messenger linking receptor activation to internal Ca release in liver. *Nature* 309:63-6.
- Burleigh BA, Andrews NW (1998): Signaling and host cell invasion by *Trypanosoma cruzi*. *Curr Opin Microbiol* 1:461-5.
- Burr GS, Mitchell CK, Keflemariam YJ, Heidelberger R, O'Brien J (2005): Calcium-dependent binding of calmodulin to neuronal gap junction proteins. *Biochem Biophys Res Commun* 335:1191-8.
- Butt AM (1995): Effect of inflammatory agents on electrical resistance across the blood-brain barrier in pial microvessels of anaesthetized rats. *Brain Res* 696:145-50.

- Cai H, Liu D, Garcia JG (2008): CaM Kinase II-dependent pathophysiological signalling in endothelial cells. *Cardiovasc Res* 77:30-4.
- Calcraft PJ, Ruas M, Pan Z, Cheng X, Arredouani A, Hao X, Tang J, Rietdorf K, Teboul L, Chuang KT, Lin P, Xiao R, Wang C, Zhu Y, Lin Y, Wyatt CN, Parrington J, Ma J, Evans AM, Galione A, Zhu MX (2009): NAADP mobilizes calcium from acidic organelles through two-pore channels. *Nature* 459:596-600.
- Camello-Almaraz MC, Pozo MJ, Murphy MP, Camello PJ (2006): Mitochondrial production of oxidants is necessary for physiological calcium oscillations. *J Cell Physiol* 206:487-94.
- Cao F, Eckert R, Elfgang C, Nitsche JM, Snyder SA, DF Hu, Willecke K, Nicholson BJ (1998): A quantitative analysis of connexin-specific permeability differences of gap junctions expressed in HeLa transfectants and *Xenopus* oocytes. *J Cell Sci* 111 (Pt 1):31-43.
- Cardoso FL, Brites D, Brito MA (2010): Looking at the blood-brain barrier: molecular anatomy and possible investigation approaches. *Brain Res Rev* 64:328-63.
- Caride AJ, Filoteo AG, Penheiter AR, Paszty K, Enyedi A, Penniston JT (2001): Delayed activation of the plasma membrane calcium pump by a sudden increase in Ca²⁺: fast pumps reside in fast cells. *Cell Calcium* 30:49-57.
- Carman CV, Jun CD, Salas A, Springer TA (2003): Endothelial cells proactively form microvilli-like membrane projections upon intercellular adhesion molecule 1 engagement of leukocyte LFA-1. *J Immunol* 171:6135-44.
- Carman CV, Sage PT, Sciuto TE, de la Fuente MA, Geha RS, Ochs HD, Dvorak HF, Dvorak AM, Springer TA (2007): Transcellular diapedesis is initiated by invasive podosomes. *Immunity* 26:784-97.
- Carman CV, Springer TA (2004): A transmigratory cup in leukocyte diapedesis both through individual vascular endothelial cells and between them. *J Cell Biol* 167:377-88.
- Carter TD, Bogle RG, Bjaaland T (1991): Spiking of intracellular calcium ion concentration in single cultured pig aortic endothelial cells stimulated with ATP or bradykinin. *Biochem J* 278 (Pt 3):697-704.
- Case RM, Eisner D, Gurney A, Jones O, Muallem S, Verkhratsky A (2007): Evolution of calcium homeostasis: from birth of the first cell to an omnipresent signalling system. *Cell Calcium* 42:345-50.
- Casey JR, Grinstein S, Orlowski J (2010): Sensors and regulators of intracellular pH. *Nat Rev Mol Cell Biol* 11:50-61.
- Cecchelli R, Dehouck B, Descamps L, Fenart L, Buee-Scherrer VV, Duhem C, Lundquist S, Rentfel M, Torpier G, Dehouck MP (1999): In vitro model for evaluating drug transport across the blood-brain barrier. *Adv Drug Deliv Rev* 36:165-178.
- Chalmers S, McCarron JG (2008): The mitochondrial membrane potential and Ca²⁺ oscillations in smooth muscle. *J Cell Sci* 121:75-85.
- Chanson M, Mollard P, Meda P, Suter S, Jongsma HJ (1999): Modulation of pancreatic acinar cell to cell coupling during ACh-evoked changes in cytosolic Ca²⁺. *J Biol Chem* 274:282-7.
- Charles AC, Merrill JE, Dirksen ER, Sanderson MJ (1991): Intercellular signaling in glial cells: calcium waves and oscillations in response to mechanical stimulation and glutamate. *Neuron* 6:983-92.
- Chatton JY, Liu H, Stucki JW (1995): Simultaneous measurements of Ca²⁺ in the intracellular stores and the cytosol of hepatocytes during hormone-induced Ca²⁺ oscillations. *FEBS Lett* 368:165-8.
- Chaytor AT, Evans WH, Griffith TM (1997): Peptides homologous to extracellular loop motifs of connexin 43 reversibly abolish rhythmic contractile activity in rabbit arteries. *J Physiol* 503 (Pt 1):99-110.
- Chekeni FB, Elliott MR, Sandilos JK, Walk SF, Kinchen JM, Lazarowski ER, Armstrong AJ, Penuela S, Laird DW, Salvesen GS, Isakson BE, Bayliss DA, Ravichandran KS (2010): Pannexin 1 channels mediate 'find-me' signal release and membrane permeability during apoptosis. *Nature* 467:863-7.
- Chen Y, McCarron RM, Golech S, Bembry J, Ford B, Lenz FA, Azzam N, Spatz M (2003): ET-1- and NO-mediated signal transduction pathway in human brain capillary endothelial cells. *Am J Physiol Cell Physiol* 284:C243-9.
- Chi F, Jong TD, Wang L, Ouyang Y, Wu C, Li W, Huang SH (2010): Vimentin-mediated signalling is required for IbeA+ *E. coli* K1 invasion of human brain microvascular endothelial cells. *Biochem J* 427:79-90.
- Chuang CF, Vanhoven MK, Fetter RD, Verselis VK, Bargmann CI (2007): An innexin-dependent cell network establishes left-right neuronal asymmetry in *C. elegans*. *Cell* 129:787-99.
- Churchill GC, Louis CF (1998): Roles of Ca²⁺, inositol trisphosphate and cyclic ADP-ribose in mediating intercellular Ca²⁺ signaling in sheep lens cells. *J Cell Sci* 111 (Pt 9):1217-25.
- Churchill GC, Lurtz MM, Louis CF (2001): Ca(2+) regulation of gap junctional coupling in lens epithelial cells. *Am J Physiol Cell Physiol* 281:C972-81.
- Clarke TC, Williams OJ, Martin PE, Evans WH (2009): ATP release by cardiac myocytes in a simulated ischaemia model: inhibition by a connexin mimetic and enhancement by an antiarrhythmic peptide. *Eur J Pharmacol* 605:9-14.
- Codazzi F, Teruel MN, Meyer T (2001): Control of astrocyte Ca(2+) oscillations and waves by oscillating translocation and activation of protein kinase C. *Curr Biol* 11:1089-97.

- Colegrove SL, Albrecht MA, Friel DD (2000): Quantitative analysis of mitochondrial Ca²⁺ uptake and release pathways in sympathetic neurons. Reconstruction of the recovery after depolarization-evoked [Ca²⁺]_i elevations. *J Gen Physiol* 115:371-88.
- Collard CD, Park KA, Montalto MC, Alapati S, Buras JA, Stahl GL, Colgan SP (2002): Neutrophil-derived glutamate regulates vascular endothelial barrier function. *J Biol Chem* 277:14801-11.
- Collins TJ, Lipp P, Berridge MJ, Bootman MD (2001): Mitochondrial Ca(2+) uptake depends on the spatial and temporal profile of cytosolic Ca(2+) signals. *J Biol Chem* 276:26411-20.
- Colosetti P, Tunwell RE, Cruttwell C, Arsanto JP, Mauger JP, Cassio D (2003): The type 3 inositol 1,4,5-trisphosphate receptor is concentrated at the tight junction level in polarized MDCK cells. *J Cell Sci* 116:2791-803.
- Comerford KM, Lawrence DW, Synnestvedt K, Levi BP, Colgan SP (2002): Role of vasodilator-stimulated phosphoprotein in PKA-induced changes in endothelial junctional permeability. *Faseb J* 16:583-5.
- Contreras JE, Saez JC, Bukauskas FF, Bennett MV (2003): Gating and regulation of connexin 43 (Cx43) hemichannels. *Proc Natl Acad Sci U S A* 100:11388-93.
- Contreras JE, Sanchez HA, Eugenin EA, Speidel D, Theis M, Willecke K, Bukauskas FF, Bennett MV, Saez JC (2002): Metabolic inhibition induces opening of unapposed connexin 43 gap junction hemichannels and reduces gap junctional communication in cortical astrocytes in culture. *Proc Natl Acad Sci U S A* 99:495-500.
- Cotrina ML, Kang J, Lin JH, Bueno E, Hansen TW, He L, Liu Y, Nedergaard M (1998a): Astrocytic gap junctions remain open during ischemic conditions. *J Neurosci* 18:2520-37.
- Cotrina ML, Lin JH, Alves-Rodrigues A, Liu S, Li J, Azmi-Ghadimi H, Kang J, Naus CC, Nedergaard M (1998b): Connexins regulate calcium signaling by controlling ATP release. *Proc Natl Acad Sci U S A* 95:15735-40.
- Cottrell GT, Lin R, Warn-Cramer BJ, Lau AF, Burt JM (2003): Mechanism of v-Src- and mitogen-activated protein kinase-induced reduction of gap junction communication. *Am J Physiol Cell Physiol* 284:C511-20.
- Crawford LE, Milliken EE, Irani K, Zweier JL, Becker LC, Johnson TM, Eissa NT, Crystal RG, Finkel T, Goldschmidt-Clermont PJ (1996): Superoxide-mediated actin response in post-hypoxic endothelial cells. *J Biol Chem* 271:26863-7.
- Crisuolo GR, Lelkes PI, Rotrosen D, Oldfield EH (1989): Cytosolic calcium changes in endothelial cells induced by a protein product of human gliomas containing vascular permeability factor activity. *J Neurosurg* 71:884-91.
- Crow JM, Atkinson MM, Johnson RG (1994): Micromolar levels of intracellular calcium reduce gap junctional permeability in lens cultures. *Invest Ophthalmol Vis Sci* 35:3332-41.
- Cruciani V, Mikalsen SO (2006): The vertebrate connexin family. *Cell Mol Life Sci* 63:1125-40.
- Csordas G, Renken C, Varnai P, Walter L, Weaver D, Buttle KF, Balla T, Mannella CA, Hajnoczky G (2006): Structural and functional features and significance of the physical linkage between ER and mitochondria. *J Cell Biol* 174:915-21.
- Dahl G, Levine E, Rabadan-Diehl C, Werner R (1991): Cell/cell channel formation involves disulfide exchange. *Eur J Biochem* 197:141-4.
- Dahl G, Werner R, Levine E, Rabadan-Diehl C (1992): Mutational analysis of gap junction formation. *Biophys J* 62:172-80; discussion 180-2.
- Dakin K, Li WH (2006): Local Ca²⁺ rise near store operated Ca²⁺ channels inhibits cell coupling during capacitative Ca²⁺ influx. *Cell Commun Adhes* 13:29-39.
- Dakin K, Zhao Y, Li WH (2005): LAMP, a new imaging assay of gap junctional communication unveils that Ca²⁺ influx inhibits cell coupling. *Nat Methods* 2:55-62.
- D'Ambrosi N, Iafrate M, Saba E, Rosa P, Volonte C (2007): Comparative analysis of P2Y4 and P2Y6 receptor architecture in native and transfected neuronal systems. *Biochim Biophys Acta* 1768:1592-9.
- Das Sarma J, Wang F, Koval M (2002): Targeted gap junction protein constructs reveal connexin-specific differences in oligomerization. *J Biol Chem* 277:20911-8.
- Davalos D, Grutzendler J, Yang G, Kim JV, Zuo Y, Jung S, Littman DR, Dustin ML, Gan WB (2005): ATP mediates rapid microglial response to local brain injury in vivo. *Nat Neurosci* 8:752-8.
- D'Aversa TG, Eugenin EA, Lopez L, Berman JW (2012): Myelin Basic Protein Induces Inflammatory Mediators from Primary Human Endothelial Cells and Blood-Brain-Barrier Disruption: Implications for the Pathogenesis of Multiple Sclerosis. *Neuropathol Appl Neurobiol*.
- Davidson JO, Green CR, LF BN, O'Carroll SJ, Fraser M, Bennet L, Jan Gunn A (2012): Connexin hemichannel blockade improves outcomes in a model of fetal ischemia. *Ann Neurol* 71:121-32.
- Davidson JS, Baumgarten IM (1988): Glycyrrhetic acid derivatives: a novel class of inhibitors of gap-junctional intercellular communication. Structure-activity relationships. *J Pharmacol Exp Ther* 246:1104-7.
- Davies DC (2002): Blood-brain barrier breakdown in septic encephalopathy and brain tumours. *J Anat* 200:639-46.

- Davis B, Tang J, Zhang L, Mu D, Jiang X, Biran V, Vexler Z, Ferriero DM (2010): Role of vasodilator stimulated phosphoprotein in VEGF induced blood-brain barrier permeability in endothelial cell monolayers. *Int J Dev Neurosci*.
- Davis RJ, Challiss J, Nahorski SR (1999): Enhanced purinoceptor-mediated Ca^{2+} signalling in L-fibroblasts overexpressing type 1 inositol 1,4,5-trisphosphate receptors. *Biochem J* 341 (Pt 3):813-20.
- Dawson AP (1997): Calcium signalling: how do IP3 receptors work? *Curr Biol* 7:R544-7.
- De Blasio BF, Iversen JG, Rottingen JA (2004a): Intercellular calcium signalling in cultured renal epithelia: a theoretical study of synchronization mode and pacemaker activity. *Eur Biophys J* 33:657-70.
- De Blasio BF, Rottingen JA, Sand KL, Giaever I, Iversen JG (2004b): Global, synchronous oscillations in cytosolic calcium and adherence in bradykinin-stimulated Madin-Darby canine kidney cells. *Acta Physiol Scand* 180:335-46.
- De Bock M, Culot M, Wang N, Bol M, Decrock E, De Vuyst E, da Costa A, Dauwe I, Vinken M, Simon AM, Rogiers V, De Ley G, Evans WH, Bultynck G, Dupont G, Cecchelli R, Leybaert L (2011): Connexin channels provide a target to manipulate brain endothelial calcium dynamics and blood-brain barrier permeability. *J Cereb Blood Flow Metab* 31:1942-1957.
- De Koninck P, Schulman H (1998): Sensitivity of CaM kinase II to the frequency of Ca^{2+} oscillations. *Science* 279:227-30.
- De Pitta M, Volman V, Levine H, Ben-Jacob E (2009): Multimodal encoding in a simplified model of intracellular calcium signaling. *Cogn Process* 10 Suppl 1:S55-70.
- De Vuyst E, De Bock M, Decrock E, Van Moorhem M, Naus C, Mabilde C, Leybaert L (2008): In situ bipolar electroporation for localized cell loading with reporter dyes and investigating gap junctional coupling. *Biophys J* 94:469-79.
- De Vuyst E, Decrock E, Cabooter L, DUBYAK GR, Naus CC, Evans WH, Leybaert L (2006): Intracellular calcium changes trigger connexin 32 hemichannel opening. *Embo J* 25:34-44.
- De Vuyst E, Decrock E, De Bock M, Yamasaki H, Naus CC, Evans WH, Leybaert L (2007): Connexin hemichannels and gap junction channels are differentially influenced by lipopolysaccharide and basic fibroblast growth factor. *Mol Biol Cell* 18:34-46.
- De Vuyst E, Wang N, Decrock E, De Bock M, Vinken M, Van Moorhem M, Lai C, Culot M, Rogiers V, Cecchelli R, Naus CC, Evans WH, Leybaert L (2009): Ca^{2+} regulation of connexin 43 hemichannels in C6 glioma and glial cells. *Cell Calcium* 46:176-87.
- de Weerd WF, Leeb-Lundberg LM (1997): Bradykinin sequesters B2 bradykinin receptors and the receptor-coupled G α subunits G α q and G α i in caveolae in DDT1 MF-2 smooth muscle cells. *J Biol Chem* 272:17858-66.
- De Young GW, Keizer J (1992): A single-pool inositol 1,4,5-trisphosphate-receptor-based model for agonist-stimulated oscillations in Ca^{2+} concentration. *Proc Natl Acad Sci U S A* 89:9895-9.
- Decrock E, De Vuyst E, Vinken M, Van Moorhem M, Vranckx K, Wang N, Van Laeken L, De Bock M, D'Herde K, Lai CP, Rogiers V, Evans WH, Naus CC, Leybaert L (2009): Connexin 43 hemichannels contribute to the propagation of apoptotic cell death in a rat C6 glioma cell model. *Cell Death Differ* 16:151-63.
- Dejana E (2004): Endothelial cell-cell junctions: happy together. *Nat Rev Mol Cell Biol* 5:261-70.
- Dejana E, Spagnuolo R, Bazzoni G (2001): Interendothelial junctions and their role in the control of angiogenesis, vascular permeability and leukocyte transmigration. *Thromb Haemost* 86:308-15.
- Dejana E, Tournier-Lasserre E, Weinstein BM (2009): The control of vascular integrity by endothelial cell junctions: molecular basis and pathological implications. *Dev Cell* 16:209-21.
- Deli MA, Joo F, Krizbai I, Lengyel I, Nunzi MG, Wolff JR (1993): Calcium/calmodulin-stimulated protein kinase II is present in primary cultures of cerebral endothelial cells. *J Neurochem* 60:1960-3.
- Dellen BK, Barber MJ, Ristig ML, Hescheler J, Sauer H, Wartenberg M (2005): $[Ca^{2+}]$ oscillations in a model of energy-dependent Ca^{2+} uptake by the endoplasmic reticulum. *J Theor Biol* 237:279-90.
- Demer LL, Wortham CM, Dirksen ER, Sanderson MJ (1993): Mechanical stimulation induces intercellular calcium signaling in bovine aortic endothelial cells. *Am J Physiol* 264:H2094-102.
- Derangeon M, Spray DC, Bourmeyster N, Sarrouilhe D, Herve JC (2009): Reciprocal influence of connexins and apical junction proteins on their expressions and functions. *Biochim Biophys Acta* 1788:768-78.
- Dermietzel R, Meier C, Bukauskas F, Spray DC (2003): Following tracks of hemichannels. *Cell Commun Adhes* 10:335-40.
- Descamps L, Coisne C, Dehouck B, Cecchelli R, Torpier G (2003): Protective effect of glial cells against lipopolysaccharide-mediated blood-brain barrier injury. *Glia* 42:46-58.
- DeVries SH, Schwartz EA (1992): Hemi-gap-junction channels in solitary horizontal cells of the catfish retina. *J Physiol* 445:201-30.

- Dhein S, Duerrschmidt N, Scholl A, Boldt A, Schulte JS, Pfanmuller B, Rojas-Gomez D, Scheffler A, Haefliger JA, Doll N, Mohr FW (2008): A new role for extracellular Ca²⁺ in gap-junction remodeling: studies in humans and rats. *Naunyn Schmiedebergs Arch Pharmacol* 377:125-38.
- D'Hondt C, Ponsaerts R, De Smedt H, Vinken M, De Vuyst E, De Bock M, Wang N, Rogiers V, Leybaert L, Himpens B, Bultynck G (2011): Pannexin channels in ATP release and beyond: An unexpected rendezvous at the endoplasmic reticulum. *Cell Signal* 23:305-16.
- D'Hondt C, Ponsaerts R, Srinivas SP, Vereecke J, Himpens B (2007a): Thrombin inhibits intercellular calcium wave propagation in corneal endothelial cells by modulation of hemichannels and gap junctions. *Invest Ophthalmol Vis Sci* 48:120-33.
- D'Hondt C, Srinivas SP, Vereecke J, Himpens B (2007b): Adenosine opposes thrombin-induced inhibition of intercellular calcium wave in corneal endothelial cells. *Invest Ophthalmol Vis Sci* 48:1518-27.
- Di Capite J, Ng SW, Parekh AB (2009): Decoding of cytoplasmic Ca²⁺ oscillations through the spatial signature drives gene expression. *Curr Biol* 19:853-8.
- Didier N, Romero IA, Creminon C, Wijkhuisen A, Grassi J, Mabondzo A (2003): Secretion of interleukin-1beta by astrocytes mediates endothelin-1 and tumour necrosis factor-alpha effects on human brain microvascular endothelial cell permeability. *J Neurochem* 86:246-54.
- Doctrow SR, Abelleira SM, Curry LA, Heller-Harrison R, Kozarich JW, Malfroy B, McCarroll LA, Morgan KG, Morrow AR, Musso GF (1994): The bradykinin analog RMP-7 increases intracellular free calcium levels in rat brain microvascular endothelial cells. *J Pharmacol Exp Ther* 271:229-37.
- Dodelet-Devillers A, Cayrol R, van Horssen J, Haqqani AS, de Vries HE, Engelhardt B, Greenwood J, Prat A (2009): Functions of lipid raft membrane microdomains at the blood-brain barrier. *J Mol Med* 87:765-74.
- Dohgu S, Takata F, Yamauchi A, Nakagawa S, Egawa T, Naito M, Tsuruo T, Sawada Y, Niwa M, Kataoka Y (2005): Brain pericytes contribute to the induction and up-regulation of blood-brain barrier functions through transforming growth factor-beta production. *Brain Res* 1038:208-15.
- Dolmetsch RE, Lewis RS (1994): Signaling between intracellular Ca²⁺ stores and depletion-activated Ca²⁺ channels generates [Ca²⁺]_i oscillations in T lymphocytes. *J Gen Physiol* 103:365-88.
- Dolmetsch RE, Xu K, Lewis RS (1998): Calcium oscillations increase the efficiency and specificity of gene expression. *Nature* 392:933-6.
- Domenighetti AA, Beny JL, Chabaud F, Frieden M (1998): An intercellular regenerative calcium wave in porcine coronary artery endothelial cells in primary culture. *J Physiol* 513 (Pt 1):103-16.
- Du F, Saitoh F, Tian QB, Miyazawa S, Endo S, Suzuki T (2006): Mechanisms for association of Ca²⁺/calmodulin-dependent protein kinase II with lipid rafts. *Biochem Biophys Res Commun* 347:814-20.
- Ducret E, Alexopoulos H, Le Feuvre Y, Davies JA, Meyrand P, Bacon JP, Fenelon VS (2006): Innexins in the lobster stomatogastric nervous system: cloning, phylogenetic analysis, developmental changes and expression within adult identified dye and electrically coupled neurons. *Eur J Neurosci* 24:3119-33.
- Duffy HS, Delmar M, Spray DC (2002): Formation of the gap junction nexus: binding partners for connexins. *J Physiol Paris* 96:243-9.
- Dupont G, Combettes L, Bird GS, Putney JW (2010): Calcium Oscillations. *Cold Spring Harb Perspect Biol*.
- Dupont G, Combettes L, Leybaert L (2007): Calcium dynamics: spatio-temporal organization from the subcellular to the organ level. *Int Rev Cytol* 261:193-245.
- Dupont G, Goldbeter A (1998): CaM kinase II as frequency decoder of Ca²⁺ oscillations. *Bioessays* 20:607-10.
- Dykes IM, Freeman FM, Bacon JP, Davies JA (2004): Molecular basis of gap junctional communication in the CNS of the leech *Hirudo medicinalis*. *J Neurosci* 24:886-94.
- Easton AS, Abbott NJ (2002): Bradykinin increases permeability by calcium and 5-lipoxygenase in the ECV304/C6 cell culture model of the blood-brain barrier. *Brain Res* 953:157-69.
- Ebihara L, Liu X, Pal JD (2003): Effect of external magnesium and calcium on human connexin46 hemichannels. *Biophys J* 84:277-86.
- Ebihara L, Steiner E (1993): Properties of a nonjunctional current expressed from a rat connexin46 cDNA in *Xenopus* oocytes. *J Gen Physiol* 102:59-74.
- Ebnet K, Suzuki A, Ohno S, Vestweber D (2004): Junctional adhesion molecules (JAMs): more molecules with dual functions? *J Cell Sci* 117:19-29.
- Eckert R (2002): pH gating of lens fibre connexins. *Pflugers Arch* 443:843-51.
- Edwards A, Pallone TL (2008): Mechanisms underlying angiotensin II-induced calcium oscillations. *Am J Physiol Renal Physiol* 295:F568-84.
- Ek CJ, Dziegielewska KM, Stolp H, Saunders NR (2006): Functional effectiveness of the blood-brain barrier to small water-soluble molecules in developing and adult opossum (*Monodelphis domestica*). *J Comp Neurol* 496:13-26.
- Ek JF, Delmar M, Perzova R, Taffet SM (1994): Role of histidine 95 on pH gating of the cardiac gap junction protein connexin43. *Circ Res* 74:1058-64.

- Ek-Vitorin JF, Calero G, Morley GE, Coombs W, Taffet SM, Delmar M (1996): PH regulation of connexin43: molecular analysis of the gating particle. *Biophys J* 71:1273-84.
- Elfgang C, Eckert R, Lichtenberg-Frate H, Butterweck A, Traub O, Klein RA, Hulser DF, Willecke K (1995): Specific permeability and selective formation of gap junction channels in connexin-transfected HeLa cells. *J Cell Biol* 129:805-17.
- Eltzschig HK, Eckle T, Mager A, Kuper N, Karcher C, Weissmuller T, Boengler K, Schulz R, Robson SC, Colgan SP (2006): ATP release from activated neutrophils occurs via connexin 43 and modulates adenosine-dependent endothelial cell function. *Circ Res* 99:1100-8.
- Engelhardt B (2003): Development of the blood-brain barrier. *Cell Tissue Res* 314:119-29.
- Eskandari S, Zampighi GA, Leung DW, Wright EM, Loo DD (2002): Inhibition of gap junction hemichannels by chloride channel blockers. *J Membr Biol* 185:93-102.
- Estrada M, Espinosa A, Gibson CJ, Uhlen P, Jaimovich E (2005): Capacitative calcium entry in testosterone-induced intracellular calcium oscillations in myotubes. *J Endocrinol* 184:371-9.
- Etienne-Manneville S, Manneville JB, Adamson P, Wilbourn B, Greenwood J, Couraud PO (2000): ICAM-1-coupled cytoskeletal rearrangements and transendothelial lymphocyte migration involve intracellular calcium signaling in brain endothelial cell lines. *J Immunol* 165:3375-83.
- Eugenin EA, Eckardt D, Theis M, Willecke K, Bennett MV, Saez JC (2001): Microglia at brain stab wounds express connexin 43 and in vitro form functional gap junctions after treatment with interferon-gamma and tumor necrosis factor-alpha. *Proc Natl Acad Sci U S A* 98:4190-5.
- Evanko DS, Zhang Q, Zorec R, Haydon PG (2004): Defining pathways of loss and secretion of chemical messengers from astrocytes. *Glia* 47:233-40.
- Evans WH, De Vuyst E, Leybaert L (2006): The gap junction cellular internet: connexin hemichannels enter the signalling limelight. *Biochem J* 397:1-14.
- Evans WH, Leybaert L (2007): Mimetic peptides as blockers of connexin channel-facilitated intercellular communication. *Cell Commun Adhes* 14:265-73.
- Falcke M, Hudson JL, Camacho P, Lechleiter JD (1999): Impact of mitochondrial Ca²⁺ cycling on pattern formation and stability. *Biophys J* 77:37-44.
- Falk MM (2000): Connexin-specific distribution within gap junctions revealed in living cells. *J Cell Sci* 113 (Pt 22):4109-20.
- Falk MM, Buehler LK, Kumar NM, Gilula NB (1997): Cell-free synthesis and assembly of connexins into functional gap junction membrane channels. *Embo J* 16:2703-16.
- Faria RX, Reis RA, Casabulho CM, Alberto AV, de Farias FP, Henriques-Pons A, Alves LA (2009): Pharmacological properties of a pore induced by raising intracellular Ca²⁺. *Am J Physiol Cell Physiol* 297:C28-42.
- Feolde E, Vigne P, Breittmayer JP, Frelin C (1995): ATP, a partial agonist of atypical P2Y purinoceptors in rat brain microvascular endothelial cells. *Br J Pharmacol* 115:1199-203.
- Ferris CD, Haganir RL, Bredt DS, Cameron AM, Snyder SH (1991): Inositol trisphosphate receptor: phosphorylation by protein kinase C and calcium calmodulin-dependent protein kinases in reconstituted lipid vesicles. *Proc Natl Acad Sci U S A* 88:2232-5.
- Ferris CD, Haganir RL, Snyder SH (1990): Calcium flux mediated by purified inositol 1,4,5-trisphosphate receptor in reconstituted lipid vesicles is allosterically regulated by adenine nucleotides. *Proc Natl Acad Sci U S A* 87:2147-51.
- Feske S, Gwack Y, Prakriya M, Srikanth S, Puppel SH, Tanasa B, Hogan PG, Lewis RS, Daly M, Rao A (2006): A mutation in Orai1 causes immune deficiency by abrogating CRAC channel function. *Nature* 441:179-85.
- Fioretti B, Franciolini F, Catacuzzeno L (2005): A model of intracellular Ca²⁺ oscillations based on the activity of the intermediate-conductance Ca²⁺-activated K⁺ channels. *Biophys Chem* 113:17-23.
- Firek L, Weingart R (1995): Modification of gap junction conductance by divalent cations and protons in neonatal rat heart cells. *J Mol Cell Cardiol* 27:1633-43.
- Fischer D, Kissel T (2001): Histochemical characterization of primary capillary endothelial cells from porcine brains using monoclonal antibodies and fluorescein isothiocyanate-labelled lectins: implications for drug delivery. *Eur J Pharm Biopharm* 52:1-11.
- Fischer S, Clauss M, Wiesnet M, Renz D, Schaper W, Karliczek GF (1999): Hypoxia induces permeability in brain microvessel endothelial cells via VEGF and NO. *Am J Physiol* 276:C812-20.
- Fischer S, Nishio M, Peters SC, Tschernatsch M, Walberer M, Weidemann S, Heidenreich R, Couraud PO, Weksler BB, Romero IA, Gerriets T, Preissner KT (2009): Signaling mechanism of extracellular RNA in endothelial cells. *Faseb J* 23:2100-9.
- Fischer S, Wiesnet M, Marti HH, Renz D, Schaper W (2004): Simultaneous activation of several second messengers in hypoxia-induced hyperpermeability of brain derived endothelial cells. *J Cell Physiol* 198:359-69.

- Fischer S, Wiesnet M, Renz D, Schaper W (2005): H₂O₂ induces paracellular permeability of porcine brain-derived microvascular endothelial cells by activation of the p44/42 MAP kinase pathway. *Eur J Cell Biol* 84:687-97.
- Fleegal MA, Hom S, Borg LK, Davis TP (2005): Activation of PKC modulates blood-brain barrier endothelial cell permeability changes induced by hypoxia and posthypoxic reoxygenation. *Am J Physiol Heart Circ Physiol* 289:H2012-9.
- Foote CI, Zhou L, Zhu X, Nicholson BJ (1998): The pattern of disulfide linkages in the extracellular loop regions of connexin 32 suggests a model for the docking interface of gap junctions. *J Cell Biol* 140:1187-97.
- Foskett JK, Wong DC (1994): [Ca²⁺]_i inhibition of Ca²⁺ release-activated Ca²⁺ influx underlies agonist- and thapsigargin-induced [Ca²⁺]_i oscillations in salivary acinar cells. *J Biol Chem* 269:31525-32.
- Franco L, Zocchi E, Usai C, Guida L, Bruzzone S, Costa A, De Flora A (2001): Paracrine roles of NAD⁺ and cyclic ADP-ribose in increasing intracellular calcium and enhancing cell proliferation of 3T3 fibroblasts. *J Biol Chem* 276:21642-8.
- Fukami K, Inanobe S, Kanemaru K, Nakamura Y (2010): Phospholipase C is a key enzyme regulating intracellular calcium and modulating the phosphoinositide balance. *Prog Lipid Res* 49:429-37.
- Furuse M, Hirase T, Itoh M, Nagafuchi A, Yonemura S, Tsukita S (1993): Occludin: a novel integral membrane protein localizing at tight junctions. *J Cell Biol* 123:1777-88.
- Furuse M, Sasaki H, Fujimoto K, Tsukita S (1998): A single gene product, claudin-1 or -2, reconstitutes tight junction strands and recruits occludin in fibroblasts. *J Cell Biol* 143:391-401.
- Furuse M, Sasaki H, Tsukita S (1999): Manner of interaction of heterogeneous claudin species within and between tight junction strands. *J Cell Biol* 147:891-903.
- Gabriels JE, Paul DL (1998): Connexin43 is highly localized to sites of disturbed flow in rat aortic endothelium but connexin37 and connexin40 are more uniformly distributed. *Circ Res* 83:636-43.
- Gaietta G, Deerinck TJ, Adams SR, Bouwer J, Tour O, Laird DW, Sosinsky GE, Tsien RY, Ellisman MH (2002): Multicolor and electron microscopic imaging of connexin trafficking. *Science* 296:503-7.
- Galione A (1994): Cyclic ADP-ribose, the ADP-ribosyl cyclase pathway and calcium signalling. *Mol Cell Endocrinol* 98:125-31.
- Galione A, Cui Y, Empson R, Iino S, Wilson H, Terrar D (1998): Cyclic ADP-ribose and the regulation of calcium-induced calcium release in eggs and cardiac myocytes. *Cell Biochem Biophys* 28:19-30.
- Galione A, Evans AM, Ma J, Parrington J, Arredouani A, Cheng X, Zhu MX (2009): The acid test: the discovery of two-pore channels (TPCs) as NAADP-gated endolysosomal Ca²⁺ release channels. *Pflugers Arch* 458:869-76.
- Garberg P, Ball M, Borg N, Cecchelli R, Fenart L, Hurst RD, Lindmark T, Mabondzo A, Nilsson JE, Raub TJ, Stanimirovic D, Terasaki T, Oberg JO, Osetrberg T (2005): In vitro models of the blood-brain barrier. *Toxicol in vitro* 19: 299-334.
- Garcia CM, Darland DC, Massingham LJ, D'Amore PA (2004): Endothelial cell-astrocyte interactions and TGF beta are required for induction of blood-neural barrier properties. *Brain Res Dev Brain Res* 152:25-38.
- Garcia JG, Davis HW, Patterson CE (1995): Regulation of endothelial cell gap formation and barrier dysfunction: role of myosin light chain phosphorylation. *J Cell Physiol* 163:510-22.
- Garcia JG, Verin AD, Schaphorst K, Siddiqui R, Patterson CE, Csontos C, Natarajan V (1999): Regulation of endothelial cell myosin light chain kinase by Rho, cortactin, and p60(src). *Am J Physiol* 276:L989-98.
- Gaudreault N, Perrin RM, Guo M, Clanton CP, Wu MH, Yuan SY (2008): Counter regulatory effects of PKCbetaII and PKCdelta on coronary endothelial permeability. *Arterioscler Thromb Vasc Biol* 28:1527-33.
- Ge S, Song L, Pachter JS (2005): Where is the blood-brain barrier ... really? *J Neurosci Res* 79:421-7.
- Gherzi-Egea JF, Leininger-Muller B, Cecchelli R, Fenstermacher JD (1995): Blood-brain interfaces: relevance to cerebral drug metabolism. *Toxicol Lett* 82-83:645-53.
- Giaume C, Fromaget C, el Aoumari A, Cordier J, Glowinski J, Gros D (1991): Gap junctions in cultured astrocytes: single-channel currents and characterization of channel-forming protein. *Neuron* 6:133-43.
- Giaume C, Theis M (2010): Pharmacological and genetic approaches to study connexin-mediated channels in glial cells of the central nervous system. *Brain Res Rev* 63:160-76.
- Giepmans BN, Moolenaar WH (1998): The gap junction protein connexin43 interacts with the second PDZ domain of the zona occludens-1 protein. *Curr Biol* 8:931-4.
- Giovannucci DR, Groblewski GE, Sneyd J, Yule DI (2000): Targeted phosphorylation of inositol 1,4,5-trisphosphate receptors selectively inhibits localized Ca²⁺ release and shapes oscillatory Ca²⁺ signals. *J Biol Chem* 275:33704-11.
- Goeckeler ZM, Wysolmerski RB (1995): Myosin light chain kinase-regulated endothelial cell contraction: the relationship between isometric tension, actin polymerization, and myosin phosphorylation. *J Cell Biol* 130:613-27.
- Goldberg GS, Lampe PD, Nicholson BJ (1999): Selective transfer of endogenous metabolites through gap junctions composed of different connexins. *Nat Cell Biol* 1:457-9.

- Goldberg GS, Moreno AP, Bechberger JF, Hearn SS, Shivers RR, MacPhee DJ, Zhang YC, Naus CC (1996): Evidence that disruption of connexon particle arrangements in gap junction plaques is associated with inhibition of gap junctional communication by a glycyrrhetic acid derivative. *Exp Cell Res* 222:48-53.
- Goldberg GS, Moreno AP, Lampe PD (2002): Gap junctions between cells expressing connexin 43 or 32 show inverse permselectivity to adenosine and ATP. *J Biol Chem* 277:36725-30.
- Goldberg GS, Valiunas V, Brink PR (2004): Selective permeability of gap junction channels. *Biochim Biophys Acta* 1662:96-101.
- Goldberg M, De Pitta M, Volman V, Berry H, Ben-Jacob E (2010): Nonlinear gap junctions enable long-distance propagation of pulsating calcium waves in astrocyte networks. *PLoS Comput Biol* 6.
- Goldbeter A, Dupont G, Berridge MJ (1990): Minimal model for signal-induced Ca²⁺ oscillations and for their frequency encoding through protein phosphorylation. *Proc Natl Acad Sci U S A* 87:1461-5.
- Goldman RD, Khuon S, Chou YH, Opal P, Steinert PM (1996): The function of intermediate filaments in cell shape and cytoskeletal integrity. *J Cell Biol* 134:971-83.
- Golovina VA (2005): Visualization of localized store-operated calcium entry in mouse astrocytes. Close proximity to the endoplasmic reticulum. *J Physiol* 564:737-49.
- Gomes P, Srinivas SP, Van Driessche W, Vereecke J, Himpens B (2005): ATP release through connexin hemichannels in corneal endothelial cells. *Invest Ophthalmol Vis Sci* 46:1208-18.
- Gomes P, Srinivas SP, Vereecke J, Himpens B (2006): Gap junctional intercellular communication in bovine corneal endothelial cells. *Exp Eye Res* 83:1225-37.
- Gomez-Hernandez JM, de Miguel M, Larrosa B, Gonzalez D, Barrio LC (2003): Molecular basis of calcium regulation in connexin-32 hemichannels. *Proc Natl Acad Sci U S A* 100:16030-5.
- Gong XQ, Nicholson BJ (2001): Size selectivity between gap junction channels composed of different connexins. *Cell Commun Adhes* 8:187-92.
- Gonzalez D, Gomez-Hernandez JM, Barrio LC (2006): Species specificity of mammalian connexin-26 to form open voltage-gated hemichannels. *Faseb J* 20:2329-38.
- Gonzalez D, Gomez-Hernandez JM, Barrio LC (2007): Molecular basis of voltage dependence of connexin channels: an integrative appraisal. *Prog Biophys Mol Biol* 94:66-106.
- Gossman DG, Zhao HB (2008): Hemichannel-mediated inositol 1,4,5-trisphosphate (IP₃) release in the cochlea: a novel mechanism of IP₃ intercellular signaling. *Cell Commun Adhes* 15:305-15.
- Gourdie RG, Ghatnekar GS, O'Quinn M, Rhatt MJ, Barker RJ, Zhu C, Jourdan J, Hunter AW (2006): The unstoppable connexin43 carboxyl-terminus: new roles in gap junction organization and wound healing. *Ann N Y Acad Sci* 1080:49-62.
- Grab DJ, Garcia-Garcia JC, Nikolskaia OV, Kim YV, Brown A, Pardo CA, Zhang Y, Becker KG, Wilson BA, de ALAP, Scharfstein J, Dumler JS (2009a): Protease activated receptor signaling is required for African trypanosome traversal of human brain microvascular endothelial cells. *PLoS Negl Trop Dis* 3:e479.
- Grab DJ, Nyarko E, Nikolskaia OV, Kim YV, Dumler JS (2009b): Human brain microvascular endothelial cell traversal by *Borrelia burgdorferi* requires calcium signaling. *Clin Microbiol Infect* 15:422-6.
- Grab DJ, Perides G, Dumler JS, Kim KJ, Park J, Kim YV, Nikolskaia O, Choi KS, Stins MF, Kim KS (2005): *Borrelia burgdorferi*, host-derived proteases, and the blood-brain barrier. *Infect Immun* 73:1014-22.
- Greenwood J, Etienne-Manneville S, Adamson P, Couraud PO (2002): Lymphocyte migration into the central nervous system: implication of ICAM-1 signalling at the blood-brain barrier. *Vascul Pharmacol* 38:315-22.
- Grimaldi M, Maratos M, Verma A (2003): Transient receptor potential channel activation causes a novel form of [Ca²⁺]_i oscillations and is not involved in capacitative Ca²⁺ entry in glial cells. *J Neurosci* 23:4737-45.
- Grynkiewicz G, Poenie M, Tsien RY (1985): A new generation of Ca²⁺ indicators with greatly improved fluorescence properties. *J Biol Chem* 260:3440-50.
- Guan X, Wilson S, Schlender KK, Ruch RJ (1996): Gap-junction disassembly and connexin 43 dephosphorylation induced by 18 beta-glycyrrhetic acid. *Mol Carcinog* 16:157-64.
- Gul R, Kim SY, Park KH, Kim BJ, Kim SJ, Im MJ, Kim UH (2008): A novel signaling pathway of ADP-ribosyl cyclase activation by angiotensin II in adult rat cardiomyocytes. *Am J Physiol Heart Circ Physiol* 295:H77-88.
- Gunduz D, Hirche F, Hartel FV, Rodewald CW, Schafer M, Pfitzer G, Piper HM, Noll T (2003): ATP antagonism of thrombin-induced endothelial barrier permeability. *Cardiovasc Res* 59:470-8.
- Guo H, Jin YX, Ishikawa M, Huang YM, van der Meide PH, Link H, Xiao BG (1998): Regulation of beta-chemokine mRNA expression in adult rat astrocytes by lipopolysaccharide, proinflammatory and immunoregulatory cytokines. *Scand J Immunol* 48:502-8.
- Guthrie PB, Knappenberger J, Segal M, Bennett MV, Charles AC, Kater SB (1999): ATP released from astrocytes mediates glial calcium waves. *J Neurosci* 19:520-8.
- Haasemann M, Cartaud J, Muller-Esterl W, Dunia I (1998): Agonist-induced redistribution of bradykinin B₂ receptor in caveolae. *J Cell Sci* 111 (Pt 7):917-28.
- Haeffliger JA, Nicod P, Meda P (2004): Contribution of connexins to the function of the vascular wall. *Cardiovasc Res* 62:345-56.

- Hagar RE, Burgstahler AD, Nathanson MH, Ehrlich BE (1998): Type III InsP3 receptor channel stays open in the presence of increased calcium. *Nature* 396:81-4.
- Hajnóczky G, Thomas AP (1997): Minimal requirements for calcium oscillations driven by the IP3 receptor. *Embo J* 16:3533-43.
- Haorah J, Heilman D, Knipe B, Chrastil J, Leibhart J, Ghorpade A, Miller DW, Persidsky Y (2005): Ethanol-induced activation of myosin light chain kinase leads to dysfunction of tight junctions and blood-brain barrier compromise. *Alcohol Clin Exp Res* 29:999-1009.
- Haorah J, Knipe B, Gorantla S, Zheng J, Persidsky Y (2007a): Alcohol-induced blood-brain barrier dysfunction is mediated via inositol 1,4,5-triphosphate receptor (IP3R)-gated intracellular calcium release. *J Neurochem* 100:324-36.
- Haorah J, Ramirez SH, Schall K, Smith D, Pandya R, Persidsky Y (2007b): Oxidative stress activates protein tyrosine kinase and matrix metalloproteinases leading to blood-brain barrier dysfunction. *J Neurochem* 101:566-76.
- Haorah J, Schall K, Ramirez SH, Persidsky Y (2008): Activation of protein tyrosine kinases and matrix metalloproteinases causes blood-brain barrier injury: Novel mechanism for neurodegeneration associated with alcohol abuse. *Glia* 56:78-88.
- Harks EG, Camina JP, Peters PH, Ypey DL, Scheenen WJ, van Zoelen EJ, Theuvenet AP (2003a): Besides affecting intracellular calcium signaling, 2-APB reversibly blocks gap junctional coupling in confluent monolayers, thereby allowing measurement of single-cell membrane currents in undissociated cells. *Faseb J* 17:941-3.
- Harks EG, Scheenen WJ, Peters PH, van Zoelen EJ, Theuvenet AP (2003b): Prostaglandin F2 alpha induces unsynchronized intracellular calcium oscillations in monolayers of gap junctionally coupled NRK fibroblasts. *Pflugers Arch* 447:78-86.
- Harris AL (2001): Emerging issues of connexin channels: biophysics fills the gap. *Q Rev Biophys* 34:325-472.
- Harris AL (2007): Connexin channel permeability to cytoplasmic molecules. *Prog Biophys Mol Biol* 94:120-43.
- Harris AL (2008): Connexin specificity of second messenger permeation: real numbers at last. *J Gen Physiol* 131:287-92.
- Hassinger TD, Guthrie PB, Atkinson PB, Bennett MV, Kater SB (1996): An extracellular signaling component in propagation of astrocytic calcium waves. *Proc Natl Acad Sci U S A* 93:13268-73.
- Hawat G, Benderdour M, Rousseau G, Baroudi G (2010): Connexin 43 mimetic peptide Gap26 confers protection to intact heart against myocardial ischemia injury. *Pflugers Arch* 460:583-92.
- Hawkins BT, Davis TP (2005): The blood-brain barrier/neurovascular unit in health and disease. *Pharmacol Rev* 57:173-85.
- He LQ, Cai F, Liu Y, Liu MJ, Tan ZP, Pan Q, Fang FY, Liang de S, Wu LQ, Long ZG, Dai HP, Xia K, Xia JH, Zhang ZH (2005): Cx31 is assembled and trafficked to cell surface by ER-Golgi pathway and degraded by proteasomal or lysosomal pathways. *Cell Res* 15:455-64.
- Heizmann CW, Hunziker W (1991): Intracellular calcium-binding proteins: more sites than insights. *Trends Biochem Sci* 16:98-103.
- Hellstrom M, Gerhardt H, Kalen M, Li X, Eriksson U, Wolburg H, Betsholtz C (2001): Lack of pericytes leads to endothelial hyperplasia and abnormal vascular morphogenesis. *J Cell Biol* 153:543-53.
- Hellstrom M, Kalen M, Lindahl P, Abramsson A, Betsholtz C (1999): Role of PDGF-B and PDGFR-beta in recruitment of vascular smooth muscle cells and pericytes during embryonic blood vessel formation in the mouse. *Development* 126:3047-55.
- Herbert JM, Augereau JM, Gleye J, Maffrand JP (1990): Chelerythrine is a potent and specific inhibitor of protein kinase C. *Biochem Biophys Res Commun* 172:993-9.
- Herve JC, Bourmeyster N, Sarrouilhe D (2004): Diversity in protein-protein interactions of connexins: emerging roles. *Biochim Biophys Acta* 1662:22-41.
- Herve JC, Derangeon M, Bahbouhi B, Mesnil M, Sarrouilhe D (2007): The connexin turnover, an important modulating factor of the level of cell-to-cell junctional communication: comparison with other integral membrane proteins. *J Membr Biol* 217:21-33.
- Herve JC, Sarrouilhe D (2002): Modulation of junctional communication by phosphorylation: protein phosphatases, the missing link in the chain. *Biol Cell* 94:423-32.
- Hess J, Jensen CV, Diemer NH (1989): Calcium-imaging with Fura-2 in isolated cerebral microvessels. *Acta Histochem* 87:107-14.
- Heyman NS, Kurjiaka DT, Ek Vitorin JF, Burt JM (2009): Regulation of gap junctional charge selectivity in cells coexpressing connexin 40 and connexin 43. *Am J Physiol Heart Circ Physiol* 297:H450-9.
- Hicks K, O'Neil RG, Dubinsky WS, Brown RC (2010): Trpc-Mediated Actin-Myosin Contraction Is Critical for Bbb Disruption Following Hypoxic Stress. *Am J Physiol Cell Physiol*.
- Hirase H, Creso J, Singleton M, Bartho P, Buzsaki G (2004): Two-photon imaging of brain pericytes in vivo using dextran-conjugated dyes. *Glia* 46:95-100.

- Hirase T, Staddon JM, Saitou M, Ando-Akatsuka Y, Itoh M, Furuse M, Fujimoto K, Tsukita S, Rubin LL (1997): Occludin as a possible determinant of tight junction permeability in endothelial cells. *J Cell Sci* 110 (Pt 14):1603-13.
- Hirose K, Kadowaki S, Tanabe M, Takeshima H, Iino M (1999): Spatiotemporal dynamics of inositol 1,4,5-trisphosphate that underlies complex Ca^{2+} mobilization patterns. *Science* 284:1527-30.
- Hisadome K, Koyama T, Kimura C, Droogmans G, Ito Y, Oike M (2002): Volume-regulated anion channels serve as an auto/paracrine nucleotide release pathway in aortic endothelial cells. *J Gen Physiol* 119:511-20.
- Hoang QV, Qian H, Ripps H (2010): Functional analysis of hemichannels and gap-junctional channels formed by connexins 43 and 46. *Mol Vis* 16:1343-52.
- Hofer A, Dermietzel R (1998): Visualization and functional blocking of gap junction hemichannels (connexons) with antibodies against external loop domains in astrocytes. *Glia* 24:141-54.
- Hofer AM (2005): Another dimension to calcium signaling: a look at extracellular calcium. *J Cell Sci* 118:855-62.
- Hofer AM, Curci S, Doble MA, Brown EM, Soybel DI (2000): Intercellular communication mediated by the extracellular calcium-sensing receptor. *Nat Cell Biol* 2:392-8.
- Hooper C, Taylor DL, Pocock JM (2005): Pure albumin is a potent trigger of calcium signalling and proliferation in microglia but not macrophages or astrocytes. *J Neurochem* 92:1363-76.
- Hori S, Ohtsuki S, Hosoya K, Nakashima E, Terasaki T (2004): A pericyte-derived angiopoietin-1 multimeric complex induces occludin gene expression in brain capillary endothelial cells through Tie-2 activation in vitro. *J Neurochem* 89:503-13.
- Hu Q, Ziegelstein RC (2000): Hypoxia/reoxygenation stimulates intracellular calcium oscillations in human aortic endothelial cells. *Circulation* 102:2541-7.
- Hu R, He ML, Hu H, Yuan BX, Zang WJ, Lau CP, Tse HF, Li GR (2009): Characterization of calcium signaling pathways in human preadipocytes. *J Cell Physiol* 220:765-70.
- Huang YJ, Maruyama Y, Dvoryanchikov G, Pereira E, Chaudhari N, Roper SD (2007): The role of pannexin 1 hemichannels in ATP release and cell-cell communication in mouse taste buds. *Proc Natl Acad Sci U S A* 104:6436-41.
- Huckstepp RT, id Bihi R, Eason R, Spyer KM, Dicke N, Willecke K, Marina N, Gourine AV, Dale N (2010): Connexin hemichannel-mediated CO_2 -dependent release of ATP in the medulla oblongata contributes to central respiratory chemosensitivity. *J Physiol* 588:3901-20.
- Hunter AW, Barker RJ, Zhu C, Gourdie RG (2005): Zonula occludens-1 alters connexin43 gap junction size and organization by influencing channel accretion. *Mol Biol Cell* 16:5686-98.
- Hurst RD, Clark JB (1998): Alterations in transendothelial electrical resistance by vasoactive agonists and cyclic AMP in a blood-brain barrier model system. *Neurochem Res* 23:149-54.
- Igarashi Y, Utsumi H, Chiba H, Yamada-Sasamori Y, Tobioka H, Kamimura Y, Furuuchi K, Kokai Y, Nakagawa T, Mori M, Sawada N (1999): Glial cell line-derived neurotrophic factor induces barrier function of endothelial cells forming the blood-brain barrier. *Biochem Biophys Res Commun* 261:108-12.
- Iino M (2000): Molecular basis of spatio-temporal dynamics in inositol 1,4,5-trisphosphate-mediated Ca^{2+} signalling. *Jpn J Pharmacol* 82:15-20.
- Iino M (2010): Spatiotemporal dynamics of Ca^{2+} signaling and its physiological roles. *Proc Jpn Acad Ser B Phys Biol Sci* 86:244-56.
- Ilyin V, Parker I (1994): Role of cytosolic Ca^{2+} in inhibition of $InsP_3$ -evoked Ca^{2+} release in *Xenopus* oocytes. *J Physiol* 477 (Pt 3):503-9.
- Innocenti B, Parpura V, Haydon PG (2000): Imaging extracellular waves of glutamate during calcium signaling in cultured astrocytes. *J Neurosci* 20:1800-8.
- Isakson BE (2008): Localized expression of an $Ins(1,4,5)P_3$ receptor at the myoendothelial junction selectively regulates heterocellular Ca^{2+} communication. *J Cell Sci* 121:3664-73.
- Isakson BE, Evans WH, Boitano S (2001): Intercellular Ca^{2+} signaling in alveolar epithelial cells through gap junctions and by extracellular ATP. *Am J Physiol Lung Cell Mol Physiol* 280:L221-8.
- Ishihara H, Wada T, Kizuki N, Asano T, Yazaki Y, Kikuchi M, Oka Y (1999): Enhanced phosphoinositide hydrolysis via overexpression of phospholipase C beta1 or delta1 inhibits stimulus-induced insulin release in insulinoma MIN6 cells. *Biochem Biophys Res Commun* 254:77-82.
- Ishii K, Hirose K, Iino M (2006): Ca^{2+} shuttling between endoplasmic reticulum and mitochondria underlying Ca^{2+} oscillations. *EMBO Rep* 7:390-6.
- Ishikawa M, Iwamoto T, Nakamura T, Doyle A, Fukumoto S, Yamada Y (2011): Pannexin 3 functions as an ER Ca^{2+} channel, hemichannel, and gap junction to promote osteoblast differentiation. *J Cell Biol* 193:1257-74.
- Ishizaki T, Chiba H, Kojima T, Fujibe M, Soma T, Miyajima H, Nagasawa K, Wada I, Sawada N (2003): Cyclic AMP induces phosphorylation of claudin-5 immunoprecipitates and expression of claudin-5 gene in blood-brain-barrier endothelial cells via protein kinase A-dependent and -independent pathways. *Exp Cell Res* 290:275-88.

- Isshiki M, Anderson RG (2003): Function of caveolae in Ca²⁺ entry and Ca²⁺-dependent signal transduction. *Traffic* 4:717-23.
- Isshiki M, Ando J, Korenaga R, Kogo H, Fujimoto T, Fujita T, Kamiya A (1998): Endothelial Ca²⁺ waves preferentially originate at specific loci in caveolin-rich cell edges. *Proc Natl Acad Sci U S A* 95:5009-14.
- Itoh M, Nagafuchi A, Moroi S, Tsukita S (1997): Involvement of ZO-1 in cadherin-based cell adhesion through its direct binding to alpha catenin and actin filaments. *J Cell Biol* 138:181-92.
- Itoh M, Yonemura S, Nagafuchi A, Tsukita S (1991): A 220-kD undercoat-constitutive protein: its specific localization at cadherin-based cell-cell adhesion sites. *J Cell Biol* 115:1449-62.
- Ivanov AI, Hunt D, Utech M, Nusrat A, Parkos CA (2005): Differential roles for actin polymerization and a myosin II motor in assembly of the epithelial apical junctional complex. *Mol Biol Cell* 16:2636-50.
- Ivanov AI, McCall IC, Parkos CA, Nusrat A (2004a): Role for actin filament turnover and a myosin II motor in cytoskeleton-driven disassembly of the epithelial apical junctional complex. *Mol Biol Cell* 15:2639-51.
- Ivanov AI, Nusrat A, Parkos CA (2004b): Endocytosis of epithelial apical junctional proteins by a clathrin-mediated pathway into a unique storage compartment. *Mol Biol Cell* 15:176-88.
- Iyer S, Deutsch K, Yan X, Lin B (2007): Batch RNAi selector: a standalone program to predict specific siRNA candidates in batches with enhanced sensitivity. *Comput Methods Programs Biomed* 85:203-9.
- Jackson JG, Thayer SA (2006): Mitochondrial modulation of Ca²⁺-induced Ca²⁺-release in rat sensory neurons. *J Neurophysiol* 96:1093-104.
- Jacobson JR, Dudek SM, Singleton PA, Kolosova IA, Verin AD, Garcia JG (2006): Endothelial cell barrier enhancement by ATP is mediated by the small GTPase Rac and cortactin. *Am J Physiol Lung Cell Mol Physiol* 291:L289-95.
- Jan CR, Ho CM, Wu SN, Tseng CJ (1998): Bradykinin-evoked Ca²⁺ mobilization in Madin Darby canine kidney cells. *Eur J Pharmacol* 355:219-33.
- Jardin I, Lopez JJ, Pariente JA, Salido GM, Rosado JA (2008): Intracellular calcium release from human platelets: different messengers for multiple stores. *Trends Cardiovasc Med* 18:57-61.
- Jin R, Yang G, Li G (2010): Molecular insights and therapeutic targets for blood-brain barrier disruption in ischemic stroke: Critical role of matrix metalloproteinases and tissue-type plasminogen activator. *Neurobiol Dis*.
- Johnson TL, Nerem RM (2007): Endothelial connexin 37, connexin 40, and connexin 43 respond uniquely to substrate and shear stress. *Endothelium* 14:215-26.
- Jones BF, Boyles RR, Hwang SY, Bird GS, Putney JW (2008): Calcium influx mechanisms underlying calcium oscillations in rat hepatocytes. *Hepatology* 48:1273-81.
- Jungmann P, Wilhelmi M, Oberleithner H, Riethmuller C (2008): Bradykinin does not induce gap formation between human endothelial cells. *Pflugers Arch* 455:1007-16.
- Kamermans M, Fahrenfort I, Schultz K, Janssen-Bienhold U, Sjoerdsma T, Weiler R (2001): Hemichannel-mediated inhibition in the outer retina. *Science* 292:1178-80.
- Kamouchi M, Kitazono T, Ago T, Wakisaka M, Ooboshi H, Ibayashi S, Iida M (2004): Calcium influx pathways in rat CNS pericytes. *Brain Res Mol Brain Res* 126:114-20.
- Kang J, Kang N, Lovatt D, Torres A, Zhao Z, Lin J, Nedergaard M (2008): Connexin 43 hemichannels are permeable to ATP. *J Neurosci* 28:4702-11.
- Kang M, Othmer HG (2007): The variety of cytosolic calcium responses and possible roles of PLC and PKC. *Phys Biol* 4:325-43.
- Kanmogne GD, Schall K, Leibhart J, Knipe B, Gendelman HE, Persidsky Y (2007): HIV-1 gp120 compromises blood-brain barrier integrity and enhances monocyte migration across blood-brain barrier: implication for viral neuropathogenesis. *J Cereb Blood Flow Metab* 27:123-34.
- Karpuk N, Burkovetskaya M, Fritz T, Angle A, Kielian T (2011): Neuroinflammation leads to region-dependent alterations in astrocyte gap junction communication and hemichannel activity. *J Neurosci* 31:414-25.
- Kawamura H, Kobayashi M, Li Q, Yamanishi S, Katsumura K, Minami M, Wu DM, Puro DG (2004): Effects of angiotensin II on the pericyte-containing microvasculature of the rat retina. *J Physiol* 561:671-83.
- Kawano S, Otsu K, Kuruma A, Shoji S, Yanagida E, Muto Y, Yoshikawa F, Hirayama Y, Mikoshiba K, Furuichi T (2006): ATP autocrine/paracrine signaling induces calcium oscillations and NFAT activation in human mesenchymal stem cells. *Cell Calcium* 39:313-24.
- Keizer J, De Young GW (1992): Two roles of Ca²⁺ in agonist stimulated Ca²⁺ oscillations. *Biophys J* 61:649-60.
- Kelley GG, Ondrako JM, Reks SE (2001): Fuel and hormone regulation of phospholipase C beta 1 and delta 1 overexpressed in RINm5F pancreatic beta cells. *Mol Cell Endocrinol* 177:107-15.
- Kennedy C, Proulx PR, Hebert RL (1997): Bradykinin-induced translocation of cytoplasmic phospholipase A2 in MDCK cells. *Can J Physiol Pharmacol* 75:563-7.

- Kerem A, Yin J, Kaestle SM, Hoffmann J, Schoene AM, Singh B, Kuppe H, Borst MM, Kuebler WM (2010): Lung endothelial dysfunction in congestive heart failure: role of impaired Ca²⁺ signaling and cytoskeletal reorganization. *Circ Res* 106:1103-16.
- Kettenmann H, Hanisch UK, Noda M, Verkhratsky A (2011): Physiology of microglia. *Physiol Rev* 91:461-553.
- Khan NA, Kim Y, Shin S, Kim KS (2007): FimH-mediated *Escherichia coli* K1 invasion of human brain microvascular endothelial cells. *Cell Microbiol* 9:169-78.
- Khodakhah K, Ogden D (1993): Functional heterogeneity of calcium release by inositol trisphosphate in single Purkinje neurones, cultured cerebellar astrocytes, and peripheral tissues. *Proc Natl Acad Sci U S A* 90:4976-80.
- Kim JV, Dustin ML (2006): Innate response to focal necrotic injury inside the blood-brain barrier. *J Immunol* 177:5269-77.
- Kim YA, Park SL, Kim MY, Lee SH, Baik EJ, Moon CH, Jung YS (2010): Role of PKC β II and PKC δ in blood-brain barrier permeability during aglycemic hypoxia. *Neurosci Lett* 468:254-8.
- Kim YH, Park TJ, Lee YH, Baek KJ, Suh PG, Ryu SH, Kim KT (1999): Phospholipase C- δ 1 is activated by capacitative calcium entry that follows phospholipase C- β activation upon bradykinin stimulation. *J Biol Chem* 274:26127-34.
- Kim YV, Di Cello F, Hillaire CS, Kim KS (2004): Differential Ca²⁺ signaling by thrombin and protease-activated receptor-1-activating peptide in human brain microvascular endothelial cells. *Am J Physiol Cell Physiol* 286:C31-42.
- Kim YV, Pearce D, Kim KS (2008): Ca²⁺/calmodulin-dependent invasion of microvascular endothelial cells of human brain by *Escherichia coli* K1. *Cell Tissue Res* 332:427-33.
- Kimura C, Oike M, Ito Y (2000): Hypoxia-induced alterations in Ca²⁺ mobilization in brain microvascular endothelial cells. *Am J Physiol Heart Circ Physiol* 279:H2310-8.
- Kiselyov K, Shin DM, Muallem S (2003): Signalling specificity in GPCR-dependent Ca²⁺ signalling. *Cell Signal* 15:243-53.
- Klingenberg D, Gunduz D, Hartel F, Bindewald K, Schafer M, Piper HM, Noll T (2004): MEK/MAPK as a signaling element in ATP control of endothelial myosin light chain. *Am J Physiol Cell Physiol* 286:C807-12.
- Kniesel U, Risau W, Wolburg H (1996): Development of blood-brain barrier tight junctions in the rat cortex. *Brain Res Dev Brain Res* 96:229-40.
- Koenig H, Goldstone AD, Lu CY, Trout JJ (1989): Polyamines and Ca²⁺ mediate hyperosmolar opening of the blood-brain barrier: in vitro studies in isolated rat cerebral capillaries. *J Neurochem* 52:1135-42.
- Koizumi S (2010): Synchronization of Ca²⁺ oscillations: involvement of ATP release in astrocytes. *Febs J* 277:286-92.
- Kojima T, Murata M, Go M, Spray DC, Sawada N (2007): Connexins induce and maintain tight junctions in epithelial cells. *J Membr Biol* 217:13-9.
- Kolosova IA, Mirzapioazova T, Adyshev D, Usatyuk P, Romer LH, Jacobson JR, Natarajan V, Pearce DB, Garcia JG, Verin AD (2005): Signaling pathways involved in adenosine triphosphate-induced endothelial cell barrier enhancement. *Circ Res* 97:115-24.
- Kolosova IA, Mirzapioazova T, Moreno-Vinasco L, Sammani S, Garcia JG, Verin AD (2008): Protective effect of purinergic agonist ATP γ S against acute lung injury. *Am J Physiol Lung Cell Mol Physiol* 294:L319-24.
- Komarova Y, Malik AB (2010): Regulation of endothelial permeability via paracellular and transcellular transport pathways. *Annu Rev Physiol* 72:463-93.
- Kondo RP, Wang SY, John SA, Weiss JN, Goldhaber JI (2000): Metabolic inhibition activates a non-selective current through connexin hemichannels in isolated ventricular myocytes. *J Mol Cell Cardiol* 32:1859-72.
- Konstantoulaki M, Kouklis P, Malik AB (2003): Protein kinase C modifications of VE-cadherin, p120, and β -catenin contribute to endothelial barrier dysregulation induced by thrombin. *Am J Physiol Lung Cell Mol Physiol* 285:L434-42.
- Kovacs M, Toth J, Hetenyi C, Malnasi-Csizmadia A, Sellers JR (2004): Mechanism of blebbistatin inhibition of myosin II. *J Biol Chem* 279:35557-63.
- Kraft P, Benz PM, Austinat M, Brede ME, Schuh K, Walter U, Stoll G, Kleinschnitz C (2010): Deficiency of vasodilator-stimulated phosphoprotein (VASP) increases blood-brain-barrier damage and edema formation after ischemic stroke in mice. *PLoS One* 5:e15106.
- Krause M, Dent EW, Bear JE, Loureiro JJ, Gertler FB (2003): Ena/VASP proteins: regulators of the actin cytoskeleton and cell migration. *Annu Rev Cell Dev Biol* 19:541-64.
- Kreft M, Stenovec M, Rupnik M, Grlic S, Krzan M, Potokar M, Pangrsic T, Haydon PG, Zorec R (2004): Properties of Ca²⁺-dependent exocytosis in cultured astrocytes. *Glia* 46:437-45.
- Kristian T, Gido G, Siesjo BK (1993): Brain calcium metabolism in hypoglycemic coma. *J Cereb Blood Flow Metab* 13:955-61.
- Kristian T, Siesjo BK (1998): Calcium in ischemic cell death. *Stroke* 29:705-18.

- Krizbai IA, Bauer H, Bresgen N, Eckl PM, Farkas A, Szatmari E, Traweger A, Wejksza K, Bauer HC (2005): Effect of oxidative stress on the junctional proteins of cultured cerebral endothelial cells. *Cell Mol Neurobiol* 25:129-39.
- Kronengold J, Trexler EB, Bukauskas FF, Bargiello TA, Verselis VK (2003): Single-channel SCAM identifies pore-lining residues in the first extracellular loop and first transmembrane domains of Cx46 hemichannels. *J Gen Physiol* 122:389-405.
- Kuhlmann CR, Gerigk M, Bender B, Closhen D, Lessmann V, Luhmann HJ (2008): Fluvastatin prevents glutamate-induced blood-brain-barrier disruption in vitro. *Life Sci* 82:1281-7.
- Kuhlmann CR, Tamaki R, Gamberdinger M, Lessmann V, Behl C, Kempfski OS, Luhmann HJ (2007): Inhibition of the myosin light chain kinase prevents hypoxia-induced blood-brain barrier disruption. *J Neurochem* 102:501-7.
- Kuhlmann CR, Zehendner CM, Gerigk M, Closhen D, Bender B, Friedl P, Luhmann HJ (2009): MK801 blocks hypoxic blood-brain-barrier disruption and leukocyte adhesion. *Neurosci Lett* 449:168-72.
- Kumar NM, Gilula NB (1996): The gap junction communication channel. *Cell* 84:381-8.
- Kuruma A, Inoue T, Mikoshiba K (2003): Dynamics of Ca²⁺ and Na⁺ in the dendrites of mouse cerebellar Purkinje cells evoked by parallel fibre stimulation. *Eur J Neurosci* 18:2677-89.
- Kwak BR, Hermans MM, De Jonge HR, Lohmann SM, Jongasma HJ, Chanson M (1995): Differential regulation of distinct types of gap junction channels by similar phosphorylating conditions. *Mol Biol Cell* 6:1707-19.
- Kyle JW, Berthoud VM, Kurutz J, Minogue PJ, Greenspan M, Hanck DA, Beyer EC (2009): The N terminus of connexin37 contains an alpha-helix that is required for channel function. *J Biol Chem* 284:20418-27.
- Lai CH, Kuo KH (2005): The critical component to establish in vitro BBB model: Pericyte. *Brain Res Brain Res Rev* 50:258-65.
- Lai CP, Bechberger JF, Thompson RJ, MacVicar BA, Bruzzone R, Naus CC (2007): Tumor-suppressive effects of pannexin 1 in C6 glioma cells. *Cancer Res* 67:1545-54.
- Laing JG, Chou BC, Steinberg TH (2005): ZO-1 alters the plasma membrane localization and function of Cx43 in osteoblastic cells. *J Cell Sci* 118:2167-76.
- Laird DW (2006): Life cycle of connexins in health and disease. *Biochem J* 394:527-43.
- Lal R, John SA, Laird DW, Arnsdorf MF (1995): Heart gap junction preparations reveal hemiplaques by atomic force microscopy. *Am J Physiol* 268:C968-77.
- Lampe PD, Lau AF (2004): The effects of connexin phosphorylation on gap junctional communication. *Int J Biochem Cell Biol* 36:1171-86.
- Landesman Y, White TW, Starich TA, Shaw JE, Goodenough DA, Paul DL (1999): Innexin-3 forms connexin-like intercellular channels. *J Cell Sci* 112 (Pt 14):2391-6.
- Langlois S, Cowan KN, Shao Q, Cowan BJ, Laird DW (2008): Caveolin-1 and -2 interact with connexin43 and regulate gap junctional intercellular communication in keratinocytes. *Mol Biol Cell* 19:912-28.
- Larson DM, Carson MP, Haudenschild CC (1987): Junctional transfer of small molecules in cultured bovine brain microvascular endothelial cells and pericytes. *Microvasc Res* 34:184-99.
- Larson DM, Haudenschild CC, Beyer EC (1990): Gap junction messenger RNA expression by vascular wall cells. *Circ Res* 66:1074-80.
- Laskey RE, Adams DJ, Cannell M, van Breemen C (1992): Calcium entry-dependent oscillations of cytoplasmic calcium concentration in cultured endothelial cell monolayers. *Proc Natl Acad Sci U S A* 89:1690-4.
- Lawrie AM, Rizzuto R, Pozzan T, Simpson AW (1996): A role for calcium influx in the regulation of mitochondrial calcium in endothelial cells. *J Biol Chem* 271:10753-9.
- Lazrak A, Peracchia C (1993): Gap junction gating sensitivity to physiological internal calcium regardless of pH in Novikoff hepatoma cells. *Biophys J* 65:2002-12.
- Lazrak A, Peres A, Giovannardi S, Peracchia C (1994): Ca-mediated and independent effects of arachidonic acid on gap junctions and Ca-independent effects of oleic acid and halothane. *Biophys J* 67:1052-9.
- LeBeau AP, Yule DI, Groblewski GE, Sneyd J (1999): Agonist-dependent phosphorylation of the inositol 1,4,5-trisphosphate receptor: A possible mechanism for agonist-specific calcium oscillations in pancreatic acinar cells. *J Gen Physiol* 113:851-72.
- Lee NP, Mruk DD, Conway AM, Cheng CY (2004): Zyxin, axin, and Wiskott-Aldrich syndrome protein are adaptors that link the cadherin/catenin protein complex to the cytoskeleton at adherens junctions in the seminiferous epithelium of the rat testis. *J Androl* 25:200-15.
- Lee TH, Avraham H, Lee SH, Avraham S (2002): Vascular endothelial growth factor modulates neutrophil transendothelial migration via up-regulation of interleukin-8 in human brain microvascular endothelial cells. *J Biol Chem* 277:10445-51.
- Lee TH, Avraham HK, Jiang S, Avraham S (2003): Vascular endothelial growth factor modulates the transendothelial migration of MDA-MB-231 breast cancer cells through regulation of brain microvascular endothelial cell permeability. *J Biol Chem* 278:5277-84.

- Lewis RS, Cahalan MD (1989): Mitogen-induced oscillations of cytosolic Ca^{2+} and transmembrane Ca^{2+} current in human leukemic T cells. *Cell Regul* 1:99-112.
- Leybaert L and De Ley G (1994): Interstitial and tissue cations and electrical potential after experimental spinal cord injury. *Exp Brain Res* 100: 369-75
- Leybaert L, Braet K, Vandamme W, Cabooter L, Martin PE, Evans WH (2003): Connexin channels, connexin mimetic peptides and ATP release. *Cell Commun Adhes* 10:251-7.
- Leybaert L, Sanderson MJ (2012) Intercellular Ca^{2+} waves: mechanisms and function. *Physiol Rev*, In Press.
- Li AF, Sato T, Haimovici R, Okamoto T, Roy S (2003): High glucose alters connexin 43 expression and gap junction intercellular communication activity in retinal pericytes. *Invest Ophthalmol Vis Sci* 44:5376-82.
- Li H, Liu TF, Lazrak A, Peracchia C, Goldberg GS, Lampe PD, Johnson RG (1996): Properties and regulation of gap junctional hemichannels in the plasma membranes of cultured cells. *J Cell Biol* 134:1019-30.
- Li L, Bressler B, Prameya R, Dorovini-Zis K, Van Breemen C (1999): Agonist-stimulated calcium entry in primary cultures of human cerebral microvascular endothelial cells. *Microvasc Res* 57:211-26.
- Li MW, Mruk DD, Lee WM, Cheng CY (2009): Connexin 43 and plakophilin-2 as a protein complex that regulates blood-testis barrier dynamics. *Proc Natl Acad Sci U S A* 106:10213-8.
- Li S, Dent JA, Roy R (2003): Regulation of intermuscular electrical coupling by the *Caenorhabditis elegans* innexin *inx-6*. *Mol Biol Cell* 14:2630-44.
- Li X, Lynn BD, Nagy JI (2012): The effector and scaffolding proteins AF6 and MUPP1 interact with connexin36 and localize at gap junctions that form electrical synapses in rodent brain. *Eur J Neurosci* 35:166-81.
- Liao CK, Wang SM, Chen YL, Wang HS, Wu JC (2010): Lipopolysaccharide-induced inhibition of connexin43 gap junction communication in astrocytes is mediated by downregulation of caveolin-3. *Int J Biochem Cell Biol* 42:762-70.
- Lin GC, Rurangirwa JK, Koval M, Steinberg TH (2004): Gap junctional communication modulates agonist-induced calcium oscillations in transfected HeLa cells. *J Cell Sci* 117:881-7.
- Lin MI, Yu J, Murata T, Sessa WC (2007): Caveolin-1-deficient mice have increased tumor microvascular permeability, angiogenesis, and growth. *Cancer Res* 67:2849-56.
- Lippoldt A, Liebner S, Andbjør B, Kalbacher H, Wolburg H, Haller H, Fuxe K (2000): Organization of choroid plexus epithelial and endothelial cell tight junctions and regulation of claudin-1, -2 and -5 expression by protein kinase C. *Neuroreport* 11:1427-31.
- Little TL, Beyer EC, Duling BR (1995): Connexin 43 and connexin 40 gap junctional proteins are present in arteriolar smooth muscle and endothelium in vivo. *Am J Physiol* 268:H729-39.
- Liu F, Arce FT, Ramachandran S, Lal R (2006): Nanomechanics of hemichannel conformations: connexin flexibility underlying channel opening and closing. *J Biol Chem* 281:23207-17.
- Liu HT, Sabirov RZ, Okada Y (2008a): Oxygen-glucose deprivation induces ATP release via maxi-anion channels in astrocytes. *Purinergic Signal* 4:147-54.
- Liu LB, Xue YX, Liu YH, Wang YB (2008b): Bradykinin increases blood-tumor barrier permeability by down-regulating the expression levels of ZO-1, occludin, and claudin-5 and rearranging actin cytoskeleton. *J Neurosci Res* 86:1153-68.
- Liu S, Taffet S, Stoner L, Delmar M, Vallano ML, Jalife J (1993): A structural basis for the unequal sensitivity of the major cardiac and liver gap junctions to intracellular acidification: the carboxyl tail length. *Biophys J* 64:1422-33.
- Liu T, Guevara OE, Warburton RR, Hill NS, Gaestel M, Kayyali US (2010a): Regulation of vimentin intermediate filaments in endothelial cells by hypoxia. *Am J Physiol Cell Physiol* 299:C363-73.
- Liu X, Hashimoto-Torii K, Torii M, Ding C, Rakic P (2010b): Gap junctions/hemichannels modulate interkinetic nuclear migration in the forebrain precursors. *J Neurosci* 30:4197-209.
- Liu X, Wang W, Singh BB, Lockwich T, Jadlowiec J, O'Connell B, Wellner R, Zhu MX, Ambudkar IS (2000): Trp1, a candidate protein for the store-operated Ca^{2+} influx mechanism in salivary gland cells. *J Biol Chem* 275:3403-11.
- Locovei S, Bao L, Dahl G (2006a): Pannexin 1 in erythrocytes: function without a gap. *Proc Natl Acad Sci U S A* 103:7655-9.
- Locovei S, Scemes E, Qiu F, Spray DC, Dahl G (2007): Pannexin1 is part of the pore forming unit of the P2X(7) receptor death complex. *FEBS Lett* 581:483-8.
- Locovei S, Wang J, Dahl G (2006b): Activation of pannexin 1 channels by ATP through P2Y receptors and by cytoplasmic calcium. *FEBS Lett* 580:239-44.
- Loewenstein WR (1981): Junctional intercellular communication: the cell-to-cell membrane channel. *Physiol Rev* 61:829-913.
- Loewenstein WR, Rose B (1978): Calcium in (junctional) intercellular communication and a thought on its behavior in intracellular communication. *Ann N Y Acad Sci* 307:285-307.

- Lok J, Gupta P, Guo S, Kim WJ, Whalen MJ, van Leyen K, Lo EH (2007): Cell-cell signaling in the neurovascular unit. *Neurochem Res* 32:2032-45.
- Lu TS, Avraham HK, Seng S, Tachado SD, Koziel H, Makriyannis A, Avraham S (2008): Cannabinoids inhibit HIV-1 Gp120-mediated insults in brain microvascular endothelial cells. *J Immunol* 181:6406-16.
- Luh C, Kuhlmann CR, Ackermann B, Timaru-Kast R, Luhmann HJ, Behl C, Werner C, Engelhard K, Thal SC (2009): Inhibition of myosin light chain kinase reduces brain edema formation after traumatic brain injury. *J Neurochem*.
- Lum H, Jaffe HA, Schulz IT, Masood A, RayChaudhury A, Green RD (1999): Expression of PKA inhibitor (PKI) gene abolishes cAMP-mediated protection to endothelial barrier dysfunction. *Am J Physiol* 277:C580-8.
- Luo D, Broad LM, Bird GS, Putney JW, Jr. (2001): Mutual antagonism of calcium entry by capacitative and arachidonic acid-mediated calcium entry pathways. *J Biol Chem* 276:20186-9.
- Luo K, Turnbull MW (2011): Characterization of nonjunctional hemichannels in caterpillar cells. *J Insect Sci* 11:6.
- Lurtz MM, Louis CF (2003): Calmodulin and protein kinase C regulate gap junctional coupling in lens epithelial cells. *Am J Physiol Cell Physiol* 285:C1475-82.
- Lurtz MM, Louis CF (2007): Intracellular calcium regulation of connexin43. *Am J Physiol Cell Physiol* 293:C1806-13.
- Ma TY, Tran D, Hoa N, Nguyen D, Merryfield M, Tarnawski A (2000): Mechanism of extracellular calcium regulation of intestinal epithelial tight junction permeability: role of cytoskeletal involvement. *Microsc Res Tech* 51:156-68.
- Ma X, Cao J, Luo J, Nilius B, Huang Y, Ambudkar IS, Yao X (2010): Depletion of Intracellular Ca²⁺ Stores Stimulates the Translocation of TRPV4-C1 Heteromeric Channels to the Plasma Membrane. *Arterioscler Thromb Vasc Biol*.
- Maass K, Shibayama J, Chase SE, Willecke K, Delmar M (2007): C-terminal truncation of connexin43 changes number, size, and localization of cardiac gap junction plaques. *Circ Res* 101:1283-91.
- Maeda S, Nakagawa S, Suga M, Yamashita E, Oshima A, Fujiyoshi Y, Tsukihara T (2009): Structure of the connexin 26 gap junction channel at 3.5 Å resolution. *Nature* 458:597-602.
- Maes K, Missiaen L, De Smet P, Vanlingen S, Callewaert G, Parys JB, De Smedt H (2000): Differential modulation of inositol 1,4,5-trisphosphate receptor type 1 and type 3 by ATP. *Cell Calcium* 27:257-67.
- Mak DO, McBride S, Foskett JK (2001a): ATP regulation of recombinant type 3 inositol 1,4,5-trisphosphate receptor gating. *J Gen Physiol* 117:447-56.
- Mak DO, McBride S, Foskett JK (2001b): Regulation by Ca²⁺ and inositol 1,4,5-trisphosphate (InsP₃) of single recombinant type 3 InsP₃ receptor channels. Ca²⁺ activation uniquely distinguishes types 1 and 3 insp₃ receptors. *J Gen Physiol* 117:435-46.
- Malarkey EB, Parpura V (2008): Mechanisms of glutamate release from astrocytes. *Neurochem Int* 52:142-54.
- Malewicz B, Kumar VV, Johnson RG, Baumann WJ (1990): Lipids in gap junction assembly and function. *Lipids* 25:419-27.
- Malli R, Frieden M, Osibow K, Zoratti C, Mayer M, Demaurex N, Graier WF (2003): Sustained Ca²⁺ transfer across mitochondria is Essential for mitochondrial Ca²⁺ buffering, store-operated Ca²⁺ entry, and Ca²⁺ store refilling. *J Biol Chem* 278:44769-79.
- Manthey D, Bukauskas F, Lee CG, Kozak CA, Willecke K (1999): Molecular cloning and functional expression of the mouse gap junction gene connexin-57 in human HeLa cells. *J Biol Chem* 274:14716-23.
- Marhl M, Schuster S, Brumen M (1998): Mitochondria as an important factor in the maintenance of constant amplitudes of cytosolic calcium oscillations. *Biophys Chem* 71:125-32.
- Mark KS, Davis TP (2002): Cerebral microvascular changes in permeability and tight junctions induced by hypoxia-reoxygenation. *Am J Physiol Heart Circ Physiol* 282:H1485-94.
- Martin SC, Shuttleworth TJ (1994): Ca²⁺ influx drives agonist-activated [Ca²⁺]_i oscillations in an exocrine cell. *FEBS Lett* 352:32-6.
- Martin-Padura I, Lostaglio S, Schneemann M, Williams L, Romano M, Fruscella P, Panzeri C, Stoppacciaro A, Ruco L, Villa A, Simmons D, Dejana E (1998): Junctional adhesion molecule, a novel member of the immunoglobulin superfamily that distributes at intercellular junctions and modulates monocyte transmigration. *J Cell Biol* 142:117-27.
- Maruyama T, Kanaji T, Nakade S, Kanno T, Mikoshiba K (1997): 2APB, 2-aminoethoxydiphenyl borate, a membrane-penetrable modulator of Ins(1,4,5)P₃-induced Ca²⁺ release. *J Biochem* 122:498-505.
- Massimini M, Amzica F (2001): Extracellular calcium fluctuations and intracellular potentials in the cortex during the slow sleep oscillation. *J Neurophysiol* 85:1346-50.
- Mauban JR, Wilkinson K, Schach C, Yuan JX (2006): Histamine-mediated increases in cytosolic [Ca²⁺]_i involve different mechanisms in human pulmonary artery smooth muscle and endothelial cells. *Am J Physiol Cell Physiol* 290:C325-36.
- Mayhan WG (2001): Regulation of blood-brain barrier permeability. *Microcirculation* 8:89-104.

- McCarthy KM, Skare IB, Stankewich MC, Furuse M, Tsukita S, Rogers RA, Lynch RD, Schneeberger EE (1996): Occludin is a functional component of the tight junction. *J Cell Sci* 109 (Pt 9):2287-98.
- McClenahan D, Hillenbrand K, Kapur A, Carlton D, Czuprynski C (2009): Effects of extracellular ATP on bovine lung endothelial and epithelial cell monolayer morphologies, apoptoses, and permeabilities. *Clin Vaccine Immunol* 16:43-8.
- McKimmie CS, Graham GJ (2010): Astrocytes modulate the chemokine network in a pathogen-specific manner. *Biochem Biophys Res Commun* 394:1006-11.
- Meacci E, Bini F, Sassoli C, Martinesi M, Squecco R, Chellini F, Zecchi-Orlandini S, Francini F, Formigli L (2010): Functional interaction between TRPC1 channel and connexin-43 protein: a novel pathway underlying S1P action on skeletal myogenesis. *Cell Mol Life Sci* 67:4269-85.
- Mehta D, Rahman A, Malik AB (2001): Protein kinase C- α signals rho-guanine nucleotide dissociation inhibitor phosphorylation and rho activation and regulates the endothelial cell barrier function. *J Biol Chem* 276:22614-20.
- Mei X, Giaume C., Koulakoff A. (2010): Changes in connexin expression and hemichannel activity in reactive astrocytes of APP/PS1 mice. *FENS Abstracts* 5:078.63.
- Meldolesi J, Pozzan T (1998): The endoplasmic reticulum Ca²⁺ store: a view from the lumen. *Trends Biochem Sci* 23:10-4.
- Meme W, Vandecasteele M, Giaume C, Venance L (2009): Electrical coupling between hippocampal astrocytes in rat brain slices. *Neurosci Res* 63:236-43.
- Meyer T, Stryer L (1988): Molecular model for receptor-stimulated calcium spiking. *Proc Natl Acad Sci U S A* 85:5051-5.
- Mignen O, Thompson JL, Shuttleworth TJ (2001): Reciprocal regulation of capacitative and arachidonate-regulated noncapacitative Ca²⁺ entry pathways. *J Biol Chem* 276:35676-83.
- Mignen O, Thompson JL, Shuttleworth TJ (2007): STIM1 regulates Ca²⁺ entry via arachidonate-regulated Ca²⁺-selective (ARC) channels without store depletion or translocation to the plasma membrane. *J Physiol* 579:703-15.
- Mignen O, Thompson JL, Shuttleworth TJ (2009): The molecular architecture of the arachidonate-regulated Ca²⁺-selective ARC channel is a pentameric assembly of Orai1 and Orai3 subunits. *J Physiol* 587:4181-97.
- Mikoshiba K, Hisatsune C, Futatsugi A, Mizutani A, Nakamura T, Miyachi K (2008): The role of Ca²⁺ signaling in cell function with special reference to exocrine secretion. *Cornea* 27 Suppl 1:S3-8.
- Missiaen L, Parys JB, Sienaert I, Maes K, Kunzelmann K, Takahashi M, Tanzawa K, De Smedt H (1998): Functional properties of the type-3 InsP₃ receptor in 16HBE14o- bronchial mucosal cells. *J Biol Chem* 273:8983-6.
- Miyakawa T, Maeda A, Yamazawa T, Hirose K, Kurosaki T, Ino M (1999): Encoding of Ca²⁺ signals by differential expression of IP₃ receptor subtypes. *Embo J* 18:1303-8.
- Moerenhout M, Himpens B, Vereecke J (2001): Intercellular communication upon mechanical stimulation of CPAE- endothelial cells is mediated by nucleotides. *Cell Calcium* 29:125-36.
- Mogensen C, Bergner B, Wallner S, Ritter A, d'Avis S, Ninichuk V, Kameritsch P, Gloe T, Nagel W, Pohl U (2011): Isolation and functional characterization of pericytes derived from hamster skeletal muscle. *Acta Physiol (Oxf)* 201:413-26.
- Monaco G, Decrock E, Akl H, Ponsaerts R, Vervliet T, Luyten T, De Maeyer M, Missiaen L, Distelhorst CW, De Smedt H, Parys JB, Leybaert L, Bultynck G (2012): Selective regulation of IP₃-receptor-mediated Ca(2+) signaling and apoptosis by the BH4 domain of Bcl-2 versus Bcl-Xl. *Cell Death Differ* 19:295-309.
- Moreno AP (2005): Connexin phosphorylation as a regulatory event linked to channel gating. *Biochim Biophys Acta* 1711:164-71.
- Moreno AP, Chanson M, Elenes S, Anumonwo J, Scerri I, Gu H, Taffet SM, Delmar M (2002): Role of the carboxyl terminal of connexin43 in transjunctional fast voltage gating. *Circ Res* 90:450-7.
- Moreno AP, Lau AF (2007): Gap junction channel gating modulated through protein phosphorylation. *Prog Biophys Mol Biol* 94:107-19.
- Morley P, Small DL, Murray CL, Mealing GA, Poulter MO, Durkin JP, Stanimirovic DB (1998): Evidence that functional glutamate receptors are not expressed on rat or human cerebrovascular endothelial cells. *J Cereb Blood Flow Metab* 18:396-406.
- Mottola A, Antoniotti S, Lovisolo D, Munaron L (2005): Regulation of noncapacitative calcium entry by arachidonic acid and nitric oxide in endothelial cells. *Faseb J* 19:2075-7.
- Muller DJ, Hand GM, Engel A, Sosinsky GE (2002): Conformational changes in surface structures of isolated connexin 26 gap junctions. *Embo J* 21:3598-607.
- Murata T, Lin MI, Stan RV, Bauer PM, Yu J, Sessa WC (2007): Genetic evidence supporting caveolae microdomain regulation of calcium entry in endothelial cells. *J Biol Chem* 282:16631-43.
- Musil LS, Goodenough DA (1991): Biochemical analysis of connexin43 intracellular transport, phosphorylation, and assembly into gap junctional plaques. *J Cell Biol* 115:1357-74.

- Musil LS, Goodenough DA (1993): Multisubunit assembly of an integral plasma membrane channel protein, gap junction connexin43, occurs after exit from the ER. *Cell* 74:1065-77.
- Musil LS, Le AC, VanSlyke JK, Roberts LM (2000): Regulation of connexin degradation as a mechanism to increase gap junction assembly and function. *J Biol Chem* 275:25207-15.
- Myllykoski M, Kuczera K, Kursula P (2009): Complex formation between calmodulin and a peptide from the intracellular loop of the gap junction protein connexin43: Molecular conformation and energetics of binding. *Biophys Chem* 144:130-5.
- Nadal A, Sul JY, Valdeolmillos M, McNaughton PA (1998): Albumin elicits calcium signals from astrocytes in brain slices from neonatal rat cortex. *J Physiol* 509 (Pt 3):711-6.
- Nagasawa K, Chiba H, Fujita H, Kojima T, Saito T, Endo T, Sawada N (2006): Possible involvement of gap junctions in the barrier function of tight junctions of brain and lung endothelial cells. *J Cell Physiol* 208:123-32.
- Nagy Z, Goehlert UG, Wolfe LS, Huttner I (1985): Ca²⁺ depletion-induced disconnection of tight junctions in isolated rat brain microvessels. *Acta Neuropathol (Berl)* 68:48-52.
- Nakagawa S, Deli MA, Nakao S, Honda M, Hayashi K, Nakaoka R, Kataoka Y, Niwa M (2007): Pericytes from brain microvessels strengthen the barrier integrity in primary cultures of rat brain endothelial cells. *Cell Mol Neurobiol* 27:687-94.
- Nash MS, Schell MJ, Atkinson PJ, Johnston NR, Nahorski SR, Challiss RA (2002): Determinants of metabotropic glutamate receptor-5-mediated Ca²⁺ and inositol 1,4,5-trisphosphate oscillation frequency. Receptor density versus agonist concentration. *J Biol Chem* 277:35947-60.
- Nash MS, Young KW, Challiss RA, Nahorski SR (2001): Intracellular signalling. Receptor-specific messenger oscillations. *Nature* 413:381-2.
- Naus CC, Laird DW (2010): Implications and challenges of connexin connections to cancer. *Nat Rev Cancer* 10:435-41.
- Neal CR, Michel CC (1995): Transcellular gaps in microvascular walls of frog and rat when permeability is increased by perfusion with the ionophore A23187. *J Physiol* 488 (Pt 2):427-37.
- Neijssen J, Herberts C, Drijfhout JW, Reits E, Janssen L, Neefjes J (2005): Cross-presentation by intercellular peptide transfer through gap junctions. *Nature* 434:83-8.
- Neuwelt EA, Bauer B, Fahlke C, Fricker G, Iadecola C, Janigro D, Leybaert L, Molnar Z, O'Donnell ME, Povlishock JT, Saunders NR, Sharp F, Stanimirovic D, Watts RJ, Drewes LR (2011): Engaging neuroscience to advance translational research in brain barrier biology. *Nat Rev Neurosci* 12:169-82.
- Nikolskaia OV, de ALAP, Kim YV, Lonsdale-Eccles JD, Fukuma T, Scharfstein J, Grab DJ (2006): Blood-brain barrier traversal by African trypanosomes requires calcium signaling induced by parasite cysteine protease. *J Clin Invest* 116:2739-47.
- Ningaraj NS, Rao MK, Black KL (2003): Adenosine 5'-triphosphate-sensitive potassium channel-mediated blood-brain tumor barrier permeability increase in a rat brain tumor model. *Cancer Res* 63:8899-911.
- Nishioku T, Dohgu S, Takata F, Eto T, Ishikawa N, Kodama KB, Nakagawa S, Yamauchi A, Kataoka Y (2009): Detachment of brain pericytes from the basal lamina is involved in disruption of the blood-brain barrier caused by lipopolysaccharide-induced sepsis in mice. *Cell Mol Neurobiol* 29:309-16.
- Nitta T, Hata M, Gotoh S, Seo Y, Sasaki H, Hashimoto N, Furuse M, Tsukita S (2003): Size-selective loosening of the blood-brain barrier in claudin-5-deficient mice. *J Cell Biol* 161:653-60.
- Noll T, Holschermann H, Koprek K, Gunduz D, Haberbosch W, Tillmanns H, Piper HM (1999): ATP reduces macromolecule permeability of endothelial monolayers despite increasing [Ca²⁺]_i. *Am J Physiol* 276:H1892-901.
- Norambuena A, Poblete MI, Donoso MV, Espinoza CS, Gonzalez A, Huidobro-Toro JP (2008): P2Y1 receptor activation elicits its partition out of membrane rafts and its rapid internalization from human blood vessels: implications for receptor signaling. *Mol Pharmacol* 74:1666-77.
- Nusrat A, Chen JA, Foley CS, Liang TW, Tom J, Cromwell M, Quan C, Mrsny RJ (2000a): The coiled-coil domain of occludin can act to organize structural and functional elements of the epithelial tight junction. *J Biol Chem* 275:29816-22.
- Nusrat A, Parkos CA, Verkade P, Foley CS, Liang TW, Innis-Whitehouse W, Eastburn KK, Madara JL (2000b): Tight junctions are membrane microdomains. *J Cell Sci* 113 (Pt 10):1771-81.
- Oancea E, Meyer T (1998): Protein kinase C as a molecular machine for decoding calcium and diacylglycerol signals. *Cell* 95:307-18.
- Oby E, Janigro D (2006): The blood-brain barrier and epilepsy. *Epilepsia* 47:1761-74.
- O'Carroll SJ, Alkadhi M, Nicholson LF, Green CR (2008): Connexin 43 mimetic peptides reduce swelling, astrogliosis, and neuronal cell death after spinal cord injury. *Cell Commun Adhes* 15:27-42.
- Oh S, Abrams CK, Verselis VK, Bargiello TA (2000): Stoichiometry of transjunctional voltage-gating polarity reversal by a negative charge substitution in the amino terminus of a connexin32 chimera. *J Gen Physiol* 116:13-31.

- Olesen SP (1985): A calcium-dependent reversible permeability increase in microvessels in frog brain, induced by serotonin. *J Physiol* 361:103-13.
- Olesen SP (1987): Regulation of ion permeability in frog brain venules. Significance of calcium, cyclic nucleotides and protein kinase C. *J Physiol* 387:59-68.
- Olesen SP (1989): An electrophysiological study of microvascular permeability and its modulation by chemical mediators. *Acta Physiol Scand Suppl* 579:1-28.
- Olesen SP, Crone C (1986): Substances that rapidly augment ionic conductance of endothelium in cerebral venules. *Acta Physiol Scand* 127:233-41.
- Olk S, Zoidl G, Dermietzel R (2009): Connexins, cell motility, and the cytoskeleton. *Cell Motil Cytoskeleton* 66:1000-16.
- O'Quinn MP, Palatinus JA, Harris BS, Hewett KW, Gourdie RG (2011): A peptide mimetic of the connexin43 carboxyl terminus reduces gap junction remodeling and induced arrhythmia following ventricular injury. *Circ Res* 108:704-15.
- Orellana JA, Saez PJ, Shoji KF, Schalper KA, Palacios-Prado N, Velarde V, Giaume C, Bennett MV, Saez JC (2009): Modulation of brain hemichannels and gap junction channels by pro-inflammatory agents and their possible role in neurodegeneration. *Antioxid Redox Signal* 11:369-99.
- Orellana JA, Diaz E, Schalper KA, Vargas AA, Bennett MV, Saez JC (2011a): Cation permeation through connexin 43 hemichannels is cooperative, competitive and saturable with parameters depending on the permeant species. *Biochem Biophys Res Commun*.
- Orellana JA, Shoji KF, Abudara V, Ezan P, Amigou E, Saez PJ, Jiang JX, Naus CC, Saez JC, Giaume C (2011b): Amyloid beta-induced death in neurons involves glial and neuronal hemichannels. *J Neurosci* 31:4962-77.
- Oshima A, Tani K, Hiroaki Y, Fujiyoshi Y, Sosinsky GE (2007): Three-dimensional structure of a human connexin26 gap junction channel reveals a plug in the vestibule. *Proc Natl Acad Sci U S A* 104:10034-9.
- Pacher P, Hajnoczky G (2001): Propagation of the apoptotic signal by mitochondrial waves. *Embo J* 20:4107-21.
- Paemeleire K, de Hemptinne A, Leybaert L (1999): Chemically, mechanically, and hyperosmolarity-induced calcium responses of rat cortical capillary endothelial cells in culture. *Exp Brain Res* 126:473-81.
- Paemeleire K, Martin PE, Coleman SL, Fogarty KE, Carrington WA, Leybaert L, Tuft RA, Evans WH, Sanderson MJ (2000): Intercellular calcium waves in HeLa cells expressing GFP-labeled connexin 43, 32, or 26. *Mol Biol Cell* 11:1815-27.
- Panchin Y, Kelmanson I, Matz M, Lukyanov K, Usman N, Lukyanov S (2000): A ubiquitous family of putative gap junction molecules. *Curr Biol* 10:R473-4.
- Pangrsic T, Potokar M, Stenovc M, Kreft M, Fabbretti E, Nistri A, Pryazhnikov E, Khiroug L, Giniatullin R, Zorec R (2007): Exocytotic release of ATP from cultured astrocytes. *J Biol Chem* 282:28749-58.
- Papadopoulos MC, Davies DC, Moss RF, Tighe D, Bennett ED (2000): Pathophysiology of septic encephalopathy: a review. *Crit Care Med* 28:3019-24.
- Parfitt AM (1993): "Handbook of Experimental Pharmacology." Springer, Heidelberg, pp 1-65.
- Park J, Fan Z, Kumon RE, El-Sayed ME, Deng CX (2010): Modulation of intracellular Ca²⁺ concentration in brain microvascular endothelial cells in vitro by acoustic cavitation. *Ultrasound Med Biol* 36:1176-87.
- Parker I, Ivorra I (1990): Inhibition by Ca²⁺ of inositol trisphosphate-mediated Ca²⁺ liberation: a possible mechanism for oscillatory release of Ca²⁺. *Proc Natl Acad Sci U S A* 87:260-4.
- Parpura V, Scemes E, Spray DC (2004): Mechanisms of glutamate release from astrocytes: gap junction "hemichannels", purinergic receptors and exocytotic release. *Neurochem Int* 45:259-64.
- Parthasarathi K, Ichimura H, Monma E, Lindert J, Quadri S, Issekutz A, Bhattacharya J (2006): Connexin 43 mediates spread of Ca²⁺-dependent proinflammatory responses in lung capillaries. *J Clin Invest* 116:2193-200.
- Pasti L, Pozzan T, Carmignoto G (1995): Long-lasting changes of calcium oscillations in astrocytes. A new form of glutamate-mediated plasticity. *J Biol Chem* 270:15203-10.
- Pasti L, Zonta M, Pozzan T, Vicini S, Carmignoto G (2001): Cytosolic calcium oscillations in astrocytes may regulate exocytotic release of glutamate. *J Neurosci* 21:477-84.
- Patel S, Joseph SK, Thomas AP (1999): Molecular properties of inositol 1,4,5-trisphosphate receptors. *Cell Calcium* 25:247-64.
- Patterson RL, Boehning D, Snyder SH (2004): Inositol 1,4,5-trisphosphate receptors as signal integrators. *Annu Rev Biochem* 73:437-65.
- Paul DL, Ebihara L, Takemoto LJ, Swenson KI, Goodenough DA (1991): Connexin46, a novel lens gap junction protein, induces voltage-gated currents in nonjunctional plasma membrane of *Xenopus* oocytes. *J Cell Biol* 115:1077-89.
- Pearson RA, Dale N, Llaudet E, Mobbs P (2005): ATP released via gap junction hemichannels from the pigment epithelium regulates neural retinal progenitor proliferation. *Neuron* 46:731-44.

- Pelegriin P, Surprenant A (2006): Pannexin-1 mediates large pore formation and interleukin-1beta release by the ATP-gated P2X7 receptor. *Embo J* 25:5071-82.
- Peltonen HM, Magga JM, Bart G, Turunen PM, Antikainen MS, Kukkonen JP, Akerman KE (2009): Involvement of TRPC3 channels in calcium oscillations mediated by OX(1) orexin receptors. *Biochem Biophys Res Commun* 385:408-12.
- Penuela S, Bhalla R, Gong XQ, Cowan KN, Celetti SJ, Cowan BJ, Bai D, Shao Q, Laird DW (2007): Pannexin 1 and pannexin 3 are glycoproteins that exhibit many distinct characteristics from the connexin family of gap junction proteins. *J Cell Sci* 120:3772-83.
- Penuela S, Bhalla R, Nag K, Laird DW (2009): Glycosylation regulates pannexin intermixing and cellular localization. *Mol Biol Cell* 20:4313-23.
- Pepper MS, Montesano R, el Aoumari A, Gros D, Orci L, Meda P (1992): Coupling and connexin 43 expression in microvascular and large vessel endothelial cells. *Am J Physiol* 262:C1246-57.
- Peracchia C (1990): Increase in gap junction resistance with acidification in crayfish septate axons is closely related to changes in intracellular calcium but not hydrogen ion concentration. *J Membr Biol* 113:75-92.
- Peracchia C (2004): Chemical gating of gap junction channels; roles of calcium, pH and calmodulin. *Biochim Biophys Acta* 1662:61-80.
- Peracchia C, Sotkis A, Wang XG, Peracchia LL, Persechini A (2000): Calmodulin directly gates gap junction channels. *J Biol Chem* 275:26220-4.
- Peracchia C, Wang XC (1997): Connexin domains relevant to the chemical gating of gap junction channels. *Braz J Med Biol Res* 30:577-90.
- Persidsky Y, Ramirez SH, Haorah J, Kanmogne GD (2006): Blood-brain barrier: structural components and function under physiologic and pathologic conditions. *J Neuroimmune Pharmacol* 1:223-36.
- Pfahnl A, Dahl G (1999): Gating of cx46 gap junction hemichannels by calcium and voltage. *Pflugers Arch* 437:345-53.
- Phelan P, Bacon JP, Davies JA, Stebbings LA, Todman MG, Avery L, Baines RA, Barnes TM, Ford C, Hekimi S, Lee R, Shaw JE, Starich TA, Curtin KD, Sun YA, Wyman RJ (1998): Innexins: a family of invertebrate gap-junction proteins. *Trends Genet* 14:348-9.
- Pizzo P, Burgo A, Pozzan T, Fasolato C (2001): Role of capacitative calcium entry on glutamate-induced calcium influx in type-I rat cortical astrocytes. *J Neurochem* 79:98-109.
- Pocock TM, Williams B, Curry FE, Bates DO (2000): VEGF and ATP act by different mechanisms to increase microvascular permeability and endothelial [Ca(2+)](i). *Am J Physiol Heart Circ Physiol* 279:H1625-34.
- Politi A, Gaspers LD, Thomas AP, Hofer T (2006): Models of IP3 and Ca2+ oscillations: frequency encoding and identification of underlying feedbacks. *Biophys J* 90:3120-33.
- Ponsaerts R, De Vuyst E, Retamal M, D'Hondt C, Vermeire D, Wang N, De Smedt H, Zimmermann P, Himpens B, Vereecke J, Leybaert L, Bultynck G (2010): Intramolecular loop/tail interactions are essential for connexin 43-hemichannel activity. *Faseb J* 24:4378-95.
- Ponsaerts R, D'Hondt C, Bultynck G, Srinivas SP, Vereecke J, Himpens B (2008): The myosin II ATPase inhibitor blebbistatin prevents thrombin-induced inhibition of intercellular calcium wave propagation in corneal endothelial cells. *Invest Ophthalmol Vis Sci* 49:4816-27.
- Praetorius HA, Leipziger J (2009): ATP release from non-excitabile cells. *Purinergic Signal* 5:433-46.
- Price LS, Langeslag M, ten Klooster JP, Hordijk PL, Jalink K, Collard JG (2003): Calcium signaling regulates translocation and activation of Rac. *J Biol Chem* 278:39413-21.
- Puljung MC, Berthoud VM, Beyer EC, Hanck DA (2004): Polyvalent cations constitute the voltage gating particle in human connexin37 hemichannels. *J Gen Physiol* 124:587-603.
- Putney JW (2009): Capacitative calcium entry: from concept to molecules. *Immunol Rev* 231:10-22.
- Putney JW, Bird GS (2008): Cytoplasmic calcium oscillations and store-operated calcium influx. *J Physiol* 586:3055-9.
- Qin H, Shao Q, Igdoura SA, Alaoui-Jamali MA, Laird DW (2003): Lysosomal and proteasomal degradation play distinct roles in the life cycle of Cx43 in gap junctional intercellular communication-deficient and -competent breast tumor cells. *J Biol Chem* 278:30005-14.
- Qiu LB, Ding GR, Li KC, Wang XW, Zhou Y, Zhou YC, Li YR, Guo GZ (2010): The role of protein kinase C in the opening of blood-brain barrier induced by electromagnetic pulse. *Toxicology* 273:29-34.
- Rackauskas M, Neverauskas V, Skeberdis VA (2010): Diversity and properties of connexin gap junction channels. *Medicina (Kaunas)* 46:1-12.
- Ramachandran S, Xie LH, John SA, Subramaniam S, Lal R (2007): A novel role for connexin hemichannel in oxidative stress and smoking-induced cell injury. *PLoS ONE* 2:e712.
- Ramos-Franco J, Fill M, Mignery GA (1998): Isoform-specific function of single inositol 1,4,5-trisphosphate receptor channels. *Biophys J* 75:834-9.
- Ramsauer M, Krause D, Dermietzel R (2002): Angiogenesis of the blood-brain barrier in vitro and the function of cerebral pericytes. *Faseb J* 16:1274-6.

- Raslan F, Schwarz T, Meuth SG, Austinat M, Bader M, Renne T, Roosen K, Stoll G, Siren AL, Kleinschnitz C (2010): Inhibition of bradykinin receptor B1 protects mice from focal brain injury by reducing blood-brain barrier leakage and inflammation. *J Cereb Blood Flow Metab* 30:1477-86.
- Rebecchi MJ, Pentylala SN (2000): Structure, function, and control of phosphoinositide-specific phospholipase C. *Physiol Rev* 80:1291-335.
- Reetz G, Reiser G (1996): $[Ca^{2+}]_i$ oscillations induced by bradykinin in rat glioma cells associated with Ca^{2+} -store-dependent Ca^{2+} influx are controlled by cell volume and by membrane potential. *Cell Calcium* 19:143-56.
- Reinhard M, Giehl K, Abel K, Haffner C, Jarchau T, Hoppe V, Jockusch BM, Walter U (1995): The proline-rich focal adhesion and microfilament protein VASP is a ligand for profilins. *Embo J* 14:1583-9.
- Reither G, Schaefer M, Lipp P (2006): PKC α : a versatile key for decoding the cellular calcium toolkit. *J Cell Biol* 174:521-33.
- Retamal MA, Cortes CJ, Reuss L, Bennett MV, Saez JC (2006): S-nitrosylation and permeation through connexin 43 hemichannels in astrocytes: induction by oxidant stress and reversal by reducing agents. *Proc Natl Acad Sci U S A* 103:4475-80.
- Retamal MA, Froger N, Palacios-Prado N, Ezan P, Saez PJ, Saez JC, Giaume C (2007a): Cx43 hemichannels and gap junction channels in astrocytes are regulated oppositely by proinflammatory cytokines released from activated microglia. *J Neurosci* 27:13781-92.
- Retamal MA, Schalper KA, Shoji KF, Bennett MV, Saez JC (2007b): Opening of connexin 43 hemichannels is increased by lowering intracellular redox potential. *Proc Natl Acad Sci U S A* 104:8322-7.
- Revest PA, Abbott NJ, Gillespie JJ (1991): Receptor-mediated changes in intracellular $[Ca^{2+}]_i$ in cultured rat brain capillary endothelial cells. *Brain Res* 549:159-61.
- Revilla A, Castro C, Barrio LC (1999): Molecular dissection of transjunctional voltage dependence in the connexin-32 and connexin-43 junctions. *Biophys J* 77:1374-83.
- Rey O, Young SH, Papazyan R, Shapiro MS, Rozengurt E (2006): Requirement of the TRPC1 cation channel in the generation of transient Ca^{2+} oscillations by the calcium-sensing receptor. *J Biol Chem* 281:38730-7.
- Rhett JM, Jourdan J, Gourdie RG (2011): Connexin 43 connexon to gap junction transition is regulated by zonula occludens-1. *Mol Biol Cell* 22:1516-28.
- Ri Y, Ballesteros JA, Abrams CK, Oh S, Verselis VK, Weinstein H, Bargiello TA (1999): The role of a conserved proline residue in mediating conformational changes associated with voltage gating of Cx32 gap junctions. *Biophys J* 76:2887-98.
- Ribatti D, Nico B, Crivellato E, Artico M (2006): Development of the blood-brain barrier: a historical point of view. *Anat Rec B New Anat* 289:3-8.
- Ripps H, Qian H, Zakevicius J (2004): Properties of connexin26 hemichannels expressed in *Xenopus* oocytes. *Cell Mol Neurobiol* 24:647-65.
- Robertson J, Lang S, Lambert PA, Martin PE (2010): Peptidoglycan derived from *Staphylococcus epidermidis* induces Connexin43 hemichannel activity with consequences on the innate immune response in endothelial cells. *Biochem J* 432:133-43.
- Roh DS, Funderburgh JL (2011): Rapid changes in connexin-43 in response to genotoxic stress stabilize cell-cell communication in corneal endothelium. *Invest Ophthalmol Vis Sci* 52:5174-82.
- Romanov RA, Rogachevskaja OA, Bystrova MF, Jiang P, Margolskee RF, Kolesnikov SS (2007): Afferent neurotransmission mediated by hemichannels in mammalian taste cells. *Embo J* 26:657-67.
- Rosado JA, Brownlow SL, Sage SO (2002): Endogenously expressed Trp1 is involved in store-mediated Ca^{2+} entry by conformational coupling in human platelets. *J Biol Chem* 277:42157-63.
- Rose B, Loewenstein WR (1976): Permeability of a cell junction and the local cytoplasmic free ionized calcium concentration: a study with aequorin. *J Membr Biol* 28:87-119.
- Rosenberg OS, Deindl S, Comolli LR, Hoelz A, Downing KH, Nairn AC, Kuriyan J (2006): Oligomerization states of the association domain and the holoenzyme of Ca^{2+} /CaM kinase II. *Febs J* 273:682-94.
- Rottingen J, Iversen JG (2000): Ruled by waves? Intracellular and intercellular calcium signalling. *Acta Physiol Scand* 169:203-19.
- Rottingen JA, Camerer E, Mathiesen I, Prydz H, Iversen JG (1997): Synchronized Ca^{2+} oscillations induced in Madin Darby canine kidney cells by bradykinin and thrombin but not by ATP. *Cell Calcium* 21:195-211.
- Rubin LL, Hall DE, Porter S, Barbu K, Cannon C, Horner HC, Janatpour M, Liaw CW, Manning K, Morales J, et al. (1991): A cell culture model of the blood-brain barrier. *J Cell Biol* 115:1725-35.
- Rutter GA (2006): Moving Ca^{2+} from the endoplasmic reticulum to mitochondria: is spatial intimacy enough? *Biochem Soc Trans* 34:351-5.
- Ryu JK, McLarnon JG (2009): A leaky blood-brain barrier, fibrinogen infiltration and microglial reactivity in inflamed Alzheimer's disease brain. *J Cell Mol Med* 13:2911-25.
- Sabourin T, Bastien L, Bachvarov DR, Marceau F (2002): Agonist-induced translocation of the kinin B(1) receptor to caveolae-related rafts. *Mol Pharmacol* 61:546-53.

- Sacks RS, Firth AL, Remillard CV, Agange N, Yau J, Ko EA, Yuan JX (2008): Thrombin-mediated increases in cytosolic $[Ca^{2+}]$ involve different mechanisms in human pulmonary artery smooth muscle and endothelial cells. *Am J Physiol Lung Cell Mol Physiol* 295:L1048-55.
- Saez JC, Berthoud VM, Branes MC, Martinez AD, Beyer EC (2003): Plasma membrane channels formed by connexins: their regulation and functions. *Physiol Rev* 83:1359-400.
- Saez JC, Retamal MA, Basilio D, Bukauskas FF, Bennett MV (2005): Connexin-based gap junction hemichannels: gating mechanisms. *Biochim Biophys Acta* 1711:215-24.
- Saez JC, Schalper KA, Retamal MA, Orellana JA, Shoji KF, Bennett MV (2010): Cell membrane permeabilization via connexin hemichannels in living and dying cells. *Exp Cell Res* 316:2377-89.
- Sage SO, Adams DJ, van Breemen C (1989): Synchronized oscillations in cytoplasmic free calcium concentration in confluent bradykinin-stimulated bovine pulmonary artery endothelial cell monolayers. *J Biol Chem* 264:6-9.
- Saitou M, Furuse M, Sasaki H, Schulzke JD, Fromm M, Takano H, Noda T, Tsukita S (2000): Complex phenotype of mice lacking occludin, a component of tight junction strands. *Mol Biol Cell* 11:4131-42.
- Salameh A, Dhein S (2005): Pharmacology of gap junctions. New pharmacological targets for treatment of arrhythmia, seizure and cancer? *Biochim Biophys Acta* 1719:36-58.
- Salido GM, Sage SO, Rosado JA (2009): Biochemical and functional properties of the store-operated Ca^{2+} channels. *Cell Signal* 21:457-61.
- Saliez J, Bouzin C, Rath G, Ghisdal P, Desjardins F, Rezzani R, Rodella LF, Vriens J, Nilius B, Feron O, Balligand JL, Dessy C (2008): Role of caveolar compartmentation in endothelium-derived hyperpolarizing factor-mediated relaxation: Ca^{2+} signals and gap junction function are regulated by caveolin in endothelial cells. *Circulation* 117:1065-74.
- Sammels E, Parys JB, Missiaen L, De Smedt H, Bultynck G (2010): Intracellular Ca^{2+} storage in health and disease: a dynamic equilibrium. *Cell Calcium* 47:297-314.
- Samuels SE, Lipitz JB, Dahl G, Muller KJ (2010): Neuroglial ATP release through innexin channels controls microglial cell movement to a nerve injury. *J Gen Physiol* 136:425-42.
- Sanchez HA, Mese G, Srinivas M, White TW, Verselis VK (2010): Differentially altered Ca^{2+} regulation and Ca^{2+} permeability in Cx26 hemichannels formed by the A40V and G45E mutations that cause keratitis ichthyosis deafness syndrome. *J Gen Physiol* 136:47-62.
- Sanchez HA, Orellana JA, Verselis VK, Saez JC (2009): Metabolic inhibition increases activity of connexin-32 hemichannels permeable to Ca^{2+} in transfected HeLa cells. *Am J Physiol Cell Physiol* 297:C665-78.
- Sanderson MJ, Charles AC, Dirksen ER (1990): Mechanical stimulation and intercellular communication increases intracellular Ca^{2+} in epithelial cells. *Cell Regul* 1:585-96.
- Sandoval KE, Witt KA (2008): Blood-brain barrier tight junction permeability and ischemic stroke. *Neurobiol Dis* 32:200-19.
- Sarker MH, Easton AS, Fraser PA (1998): Regulation of cerebral microvascular permeability by histamine in the anaesthetized rat. *J Physiol* 507 (Pt 3):909-18.
- Sarker MH, Fraser PA (2002): The role of guanylyl cyclases in the permeability response to inflammatory mediators in pial venular capillaries in the rat. *J Physiol* 540:209-18.
- Sarker MH, Hu DE, Fraser PA (2000): Acute effects of bradykinin on cerebral microvascular permeability in the anaesthetized rat. *J Physiol* 528 Pt 1:177-87.
- Sarker MH, Hu DE, Fraser PA (2010): Regulation of Cerebromicrovascular Permeability by Lysophosphatidic Acid. *Microcirculation* 17:39-46.
- Satpathy M, Gallagher P, Jin Y, Srinivas SP (2005): Extracellular ATP opposes thrombin-induced myosin light chain phosphorylation and loss of barrier integrity in corneal endothelial cells. *Exp Eye Res* 81:183-92.
- Saunders NR, Ek CJ, Habgood MD, Dziegielewska KM (2008): Barriers in the brain: a renaissance? *Trends Neurosci* 31:279-86.
- Saunders NR, Habgood MD, Dziegielewska KM (1999): Barrier mechanisms in the brain, II. Immature brain. *Clin Exp Pharmacol Physiol* 26:85-91.
- Savi P, Zacharyus JL, Delesque-Touchard N, Labouret C, Herve C, Uzabiaga MF, Pereillo JM, Culouscou JM, Bono F, Ferrara P, Herbert JM (2006): The active metabolite of Clopidogrel disrupts P2Y12 receptor oligomers and partitions them out of lipid rafts. *Proc Natl Acad Sci U S A* 103:11069-74.
- Scemes E, Duval N, Meda P (2003): Reduced expression of P2Y1 receptors in connexin43-null mice alters calcium signaling and migration of neural progenitor cells. *J Neurosci* 23:11444-52.
- Scemes E, Giaume C (2006): Astrocyte calcium waves: what they are and what they do. *Glia* 54:716-25.
- Scemes E, Suadicani SO, Spray DC (2000): Intercellular communication in spinal cord astrocytes: fine tuning between gap junctions and P2 nucleotide receptors in calcium wave propagation. *J Neurosci* 20:1435-45.
- Schalper KA, Palacios-Prado N, Retamal MA, Shoji KF, Martinez AD, Saez JC (2008): Connexin hemichannel composition determines the FGF-1-induced membrane permeability and free $[Ca^{2+}]_i$ responses. *Mol Biol Cell* 19:3501-13.

- Schalper KA, Sanchez HA, Lee SC, Altenberg GA, Nathanson MH, Saez JC (2010): Connexin43 hemichannels mediate the Ca²⁺ influx induced by extracellular alkalization. *Am J Physiol Cell Physiol*.
- Scharbrodt W, Abdallah Y, Kassekert SA, Gligorievski D, Piper HM, Boker DK, Deinsberger W, Oertel MF (2009): Cytosolic Ca²⁺ oscillations in human cerebrovascular endothelial cells after subarachnoid hemorrhage. *J Cereb Blood Flow Metab* 29:57-65.
- Schinkel AH (1999): P-Glycoprotein, a gatekeeper in the blood-brain barrier. *Adv Drug Deliv Rev* 36:179-194.
- Schipke CG, Boucsein C, Ohlemeyer C, Kirchhoff F, Kettenmann H (2002): Astrocyte Ca²⁺ waves trigger responses in microglial cells in brain slices. *Faseb J* 16:255-7.
- Schoch HJ, Fischer S, Marti HH (2002): Hypoxia-induced vascular endothelial growth factor expression causes vascular leakage in the brain. *Brain* 125:2549-57.
- Schubert AL, Schubert W, Spray DC, Lisanti MP (2002a): Connexin family members target to lipid raft domains and interact with caveolin-1. *Biochemistry* 41:5754-64.
- Schubert W, Frank PG, Woodman SE, Hyogo H, Cohen DE, Chow CW, Lisanti MP (2002b): Microvascular hyperpermeability in caveolin-1 (-/-) knock-out mice. Treatment with a specific nitric-oxide synthase inhibitor, L-NAME, restores normal microvascular permeability in Cav-1 null mice. *J Biol Chem* 277:40091-8.
- Schulz I, Krause E (2004): Inositol 1,4,5-trisphosphate and its co-players in the concert of Ca²⁺ signalling--new faces in the line up. *Curr Mol Med* 4:313-22.
- Schuster A, Oishi H, Beny JL, Stergiopoulos N, Meister JJ (2001): Simultaneous arterial calcium dynamics and diameter measurements: application to myoendothelial communication. *Am J Physiol Heart Circ Physiol* 280:H1088-96.
- Schwaninger M, Sallmann S, Petersen N, Schneider A, Prinz S, Libermann TA, Spranger M (1999): Bradykinin induces interleukin-6 expression in astrocytes through activation of nuclear factor-kappaB. *J Neurochem* 73:1461-6.
- Schwiebert EM, Zsembery A (2003): Extracellular ATP as a signaling molecule for epithelial cells. *Biochim Biophys Acta* 1615:7-32.
- Segretain D, Falk MM (2004): Regulation of connexin biosynthesis, assembly, gap junction formation, and removal. *Biochim Biophys Acta* 1662:3-21.
- Seki A, Duffy HS, Coombs W, Spray DC, Taffet SM, Delmar M (2004): Modifications in the biophysical properties of connexin43 channels by a peptide of the cytoplasmic loop region. *Circ Res* 95:e22-8.
- Seminario-Vidal L, Kreda S, Jones L, O'Neal W, Trejo J, Boucher RC, Lazarowski ER (2009): Thrombin promotes release of ATP from lung epithelial cells through coordinated activation of rho- and Ca²⁺-dependent signaling pathways. *J Biol Chem* 284:20638-48.
- Sharp CD, Hines I, Houghton J, Warren A, Jackson THt, Jawahar A, Nanda A, Elrod JW, Long A, Chi A, Minagar A, Alexander JS (2003): Glutamate causes a loss in human cerebral endothelial barrier integrity through activation of NMDA receptor. *Am J Physiol Heart Circ Physiol* 285:H2592-8.
- Sharp CD, Houghton J, Elrod JW, Warren A, Jackson THt, Jawahar A, Nanda A, Minagar A, Alexander JS (2005): N-methyl-D-aspartate receptor activation in human cerebral endothelium promotes intracellular oxidant stress. *Am J Physiol Heart Circ Physiol* 288:H1893-9.
- Shasby DM, Ries DR, Shasby SS, Winter MC (2002): Histamine stimulates phosphorylation of adherens junction proteins and alters their link to vimentin. *Am J Physiol Lung Cell Mol Physiol* 282:L1330-8.
- Shepro D, Morel NM (1993): Pericyte physiology. *Faseb J* 7:1031-8.
- Shibata T, Misawa N, Takeo C, Saeki N, Saito Y, Tatsuno I (2005): Analysis of genes dominantly expressed in rat cerebral endothelial cells using suppression subtractive hybridization. *J Atheroscler Thromb* 12:330-7.
- Shintani-Ishida K, Uemura K, Yoshida K (2007): Hemichannels in cardiomyocytes open transiently during ischemia and contribute to reperfusion injury following brief ischemia. *Am J Physiol Heart Circ Physiol* 293:H1714-20.
- Shirakawa H, Sakimoto S, Nakao K, Sugishita A, Konno M, Iida S, Kusano A, Hashimoto E, Nakagawa T, Kaneko S (2010): Transient receptor potential canonical 3 (TRPC3) mediates thrombin-induced astrocyte activation and upregulates its own expression in cortical astrocytes. *J Neurosci* 30:13116-29.
- Shuttleworth TJ (1999): What drives calcium entry during [Ca²⁺]_i oscillations?--challenging the capacitative model. *Cell Calcium* 25:237-46.
- Shuttleworth TJ (2009): Arachidonic acid, ARC channels, and Orai proteins. *Cell Calcium* 45:602-10.
- Shuttleworth TJ, Mignen O (2003): Calcium entry and the control of calcium oscillations. *Biochem Soc Trans* 31:916-9.
- Shuttleworth TJ, Thompson JL (1996): Ca²⁺ entry modulates oscillation frequency by triggering Ca²⁺ release. *Biochem J* 313 (Pt 3):815-9.
- Sigma-RBI P2 Receptors: "RBI eHandbook of Receptor Classification and Signal Transduction." pp 130-137. <http://www.sigmaldrich.com/life-science/cell-biology/learning-center/ehandbook.html>
- Siller-Jackson AJ, Burra S, Gu S, Xia X, Bonewald LF, Sprague E, Jiang JX (2008): Adaptation of connexin 43-hemichannel prostaglandin release to mechanical loading. *J Biol Chem* 283:26374-82.

- Silverman WR, de Rivero Vaccari JP, Locovei S, Qiu F, Carlsson SK, Scemes E, Keane RW, Dahl G (2009): The pannexin 1 channel activates the inflammasome in neurons and astrocytes. *J Biol Chem* 284:18143-51.
- Simard M, Arcuino G, Takano T, Liu QS, Nedergaard M (2003): Signaling at the gliovascular interface. *J Neurosci* 23:9254-62.
- Simon AM, Chen H, Jackson CL (2006): Cx37 and Cx43 localize to zona pellucida in mouse ovarian follicles. *Cell Commun Adhes* 13:61-77.
- Simon J, Filippov AK, Goransson S, Wong YH, Frelin C, Michel AD, Brown DA, Barnard EA (2002): Characterization and channel coupling of the P2Y(12) nucleotide receptor of brain capillary endothelial cells. *J Biol Chem* 277:31390-400.
- Simon J, Vigne P, Eklund KM, Michel AD, Carruthers AM, Humphrey PP, Frelin C, Barnard EA (2001): Activity of adenosine diphosphates and triphosphates on a P2Y(T) -type receptor in brain capillary endothelial cells. *Br J Pharmacol* 132:173-82.
- Sipos I, Domotor E, Abbott NJ, Adam-Vizi V (2000): The pharmacology of nucleotide receptors on primary rat brain endothelial cells grown on a biological extracellular matrix: effects on intracellular calcium concentration. *Br J Pharmacol* 131:1195-203.
- Skerrett IM, Aronowitz J, Shin JH, Cymes G, Kasperek E, Cao FL, Nicholson BJ (2002): Identification of amino acid residues lining the pore of a gap junction channel. *J Cell Biol* 159:349-60.
- Sneyd J, Keizer J, Sanderson MJ (1995): Mechanisms of calcium oscillations and waves: a quantitative analysis. *Faseb J* 9:1463-72.
- Sneyd J, Tsaneva-Atanasova K, Reznikov V, Bai Y, Sanderson MJ, Yule DI (2006): A method for determining the dependence of calcium oscillations on inositol trisphosphate oscillations. *Proc Natl Acad Sci U S A* 103:1675-80.
- Sneyd J, Tsaneva-Atanasova K, Yule DI, Thompson JL, Shuttleworth TJ (2004): Control of calcium oscillations by membrane fluxes. *Proc Natl Acad Sci U S A* 101:1392-6.
- Sohl G, Willecke K (2003): An update on connexin genes and their nomenclature in mouse and man. *Cell Commun Adhes* 10:173-80.
- Sohl G, Willecke K (2004): Gap junctions and the connexin protein family. *Cardiovasc Res* 62:228-32.
- Solan JL, Lampe PD (2007): Key connexin 43 phosphorylation events regulate the gap junction life cycle. *J Membr Biol* 217:35-41.
- Solan JL, Lampe PD (2009): Connexin43 phosphorylation: structural changes and biological effects. *Biochem J* 419:261-72.
- Somjen GG (2004): The regulation of brain ions. *Ions in the brain: normal function, seizures and stroke*, Oxford University Press, pp. 13-62.
- Somjen GG, Aitken PG, Giacchino JL, McNamara JO (1986): Interstitial ion concentrations and paroxysmal discharges in hippocampal formation and spinal cord. *Adv Neurol* 44:663-80.
- Song L, Ge S, Pachter JS (2007): Caveolin-1 regulates expression of junction-associated proteins in brain microvascular endothelial cells. *Blood* 109:1515-23.
- Sosinsky GE, Nicholson BJ (2005): Structural organization of gap junction channels. *Biochim Biophys Acta* 1711:99-125.
- Sporbert A, Mertsch K, Smolenski A, Haseloff RF, Schonfelder G, Paul M, Ruth P, Walter U, Blasig IE (1999): Phosphorylation of vasodilator-stimulated phosphoprotein: a consequence of nitric oxide- and cGMP-mediated signal transduction in brain capillary endothelial cells and astrocytes. *Brain Res Mol Brain Res* 67:258-66.
- Spray DC, Stern JH, Harris AL, Bennett MV (1982): Gap junctional conductance: comparison of sensitivities to H and Ca ions. *Proc Natl Acad Sci U S A* 79:441-5.
- Spray DC, Ye ZC, Ransom BR (2006): Functional connexin "hemichannels": a critical appraisal. *Glia* 54:758-73.
- Spyridopoulos I, Luedemann C, Chen D, Kearney M, Murohara T, Principe N, Isner JM, Losordo DW (2002): Divergence of angiogenic and vascular permeability signaling by VEGF: inhibition of protein kinase C suppresses VEGF-induced angiogenesis, but promotes VEGF-induced, NO-dependent vascular permeability. *Arterioscler Thromb Vasc Biol* 22:901-6.
- Srinivas M, Kronengold J, Bukauskas FF, Bargiello TA, Verselis VK (2005): Correlative studies of gating in Cx46 and Cx50 hemichannels and gap junction channels. *Biophys J* 88:1725-39.
- Srinivas M, Rozental R, Kojima T, Dermietzel R, Mehler M, Condorelli DF, Kessler JA, Spray DC (1999): Functional properties of channels formed by the neuronal gap junction protein connexin36. *J Neurosci* 19:9848-55.
- Stamatovic SM, Dimitrijevic OB, Keep RF, Andjelkovic AV (2006): Protein kinase Calpha-RhoA cross-talk in CCL2-induced alterations in brain endothelial permeability. *J Biol Chem* 281:8379-88.
- Stamatovic SM, Keep RF, Andjelkovic AV (2008): Brain endothelial cell-cell junctions: how to "open" the blood brain barrier. *Curr Neuropharmacol* 6:179-92.

- Stergiopoulos K, Alvarado JL, Mastroianni M, Ek-Vitorin JF, Taffet SM, Delmar M (1999): Hetero-domain interactions as a mechanism for the regulation of connexin channels. *Circ Res* 84:1144-55.
- Stout C, Charles A (2003): Modulation of intercellular calcium signaling in astrocytes by extracellular calcium and magnesium. *Glia* 43:265-73.
- Stout CE, Costantin JL, Naus CC, Charles AC (2002): Intercellular calcium signaling in astrocytes via ATP release through connexin hemichannels. *J Biol Chem* 277:10482-8.
- Strahonja-Packard A, Sanderson MJ (1999): Intercellular Ca(2+) waves induce temporally and spatially distinct intracellular Ca(2+) oscillations in glia. *Glia* 28:97-113.
- Streb H, Irvine RF, Berridge MJ, Schulz I (1983): Release of Ca²⁺ from a nonmitochondrial intracellular store in pancreatic acinar cells by inositol-1,4,5-trisphosphate. *Nature* 306:67-9.
- Stridh MH, Correa F, Nodin C, Weber SG, Blomstrand F, Nilsson M, Sandberg M (2010): Enhanced glutathione efflux from astrocytes in culture by low extracellular Ca²⁺ and curcumin. *Neurochem Res* 35:1231-8.
- Stridh MH, Tranberg M, Weber SG, Blomstrand F, Sandberg M (2008): Stimulated efflux of amino acids and glutathione from cultured hippocampal slices by omission of extracellular calcium: likely involvement of connexin hemichannels. *J Biol Chem* 283:10347-56.
- Su J, Cui M, Tang Y, Zhou H, Liu L, Dong Q (2009): Blockade of bradykinin B2 receptor more effectively reduces postischemic blood-brain barrier disruption and cytokines release than B1 receptor inhibition. *Biochem Biophys Res Commun* 388:205-11.
- Suadcani SO, Brosnan CF, Scemes E (2006): P2X7 receptors mediate ATP release and amplification of astrocytic intercellular Ca²⁺ signaling. *J Neurosci* 26:1378-85.
- Suadcani SO, Flores CE, Urban-Maldonado M, Beelitz M, Scemes E (2004): Gap junction channels coordinate the propagation of intercellular Ca²⁺ signals generated by P2Y receptor activation. *Glia* 48:217-29.
- Suchyna TM, Nitsche JM, Chilton M, Harris AL, Veenstra RD, Nicholson BJ (1999): Different ionic selectivities for connexins 26 and 32 produce rectifying gap junction channels. *Biophys J* 77:2968-87.
- Suchyna TM, Xu LX, Gao F, Fournier CR, Nicholson BJ (1993): Identification of a proline residue as a transduction element involved in voltage gating of gap junctions. *Nature* 365:847-9.
- Sukumaran SK, Prasadarao NV (2002): Regulation of protein kinase C in Escherichia coli K1 invasion of human brain microvascular endothelial cells. *J Biol Chem* 277:12253-62.
- Sukumaran SK, Prasadarao NV (2003): Escherichia coli K1 invasion increases human brain microvascular endothelial cell monolayer permeability by disassembling vascular-endothelial cadherins at tight junctions. *J Infect Dis* 188:1295-309.
- Sumi N, Nishioku T, Takata F, Matsumoto J, Watanabe T, Shuto H, Yamauchi A, Dohgu S, Kataoka Y (2010): Lipopolysaccharide-activated microglia induce dysfunction of the blood-brain barrier in rat microvascular endothelial cells co-cultured with microglia. *Cell Mol Neurobiol* 30:247-53.
- Sun J, Usune S, Zhao Y, Migita K, Katsuragi T (2010): Multidrug resistance protein transporter and Ins(1,4,5)P₃-sensitive Ca²⁺-signaling involved in adenosine triphosphate export via Gq protein-coupled NK2-receptor stimulation with neurokinin A. *J Pharmacol Sci* 114:92-8.
- Suzuki T, Du F, Tian QB, Zhang J, Endo S (2008): Ca²⁺/calmodulin-dependent protein kinase II α clusters are associated with stable lipid rafts and their formation traps PSD-95. *J Neurochem* 104:596-610.
- Swann K, Yu Y (2008): The dynamics of calcium oscillations that activate mammalian eggs. *Int J Dev Biol* 52:585-94.
- Swatton JE, Morris SA, Cardy TJ, Taylor CW (1999): Type 3 inositol trisphosphate receptors in RINm5F cells are biphasically regulated by cytosolic Ca²⁺ and mediate quantal Ca²⁺ mobilization. *Biochem J* 344 Pt 1:55-60.
- Szalai G, Krishnamurthy R, Hajnoczky G (1999): Apoptosis driven by IP(3)-linked mitochondrial calcium signals. *Embo J* 18:6349-61.
- Szente M, Gajda Z, Said Ali K, Hermes E (2002): Involvement of electrical coupling in the in vivo ictal epileptiform activity induced by 4-aminopyridine in the neocortex. *Neuroscience* 115:1067-78.
- Tai CJ, Kang SK, Leung PC (2001): Adenosine triphosphate-evoked cytosolic calcium oscillations in human granulosa-luteal cells: role of protein kinase C. *J Clin Endocrinol Metab* 86:773-7.
- Takens-Kwak BR, Jongsma HJ, Rook MB, Van Ginneken AC (1992): Mechanism of heptanol-induced uncoupling of cardiac gap junctions: a perforated patch-clamp study. *Am J Physiol* 262:C1531-8.
- Takeuchi H, Jin S, Wang J, Zhang G, Kawanokuchi J, Kuno R, Sonobe Y, Mizuno T, Suzumura A (2006): Tumor necrosis factor- α induces neurotoxicity via glutamate release from hemichannels of activated microglia in an autocrine manner. *J Biol Chem* 281:21362-8.
- Takeuchi H, Mizoguchi H, Doi Y, Jin S, Noda M, Liang J, Li H, Zhou Y, Mori R, Yasuoka S, Li E, Parajuli B, Kawanokuchi J, Sonobe Y, Sato J, Yamanaka K, Sobue G, Mizuno T, Suzumura A (2011): Blockade of gap junction hemichannel suppresses disease progression in mouse models of amyotrophic lateral sclerosis and Alzheimer's disease. *PLoS One* 6:e21108.

- Tanaka N, Nejime N, Kagota S, Kubota Y, Yudo K, Nakamura K, Kunitomo M, Takahashi K, Hashimoto M, Shinozuka K (2006): ATP participates in the regulation of microvessel permeability. *J Pharm Pharmacol* 58:481-7.
- Tanaka N, Nejime N, Kubota Y, Kagota S, Yudo K, Nakamura K, Kunitomo M, Takahashi K, Hashimoto M, Shinozuka K (2005): Myosin light chain kinase and Rho-kinase participate in P2Y receptor-mediated acceleration of permeability through the endothelial cell layer. *J Pharm Pharmacol* 57:335-40.
- Tang Q, Dowd TL, Verselis VK, Bargiello TA (2009): Conformational changes in a pore-forming region underlie voltage-dependent "loop gating" of an unapposed connexin hemichannel. *J Gen Physiol* 133:555-70.
- Tanimura A, Nezu A, Morita T, Hashimoto N, Tojyo Y (2002): Interplay between calcium, diacylglycerol, and phosphorylation in the spatial and temporal regulation of PKC α -GFP. *J Biol Chem* 277:29054-62.
- Tao L, Harris AL (2007): 2-aminoethoxydiphenyl borate directly inhibits channels composed of connexin26 and/or connexin32. *Mol Pharmacol* 71:570-9.
- Taylor CW, Laude AJ (2002): IP3 receptors and their regulation by calmodulin and cytosolic Ca²⁺. *Cell Calcium* 32:321-34.
- Taylor HJ, Chaytor AT, Evans WH, Griffith TM (1998): Inhibition of the gap junctional component of endothelium-dependent relaxations in rabbit iliac artery by 18- α glycyrrhetic acid. *Br J Pharmacol* 125:1-3.
- Teubner B, Odermatt B, Guldenagel M, Sohl G, Degen J, Bukauskas F, Kronengold J, Verselis VK, Jung YT, Kozak CA, Schilling K, Willecke K (2001): Functional expression of the new gap junction gene connexin47 transcribed in mouse brain and spinal cord neurons. *J Neurosci* 21:1117-26.
- Theis M, de Wit C, Schlaeger TM, Eckardt D, Kruger O, Doring B, Risau W, Deutsch U, Pohl U, Willecke K (2001): Endothelium-specific replacement of the connexin43 coding region by a lacZ reporter gene. *Genesis* 29:1-13.
- Thimm J, Mechler A, Lin H, Rhee S, Lal R (2005): Calcium-dependent open/closed conformations and interfacial energy maps of reconstituted hemichannels. *J Biol Chem* 280:10646-54.
- Thomas AP, Bird GS, Hajnoczky G, Robb-Gaspers LD, Putney JW, Jr. (1996): Spatial and temporal aspects of cellular calcium signaling. *Faseb J* 10:1505-17.
- Thomas T, Jordan K, Simek J, Shao Q, Jedeszko C, Walton P, Laird DW (2005): Mechanisms of Cx43 and Cx26 transport to the plasma membrane and gap junction regeneration. *J Cell Sci* 118:4451-62.
- Thomas WE (1999): Brain macrophages: on the role of pericytes and perivascular cells. *Brain Res Brain Res Rev* 31:42-57.
- Thompson RJ, Zhou N, MacVicar BA (2006): Ischemia opens neuronal gap junction hemichannels. *Science* 312:924-7.
- Thore S, Dyachok O, Gylfe E, Tengholm A (2005): Feedback activation of phospholipase C via intracellular mobilization and store-operated influx of Ca²⁺ in insulin-secreting beta-cells. *J Cell Sci* 118:4463-71.
- Thore S, Dyachok O, Tengholm A (2004): Oscillations of phospholipase C activity triggered by depolarization and Ca²⁺ influx in insulin-secreting cells. *J Biol Chem* 279:19396-400.
- Thuringer D, Maulon L, Frelin C (2002): Rapid transactivation of the vascular endothelial growth factor receptor KDR/Flk-1 by the bradykinin B2 receptor contributes to endothelial nitric-oxide synthase activation in cardiac capillary endothelial cells. *J Biol Chem* 277:2028-32.
- Tian GF, Takano T, Lin JH, Wang X, Bekar L, Nedergaard M (2006): Imaging of cortical astrocytes using 2-photon laser scanning microscopy in the intact mouse brain. *Adv Drug Deliv Rev* 58:773-87.
- Tiruppathi C, Ahmmed GU, Vogel SM, Malik AB (2006): Ca²⁺ signaling, TRP channels, and endothelial permeability. *Microcirculation* 13:693-708.
- Toma I, Bansal E, Meer EJ, Kang JJ, Vargas SL, Peti-Peterdi J (2008): Connexin 40 and ATP-dependent intercellular calcium wave in renal glomerular endothelial cells. *Am J Physiol Regul Integr Comp Physiol* 294:R1769-76.
- Tomida T, Hirose K, Takizawa A, Shibasaki F, Iino M (2003): NFAT functions as a working memory of Ca²⁺ signals in decoding Ca²⁺ oscillation. *Embo J* 22:3825-32.
- Torres A, Wanf F, Xu Q, Fujita T, Dobrowolski R, Willecke K, Takano T, Nedergaard M (2012): Extracellular Ca²⁺ acts as a mediator of communication from neurons to glia. *Sci Signal* 5: ra8
- Toubas J, Beck S, Pageaud AL, Huby AC, Mael-Ainin M, Dussaulte JC, Chatziantoniou C, Chadjichristos CE (2011): Alteration of connexin expression is an early signal for chronic kidney disease. *Am J Physiol Renal Physiol* 301:F24-32.
- Tovey SC, de Smet P, Lipp P, Thomas D, Young KW, Missiaen L, De Smedt H, Parys JB, Berridge MJ, Thuring J, Holmes A, Bootman MD (2001): Calcium puffs are generic InsP(3)-activated elementary calcium signals and are downregulated by prolonged hormonal stimulation to inhibit cellular calcium responses. *J Cell Sci* 114:3979-89.

- Traub O, Hertlein B, Kasper M, Eckert R, Krisciukaitis A, Hulser D, Willecke K (1998): Characterization of the gap junction protein connexin37 in murine endothelium, respiratory epithelium, and after transfection in human HeLa cells. *Eur J Cell Biol* 77:313-22.
- Trexler EB, Bennett MV, Bargiello TA, Verselis VK (1996): Voltage gating and permeation in a gap junction hemichannel. *Proc Natl Acad Sci U S A* 93:5836-41.
- Trexler EB, Bukauskas FF, Bennett MV, Bargiello TA, Verselis VK (1999): Rapid and direct effects of pH on connexins revealed by the connexin46 hemichannel preparation. *J Gen Physiol* 113:721-42.
- Trexler EB, Bukauskas FF, Kronengold J, Bargiello TA, Verselis VK (2000): The first extracellular loop domain is a major determinant of charge selectivity in connexin46 channels. *Biophys J* 79:3036-51.
- Tsukamoto A, Hayashida Y, Furukawa KS, Ushida T (2010): Spatio-temporal PLC activation in parallel with intracellular Ca²⁺ wave propagation in mechanically stimulated single MDCK cells. *Cell Calcium* 47:253-63.
- Tu H, Wang Z, Bezprozvanny I (2005a): Modulation of mammalian inositol 1,4,5-trisphosphate receptor isoforms by calcium: a role of calcium sensor region. *Biophys J* 88:1056-69.
- Tu H, Wang Z, Nosyreva E, De Smedt H, Bezprozvanny I (2005b): Functional characterization of mammalian inositol 1,4,5-trisphosphate receptor isoforms. *Biophys J* 88:1046-55.
- Ueda T, Shikano M, Kamiya T, Joh T, Ugawa S (2011): The TRPV4 channel is a novel regulator of intracellular Ca²⁺ in human esophageal epithelial cells. *Am J Physiol Gastrointest Liver Physiol* 301:G138-47.
- Uehara K, Uehara A (2011): P2Y1, P2Y6, and P2Y12 receptors in rat splenic sinus endothelial cells: an immunohistochemical and ultrastructural study. *Histochem Cell Biol* 136:557-67.
- Uhlen P, Fritz N (2010): Biochemistry of calcium oscillations. *Biochem Biophys Res Commun* 396:28-32.
- Unger VM, Kumar NM, Gilula NB, Yeager M (1999): Three-dimensional structure of a recombinant gap junction membrane channel. *Science* 283:1176-80.
- Unwin PN, Ennis PD (1983): Calcium-mediated changes in gap junction structure: evidence from the low angle X-ray pattern. *J Cell Biol* 97:1459-66.
- Utsumi H, Chiba H, Kamimura Y, Osanai M, Igarashi Y, Tobioka H, Mori M, Sawada N (2000): Expression of GFRalpha-1, receptor for GDNF, in rat brain capillary during postnatal development of the BBB. *Am J Physiol Cell Physiol* 279:C361-8.
- Vaca L (2010): SOCIC: the store-operated calcium influx complex. *Cell Calcium* 47:199-209.
- Vajanaphanich M, Schultz C, Tsien RY, Traynor-Kaplan AE, Pandolfi SJ, Barrett KE (1995): Cross-talk between calcium and cAMP-dependent intracellular signaling pathways. Implications for synergistic secretion in T84 colonic epithelial cells and rat pancreatic acinar cells. *J Clin Invest* 96:386-93.
- Valiunas V (2002): Biophysical properties of connexin-45 gap junction hemichannels studied in vertebrate cells. *J Gen Physiol* 119:147-64.
- Valiunas V, Niessen H, Willecke K, Weingart R (1999): Electrophysiological properties of gap junction channels in hepatocytes isolated from connexin32-deficient and wild-type mice. *Pflugers Arch* 437:846-56.
- Valiunas V, Polosina YY, Miller H, Potapova IA, Valiuniene L, Doronin S, Mathias RT, Robinson RB, Rosen MR, Cohen IS, Brink PR (2005): Connexin-specific cell-to-cell transfer of short interfering RNA by gap junctions. *J Physiol* 568:459-68.
- Valiunas V, Weingart R (2000): Electrical properties of gap junction hemichannels identified in transfected HeLa cells. *Pflugers Arch* 440:366-79.
- Van der Goes A, Wouters D, Van Der Pol SM, Huizinga R, Ronken E, Adamson P, Greenwood J, Dijkstra CD, De Vries HE (2001): Reactive oxygen species enhance the migration of monocytes across the blood-brain barrier in vitro. *Faseb J* 15:1852-4.
- Van Moorhem M, Decrock E, Coussee E, Faes L, De Vuyst E, Vranckx K, De Bock M, Wang N, D'Herde K, Lambain F, Callewaert G, Leybaert L (2010): L-beta-ODAP alters mitochondrial Ca²⁺ handling as an early event in excitotoxicity. *Cell Calcium* 47:287-96.
- van Veen TA, van Rijen HV, Jongsma HJ (2000): Electrical conductance of mouse connexin45 gap junction channels is modulated by phosphorylation. *Cardiovasc Res* 46:496-510.
- van Zeijl L, Ponsioen B, Giepmans BN, Ariaens A, Postma FR, Varnai P, Balla T, Divecha N, Jalink K, Moolenaar WH (2007): Regulation of connexin43 gap junctional communication by phosphatidylinositol 4,5-bisphosphate. *J Cell Biol* 177:881-91.
- Vandamme W, Braet K, Cabooter L, Leybaert L (2004): Tumour necrosis factor alpha inhibits purinergic calcium signalling in blood-brain barrier endothelial cells. *J Neurochem* 88:411-21.
- Vanden Abeele F, Bidaux G, Gordienko D, Beck B, Panchin YV, Baranova AV, Ivanov DV, Skryma R, Prevarskaya N (2006): Functional implications of calcium permeability of the channel formed by pannexin 1. *J Cell Biol* 174:535-46.
- Vanderheyden V, Devogelaere B, Missiaen L, De Smedt H, Bultynck G, Parys JB (2009): Regulation of inositol 1,4,5-trisphosphate-induced Ca²⁺ release by reversible phosphorylation and dephosphorylation. *Biochim Biophys Acta* 1793:959-70.

- Vanslyke JK, Naus CC, Musil LS (2009): Conformational maturation and post-ER multisubunit assembly of gap junction proteins. *Mol Biol Cell* 20:2451-63.
- Veenstra RD, Wang HZ, Beyer EC, Ramanan SV, Brink PR (1994): Connexin37 forms high conductance gap junction channels with subconductance state activity and selective dye and ionic permeabilities. *Biophys J* 66:1915-28.
- Veliz LP, Gonzalez FG, Duling BR, Saez JC, Boric MP (2008): Functional role of gap junctions in cytokine-induced leukocyte adhesion to endothelium in vivo. *Am J Physiol Heart Circ Physiol* 295:H1056-H1066.
- Verderio C, Bruzzone S, Zocchi E, Fedele E, Schenk U, De Flora A, Matteoli M (2001a): Evidence of a role for cyclic ADP-ribose in calcium signalling and neurotransmitter release in cultured astrocytes. *J Neurochem* 78:646-57.
- Verderio C, Matteoli M (2001b): ATP mediates calcium signaling between astrocytes and microglial cells: modulation by IFN-gamma. *J Immunol* 166:6383-91.
- Verin AD, Gilbert-McClain LI, Patterson CE, Garcia JG (1998): Biochemical regulation of the nonmuscle myosin light chain kinase isoform in bovine endothelium. *Am J Respir Cell Mol Biol* 19:767-76.
- Verma V, Hallett MB, Leybaert L, Martin PE, Evans WH (2009): Perturbing plasma membrane hemichannels attenuates calcium signalling in cardiac cells and HeLa cells expressing connexins. *Eur J Cell Biol* 88:79-90.
- Verselis VK, Ginter CS, Bargiello TA (1994): Opposite voltage gating polarities of two closely related connexins. *Nature* 368:348-51.
- Verselis VK, Srinivas M (2008): Divalent cations regulate connexin hemichannels by modulating intrinsic voltage-dependent gating. *J Gen Physiol* 132:315-27.
- Verselis VK, Trelles MP, Rubinos C, Bargiello TA, Srinivas M (2009): Loop gating of connexin hemichannels involves movement of pore-lining residues in the first extracellular loop domain. *J Biol Chem* 284:4484-93.
- Vestweber D (2000): Molecular mechanisms that control endothelial cell contacts. *J Pathol* 190:281-91.
- Vezzani A, Wu HQ, Angelico P, Stasi MA, Samanin R (1988): Quinolinic acid-induced seizures, but not nerve cell death, are associated with extracellular Ca²⁺ decrease assessed in the hippocampus by brain dialysis. *Brain Res* 454:289-97.
- Vial C, Fung CY, Goodall AH, Mahaut-Smith MP, Evans RJ (2006): Differential sensitivity of human platelet P2X₁ and P2Y₁ receptors to disruption of lipid rafts. *Biochem Biophys Res Commun* 343:415-9.
- Victorino GP, Newton CR, Curran B (2004): Endothelin-1 decreases microvessel permeability after endothelial activation. *J Trauma* 56:832-6.
- Vigne P, Feolde E, Breittmayer JP, Frelin C (1994): Characterization of the effects of 2-methylthio-ATP and 2-chloro-ATP on brain capillary endothelial cells: similarities to ADP and differences from ATP. *Br J Pharmacol* 112:775-80.
- Vinken M, Decrock E, De Vuyst E, De Bock M, Vandenbroucke RE, De Geest BG, Demeester J, Sanders NN, Vanhaecke T, Leybaert L, Rogiers V (2010): Connexin32 hemichannels contribute to the apoptotic-to-necrotic transition during Fas-mediated hepatocyte cell death. *Cell Mol Life Sci* 67:907-18.
- Violin JD, Zhang J, Tsien RY, Newton AC (2003): A genetically encoded fluorescent reporter reveals oscillatory phosphorylation by protein kinase C. *J Cell Biol* 161:899-909.
- Visentin S, Nuccio CD, Bellenchi GC (2006): Different patterns of Ca²⁺(+) signals are induced by low compared to high concentrations of P2Y agonists in microglia. *Purinergic Signal* 2:605-17.
- Vogel C, Bauer A, Wiesnet M, Preissner KT, Schaper W, Marti HH, Fischer S (2007): Flt-1, but not Flk-1 mediates hyperpermeability through activation of the PI3-K/Akt pathway. *J Cell Physiol* 212:236-43.
- Wakui M, Potter BV, Petersen OH (1989): Pulsatile intracellular calcium release does not depend on fluctuations in inositol trisphosphate concentration. *Nature* 339:317-20.
- Wang HZ, Veenstra RD (1997): Monovalent ion selectivity sequences of the rat connexin43 gap junction channel. *J Gen Physiol* 109:491-507.
- Wang J, Ma M, Locovei S, Keane RW, Dahl G (2007): Modulation of membrane channel currents by gap junction protein mimetic peptides: size matters. *Am J Physiol Cell Physiol* 293:C1112-9.
- Wang N, De Bock M, Bol M, De Vuyst E, Decrock E, Bukauskas F, Leybaert L (Unpublished observations): The connexin mimetic peptides Gap26 and Gap27 inhibit connexin unitary current activities.
- Wang SS, Denk W, Hausser M (2000): Coincidence detection in single dendritic spines mediated by calcium release. *Nat Neurosci* 3:1266-73.
- Wang XG, Peracchia C (1996): Connexin 32/38 chimeras suggest a role for the second half of inner loop in gap junction gating by low pH. *Am J Physiol* 271:C1743-9.
- Wang Z, Ginnan R, Abdullaev IF, Trebak M, Vincent PA, Singer HA (2010): Calcium/calmodulin-dependent protein kinase II delta6 (CaMKIIdelta6) and RhoA involvement in thrombin-induced endothelial barrier dysfunction. *J Biol Chem*.
- Warner A, Clements DK, Parikh S, Evans WH, DeHaan RL (1995): Specific motifs in the external loops of connexin proteins can determine gap junction formation between chick heart myocytes. *J Physiol* 488 (Pt 3):721-8.

- Webb TE, Feolde E, Vigne P, Neary JT, Runberg A, Frelin C, Barnard EA (1996): The P2Y purinoceptor in rat brain microvascular endothelial cells couple to inhibition of adenylate cyclase. *Br J Pharmacol* 119:1385-92.
- Weber PA, Chang HC, Spaeth KE, Nitsche JM, Nicholson BJ (2004): The permeability of gap junction channels to probes of different size is dependent on connexin composition and permeant-pore affinities. *Biophys J* 87:958-73.
- Wedel B, Boyles RR, Putney JW, Jr., Bird GS (2007): Role of the store-operated calcium entry proteins Stim1 and Orail1 in muscarinic cholinergic receptor-stimulated calcium oscillations in human embryonic kidney cells. *J Physiol* 579:679-89.
- Weerth SH, Holtzclaw LA, Russell JT (2007): Signaling proteins in raft-like microdomains are essential for Ca²⁺ wave propagation in glial cells. *Cell Calcium* 41:155-67.
- Wei CJ, Francis R, Xu X, Lo CW (2005): Connexin43 associated with an N-cadherin-containing multiprotein complex is required for gap junction formation in NIH3T3 cells. *J Biol Chem* 280:19925-36.
- Weiss N, Miller F, Cazaubon S, Couraud PO (2009): The blood-brain barrier in brain homeostasis and neurological diseases. *Biochim Biophys Acta* 1788:842-57.
- White TW, Bruzzone R, Wolfram S, Paul DL, Goodenough DA (1994): Selective interactions among the multiple connexin proteins expressed in the vertebrate lens: the second extracellular domain is a determinant of compatibility between connexins. *J Cell Biol* 125:879-92.
- Wilhelm I, Farkas AE, Nagyoszi P, Varo G, Balint Z, Vegh GA, Couraud PO, Romero IA, Weksler B, Krizbai IA (2007): Regulation of cerebral endothelial cell morphology by extracellular calcium. *Phys Med Biol* 52:6261-74.
- Willars GB, Muller-Esterl W, Nahorski SR (1999): Receptor phosphorylation does not mediate cross talk between muscarinic M₃ and bradykinin B₂ receptors. *Am J Physiol* 277:C859-69.
- Willecke K, Eiberger J, Degen J, Eckardt D, Romualdi A, Guldenagel M, Deutsch U, Sohl G (2002): Structural and functional diversity of connexin genes in the mouse and human genome. *Biol Chem* 383:725-37.
- Wilson AC, Clemente L, Liu T, Bowen RL, Meethal SV, Atwood CS (2008): Reproductive hormones regulate the selective permeability of the blood-brain barrier. *Biochim Biophys Acta* 1782:401-7.
- Wolburg H, Lippoldt A (2002): Tight junctions of the blood-brain barrier: development, composition and regulation. *Vascul Pharmacol* 38:323-37.
- Wong CW, Christen T, Roth I, Chadjichristos CE, Derouette JP, Foglia BF, Chanson M, Goodenough DA, Kwak BR (2006): Connexin37 protects against atherosclerosis by regulating monocyte adhesion. *Nat Med* 12:950-4.
- Wood PG, Gillespie JI (1998): Evidence for mitochondrial Ca²⁺-induced Ca²⁺ release in permeabilised endothelial cells. *Biochem Biophys Res Commun* 246:543-8.
- Wu CY, Hsieh HL, Sun CC, Yang CM (2009): IL-1 β induces MMP-9 expression via a Ca²⁺-dependent CaMKII/JNK/c-JUN cascade in rat brain astrocytes. *Glia* 57:1775-89.
- Wu JC, Tsai RY, Chung TH (2003): Role of catenins in the development of gap junctions in rat cardiomyocytes. *J Cell Biochem* 88:823-35.
- Wu X, Babnigg G, Zagranichnaya T, Villereal ML (2002): The role of endogenous human Trp4 in regulating carbachol-induced calcium oscillations in HEK-293 cells. *J Biol Chem* 277:13597-608.
- Xing J, Strange K (2010): Phosphatidylinositol 4,5-bisphosphate and loss of PLC γ activity inhibit TRPM channels required for oscillatory Ca²⁺ signaling. *Am J Physiol Cell Physiol* 298:C274-82.
- Xiong ZG, MacDonald JF (1999): Sensing of extracellular calcium by neurones. *Can J Physiol Pharmacol* 77:715-21.
- Xu SZ, Beech DJ (2001): TrpC1 is a membrane-spanning subunit of store-operated Ca²⁺ channels in native vascular smooth muscle cells. *Circ Res* 88:84-7.
- Yamada T, Kawamata T, Walker DG, McGeer PL (1992): Vimentin immunoreactivity in normal and pathological human brain tissue. *Acta Neuropathol (Berl)* 84:157-62.
- Yan X, Xing J, Lorin-Nebel C, Estevez AY, Nehrke K, Lamitina T, Strange K (2006): Function of a STIM1 homologue in *C. elegans*: evidence that store-operated Ca²⁺ entry is not essential for oscillatory Ca²⁺ signaling and ER Ca²⁺ homeostasis. *J Gen Physiol* 128:443-59.
- Yang T, Roder KE, Bhat GJ, Thekkumkara TJ, Abbruscato TJ (2006): Protein kinase C family members as a target for regulation of blood-brain barrier Na,K,2Cl-cotransporter during in vitro stroke conditions and nicotine exposure. *Pharm Res* 23:291-302.
- Yang Z, Sun W, Hu K (2009): Adenosine A₁ receptors selectively target protein kinase C isoforms to the caveolin-rich plasma membrane in cardiac myocytes. *Biochim Biophys Acta* 1793:1868-75.
- Yao H, Haddad GG (2004): Calcium and pH homeostasis in neurons during hypoxia and ischemia. *Cell Calcium* 36:247-55.
- Ye ZC, Wyeth MS, Baltan-Tekkok S, Ransom BR (2003): Functional hemichannels in astrocytes: a novel mechanism of glutamate release. *J Neurosci* 23:3588-96.

- Yeager M, Harris AL (2007): Gap junction channel structure in the early 21st century: facts and fantasies. *Curr Opin Cell Biol* 19:521-8.
- Yeager M, Nicholson BJ (1996): Structure of gap junction intercellular channels. *Curr Opin Struct Biol* 6:183-92.
- Yen MR, Saier MH, Jr. (2007): Gap junctional proteins of animals: the innexin/pannexin superfamily. *Prog Biophys Mol Biol* 94:5-14.
- Yi FX, Boeldt DS, Gifford SM, Sullivan JA, Grummer MA, Magness RR, Bird IM (2010): Pregnancy enhances sustained Ca²⁺ bursts and endothelial nitric oxide synthase activation in ovine uterine artery endothelial cells through increased connexin 43 function. *Biol Reprod* 82:66-75.
- Yokoyama K, Su IH, Tezuka T, Yasuda T, Mikoshiba K, Tarakhovskiy A, Yamamoto T (2002): BANK regulates BCR-induced calcium mobilization by promoting tyrosine phosphorylation of IP(3) receptor. *Embo J* 21:83-92.
- Young KW, Nash MS, Challiss RA, Nahorski SR (2003): Role of Ca²⁺ feedback on single cell inositol 1,4,5-trisphosphate oscillations mediated by G-protein-coupled receptors. *J Biol Chem* 278:20753-60.
- Yu J, Bippes CA, Hand GM, Muller DJ, Sosinsky GE (2007): Aminosulfonate modulated pH-induced conformational changes in connexin26 hemichannels. *J Biol Chem* 282:8895-904.
- Yule DI, Betzenhauser MJ, Joseph SK (2010): Linking structure to function: Recent lessons from inositol 1,4,5-trisphosphate receptor mutagenesis. *Cell Calcium* 47:469-79.
- Yum SW, Zhang J, Valiunas V, Kanaporis G, Brink PR, White TW, Scherer SS (2007): Human connexin26 and connexin30 form functional heteromeric and heterotypic channels. *Am J Physiol Cell Physiol* 293:C1032-48.
- Zanotti S, Charles A (1997): Extracellular calcium sensing by glial cells: low extracellular calcium induces intracellular calcium release and intercellular signaling. *J Neurochem* 69:594-602.
- Zhang BX, Muallem S (1992): Feedback inhibition of Ca²⁺ release by Ca²⁺ is the underlying mechanism of agonist-evoked intracellular Ca²⁺ oscillations in pancreatic acinar cells. *J Biol Chem* 267:24387-93.
- Zhang SW, Liu Y, Huang GZ, Liu L (2007): Aconitine alters connexin43 phosphorylation status and [Ca²⁺] oscillation patterns in cultured ventricular myocytes of neonatal rats. *Toxicol In Vitro* 21:1476-85.
- Zhang X, Qi Y (2005): Role of intramolecular interaction in connexin50: mediating the Ca²⁺-dependent binding of calmodulin to gap junction. *Arch Biochem Biophys* 440:111-7.
- Zhang X, Tan F, Zhang Y, Skidgel RA (2008): Carboxypeptidase M and kinin B1 receptors interact to facilitate efficient b1 signaling from B2 agonists. *J Biol Chem* 283:7994-8004.
- Zhao XS, Shin DM, Liu LH, Shull GE, Muallem S (2001): Plasticity and adaptation of Ca²⁺ signaling and Ca²⁺-dependent exocytosis in SERCA2(+/-) mice. *Embo J* 20:2680-9.
- Zhao Y, Migita K, Sun J, Katsuragi T (2010): MRP transporters as membrane machinery in the bradykinin-inducible export of ATP. *Naunyn Schmiedebergs Arch Pharmacol* 381:315-20.
- Zhong Y, Smart EJ, Weksler B, Couraud PO, Hennig B, Toborek M (2008): Caveolin-1 regulates human immunodeficiency virus-1 Tat-induced alterations of tight junction protein expression via modulation of the Ras signaling. *J Neurosci* 28:7788-96.
- Zhou XW, Pfahnl A, Werner R, Hudder A, Llanes A, Luebke A, Dahl G (1997): Identification of a pore lining segment in gap junction hemichannels. *Biophys J* 72:1946-53.
- Zhu DM, Tekle E, Chock PB, Huang CY (1996): Reversible phosphorylation as a controlling factor for sustaining calcium oscillations in HeLa cells: Involvement of calmodulin-dependent kinase II and a calyculin A-inhibitable phosphatase. *Biochemistry* 35:7214-23.
- Zlokovic BV (2008): The blood-brain barrier in health and chronic neurodegenerative disorders. *Neuron* 57:178-201.

Dankwoord

EEN DIKKE MERCI!

En ik die dacht dat het moeilijkste geschreven was...

Eerst en vooral een dikke merci aan m'n promotor, Prof. Dr. Luc Leybaert. Zeven jaar geleden stapte ik het labo binnen als thesisstudent om er de volgende jaren niet meer weg te gaan en dat had niet mogelijk geweest dankzij jouw hulp. Je deur stond (letterlijk) altijd open voor het aanklaarten van problemen. Bedankt voor je vertrouwen, steun en 'fresh ideas' die het werk altijd voortstuwden!

This thesis would not have been complete without the unfailing help of a whole group of people in the 'LBHE' (Université d'Artois), especially Prof. Romeo Cecchelli, Dr. Maxime Culot and Anaëlle. Maxime and Anaëlle, thank you for exploring this rather unknown territory with me. I hope this is not the end of it and I can still drive to Lens from time to time! Actually, I would just like to thank everyone in the LBHE, it was amazing how you were always ready to help that girl that wandered in from time to time and that you barely knew. Un grand Merci! Een belangrijke dankjewel gaat ook uit naar onze Belgische 'connexine-connectie': Prof. Geert Bultynck, Dr. Raf Ponsaerts (KULeuven) en Prof. Dr. Mathieu Vinken (VUB), en naar Prof. Geneviève Dupont (VUB), een krak in Ca²⁺ signaal mechanismen. Onze wetenschappelijke onderonsjes (al dan niet via e-mail) zijn altijd heel leerrijk geweest en hebben aanleiding gegeven tot enkele interessante pistes. Merci daarvoor! I would also like to thank the members of the examination committee for their careful and critical reading of this thesis and providing me with their constructive feedback.

Uiteraard moet er nu ook een heel grote dankjewel volgen aan m'n labogenootjes. We were a great team! First of all, Nan, more than being 'just' colleagues, we are roommates and friends. May our shopping-addiction, weekends and (secret ☺) city trips be our witness! I don't know where we'll be in a few years, but I'm quite sure that, if we once go our separate ways, we'll keep in touch, no matter if we're on the other side of the world. Thank you for always being there, in the lab and at home 谢谢! (my first words in Chinese, I truly hope I'm not cursing right now). Kirsten, nu ik er op terugkijk hebben wij eigenlijk niet echt zo lang samengewerkt, maar jouw passage door het labo is een verademing geweest. We hebben heel wat opgestoken van jouw efficiëntie. Je werkt nu wel niet meer in Blok B, maar we gaan samen nog wel wat groupon-bonnekes verslijten hè! Elke (DC) en Marijke, we zijn samen aan dit avontuur begonnen en als laatste in rij zie ik nu eindelijk ook het einde in zicht. Bedankt voor de toffe jaren int labo. Méliissa, merci om ons altijd op de hoogte te houden van alle Blok B-weetjes ☺! Elke (DV), jij was het die me duidelijk maakte dat doctoreren niet alleen voor de 'bollebozen' was en je hebt me gestimuleerd om een beurs aan te vragen. Jouw passie voor de wetenschap en kracht om door te zetten hebben me enorm gemotiveerd. Ashish, being the new guy in the lab isn't always easy, especially when you come from the other side of the globe and you end up in a girl clique, but I wish you all the best! Ezequiel, being an exchange PhD-student, you joined us only for a short time, but oh what a time! Our Parisian nights and visits to Escala/Barcelona were unforgettable! Tenslotte nog een welgemeende danku aan m'n thesisstudenten: Iris, Gilles, Jeroen, Katrien, Muhammed, Yuliya, Nana, Ilse en Ana; jullie hebben allemaal een steentje bijgedragen en ik ben blij dat sommigen onder jullie de smaak te pakken hebben gekregen en dezelfde weg zijn ingeslagen als ik indertijd.

En we blijven nog even in Blok B, waar nog veel meer mensen op hún dankwoordje wachten. Eerst en vooral Eric, elke keer opnieuw was je trouw op post om m'n celwerk te doen en me daardoor ook een beetje ademruimte te geven. André, onze schatbewaarder, je bent zelf altijd

een schat geweest! Julien en Prof. Gaspard De Ley, jullie hebben me geïntroduceerd in de wereld van de proefdierdjes, het is een fijn samenwerken geweest! Julien, toch ook nog een extra bedankje om paashaas, Sinterklaas en zonnetje in huis te zijn. De jonge garde wuift de oude uit, geniet van jullie pensioen, jullie hebben het verdiend! Tom, Diego, Bart, Cyriel en Dirk, de TOWO-broeders, bedankt; een technisch probleem of een PC die lastig doet, jullie weten telkens van wanten. En tenslotte nog Raoul, die de pakjesbedeling en reservaties van leslokaaltjes in goede banen heeft geleid. Eneuh, sorry da ik altijd 'inbrak' in je bureau om je scanner te stelen! ☺

Lieve vrienden, nonkels, tantes, neefjes, nichtjes, bomma's en bompa's (kga geen namen noemen, kwil zeker niemand vergeten!); hoewel het voor julie niet helemaal duidelijk was waar ik nu juist mee bezig ben geweest de laatste jaren, verdienen jullie ook een dikke knuffel! Jullie beseffen misschien niet helemaal waarom, maar jullie zorgden voor mijn portie ontspanning. Effe niet aan het werk moeten denken, da's goud waard! Als ik ooit eens iets terug kan doen, je weet me te vinden!

Mijn allerlaaste, maar wel belangrijkste dankuwel gaat natuurlijk naar mam, pap, Ellen en Koen. Merci voor alle kansen, jullie hulp, interesse, enthousiasme. Jullie weten dat ik een meisje van weinig woorden ben ☺, maar ik hoop dat jullie weten dat ik jullie heel erg dankbaar ben!

Xx..
Marijke

CV



CURRICULUM VITAE

Personal details

Name: Marijke De Bock
Date of Birth: 19/11/1983 (Wilrijk - Antwerp)
Address: J.A. Carennalaan 10
2070 Zwijndrecht
E-mail : mgdebock@gmail.com

Working Experience

2010 - Current: SGS Life Sciences, Antwerp, Belgium

Freelance Scientific Co-operator

2005 - 2010: Ghent University, Ghent, Belgium

PhD Research Project at the department of Basic Medical Sciences, Physiology
Promotor: Prof. Dr. Luc Leybaert

PhD thesis 'Connexin channels provide a target to manipulate Ca²⁺ dynamics and blood brain barrier permeability'.

Granted by the Institute for the Promotion of Innovation through Science and Technology in Flanders (IWT)

Training

2009: Université Descartes, Paris, France

Course on glial cell biology and disease

2007-2008: Ghent University, Ghent, Belgium

Basic Course in Laboratory Animal Science Partim 1: General Topics
Basic Course in Laboratory Animal Science Partim 1: Specific Topics

2001-2005: Ghent University, Ghent, Belgium

Master in Biomedical Sciences, Option Neurosciences (Graduated with distinction)

Master thesis: 'Electroporation and dye transfer as a method for detection of gap junctional coupling'. Laboratory of Physiology and Pathophysiology (Promotor: Prof. Dr. Luc Leybaert)

1995-2001: St. Ludgardisschool, Antwerp, Belgium

Secondary Education
Modern languages - Mathematics

A1 Publications

De Vuyst E., Decrock E., De Bock M., Yamasaki H., Naus C.C., Evans W.H. and Leybaert L. (2007). Connexin hemichannels and gap junction channels are differentially influenced by lipopolysaccharide and basic fibroblast growth factor. *Mol. Biol. Cell.* **18** (1): 34-46 (IF 6.52).

Leybaert L., De Bock M., Van Moorhem M., Decrock E. and De Vuyst E. (2007). Neurobarrier coupling in the brain: adjusting glucose entry with demand. *J. Neurosc. Res.* **85**:3213-3220 (IF 3.48).

De Vuyst E., De Bock M., Naus C., Mabilde C. and Leybaert L. (2008). Bipolar pulsed high frequency electroporation: a technique to load a restricted zone of cells and to investigate dye spread via gap junctions. *Biophys. J.* **94** (2): 469-479 (IF 4.76).

Decrock E., De Vuyst E., Van Moorhem M., Van Laeken L., De Bock M., Vinken M., Rogiers V., D'Herde K., Evans W.H., Naus C.C. and Leybaert L. (2009). Connexin 43 hemichannels contribute to the propagation of apoptotic cell death in a rat C6 glioma cell model. *Cell Death Diff* **16** (1):151-163 (IF 7.463).

De Vuyst E., Wang N., Decrock E., De Bock M., Vinken M., Van Moorhem M., Lai C., Culot M., Rogiers V., Cecchelli R., Naus C.C., Evans W.H. and Leybaert L. (2009). Ca²⁺ regulation of connexin 43 hemichannels in C6 glioma and glial cells. *Cell Calcium* **46** (3):176-87 (IF 4.481).

Vinken M., Decrock E., De Vuyst E., De Bock M., Leybaert L., Vandenbroucke R., De Geest B., Demeester J., Sanders N., Vanhaecke T. and Rogiers V. (2009). Connexin 32 hemichannels facilitate the apoptotic-to-necrotic transition during Fas-mediated hepatocyte cell death. *Cell Mol Life Sci.* **67** (6): 907-18 (IF 5.511)

Van Moorhem M., Decrock E., Coussee E., Faes L., De Vuyst E., Vranckx K., De Bock M., Wang N., Lambein F., Callewaert G. and Leybaert L. (2010). β -ODAP alters mitochondrial Ca²⁺ handling as an early event in excitotoxicity. *Cell Calcium.* **47** (3): 287-96 (IF 4.481).

D'hondt C., Ponsaerts R., De Smedt H., Vinken M., De Vuyst E., De Bock M., Wang N., Rogiers V., Leybaert L., Himpens B. and Bultynck G. (2010). Pannexin channels in ATP release and beyond: An unexpected rendezvous at the endoplasmic reticulum. *Cell Signal.* **23** (2): 302-16 (IF 4.481) *REVIEW ARTICLE*

Van Moorhem M., Decrock E., De Vuyst E., De Bock M., Wang N., Lambein F., Van Den Bosch L., Leybaert L. (2011). L- β -N-oxalyl- α,β -diaminopropionic acid toxicity in motor neurons. *Neuroreport.* **22** (3):131-5. (IF 1.822)

De Bock M., Culot M., Wang N., Bol M., Decrock E., De Vuyst E., da Costa A., Dauwe I., Vinken M., Simon A.M., Rogiers V., De Ley G., Evans W.H., Bultynck G., Dupont G., Cecchelli R., Leybaert L. (2011). Connexin channels provide a target to manipulate brain endothelial calcium dynamics and blood-brain barrier permeability. *J Cereb Blood Flow Metab.* **31**(9):1942-57. (IF 5.457)

Decrock E., Krysko D.V., Vinken M., Kaczmarek A., Crispino G., Bol M., Wang N., De Bock M., De Vuyst E., Naus C.C., Rogiers V., Vandenabeele P., Erneux C., Mammano F., Bultynck G., Leybaert L. (2011). Transfer of IP(3) through gap junctions is critical, but not sufficient, for the spread of apoptosis. *Cell Death Differ.* **19**(6):947-57. (IF 7.463)

De Bock M., Wang N., Bol M., Decrock E., Ponsaerts R., Bultynck G., Dupont G., Leybaert L. (2012). Connexin-43 hemichannels contribute to cytoplasmic Ca^{2+} oscillations by providing a bimodal Ca^{2+} -dependent Ca^{2+} -entry pathway. *J Biol Chem.* **287**(15):12250-66 (IF 5.328)

De Bock M., Culot M., Wang N., da Costa A., Decrock E., Bol M., Bultynck G., Cechelli R., Leybaert L. Low extracellular Ca^{2+} conditions induce an increase in brain endothelial permeability that is largely mediated by triggering intercellular Ca^{2+} waves. *Brain Res.* Revision submitted

Abstracts, Posters and Oral communications

National

De Bock M., De Vuyst E., Van Moorhem M., Decrock E. and Leybaert L. (2006). A role for endothelial calcium changes in neurobarrier coupling. Neurobelgium 2006. Genval, Belgium. November 10-11, 2006 (*Acta Neurologica Belgica, supp 2006, 106, 1-2: P57*). **Poster presentation**

De Bock M., De Vuyst E., Decrock E., Van Moorhem M. and Leybaert L. (2007). Connexin hemichannels and calcium signaling between blood-brain barrier endothelial cells. Autumn meeting of the Belgian society of fundamental and clinical physiology and pharmacology. Leuven, Belgium. November 17, 2007. (*Acta Physiologica 2008; 192, Supplement 662: P-06*). **Poster presentation**

De Bock M., Culot M., De Vuyst E., Wang N., Decrock E., Van Moorhem M., Cecchelli R. and Leybaert L. (2008). Mechanisms and effects of calcium oscillations/waves in blood brain barrier endothelial cells. Belgian Brain Congress 2008. Oostende, Belgium. October 24-25, 2008. (*Acta Neurologica Belgica, supp 2008, 108, P63*). **Poster presentation**

De Bock M., Culot M., De Vuyst E., Wang N., Decrock E., Van Moorhem M., Cecchelli R. and Leybaert L. (2008). Mechanisms and effects of calcium oscillations/waves in blood brain barrier endothelial cells. Autumn meeting of the Belgian society of fundamental and clinical physiology and pharmacology. Louvain-La-Neuve, Belgium. November 8, 2008. (*Acta Physiologica 2008; 194, Supplement 668: P-17*). **Poster presentation**

De Bock M., Culot M., De Vuyst E., Wang N., Decrock E., Van Moorhem M., Cecchelli R. and Leybaert L. (2009). Mechanisms and effects of calcium oscillations in blood brain barrier endothelial cells. Annual meeting interuniversity attraction poles: Molecular and cellular mechanisms of electrical excitability. Leuven, Belgium. January 7, 2009. **Poster presentation**

De Bock M. (2009). Connexin channels contribute to endothelial Ca^{2+} dynamics and alter blood-brain barrier function. Autumn meeting of the Belgian society of fundamental and clinical physiology and pharmacology. Brussels, Belgium. October 24, 2009. (*Acta Physiologica 2009, 197, Supplement 674: O-08*). **Oral communication.**

De Bock M., Wang N., Bol M., Decrock E., De Vuyst E., Bultynck G., Dupont G., Leybaert L. (2011). Connexin-43 hemichannels contribute to cytoplasmic Ca²⁺ oscillations by introducing positive and negative feedback that combines with the bimodal Ca²⁺ dependency of inositol 1,4,5-trisphosphate receptors. Molecular and Cellular Mechanisms of Electrical Excitability, Interuniversity Attraction Poles (IUAP). Ghent, Belgium. December 16, 2011. **Poster presentation**

De Bock M., Culot M., Cecchelli R., Leybaert L. (2012). Control of blood brain barrier by calcium and connexin channels. Spring meeting of the Belgian society of fundamental and clinical physiology and pharmacology. Brussels, Belgium. March 16, 2012. **Oral communication.**

International

De Bock M. (2008). Connexin hemichannel involvement in calcium oscillations/waves in blood-brain barrier endothelial cells. La communication jonctionnelle intercellulaire "etat des lieux" IV. Poitiers, France. July 3-4, 2008. **Oral communication**

De Bock M., Culot M., De Vuyst E., Wang N., Decrock E., Van Moorhem M., Vranckx K., Cecchelli R. and Leybaert L. (2008). Connexin hemichannel involvement in calcium oscillations/waves in blood-brain barrier endothelium. 11th international symposium on signal transduction in the blood brain barriers. Amsterdam, The Netherlands. September 18-20, 2008. **Poster presentation**

De Bock M. De Vuyst E., Wang N., Decrock E., Van Moorhem M., Culot M., Simon A.M., Cecchelli R. and Leybaert L. (2009). Involvement of connexin hemichannels in dynamic calcium changes and permeability of blood-brain barrier endothelial cells. International Gap Junction Conference. Sedona, Arizona, USA. July 25-30, 2009. **Poster presentation**

De Bock M. De Vuyst E., Wang N., Decrock E., Van Moorhem M., Culot M., Simon A.M., Cecchelli R. and Leybaert L. (2009). Involvement of connexin hemichannels in dynamic calcium changes and permeability of blood-brain barrier endothelial cells. 9th european conference on glial cells in health and disease. Paris, France. September 8-12, 2009. (*Glia* 2009, 57, S13: P 170). **Poster presentation**

De Bock M., Culot M., Wang N., Bol M., Decrock E., De Vuyst E., da Costa A., De Ley G., Evans W.H., Bultynck G., Dupont G., Cecchelli R., Leybaert L. (2011). Connexin channels provide a target to manipulate brain endothelial calcium dynamics and blood-brain barrier permeability. 9th international conference on cerebral vascular biology. Leiden, The Netherlands. June 21-25, 2011. **Oral & Poster presentation**

De Bock M., Wang N., Bol M., Decrock E., De Vuyst E., Bultynck G., Dupont G., Leybaert L. (2011). Connexin-43 hemichannels contribute to cytoplasmic Ca²⁺ oscillations by introducing positive and negative feedback that combines with the bimodal Ca²⁺ dependency of inositol 1,4,5-trisphosphate receptors. International Gap Junction Conference. Ghent, Belgium. August 6-11, 2011. **Poster presentation**

International mobility

March 6-10, 2006. Internship: cell culture to establish an in vitro model of the blood brain barrier. 'Laboratoire de Physiopathologie de la Barrière Hemato-Encéphalique', Université d'Artois, France.

September 17-28, 2007. Internship granted by the French government (PAI Tournesol grant). Régulation de la perméabilité de la barrière hémato-encéphalique par des signaux calciques. 'Laboratoire de Physiopathologie de la Barrière Hemato-Encéphalique'.

